UNIVERSITÉ DE MONTRÉAL

NEW COMPOSITE MEMBRANES BASED ON MODIFIED NAFION OR FLEMION FOR PEM FUEL CELL APPLICATION

HUIMIN TIAN
DÉPARTEMENT DE GÉNIE CHIMIQUE
ÉCOLE POLYTECHNIQUE DE MONTRÉAL

THÈSE PRÉSENTÉE EN VUE DE L'OBTENTION
DU DIPLÔME DE PHILOSOPHIAE DOCTOR
(GÉNIE MÉTALLURGIQUE)
DÉCEMBRE 2004

UNVERSITÉ DE MONTRÉAL

ÉCOLE POLYTECHNIQUE DE MONTRÉAL

Cette thèse intitulée:

NEW COMPOSITE MEMBRANES BASED ON MODIFIED NAFION OR FLEMION FOR PEM FUEL CELL APPLICATION

présentée par : TIAN Huimin

en vue de l'obtention du diplôme de : Philosophiae Doctor

a été dûment acceptée par le jury d'examen constitué de:

M. AJERSCH Frank, Ph.D., président

M. SAVADOGO Oumarou, D.Sc., membre et directeur du recherche

M. SACHER Edward, Ph.D., membre

M. GUAY Daniel, Ph.D., membre

To my parents

To my family

ACKNOWLEDGEMENTS

I am deeply grateful to my dissertation director Professor Oumarou Savadogo for providing me with the opportunity to study under his guidance. I am also very indebted to him for his patience, encouragement, financial support and supervision in this work. Without his extensive and comprehensive help, this dissertation would not have been possible.

I am also grateful to all my fellow graduate students and staff of the "Laboratoire d'Électrochimie et de Matériaux Énergétiques (LÉcMÉn)" for their assistance and friendship. I would like to give my thanks to Mr. Rene Charette, Mr. Benoit Julien, Mrs. Suzie Poulin, Mrs. Carole Massicotte, for their considerable and continuous assistance with all aspects of experiments carried out.

I would like to express my sincere thanks to my parents for their continuous encouragement. Finally, I would like to extend my appreciation to my husband, Yunli Fang, and my lovely daughter, Wendy Fang, for their love, care, passion and understanding.

RÉSUMÉ

Une nouvelle membrane composite à base de Nafion ou de Flemion et de l'acide Silicotungstique (STA) a été fabriquée en utilisant une simple procédure d'évaporation du solvant. La température d'évaporation optimale et la quantité de STA requise ont été identifiées. L'évaporation du solvant peut être divisée en deux étapes pendant la préparation de la membrane. Premièrement, le solvant à été évaporé à 70°C pour deux heures. Deuxièmement, la membrane évaporée a été gardée pendant la nuit dans un four à vide à 135°C. La quantité optimale de STA dans la solution électrolytique de préparation est dan la gamme de 5×10^{-4}M à 5×10^{-3}M. Les membranes composites ainsi obtenues présentent de bonnes propriétés thermiques et mécaniques.

L'étude de la conductivité ionique montre que la membrane composite avec STA donne une plus grande conductivité ionique que sans STA. La conductivité de la membrane composite augmente avec une de la concentration du STA. Quand la concentration en STA dans 10 mL de solution électrolytique de preparation est 5×10^{-3}M, la conductivité des membranes composites peut atteindre jusqu'à 0.120 $S\cdot cm^{-1}$ dans le cas de la membrane Nafion/STA et 0.133 $S\cdot cm^{-1}$ pour la membrane Flemion/STA. Par contre, des mesures de la rétention en eau montrent que le contenu en eau dans la membrane composite avec STA est plus élevée que celle de la membrane composite sans STA. Par conséquent, avec une conductivité et une abilité elevée d'hydratation du STA, la conductivité ionique et la rétention en eau de la membrane composite peuvent être améliorées considérablement par addition de STA.

La morphologie de la membrane composite a été étudiée par microscopie à force atomique (AFM) et par microscopie par balayage d'électrons (SEM). Les résultats de l'AFM et du SEM ont montré que le STA fut dispersé uniformément dans les membranes composites à basse de Nafion et Flemion. La structure d'une membrane

composite avec STA a été étudiée par diffraction de rayons-X (XRD), FTIR, analyse thermique et XPS. Les résultats ont indiqué que le STA fut incorporé avec succès dans la structure de Nafion et Flemion pendant la procédure de préparation des membranes composites l'analyse par FTIR a montré l'existence de l'interaction entre les groupes d'acide sulphonique et le STA. L'analyse par XPS a montré l'existence de liaisons W-S et W-C dans la membrane composite. Cela peut être utilisé pour expliquer l'observation expérimentale antérieure, c'est-à-dire, que la membrane composite avec STA a une plus grande conductivité et rétention en eau que la membrane composite sans STA. Les études effectuées nous ont permis de conclure que les améliorations dans la conductivité ionique et de la rétention en eau sont dues à un changement dans la composition chimique des membranes composites par l'addition d'acide silicotungstique.

Les caractéristiques densité de courant vs. potentiel des piles PEM à base des membranes composites Nafion/STA et Flemion/STA ont été déterminées dans une pile PEM H_2/O_2. Les performances des membranes composites à base de Nafion/STA et Flemion/STA sont toujours meilleures que celles des membranes fabriquées à base de Nafion ou de Flemion sans STA. L'amélioration des les caractéristiques montrées par les membranes composites Nafion/STA et Flemion/STA dans la pile à combustible est due à un effet combiné du polymère et du STA. L'existence de STA dans les membranes améliore leur performance dans une pile à combustible et rend cette opération faisable à haute température.

ABSTRACT

A new composite membrane based on Nafion or Flemion and Silicotungstic acid (STA) was fabricated using a simple solvent evaporation procedure. The optimum evaporation temperature and the amount of STA have been investigated. The evaporation of solvent can be divided into two steps during membrane preparation. Firstly, the solvent was evaporated at 70°C for two hours. Secondly, the evaporated membrane was kept in an vacuum oven at 135°C overnight. The optimum amount of STA in the casting electrolyte solution is in the range from 5×10^{-4} to $5\times10^{-3}M$. The obtained cast composite membranes exhibit good thermal and mechanical properties.

Study of the ionic conductivity shows that the composite membrane with STA gives a higher ionic conductivity than that without STA. The conductivity of composite membrane increases with the increase of STA concentration. When the STA concentration in the 10mL casting electrolyte solution is $5\times10^{-3}M$, the conductivities of the composite membranes can reach up to 0.120 $ohm^{-1}\cdot cm^{-1}$ for Nafion/STA membrane and 0.133 $ohm^{-1}\cdot cm^{-1}$ for Flemion/STA membrane. On the other hand, the water uptake measurement shows that the water content of the composite membrane with STA is higher than that of composite membrane without STA. Consequently, due to the high conductivity and the high hydrated abiliy of STA, ionic conductivity and water uptake of the composite membrane can be significantly improved by the addition of STA.

The morphology of the composite membrane was studied using atomic force microscopy (AFM) and scanning electron microscopy (SEM). The results of AFM and SEM showed that the STA was uniformly dispersed in the Nafion and Flemion composite membranes. The structure of a composite membrane with STA has been studied by X-ray diffraction (XRD), the fourier transform infrared spectroscopy (FTIR), thermoanalysis and X-ray photoelectron spectroscopy (XPS). The results indicated that

STA was successfully introduced into the structure of Nafion and Flemion during the procedure of casting composite membrane and there was the interaction between the sulphonic acid group and STA. X-ray photoelectron spectroscopy shows the existence of *W-S* and *W-C* bonds in composite membrane. This can be used to explain the previous experimental observation that the composite membrane with STA has higher conductivity and water uptake than the compositre membrane without STA. The above studies allowed us to conclude that the improvements in ionic conductivity and water uptake are due to the change of the chemical composition of the composite membranes by the addition of silicotungstic acid.

The current-potential polarization characterization of composite Nafion/STA and Flemion/STA membranes was measured using H_2/O_2 single polymer electrolyte membrane (PEM) fuel cell system. The performance based on composite Nafion/STA and Flemion/STA membranes is always better than that based on cast Nafion or cast Flemion without STA membranes. The improvement in the fuel cell characteristics for the composite Nafion/STA and Flemion/STAmembrane is due to a combined effect of the polymer and STA. The existence of STA improves the fuel cell performance and make this operation feasible under high temperature.

CONDENSÉ EN FRANÇAIS

1. INTRODUCTION

La pile à combustible à électrolyte polymère solide (Polymer Electrolyte Membrane Fuel Cell, PEMFC) ou pile PEM est considerée comme la source d'énergie la plus adaptée pour les véhicules à faible émission de rejets polluants. La pile PEM présente beaucoup d'avantages sur les autres types de piles à combustible. Premièrement, c'est un système tout solide, compact et simple. Deuxièmement, il peut fournir des densités de courant élevées à de faibles températures. Troisièmement, la pile PEM offre une densité de puissance élevée et une capacité rapide de démarrage à la température ambiante, ce qui réduit les problèmes de corrosion. Ces caractéristiques permettent à la pile PEM de présenter beaucoup d'avantages comme une source d'énergie pour les applications mobiles. Ceci explique qu'au cours des dernières années, la recherche sur la pile PEM est devenue de plus en plus importante.

Dans le système PEMFC, l'assemblage membrane-électrodes (MEA) est le composant de base de la pile. La membrane polymérique (PEM) est l'élément clé de ce composant, parce qu'elle détermine les propriétés exigées aux autres éléments utilisés dans le système. Les membranes les plus utilisées dans les piles PEM sont les polymères perfluorés et sulfonés (PFSAs). Ces membranes sont commercialement disponibles chez trois compagnies: le Nafion® (DuPont), le Flemion® (Asahi Glass Corporation) et la membrane Aciplex® (Asahi Chemicals).

Les avantages des membranes du type PFSA sont: (1) une bonne stabilité dans des milieux oxidants et reducteurs, ainsi que de bonnes propriétés mécaniques dues à la structure de la chaîne principale du polytétrafluoroéthylène dans le polymère; (2) leur conductivité protonique élevée, qui peut atteindre des valeurs de 0.2 $S \cdot cm^{-1}$ dans les piles à combustible. Cependant, ces membranes présentent une perméabilité élevée à

l'hydrogène. En plus, le coût de la membrane de Nafion est onéreux (environ 600 US$/m2). Un autre inconvénient du Nafion est qu'il ne peut pas fonctionner à des températures relativement élevées (supérieures à 90°C) parce que dans ces conditions d'opérations la membrane se déshydrate, ce qui engendre une perte importante de la conductivité protonique. Il y a plusieurs aspects de l'effet de l'eau sur le performance des piles PEM. La conductivité protonique d'une pile PEM augmente linéairement avec le contenu de l'eau dans la membrane et la plus haute conductivité correspond à une membrane complètement hydratée. Dans une pile à combustible fonctionnant à une température au-dessus du point d'ébullition de l'eau, la membrane perdra la conductivité par déshydratation. Une membrane sèche se rétrécit, ce qui réduit le contact entre la membrane et les électrodes et diminue la conduction protonique. En outre, il peut résulter en une augmentation dans la permeation du gaz due à l'augmentation des chemins de diffusion de la phase gazeuse dans les pores de la membrane. Ainsi, il est important de développer de nouvelles membranes polymériques capables de l'opérer à haute température, avec un bas coût, une haute hydratation et une faible perméabilité aux combustibles.

2. OBJECTIFS DE CE TRAVAIL

Présentement, le développement de nouvelles membranes est basé sur les concepts suivants: (i) l'amélioration de la capacité de rétention en eau de l'électrolyte polymère; ou (ii) l'augmentation de la conductivité protonique, laquelle est indépendante de l'humidification de la membrane. Une nouvelle classe d'ionomères qui sont développés pour les applications dans des piles PEM est le composite à base d'ionomère perfluorés (PFICMs). Les membranes composites doivent présenter une conductivité ionique élevée et une bonne résistance mécanique. Elles doivent aussi résister à la déshydratation et exhiber une faible perméabilité aux combustibles. Habituellement, les PFICMs sont des combinaisons de polymères avec un composé organique ou inorganique. Ce projet est principalement concentré sur les PFICMs que

sont basés sur l'utilisation d'un polymère perfluoré avec l'acide silicontungstique (STA) comme composé inorganique.

Des additifs inorganiques sont de plus en plus utilisés pour modifier la structure des membranes polymériques. Des matériaux inorganiques ont été employés afin de réduire la résistance ionique de ces membranes (par exemple le Nafion). Plusieurs matériaux hidrophiles ont été étudiés en considérant des propriétés chimiques et physiques telles que la liaison d'hydrogène, l'acidité, le point d'ébullition et la conductivité protonique. Ces matériaux incluent des hétéropolyacides (par exemple l'acide phosphotungstique, l'acide phosphomolibdique et l'acide silicontungstique), l'oxyde de silicium, des particules d'oxydes métalliques, zéolites, verres conducteurs de protons, zirconia sulfaté et phosphate de zirconium. Dans ces approches, les additifs inorganiques, en particulier les HPAs sont introduits dans le polymer à une pourcentage très élevé pouvant atteindre 60% en poids. Les composés inorganiques ne sont pas introduits sous forme dissoute mais à l'état solide dans la membrane composite. Les hétéropolyacids (HPAs) sont des modificateurs inorganiques très attractifs parce que ce type de matériaux inorganiques, ayant une structure cristalline, a montré une conductivité élevée et une bonne stabilité thermique. Dans ce travail, l'acide silicontungstique (STA) est utilisé comme additif pour modifier le Nafion ou le Flemion. Le STA est un hétéropolyacide solide. La formule chimique du STA est $H_4SiW_{12}O_{40} \cdot 26$ H_2O à la température ambiante. Normalement, le STA est hydraté avec au moins 26 molécules d'eau pour chaque anion et très souvent cet acide peut former des hydrates solides. En plus, le STA possède une bonne conductivité et peut donner une concentration élevée de protons. La conductivité d'un seul cristal de STA (28 H_2O) est de 2.7×10^{-2} *S/cm* à la température ambiante, ce qui indique qu'il pourrait être utilisé pour élaborer des polymères composites solides avec une conductivité assez importante pour être employés dans une pile PEM à la température ambiante.

Ce projet porte sur la modification des membranes de Nafion ou de Flemion avec l'acide silicontungstique (STA) comme additif à de faibles concentrations (inférieures à 0.1 M). Les nouvelles membranes seront produites par évaporation de l'électrolyte polymère formée d'une solution de Nafion ou du Flemion contenant le Dimethylformamide (DMF) comme solvant et de faibles concentrations en STA.

Les objectifs de ce travail sont:

- Établir le processus de préparation des membranes de Nafion ou de Flemion à partir d'une solution polymérique contenant le STA dans le DMF.
- Déterminer l'effet du STA sûr les propriétés de la membrane composite, e.g., la conductivité ionique, les propriétés mécaniques et la capacité de rétention en eau, etc.
- Déterminer la structure et la composition chimique de ces membranes composites.
- Étudier la performance d'une pile PEM munie de ce nouveau type de membrane.
- Déterminer les corrélations entre les propriétés des membranes et leur performance dans les PEM.

3. EXPÉRIMENTAL

3. 1. PRÉPARATION DES MEMBRANES COMPOSITES

Les nouvelles membranes composées ont été fabriquées par une procédure simple d'évaporation du solvant. Le STA a été mélangé premièrement avec une solution de Nafion 5% en poids (ou bien une solution de Flemion 8.9% en poids), ensuite, le solvant *N, N'*-dimethylformamide (DMF) a été ajouté dans la solution, où le rapport en volume entre la solution du polymère perfluoré et la DMF est de 10:3. L'électrolyte du

mélange est ensuite évaporé à des températures supérieures à 100°C. Finalement, les membranes composées de Nafion/STA (ou Flemion/STA) ont été obtenues.

3. 2. DETERMINATION DE LA RETENTION EN EAU

La rétention en eau de la membrane et la perte du STA dans la membrane composite Nafion/STA (ou Flemion/STA) ont été mesurées en immergeant un morceau de membrane dans de l'eau désionisée bouillant ou dans l'acide sulfurique bouillant pendant 4 heures. La procédure de mesure peut être divisée en 3 étapes: premièrement, la membrane a été séchée pendant la nuit dans un four à vide à 70°C et le poids de la membrane séchée est de $W_1(g)$; deuxièmement, la membrane a été immergée dans de l'eau désionisée bouillant pendant 4 heures et le poids de la membrane non séchée est de $W_2(g)$; troisièmement, la membrane a été séchée pendant la nuit, dans un four à vide à 70°C et le poids de la membrane séchée est de W3(g). La rétention en eau et le pourcentage de la perte de STA peuvent être exprimés comme suit:

$$\text{Rétention en eau } \% = \frac{W_2(g) - W_3(g)}{W_3(g)} \times 100\%$$

$$\text{Perte de STA } \% = \left(\frac{W_1(g) - W_3(g)}{W_1(g)} / [STA]_0\right) \times 100\%$$

où $[STA]_0$ est le pourcentage en poids initial du STA dans la membrane séché.

3. 3. MESURE DE LA CONDUCTIVITÉ IONIQUE

La conductivité ionique de la membrane composite Nafion/STA (ou Flemion/STA) a été détermine en utilisant une cellule pour mesurer de la conductivité fabriquée dans notre laboratoire. La membrane a été insérée entre une paire de blocs du Téflon avec les ouvertures (le diamètre est 1 centimètre), où une solution H_2SO_4 1 M a

été ajoutée afin d'éviter de sécher la membrane pendant les expériences. Des fils de platine lisse ont été utilisés comme électrodes. La résistance de la membrane peut être obtenue en mesurant la chute de potentiel à travers de la membrane composite sous plusieurs valeurs de courant. La conductivité ionique de la membrane peut être calculée comme suit:

$$\kappa = \frac{L}{S \cdot R}$$

où: L (cm) est l'épaisseur de la membrane; ; S (cm^2) est la surface de la membrane laquelle est 0.785cm^2 dans nos expériences; R (ohm): est la résistance de la membrane; κ $(ohm^{-1} \cdot cm^{-1})$: est la conductivité ionique de la membrane.

3. 4. MORPHOLOGIE

Les morphologies des surfaces et des sections transversales des membranes composites ont été obtenues en utilisant un microscope à force atomique (AFM) et un microscope électronique à balayage (SEM), respectivement. Les mesures ont été prises avec un instrument AFM de Digital NanoScope (R) III et un instrument SEM JSM-840 de JEOL.

3.5. STABILITÉ THERMIQUE ET MÉCANIQUE DES MEMBRANES COMPOSITES

La stabilité thermique des membranes composites a été étudiée par analyse thermogravimétrique (TGA). Les spectres TGA des membranes composites ont été obtenus avec un instrument SETARAM Thermal Analyser. Ceci peuvent d'obtenir les caractéristiques principales de stabilité thermique et du processus de déshydratation du HPA, du polymère et des membranes composites. Pour la caractérisation de la stabilité thermique, les échantillons ont été placés dans le récipient et chauffés de 25°C à 800°C

à 10°C/min, en mesurant la perte de poids comme une fonction de la température dans une atmosphère d'azote.

Les propriétés d'allongement des membranes composites ont été mesurées avec un Instron (modèle 4400R) utilisant une vitesse d'étirement de 10 mm/min. Les films ayant une épaisseur de 180 μm ont été préparés d'après les normes ASTM D882-02.

3. 6. CARACTÉRISATION DE MEMBRANES COMPOSITES PAR XRD, FTIR ET XPS

Les analyses par diffraction de rayons-X (XRD) des différents échantillons ont été effectuées avec le Diffractometer instrument Philips X-Pert; Les mesures de spectroscopie FTIR ont été faites en utilisant un spectromètre Perkin Elmer 2000 FTIR. Les spectres XPS ont été enregistrés avec un ESCALAB MKII photoelectron spectrometer (VGScientific) en utilisant un Source Mg Kα et 240 W de pouissance à 12 KV. La gamme du scanner est de 1200 eV ~ 0 eV (Mg excitation) énergie de liaison. La surface de l'échantillon analysé est 2 mm x 3 mm et la profondeur analytique de l'échantillon est de 50 Å. La déconvolution des spectres XPS détaillés de carbone, du fluor, de l'oxygène, du silicium, du tungstène et du soufre a été utilisée pour analyser la composition chimique de chaque membrane et le type d'espèce chimique dans la quelle l'élement se trouve dans les membranes composites.

3. 7. APPLICATION DANS UNE PILE À COMBUSTIBLE H_2/O_2

L'évaluation de la performance des membranes composites dans une pile H_2/O_2 a été effectuée à plusieurs températures et différentes pressions de H_2 et O_2. Les courbes de la polarisation potentiel vs. densité de courant de la pile ont été obtenues avec des MEAs ayant une surface de 2.25 cm^2, lesquels sont fabriqués avec des électrodes à diffusion de gaz commerciales (E-TEK) sur les quelles sont déposées des couches

catalytiques de platine (Pt/cm2 de 1 mg, 20% Pt/C) et les membranes polymériques avec ou sans STA. La concentration du STA dans l'électrolyte de fabrication est de 3×10^{-3} M pour la membrane préparée avec STA. Les pressions utilisées pour les gaz H_2 et O_2 ont été de 1, 2 et 4 atm, respectivement et les températures de la pile ont été de 50°C, 80°C ou 110°C.

4. RÉSULTATS ET DISCUSSIONS

Les résultats essentiels obtenus dans ce travail sont les suivants. Dans un premier temps, il a été montré qu'une nouvelle famille de membranes composites a basse de Nafion ou de Flemion et de l'acide silicotungstique (STA) a été fabriquée en utilisant une procédure très simple d'évaporation de solvant. La température optimale d'évaporation et les quantités de STA qui conduisent à de bonnes membranes ont été identifiées. La préparation de la membranes effectue en deux étapes : Le solvant a été d'abord évaporé à 70°C pendant deux heures. Ensuite, la membrane obtenue a été gardée pendant 12 heures dans un four sous vide à 135°C. La quantité optimale de STA introduite dans la solution électrolytique est dans l'intervalle de 5×10^{-4} à 5×10^{-3}M. Les membranes composites obtenues présentent de bonnes propriétés thermiques et mécaniques. Les membranes composites préparées à des températures inférieures à 70°C à partir d'une solution de Nafion sans DMF, sont très fragiles alors que les membranes composites préparées avec DMF à 135°C sont très flexibles. Les deuxièmes séries de membranes ont été étudiées dans ce travail.

Dans un deuxième temps, les études de la morphologie des membranes composites Nafion/STA et Flemion/STA par AFM et SEM ont montré que le STA solide est distribué uniformément dans les membranes à base de Nafion et Flemion et ne présente aucune agglomération. L'analyse par SEM a montré que les particules de STA possèdent des dimensions estimées entre 0.1 et 0.2 μm de diamètre dans la membrane Nafion/STA et entre 0.05 et 0.1 μm de diamètre dans la membrane Flemion/STA.

La conductivité ionique des membranes composites Nafion/STA ou Flemion/STA a été mesurée sous différentes conditions, incluant l'effet de la concentration du STA utilisée pour élaborer la membrane et méthodes de prétraitement de la membrane composite avant les mesures. Il a été montré que la conductivité ionique des membranes composites augmente avec la concentration de STA utilisée lors de la fabrication de la membrane. La conductivité ionique des membranes préparées avec STA est plus élevée que celle des membranes fabriquées sans STA et peut atteindre jusqu'à 0.120 $ohm^{-1} \cdot cm^{-1}$ dans le cas de la membrane Nafion/STA et 0.133 $ohm^{-1} \cdot cm^{-1}$ dans le cas de la membrane Flemion/STA. Augmentation de la conductivité est attribuée à la haute concentration de protons fournis par le STA introduit dans la membrane. Les membranes composites étaient stables à la température ambiante dans de l'eau déionisée et leur conductivité ionique augmente avec la concentration du STA utilisée pour fabriquer la membrane quand la membrane composite a été immergée dans de l'eau déionisée ou dans une solution de H_2SO_4 1M à la température de la pièce. Cependant, la conductivité ionique est indépendante de la concentration du STA quand les membranes composites ont été prétraitées dans de l'eau déionisée bouillante. Cette dernière conductivité reste supérieure à celle des membranes élaborées sans STA. Ce résultat a été attribué à la perte de STA dans la membrane composite. La perte de STA dans la membrane composite peut aussi être observée par analyse SEM et peut être confirmée par analyse de la rugosité de la surface. La conductivité ionique des membranes composites prétraitées dans 1 M H_2SO_4 est toujours plus élevée que celle des membranes prétraitées dans de l'eau déionisée. Ceci indique qu'il y à un effet synergétique entre l'acide sulfurique et le STA. Ceci est en accord avec les résultats obtenus par SEM et AFM, lesquels ont montré que la présence d'acide sulfurique dans la membrane composite peut réduire la perte de STA dans la membrane composite.

Dans un troisième temps, la rétention en eau des membranes a été déterminée. Il a été aussi montré que la rétention en eau des membranes composites avec STA est plus

élevée que celles sans STA lorsqu'elles sont traités dans de l'eau déionisée bouillante ou dans une solution 1 M H_2SO_4 bouillante. Ceci est dû à la capacité d'hydratation élevée du STA. L'analyse thermique du STA a montré que le STA dans les membranes composites pourrait absorber plus de 18 molécules d'eau. En conséquence, la rétention en eau des membranes compostes augmente avec la concentration du STA dans la membrane. En outre, nous avons trouvé que la perte de STA de la membrane traitée dans la solution 1 M H_2SO_4 bouillant est inférieure à celle de la membrane traitée dans l'eau déionisée bouillante qui peut être utilisée pour expliquer que la membrane composite a base de Nafion/STA traitée dans une solution de H_2SO_4 bouillant conduit à la plus grande conductivité que la membrane traitée dans de l'eau déionisée bouillante. La différence de perte de STA obtenue après traitement dans de l'eau déionisée et celle obtenue après traitement dans la solution 1M H_2SO_4 bouillantes indique aussi les effets synergétiques entre l'acide sulfurique et le STA.

Les données obtenues par analyse thermique des membranes composites ont montré que ces membranes présentent une dégradation en deux étapes dans l'intervalle de température étudié (25°C~800°C). La première étape peut être associée à un processus de desulfonation, alors que la deuxième étape peut être associée à une décomposition de la chaîne principale du polymère. Nous pouvons trouver que la première température de dégradation de la membrane composite diminue avec une réduction de la concentration de STA dans la membrane. Comme la première dégradation correspond à la réaction et/ou à la dégradation des groupes acides sulfonés, l'existence du STA dans la membrane composite a une influence sur la dégradation des groupes acides sulfuriques. Ce résultat suggère une interaction spécifique possible entre le STA et l'acide sulfurique. L'analyse TG a montré que la membrane composite possède une stabilité thermique tout à fait suffisante dans la région de température acceptable pour des applications dans une pile PEM. Les propriétés mécaniques des membranes composites Nafion/STA ont montré que les membranes composites

deviennent plus rigides et leur ductilité s'est détériorée avec l'addition d'une certaine quantité de STA.

Dans un quatrième temps, nous avons utilisé la technique de diffraction de rayons-x (XRD) pour déterminer la structure de la membrane composite. Un nouveau pic de diffraction a été observé à $2\theta = 9.20$ pour la membrane composite avec STA. Par comparaison au spectre de diffraction de la membrane sans STA, ce nouveau pic a été attribué à l'interaction entre le STA et le Nafion. En conséquence, il a été conclu que quelques espèces de STA sont détectées dans la matrice de la membrane et sont combinées au polymère perfluoré.

Dans un cinquième temps, nous avons utilisé la spectroscopie infrarouge (IR) pour analyser les échantillons. Le spectre IR a montré clairement l'existence de STA dans la membrane composite. Nous avons trouvé que les bandes à 922 cm^{-1} ($W=O$) pour la membrane Nafion/STA et 928 922 cm^{-1} ($W=O$) pour la membrane Flemion/STA; 881 cm^{-1} ($W\text{-}O_c\text{-}W$) pour la membrane Nafion/STA et 877 cm^{-1} ($W\text{-}O_c\text{-}W$) pour la membrane Flemion/STA, 795 cm^{-1} ($W\text{-}O_e\text{-}W$) pour la membrane Nafion/STA et 803 cm^{-1} ($W\text{-}O_e\text{-}W$) pour la membrane Flemion/STA. Les résultats indiquent que des espèces provenant du STA sont dans les membranes. L'étirement symétrique de SO_3 est observé à 1021 cm^{-1} dans la membrane à base de Nafion ou Flemion et a changé à 1017 cm^{-1} quand la membrane polymérique a été mélangée avec du STA. Ce résultat indique que les particules de STA réagissent réciproquement avec les groupes fonctionnels de l'acide sulfurique dans la membrane composite.

Dans un sixième temps, les échantillons des membranes Nafion/STA et Flemion/STA ont été évalués en utilisant la spectroscopie photoélectronique des rayons X (XPS) afin d'analyser la composition chimique des membranes composites. L'observation de W dans les spectres du Nafion/STA et Flemion/STA suggère la présence de STA dans les membranes composites. La détection des liaisons W-S et W-

C dans les membranes Nafion/STA et Flemion/STA confirment les interactions entre le STA et l'acide sulfurique, ainsi qu'entre le STA et la chaîne principale du polymère. Les résultats obtenus par XRD, FTIR, TG, XPS supportent l'existence d'un effet synergétique entre l'acide sulphonique et le STA. Cette conclusion peut être utilisée pour expliquer l'augmentation de la conductivité ionique et de la rétention en eau des membranes composites avec l'augmentation de la concentration en STA dans la membrane. Il est possible de montre que l'amélioration de la conductivité pour les membranes Nafion/STA ou Flemion/STA peut être due à l'augmentation de la concentration des sites protoniques, lesquels viennent de l'introduction de STA dans les membranes composites. L'utilization des résultats par XPS, nous ont permis de déterminer la concentration relative totale des sites protoniques actifs qui proviendraient des groupes d'acide sulfurique et l'addition de l'espèce STA dans les membranes: 1.1% de SO_3^- pour le Nafion seul, 1.27% de SO_3^- et STA pour la membrane composite de Nafion/STA, 1.4% de SO_3^- pour le Flemion seul et 1.6% de SO_3^- et STA pour la membrane composite de Flemion/STA. Évidemment, les sites protoniques actifs des membranes composites avec STA sont plus nombreux que sans STA. La concentration élevée des sites protonique devraient correspondre à la conductivité élevée.

L'évaluation de la performance des membranes composites dans une pile à combustible a été déterminée à plusieurs températures et différentes pressions de H_2 et O_2. La membrane composite élaborée avec STA possède de meilleure caractéristique que celles sans STA à chaque densité courant, température et pression. Quand la température de la pile est de 80°C et les pressions de H_2 et O_2 sont de 4 atm, les densités de courant des MEAs faites avec une membrane composite à base de Nafion/STA et la membrane de Nafion fabriquée sans STA à 0.6V sont de 708 et 477 mA/cm^2, respectivement. Par rapport à la membrane de Nafion élaborée sans STA, l'amélioration de la densité de courant de la pile à 0.6V pour une membrane composite Nafion/STA est de 231 mA/cm^2. En outre, comme la température est augmentée à 110°C, les différences de la densité de courant entre la membrane composite Nafion/STA et la

membrane de Nafion sans STA est de 141 mA/cm^2 (4 atm). Et en comparant la membrane composite Flemion/STA avec la Flemion fabriquée sans STA, nous pouvons trouver des améliorations dans la densité de courant de la pile à 0.6V est de 238 mA/cm^2 (à 80°C), 283 mA/cm^2 (à 110°C) et 37 mA/cm^2 (à 120°C) sous la même pression d'opération. Ceci montre que la membrane composite avec STA peut permettre à une pile PEM d'avoir une bonne performance même à une température de 120°C, ce qui nous donne une indication que les propriétés électrochimiques de la membrane composite peuvent être améliorées avec l'addition de STA dans la membrane.

5. CONCLUSIONS

De nouvelles membranes composites a base de Nafion/STA et Flemion/STA ont été préparées avec succès et leurs propriétés ont été étudiées. Les nouvelles membranes composites obtenues exposent des bonnes propriétés thermiques et mécaniques à la température d'évaporation optimale. Les résultats d'AFM et SEM ont montré que le STA a été dispersé uniformément dans les membranes composites de Nafion et Flemion.

L'addition de STA aux solutions de Nafion ou de Flemion pendant la fabrication de la membrane peut améliorer efficacement la conductivité ionique et la rétention en eau de la membrane composite. La conductivité ionique et la rétention en eau augmentent avec l'augmentation de la concentration de STA dans les membranes. L'introduction de STA dans la membrane est responsable de l'amélioration des conductivités ioniques et la capacité d'absorption d'eau. Les résultats expérimentaux ont montré que la conductivité de la membrane fabriquée avec STA trempé dans de l'acide sulfurique est plus élevée que celle trempée dans de l'eau désionisée bouillante. Se a été montré que la perte de STA dans une solution de H_2SO_4 1 M est inférieure à celle déterminée sur la membrane traitée dans de l'eau désionisée bouillante. Ceci est indicatif de l'effet synergétique entre le STA et les groupes sulfonés (- SO_3H) ou / et l'augmentation des sites protoniques.

Les résultats d'analyse thermique, de XRD et l'analyse par FTIR ont montré l'existence de STA dans la membrane composite et les interactions possibles entre le STA et le polymère. Ces interactions ont été supportées par l'analyse XPS qui a montré la présence des liaisons W-C et W-S dans le membranes Nafion/STA et Flemion/STA. La présence de STA est responsable de l'amélioration des conductivités ioniques, la capacité d'absorption de l'eau par les membranes aussi bien que les performances des membranes composites dans une pile H_2/O_2. L'addition de STA peut améliorer les propriétés électrochimiques des membranes composites. Cette addition de STA améliore aussi la performance des membranes échangeuses de protons par des applications dans les piles à combustible PEM à haute température.

6. RECOMMANDATIONS

Pour poursuivre ce travail, les recommandations suivantes méritent d'être considérées:

1) la capacité d'échange des ions de la membrane composite avec STA devrait être déterminée.

2) Il est nécessaire d'étudier la rétention en eau de la membrane composite avec STA dans une atmosphère de vapeur d'eau. C'est très important d'étudier les propriétés électrochimiques de la membrane composite dans une pile à combustible opérant à haute température.

3) Il faut déterminer comment on peut réduire la perte de STA dans la membrane composite.

4) Le Flemion est un polymère perfluoré développé par Asahi Glass Company. Ce polymère présente une structure très similaire à celle du Nafion. L'étude des membranes composites de Flemion avec STA devrait être explorée plus en détail.

TABLE OF CONTENTS

LIST OF TABLES

CHAPTER 1

CHAPTER 3

LIST OF FIGURES

CHAPTER 1

CHAPTER 2

CHAPTER 3

NOMENCLATURE

b	Tafel Slope (mV/dec)
E	Fuel cell potential (V)
E_r	Fuel cell reversible potential (V)
EWs	Equivalent weights
I	Current (mA)
i_0	Exchange current density (mA/cm^2)
L	Thickness (cm)
n_{water}	Electro-osmotic drag coefficient
pK_A	Acidity constant
R	Resistance (ohm)
R_{elt}	Electric resistance of electrolyte (ohm)
R_m	Electric resistance of membrane (ohm)

Abbreviation

AFC	Alkaline Fuel Cell
AFM	Atomic Force Microscopy
DMF	*N, N'*-Dimethylformamide
DSC	Differential Scanning Calorimetry
DTG	Differential Thermogravimetry
FC	Fuel Cell
FTIR	Fourier Transform Infrared Spectroscopy
HPA	Heteropolyacid
MEA	Membrane Electrode Aassembly

MCFC	Molten Carbonate Fuel Cell
PAFC	Phosphoric Acid Fuel Cell
PEM	Polymer Electrolyte Membrane
PEMFC	Polymer Electrolyte Membrane Fuel Cell
PFICM	Per-fluorinated Inomer Composite Membrane
PFSA	Per-fluorinated Sulphonic Acid Membrane
SOFC	Solid Oxide Fuel Cell
STA	Silicotungstic Acid
SAXS	Small-angle X-ray scattering
TG	Thermogravimetry
WAXD	Wide-angle X-ray diffraction
XRD	X-ray diffraction
XPS	X-ray Photoelectron Spectroscopy

Greek Letters

κ	the ionic conductivity of the membrane ($ohm^{-1} \cdot cm^{-1}$)
η	Overpotential (V)
η_a	Overpotential at anode (V)
η_c	Overpotential at cathode (V)
η_{act}	Activation overpotential (V)
η_{mt}	Mass transport overpotential (V)
λ	mol H_2O/mol SO_3H

INTRODUCTION

Human beings can not survive without energy. As the development of the society, more and more energies are needed in industries and people's daily life. The main source of energy comes from fossil fuel. The energy in fossil fuel is in the form of chemical energy. However, the energies most frequently used are mechanical and electricity energies. It is the heat engine which converts the fossil fuel into mechanical energy or electricity through combustion. It is well known that the direct combustion of fossil fuel causes pollution and the released CO_2 causes global warming. The impurities in fossil fuel containing nitrogen and sulphur produce harmful substances, such as NO_N, and SO_2, during the combustion at high temperature. The incomplete oxidation produces multicycle aromatic substances that may cause cancer and other serious diseases. To solve the problems mentioned above, new technologies which can not only avoid pollution and improve the efficiency but also meet the application pre-requisite (can be operated under low temperature, ie.) are mandatory. It cannot be denied that the fuel cell is one of the most important candidates.

At present, the polymer electrolyte membrane fuel cells (PEMFCs) are suggested as the most probable power plant for the next generation, non-polluting automobile engine due to the very high power density available from PEMFCs combined with the potential for very low cost [1,2]. The difference of PEM fuel cell from other fuel cells is the choice of electrolyte. It is the unique physical and mechanical properties of the polymer membrane electrolyte, which can provide significant advantages over liquid and high temperature solid electrolytes in materials selection, component design and manufacturing, and power plant systems design, that makes PEMFCs superior to others. Nowadays, the technical challenges related to the development of commercial polymer electrolyte membrane fuel cells are the followings:

(i) mass production and cost reduction of components (bipolar plates, membranes, catalysts, etc.); (ii) installation of the infrastructure for low-cost, clean and efficient fuel; (iii) simplification of the stack and system; (iv) introduction of low-cost/high-volume and environmentally friendly materials processes; and (v) automation of materials processes; while at the same time maintaining or increasing performance and reliability. Accordingly, the development of new thin films materials and surface modification technologies is essential for mass production of PEMFC.

The membranes most commonly used for polymer electrolyte membrane fuel cell applications are per-fluorinated sulphonic acid membranes (PFSAs). These membranes are commercially available from four companies: Nafion® membrane from DuPont, Dow membrane from Dow chemical, Flemion® membrane from Asahi Glass Corporation and Aciplex® membrane from Asahi Chemicals [3-6]. The polymer used as electrolyte in PEMFC consists of a fluorocarbon polymer backbone, similar to Teflon, to which sulfuric acid groups have been chemically bonded. The acid molecules are fixed to the polymer and cannot leak out, but the protons on these acid groups are free to migrate through the electrolyte. Therefore, the polymer membrane is not only an electronic insulator but also an excellent conductor of hydrogen ions.

The advantages of PFSA membranes are: (1) their stability in oxidative and reductive media due to the structure of the polytetrafluoroethylene backbone; (2) their good proton conductivity, which can be as high as 0.2 $S \cdot cm^{-1}$ in polymer electrolyte fuel cells. However, the PEMFC performance decreases when it is used at elevated temperatures. This is due to the following reasons. As the temperature increases, the polymer membrane may dehydrate and its ionic conductivity will decrease. In addition, the mechanical strength of the membrane deteriorates because of deformation of the polymer chain at a high temperature. Therefore, it is necessary to develop a new membrane. Furthermore, the importance of developing a new membrane can also be due to the following reasons:

(i) The operation of PEMFC at temperature above 140°C is of great interest because, in this temperature range, anode catalyst poisoning by CO is less important and the kinetics of fuel oxidation will be improved and the efficiency of the cell will also be significantly enhanced. High temperature cell operation will contribute to reducing the complexity of the hydrocarbon fuel cell system. Some other advantages of operating PEMFC at high temperatures are: a reduction in the use of expensive catalysts because the catalyst poisoning problem by CO can be solved at high temperatures; and minimization of the problems related to electrode flooding.

(ii) On the other hand, high operating temperature may enhance the gas transport in the electrode layers since no liquid water can be present in the cell at these temperatures. This may help to improve the kinetics of mass transport and simplify the fuel cell system. In particular, the kinetics of the oxygen reduction reaction could be improved. This improvement will be at least three orders of magnitude higher if we increase the operating temperature from 25 to 130°C. Per-fluorinated membranes can not be used in PEFC operation above the temperatures of around 100 °C due to the loss of the mechanical properties and the dehydration at these temperatures. They do not perform well above 90°C in a hydrocarbon PEMFC and above 85 °C in hydrogen PEMFC. The boiling point of water can be raised by increasing the operating pressure above 3 bars, which may correspond to a boiling point of water of about 135 °C. However, raising the pressure of PEMFC is undesirable from an efficiency point of view. Accordingly, the development of polymer electrolytes which may permit operations at higher temperatures and lower water vapor pressure is a very important and interesting approach to improve PEMFC technology.

(iii) Environmental concerns of materials processes may favor using protonated membranes rather than fluorinated ones, in particular in the case of the mass production of membranes;

(iv) Normally, a membrane surface area of at least 5~12 m^2 is necessary to get 40~60 kW power for a mid-sized electrical car. However, the current market price (US$ 650 /m2 or less) is still rather high. Even though mass production could relatively reduce the membrane costs, it is not enough to cut the costs by one order of magnitude for PEMFC application in electrical vehicles. High-volume fabrication of PEMFC products would be seriously limited if the process of making available and reliable materials for the industry were not accelerated. It is essential that the focus is placed on the development and production of low-cost ionomer membranes.

The development of new membranes should be based on the following concepts: (i) improvement of water uptake of the polymer electrolyte; or (ii) achievement of high proton conductivity which is independent of membrane humidification.

A new class of ionomer materials being developed for PEMFC applications is Per-fluorinated ionomer composite membranes (PFICMs). Composite membranes must exhibit high ionic conductivity and mechanical strength. They must also resist dehydration and exhibit fuel non-permeation. Their use in fuel-cell systems is very attractive because they will enhance the efficiency of the cell significantly. Two types of PFICMs are currently being developed [7]: (i) the macro-composite membrane, which is a combination of the polymer with an organic or inorganic structure at the micron scale; and (ii) the nano-composite membrane, which is a combination of the polymer with an organic or inorganic compound of nano-meter scale.

My project is focused on one type of nano-composite membrane, which is based on the casting of perfluorinated membranes with Silicotungstic acid (STA). STA is a heteropolyacid, which has been used in catalysis [8,9], analytical chemistry [10], solid- and high hydration capacity. Nowadays, the application of heteropolyacid in fuel cell system state cell and electrochromic devices [11-16] due to its high conductivity is

becoming more and more active. In this work, the silicotungstic acid (STA) is used as additive to modify the Nafion or Flemion membrane.

Nafion and Flemion membranes can be modified either by immersing the commercial membrane in STA electrolyte or by casting from the Nafion or Flemion solution containing STA. Unfortunately, the result of immersion is not quite satisfactory. Therefore, this project is devoted to the fabrication of membranes using casting. In order to improve the mechanical properties of composite membrane, a high boiling point polar solvent (DMF) is used in the casting procedure. This is different from the membrane cast from aqueous solution.

The objectives of this study are:

- Establish the procedure of casting thin Nafion and Flemion membranes from polymer solution with STA in Dimethylformamide.
- Determine the optimum condition of membrane fabrication.
- Determine the effect of STA on the properties of composite membranes, e.g. ionic conductivity and water uptake, etc.
- Study the structure and chemical composition of these composite membranes.
- Study the fuel cell performance using the new type of membranes.

CHAPTER 1

LITERATURE REVIEW

1.1. FUEL CELLS AND POLYMER ELECTROLYTE MEMBRANE FUEL CELL

A fuel cell is an electrochemical cell which can continuously convert the chemical energy of fuel and oxidant to electrical energy by a process involving an essentially invariant electrode-electrolyte system. Since the only by-products of the reaction in a fuel cell are heat and water, FC technology offers the prospect of zero emission energy production for applications ranging from stationary power generation for electric utility networks to automotive transportation. Because of high efficiency in energy conversion, reduction in transmission and distribution losses and relatively low pollution to the environment, the fuel cell has been found in many industrial applications [17, 18, 19, 20].

Fuel cell systems normally are simply distinguished by the type of electrolyte used and the following names and abbreviations are now frequently used in publications: Alkaline Fuel Cells (AFC), Phosphoric Acid Fuel Cells (PAFC), Molten Carbonate Fuel Cells (MCFC), Solid Oxide Fuel Cells (SOFC) and Polymer Electrolyte Membrane Fuel Cells (PEMFC).

In the above fuel cell systems, PEMFCs have many advantages over the others. Firstly, they are all solid state, compact and simple. Secondly, they can provide high current density and run at low temperatures. Thirdly, they provide room temperature startup, elimination of many corrosion problems, and the potential for low resistance losses. These advantages make them suitable for portable power sources and for electric vehicles application. In recent years, PEMFCs have been identified as

promising power sources for vehicular transportation and for other applications requiring clean, quite and portable power [22]. Accordingly, the research of PEMFCs is becoming more and more active [21, 27].

1.1.1. PRINCIPLE OF POLYMER ELECTROLYTE MEMBRANE FUEL CELL

A PEMFC consists of a polymer electrolyte membrane, which acts as an electrolyte, and porous electrodes. The membrane is sandwiched between two platinum – catalyzed porous electrodes such as carbon paper and mesh. Fig. 1-1 shows the basic operation of this type of fuel cell. The fuel cell requires humidified gases, hydrogen and oxygen.

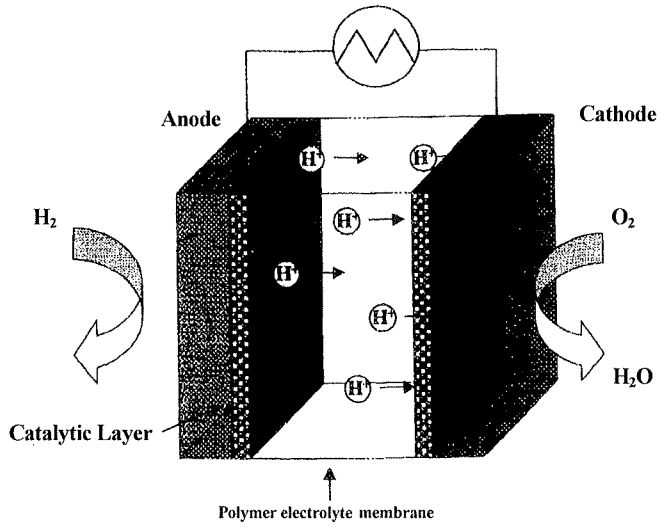

Figure 1- 1. Schematic diagram of PEMFC [34].

The fuel cell reactions are reduction of the oxidant, *OX* (in nearly all cases oxygen), which takes place at the cathode, and oxidation of the reductant, *RED* (fuel), at the anode. If the fuel is hydrogen, the electrochemical reactions that occur at the platinum electrocatalyst sites can be expressed as follows:

Anode: $H_2 \rightarrow 2H^+ + 2e^-$

Cathode: $\frac{1}{2}O_2 + 2H^+ + 2e^- \rightarrow H_2O$

Cell reaction: $2H_2 + O_2 \rightarrow 2H_2O$

At open-circuit, when the fuel cell is not producing electric energy, the fuel cell reversible potential (E_r) is given by the Nernst equation. However, if the fuel cell produces electric energy, a current I is passing through the cell. And then, E_r decreases to some value E due to the following reasons [27]:

The ohmic drop, caused by the electric resistance of the electrolyte, R_{elt}, or the membrane, R_m, if present, etc.;

Overpotentials, at both the anode and cathode.

Both effects cause E to decrease:

$$E = E_r - I(R_{elt} + R_m + \cdots) - |\eta_a| - |\eta_c| \quad (1)$$

where η_a and η_c are the overpotentials at the anode and the cathode, respectively.

In principle, the measured overpotential η is the sum of the activation overpotential (caused by kinetics resistance which comes from the adsorption, desorption and electrochemical reaction), the concentration overpotential (caused by mass transport resistance which comes from the mass transport of the reactant and the products) and ohmic resistance (which comes from the transportation of protons

through electrolyte and electrons through electrodes). The expression for the fuel cell potential (E), as a function of the reversible potential (E_r) and of the overpotentials (η) is:

$$E = E_r - \eta_{act} - \eta_{mt} - \eta_{iR} \tag{2}$$

The subscripts *act* and *mt* denote the activation and mass transport overpotentials at electrodes, respectively.

Fig. 1-2 shows the typical cell potential versus current density plot of fuel cells [28]. The semiexponential low current density region is due to the activation overpotential of the oxygen reduction reaction; the pseudo-linear intermediate current density region is caused predominantly by ohmic losses and, to a considerably lesser extent, by the charge-transfer resistance of the hydrogen oxidation reaction and the rapid decay rate of cell potential with current density is due to mass-transfer limitations. It is well accepted that the performance of the cell increase when the decrease of cell potential is reduced.

Up to the end of the linear region of the E vs. i plot, the equation:

$$E = E_0 - b\log i - Ri \tag{3}$$

where:

$$E_0 = E_r + b\log i_0 \tag{4}$$

has been used to fit the experimental data [28-33]. In these equations, E_0 is the observed open cell potential; b and i_0 are respectively the Tafel parameters and exchange current density for the oxygen reduction reaction. R represents the resistance, which causes a linear variation of the cell potential with current density. The contributions to R are due

to the charge-transfer resistance of the hydrogen oxidation reactions as well as the ohmic resistance in the cell and the mass-transfer resistance of the oxygen electrode reaction. The ohmic resistance is mainly coming from the electrolyte. The mass-transfer resistance of the oxygen electrode reaction is apparently constant over a limited current density range, but then increases rapidly causing a considerably faster decerase rate of the cell potential, leading to a limiting-current behavior.

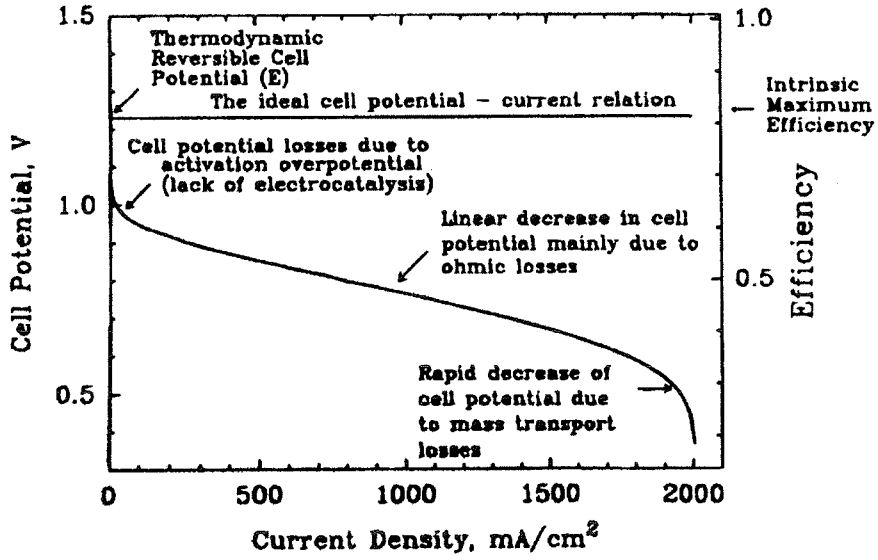

Figure 1- 2. Typical cell potential vs. current density plot for PEMFC, operating at low to intermediate temperatures, illustrating activation controlled, mass-transfer controlled and ohmic controlled regions. [28]

1.2. PERFLUORINATED IONOMER MEMBRANE

In the PEMFC system, the membrane electrode assembly (MEA) is the basic component of the single cell of a stack. The polymer electrolyte membrane (PEM) is the key element of this component, since it determines the properties required for other materials in the system. The polymer electrolyte membrane, from 50 to 250 microns thick, should provide an electrolyte capable of withstanding high-pressure differences

without any free corrosive liquids. Besides functioning as an acid electrolyte, the membrane separates the fuel gas (hydrogen or a hydrogen rich mixture) from the oxidant gas (oxygen or air) to prevent the mixing of reactant gases.

The desired properties of PEM used in PEMFCs include [35]:

a) good chemical and electrochemical stability during system operating conditions;
b) good mechanical strength and stability during operating conditions;
c) chemical properties of components compatible with the bonding requirements of PEMFCs;
d) extremely low permeability to reactant species in order to maximize coulombic efficiency;
e) high electrolyte transport to maintain uniform electrolyte content and to prevent localized drying;
f) high proton conductivity to support high currents with minimal resistive losses and zero electronic conductivity;
g) production costs compatible with the application.

In recent years, the PEMFCs have been greatly improved, mainly due to the success at Dupont and Dow Chemical companies in developing perfluorinated sulfuric acid membranes. The Nafion® family of Perfluorinated ionomer membranes was introduced by Dupont in 1966. Furthermore, Dow membrane was produced by Dow Chemical in 1988.

1.2.1. CHEMICAL STRUCTURE AND GENERAL PROPERTIES OF PERFLUORINATED IONOMER MEMBRANE

The perfluorinated ionomer membranes are of two types. One is based on strong acid functions like perfluorosulfuric acid, for example, Nafion®, Flemion® and Dow

membranes. Figure 1-3 shows the chemical structure of Nafion and other perfluorinated electrolyte membranes [37]. The values of x, y and z can be varied to produce materials at different equivalent weights (*EWs*) and pendant chain lengths. Here, the *EW* is the number of grams of polymer per mole of fixed SO_3 site. The general properties of Nafion®, Flemion®, Aciplex® and Dow® are summarized in Table 1-1.

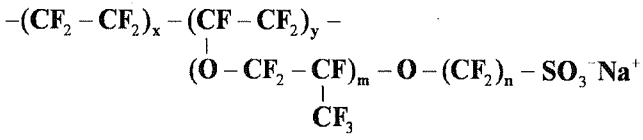

Nafion® 117	m ≥ 1, n=2, x=5-13.5, y=1000
Flemion®	m=0,1 ; n=1-5
Aciplex®	m=0,3; n=2-5, x=1.5-14
Dow membrane	m=0, n=2, x=3.6-10

Figure 1- 3. Chemical structures of perfluorinated polymer electrolyte membranes [37].

The Nafion® membrane (by Dupont) and Dow® membrane (by Dow Chemical) are the most effective and advanced membranes which are available in the market and still used in practical systems. Nafion membrane is a long-side-chain perfluorinated sulfuric acid membrane and has high *EW*s. These high *EW*s have limited the use of perfluorinated membranes in fuel cells because they lower their power density. The Dow membrane overcomes this disadvantage by shortening the side chain (m = 0 for Dow® and m ≥ 1 for Nafion®) (see Fig. 1-3). Therefore, the Dow and Nafion membranes differ in their *EW*s (for Dow membrane, the *EW* is typically in the 800~850 range; for Nafion 117 membrane, the *EW* always equals to 1100), even though they are structurally and morphologically similar. The specific conductance of 800, 850 and 1100 *EW* experimental membranes have been reported as 0.20, 0.12 and 0.081 $\Omega^{-1} \cdot cm^{-1}$, respectively [36, 38]. Accordingly, the electrochemical performance of Dow® membrane is superior to that of Nafion® 117 membrane. However, the

utilizations of Dow membrane for PEMFCs application are limited due to their higher cost resulting from its more complicated synthesis process [36] when compared to that of Nafion.

Table 1- 1. Properties of perfluorinated ionomer membranes e.g. Nafion®/Flemion®/Aciplex®/Dow® [35].

EW range	800-1500
Conductivity range (*S/cm*)	0.20-0.50; for example: 1100*EW* = 0.10 and *EW* 850 = 0.15
Conductance range (S/cm^2)	2-20: for example: 1 100 *EW* (7 and 2 mils membrane) = and 17 respectively
Dimensional stability	10-30% expansion X and Y direction from 50% RH liquid water (25°*C*. For example 1100 *EW* = 16% expansion)
Proven lifetime	> 50000 hours for Nafion®; Flemion® and Aciplex®; > 10000 hours for Dow
Thickness (*μm*)	250-50

Nowadays, the long-side-chain perfluorinated polymer electrolytes have been proven to have a prolonged service life under electrolysis and electrosynthesis and in fuel cell systems [39-41]. However, there is no large-scale industrial electrochemical system using the Dow membrane presently, so we will mainly focus on the various properties of Nafion in the following sections.

Another type of the perfluorinated ionomer membranes is based on weak-acid function. This type of membrane has been developed by Asahi Chemicals (Japan). Its

general structure is shown in Figure 1-4 [35]. This membrane has been used in chlor-alkali industry as a bilayer membrane. The comparison of membrane properties between *-SO_3H ($pK_A<1$)* and *–COOH ($pK_A=3$)* ion exchange groups has shown that the water content and the ionic conductivity of the (*-SO_3H*) based membranes are higher than those of the (*-COOH*) based membranes. Therefore, the weak-acid membranes (like Asahi) are less suitable for fuel cell applications.

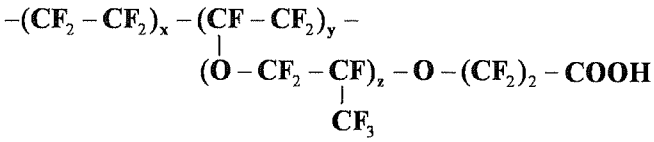

Figure 1- 4. The general structure of the Asahi chemical membrane: x = 6-8; y = 0-1 and z =1. [35]

1.2.2. MECHANISM OF PROTON TRANSPORT IN PERFLUORINATED IONOMER MEMBRANE

As a proton conductor, the perfluorinated ionomer membrane should have high proton conductivity. Therefore, it is very important and necessary to understand the mechanism of proton transport in perfluorinated ionomer membrane.

It is well known that the perfluorosulfonated polymer consists of a linear backbone of fluorocarbon chains and ethylether pendant groups with sulfuric acid cation exchange sites. Proton transport mechanism in polymer electrolyte membranes has been discussed by other authors [39, 42-44]. Yeager [42], Gierke and Hsu [43] described a structural three-zone pore model, namely, (I) A low dielectric constant region consisting of the hydrophobic fluorocarbon polymer matrix, (II) A high dielectric constant inverted miscellar region containing ion clusters including the sulfonate exchange sites, counterions, and sorbed water, and (III) The interfacial region consisting

mostly of the pendant side chains of the sulfonate groups and a small amount of water. Fig. 1-5 gives the structural model for Nafion.

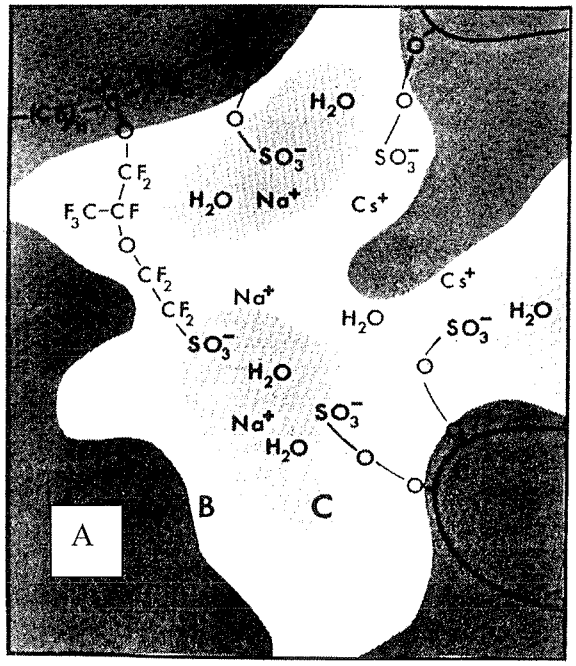

Figure 1- 5. Three region structural model for Nafion: (A) fluorocarbon; (B) interfacial zone; (C) ionic clusters. [42]

In fully hydrated Nafion, these ion clusters are about 4 *nm* in diameter. Moreover, they will shrink to about 1.9 *nm* at low water concentrations [43, 45]. The inter-connection of such spherical micelles within the membrane pores by channels creates a network for ions to transport [39, 45]. Fig. 1-6 shows the schematic diagram of a pore with an ion-exchange membrane in which the interconnected cellular geometry of the ion-cluster network is approximated by straight-cylindrical geometry.

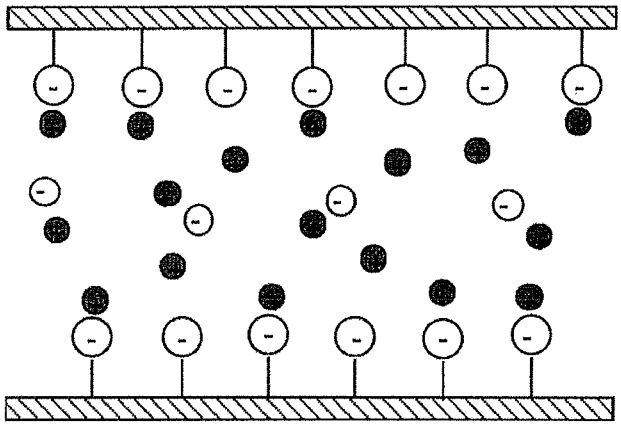

Figure 1- 6. Schematic diagram of a pore within an ion-exchange membrane with fixed anions ($-SO_3^-$) and cations, some of which are attached (Stern layer), while others form a diffuse layer. In addition, ions of any free-supported acid through self-ionization are shown. [39]

The anionic groups ($-SO_3^-$) are tethered to the pore surface and extended into the electrolyte phase, providing sites for cation exchange. In a dry membrane, a proton is firmly attached to each anionic group on the surface so that electroneutrality is maintained. The low dielectric environment promotes strong anion-cation coulombic interaction, so that the $-SO_3H$ is essentially undissociated and, consequently, there is little mobility of the protons. There is also evidence of very strong hydrogen bonding in the dry membranes, likely between the $-SO_3H$ groups. In the presence of water, the protons become solvated and form hydronium ions, $H^+ \cdot xH_2O$, within the hydrophilic core, and thus make the membrane exhibits high conductivity. Since the conductivity is proportional to the concentration of the mobile protons within the membrane, improving water uptake or increasing mobile protons can enhance the conductivity.

Water transport in the membrane will be discussed later.

1.2.3. WATER UPTAKE AND IONIC CONDUCTIVITY OF PERFLUOROSULFONIC ACID MEMBRANE

1.2.3.1. Water uptake of perfluorosulfonic acid membrane

For PEMFC, one important factor that can affect the performance of PEMFC is the hydration of the polymer electrolyte membranes [46, 49]. The membrane can be neither too dry (in which case the membrane conductivity decreases) nor too wet (in which case electrode flooding may result) [46, 47]. In PEMFC, the membranes are humidified by contact with humidified gases or liquid water, and therefore the water uptake characteristics of membranes from both liquid water and water vapor are of interest and importance.

1.2.3.1.1. Water uptake from liquid water

The water uptake of perfluorosulfonic acid membranes from liquid water has been widely reported. Firstly, the water uptake depends on the pretreatment of the membrane. Upon immersion in water at a given temperature, preboiled membranes absorb much more water than the membranes previously dried at elevated temperatures [46, 50, 51]. These effects are thought to be related to the formation and breakup of hydrated ion clusters in the membranes. The high water uptake of boiled membranes is thought to result from the development of an open structure caused by the formation of large ionic clusters [46, 50-52]. Drying membranes by heating result in pore shrinkage and reorientation of the side chains, and the reversal of which requires exposure to water at elevated temperatures [29, 53].

Fig. 1-7 [54] shows the water contents of cleaned samples of Nafion® 117 (i.e., samples that had been boiled) that were dried under vacuum at room temperature, at 80°C and at 105°C for various periods, and then re-equilibrated with water at 25°C. The samples dried at room temperature were rehydrated to the same water content as before

drying. However, the water contents of samples that were dried at elevated temperatures decreased rapidly with increasing drying time to much lower values, indicating a considerable increase in the resistance to ion cluster growth and the accompanying re-expansion of the microstructure. The water uptake after predrying at 105°C was less than that after predrying at 80°C, indicating a significantly greater degree of shrinkage of the microstructure at 105°C than that at 80°C.

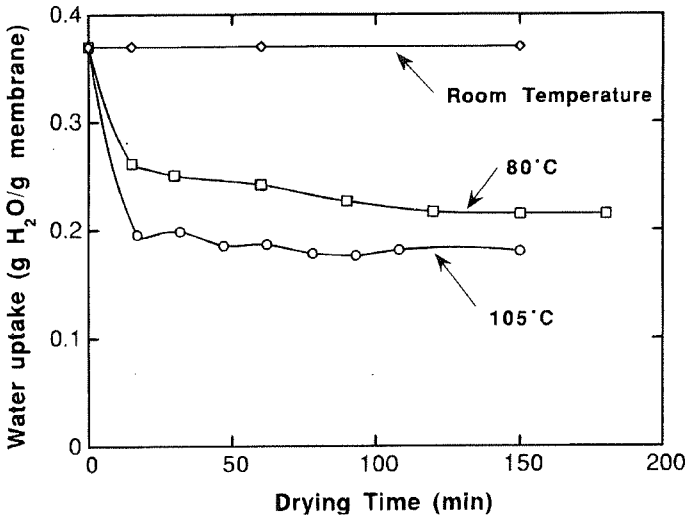

Figure 1- 7. Variations of water uptake of Nafion®117 upon immersion in water at 25°C with drying time under vacuum at different temperatures. [54]

The explanation of these results lies in the consideration of the formation and breakup of the ionic clusters as the membrane is dried [50]. Immersing the membrane in boiling water during pretreatment provides sufficient energy to form hydrated ionic clusters. When the pore is hydrated, electrostatic factors govern its internal morphology. Reorientation of the polymer chains require the cluster breakup. Therefore, a provision of sufficient energy is entailed for the sidechains to overcome barriers to motion. As long as any water is present, the sulfuric acid moieties are at least partly ionized. It is well known that trifluoromethane sulfuric acid monohydrate, a good analog of Nafion-*H* with λ (*mol H_2O/mol SO_3H*) = 1, has an ionic form: $CF_3SO_3\text{-}H_3O^+$. As the

polymer is partly dried, the ionic clusters shrink in size but remain agglomerated. When the final traces of water are removed, the sulfuric acid group is no longer ionized, the coulombic barrier for reorientation is removed, and the disintegration of the cluster is possible. However, once all the water is gone, a temperature close to the glass transition temperature of the polymer must be applied to allow sufficient reorientation of the polymer for cluster disintegration to occur. This explanation is in accordance with the concepts presented by Eisenberg [55], who suggested that cluster formation is a balance between dipole-dipole interactions favoring, and elastic forces opposing, clustering. Thus, there is a tendency for clusters to disintegrate in the dry polymer with increasing temperature.

The dependence of water uptake on membranes dehydration conditions may have important implications in their use in fuel cells. The PEMFC membrane electrode assemblies are constructed by hot-pressing the membrane between a pair of gas diffusion electrodes at high temperature (110°C~120°C). During this process, all the water is lost from the membrane, and the high dehydration temperature is expected to cause incomplete subsequent rehydration. If less water is taken up by the membrane during cell operation, a decrease in the maximum obtainable membrane conductivity occurs, since the conductivity depends roughly linearly on membrane water content.

The immersion temperature can also affect the water uptake of the membrane from the liquid water. Fig. 1-8 [54] shows the variation of water uptake with immersion temperature of the various membranes. The general behaviors are similar for all the different membranes. The water uptake increases with immersion temperature for both N-form and S-form membranes over the entire temperature range investigated (25 to 130°C), but remained constant for E-form membranes (Fig. 1-7) when the immersion temperature is up to approximately 100°C. The data for each of the S-form membranes followed smooth second-order curves over the entire temperature range investigated; similar behavior has been reported for immersion temperature up to 200°C. The water

uptake of the N-form membranes increases approximately linearly with increasing immersion temperature up to 100 or 110°C.

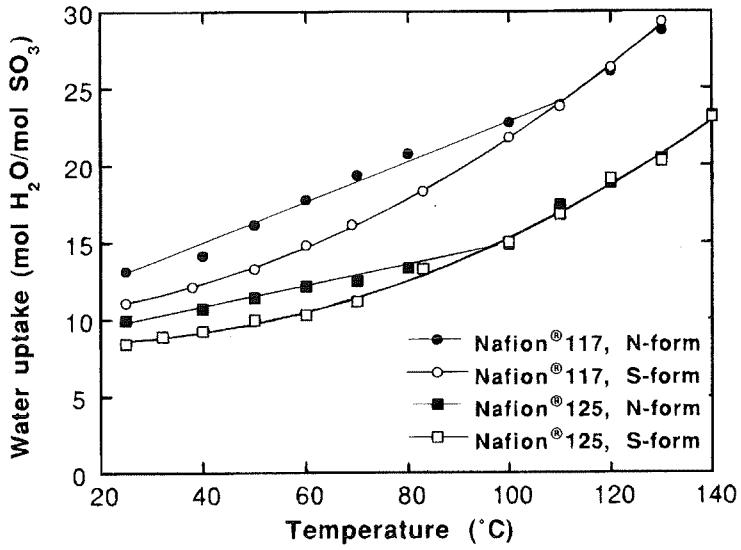

Figure 1- 8. Water uptakes of various perfluorosulfonic acid membranes upon immersion in liquid water at different temperatures after drying under vacuum at 80°C (N-form) and 105°C (S-form) [54].

The N-form membranes absorb more water than the various S-form membranes at temperatures up to 100 or 110°C. This is indicative of relatively easy ion cluster hydration in the case of N-form membranes. Accordingly, in comparison with the membranes dried at 105°C (S-form), the membrane dried at 80°C (N-form) has a lesser degree of cluster breakup and reorientation of the polymer. At immersion temperature higher than 100 or 110°C, the water uptake values for different membrane forms become the same, and the water uptake follow along the same curve observed for the S-form membranes. The above transition temperature of 100 or 110°C corresponds to the glass-transition temperature of perfluorosulfonic acid membranes [56].

Thus, the results suggest that the immersion of polymer membrane in water should be at the glass-transition temperature or above, where molecules can move more easily. In addition, the difference of membrane molecular structures caused by predrying at different temperatures will be eliminated. Consequently, predrying of the membranes at elevated temperatures (for example, during hot-pressing of membrane-electrode assembles) should not adversely affect their rehydration or conductivity during operation.

1.2.3.1.2. Water uptake from water vapor

As expected, the amount of water taken up from water vapor is less than the corresponding amount from liquid water. Table 1-2 shows the water uptake of different membrane from liquid water at 100°C and from saturated vapor water at 30°C. One possible explanation for this phenomenon is that water sorption from the liquid phase is direct, whereas sorption from the vapor phase involves the additional process of condensation of water onto the interior pore walls, which is made difficult by the hydrophobic nature of the fluorinated surfaces [50, 57].

Table 1- 2. Liquid vs.vapor phase water sorption. (For a membrane pretreated by immersion in boiling water). [46]

membrane	Uptake from	
	Liquid water at 100°C λ ($mol\ H_2O/mol\ SO_3H$)	Saturated Vapor water at 30°C λ ($mol\ H_2O/mol\ SO_3H$)
Nafion 117	21 to 22	14
Dow membrane	24 to 26	14

The values for water uptake from water vapor at 80°C are smaller than the corresponding values for 30°C [46, 50]. This temperature effect may also be related to the difficulty in condensing water on the membrane surfaces, which probably becomes even more difficult at elevated temperatures.

The observed relatively low water uptake at 80°C may be of importance if the isothermal data are to be used in PEMFC application, since PEMFCs are commonly operated at similar elevated temperature. Such guidelines are important because cell performance can be adversely affected if the membrane is allowed to be dried out (resulting in lower membrane conductivity), or if excess water is accumulated (which could result in electrode flooding) in the cell.

A related observation is that although S-form membranes take up less water from liquid water than, for example, N-form membranes, this was not found to be the case for water uptake from the vapor phase. This has an interesting implication with regard to PEMFC. One common method of preparing PEMFC membrane-electrode assemblies is hot-press the electrodes onto the membrane. The hot-pressing leads to the S-form membrane. According to the above results, that hot-pressing should not result in reducing the water uptake from the water vapor. This is important because the humidification in PEMFCs may come from the water uptake by the membrane.

1.2.3.1.3. Transport of water through the membrane

Water in the membrane is transported in two main ways: diffusion down concentration gradients that build up and electro-osmotic drag of water by protons transported from anode to cathode.

Fig. 1-9 shows the *H* intra-(self-) diffusion coefficients at 30°*C* for Nafion membranes in various states of hydration as a function of membrane water content [50]. The point for the highest water content (λ = 22) shown in Fig. 1-9 was obtained for a membrane immersed in bulk liquid water. Self-diffusion coefficients for all membranes studied are similar at a given water/sulfonate ratio and vary by more than an order of magnitude over the range of water content from λ = 2 to 22. The self-diffusion coefficients obtained are smaller than the self-diffusion coefficient of water molecules in water ($2.13\times10^{-5} cm^2/s$ at 25°*C*) [58]. This is expected due at least to the increase of tortuosity of the diffusion path in the membrane. Nevertheless, sidechain intrusions into the ion-lined pores and the hydrophobic backbone also restrict the diffusive motion of water molecules.

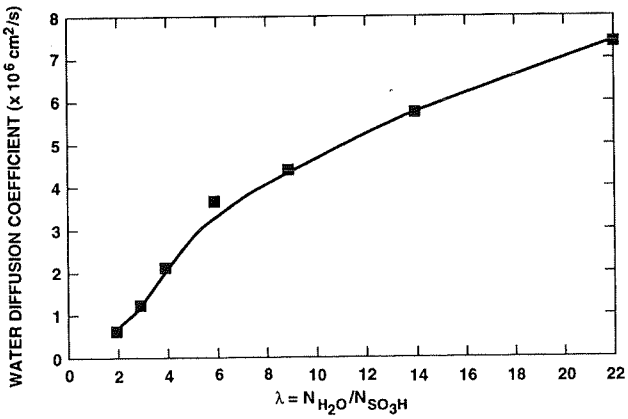

Figure 1- 9. Self-diffusion coefficient of water in Nafion as a function of extent of membrane hydration. [50]

Self-diffusion coefficients are obtained in the absence of a concentration gradient. Diffusion in a membrane across which a concentration gradient exists, is driven by an activity gradient. In a two-component system with a concentration gradient, we must describe the interdiffusion of the components. The negligible mobility of the polymer matrix allows us to approximate the interdiffusion coefficient as the

intradiffusion coefficient corrected for thermodynamic factors. The situation differs from case that the concentration profile is flat in that the water activity coefficient varies with the water concentration and these variations can alter the driving force for diffusion. To use the Fick's law to calculate water flux we must include the variation of the water activity coefficient in the effective diffusion coefficient. This result is a much smaller variation in the value of the diffusion coefficient with membrane water content [53].

The electro-osmotic drag coefficient, n_{water}, is the number of water molecules carried per proton across the membrane as protonic current is passed in the absence of activity gradients. Table 1-3 gives the electro-osmotic drag coefficient for Nafion membranes [46]. For a fully hydrated membrane at room temperature, 2.5 water molecules (average value) are dragged across the membrane per H^+ transported. While for a partially hydrated membrane (λ = 11), the drag is only 0.9. The data collected at lower membrane hydration suggest a substantial decrease in the electro-osmotic drag with water content. The main factor determining the number of water molecules dragged per ion of the membrane is the size of the charge carrier relative to the pore size through which they can move [59].

Table 1- 3. Electro-osmotic water drag by protonic current. [46]

Membrane	*Measured drag, H_2O/H^+ (30°C)*
Nafion 117, 22 H_2O/SO_3H	2.5 to 2.9
Nafion 117, 11 H_2O/SO_3H	0.9

The net transport of water across an operating fuel cell can be measured and calculated by collecting water from the anode and cathode outlets under current and at open circuit. Because water concentration gradients could exist in the membrane at an

operating fuel cell, back-diffusion could occur. The net water transport across the cell (from an anode to a cathode) is low (0.2 H_2O/H^+) contrasted with the electro-osmotic water drag for fully hydrated membranes under a uniform water concentration profiles (typically 2.5 H_2O/H^+). The low net flux of water through the operating cell is the combined results of a lowered electro-osmotic drag coefficient in partly hydrated membranes and the back-diffusion of water from a cathode to an anode.

1.2.3.2. Protonic Conductivity of Perfluorosulfonic Acid Membrane

The protonic conductivity of the membranes has been reported when the membranes were immersed in water and partially hydrated. For immersed mermbranes, the temperature dependence of the conductivity was also probed. In Fig. 1-10, the conductivity of N, C, and D at 30°C is plotted vs. the membrane water content [46]. Here, N stands for Nafion 117, D for Dow membane, C for Membrane C (Chlorine Engineers, Japan). These are all perfluorosulfonic acid membrane and they will be referred to as N, D and C hereafter respectively.

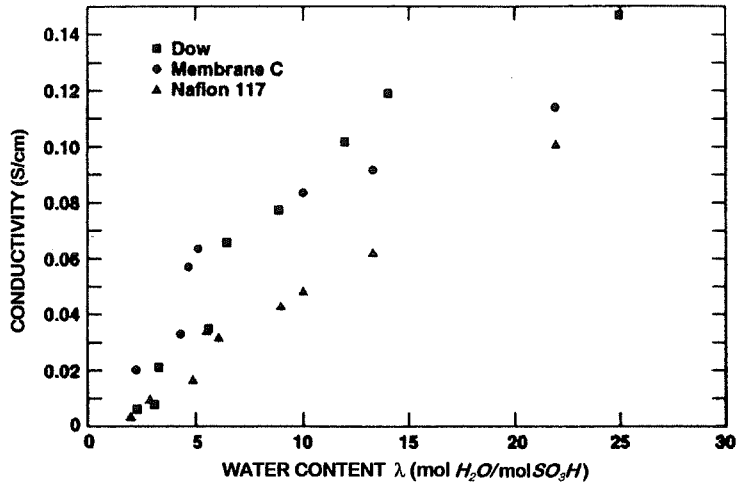

Figure 1- 10. Conductivity of N, C and D membranes at 30°C as a function of state of membrane hydration. [46]

The conductivity of N decreases roughly linearly with the decrease of water content. The value of the conductivity at $\lambda = 14$, 0.06 *S/cm* is in good agreement with that value reported by Rieke *et al.*[60]. The dependence of conductivity on water content for membrane C and Dow membranes is more complicated. In both cases, the conductivity decreases roughly linearly with decreasing water content till a threshold is apparently reached, at which point the conductivity drops substantially. Above this threshold of the water content, the conductivity of both membranes is substantially larger than that of Nafion 117. This is expected based on the higher ion-exchange capacities, and thus larger concentrations of charge carriers, in C and D relative to N. The conductivity of D is higher than that of C at higher water contents, reflecting again the higher protonic concentration in D membranes. The steep drop in conductivity observed in C and D occurs at around $\lambda = 5$ (Figure 1-10) and results in similar values of conductivity to that in N. The sharp drop in conductivity may be due to the sequestering of protons as undissociated sulfuric acid at low water contents.

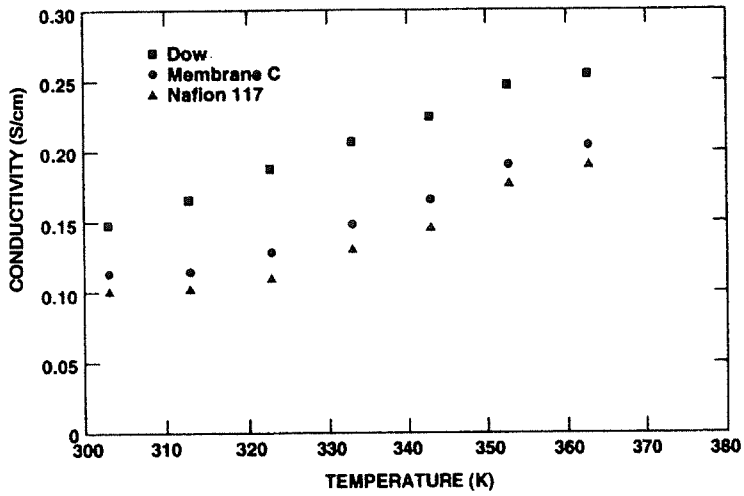

Figure 1- 11. Conductivity of N, C and D membranes, immersed in water, as a fuction of temperature. [46]

A plot illustrating the temperature dependence of the conductivity over the temperature range 25 to 90°C of immersed N, D, and C samples is shown in Fig. 1-11 [46]. Note that the water content of immersed membranes pre-equilibrated in boiling water is constant (λ = 22) over this temperature range. The specific conductivity of immersed membranes C and D is respectively larger by about 10 and 50% than that of immersed Nafion 117.

1.2.4. THERMAL STABILITY OF PERFLUOROSULFONIC ACID MEMBRANE

1.2.4.1. Thermogravimetric (TG) analysis

Figs. 1-12 show TG curves of Nafion-H. The solid curve relates to the percentage mass loss, and the dashed one to the first derivative trace (DTG).

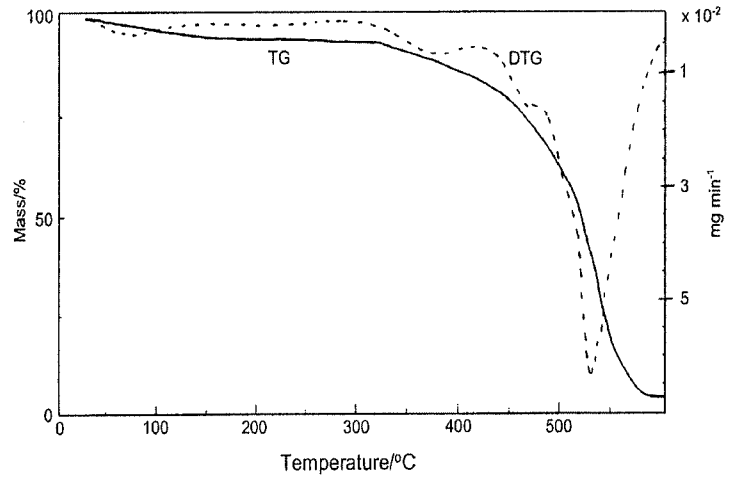

Figure 1- 12. TG (—) and DTG (- - -) traces of Nafion-*H* membrane at a heating rate of 20°C min^{-1} under N_2 atmosphere. [61]

The Nafion-*H* membrane seems to be decomposed in at least 3 stages, which can be clearly seen in the derivative curve. The gradual mass loss of about 6.4% on heating

from 25 to about 290°C can be attributed mainly to the loss of water molecules. The first stage (290–400°C) may be associated with a desulfonation process, while the second stage (400–470°C) may be related to side-chain decomposition and the third stage (470–560°C) to PTFE backbone decomposition. Wilkie *et al.* [62] reported that in the temperature range 25–355°C the gases liberated during the thermolysis of Nafion-*H* were H_2O, SO_2 and CO_2, while at higher temperatures typical gases from the degradation of fluorinated compounds, such as *HF*, and COF_2, were liberated.

1.2.4.2. Differential scanning calorimetry (DSC)

Fig. 1-13 depicts DSC curves of Nafion-*H* concerning the first run at a heating rate of 20°C per minute. It shows a strong endothermic peak at 115°C (T_1) and a weak and broad endothermic peak near 230°C (T_2). The thermal events above 250°C may be associated with thermal degradation of the Nafion-*H* membrane, according to the TG curve of this ionomer (Fig. 1-12). Between 250 and 300°C, a sharp peak is observed, which could be related to SO_2 liberation [62, 63]. A weak endothermic peak at 325°C in the DSC curves of Nafion-*H* could be related to the desulfonation process that occurred during the heating, as observed in the TG curve of Nafion-*H* .

Kyu *et al.* [64] observed two distinct thermal relaxations in the Nafion-*Na* membrane (*EW*=1365) in a dynamic mechanical analysis (DMA) study. These relaxations were attributed to the glass transition of the polymeric matrix (235°C) and to the glass transition inside the ionic clusters (140°C). In Nafion-*H*, these relaxations were observed at lower temperatures than those found for Nafion salts. The similar results for Nafion-*H* were observed at 230 and 111°C, respectively. Investigations on Nafion-117 in the acid form [61] showed two endothermic peaks; the first endotherm, at 145°C, was attributed to a transition in the ionic clusters, while the transition at 230°C was assigned to the melting of crystalline regions.

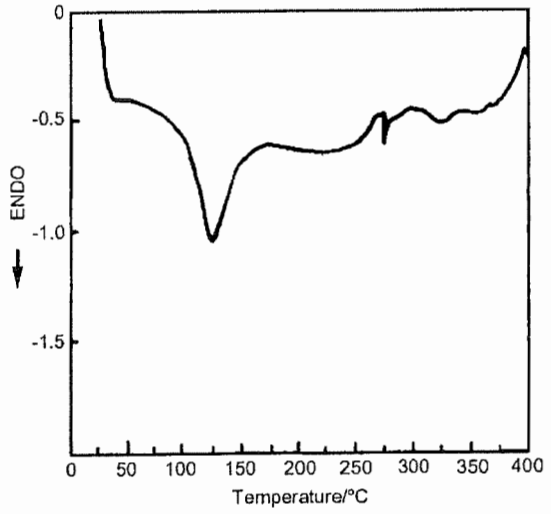

Figure 1- 13. DSC traces of the first heating for Nafion-*H* membranes at a heating rate of 20 °C min^{-1} under N_2 atmosphere. [61]

1.2.5. THE LIMITATION OF PERFLUORINATED IONOMER MEMBRANE IN FUEL CELL APPLICATION

Nafion perfluorinated ionomer membrane is widely used in PEMFCs due to its high ionic conductivity, good stability and mechanical properties (due to the strong polytetrafluoroethylene PTFE backbone). However, it has relatively high permeability for hydrogen in a fuel cell and the price of the Nafion membrane is too high (~600 *US$*/$m^2$ in mass production). Another drawback of Nafion membrane is that it can not work at high temperature because the dehydration of membrane. The current PEM fuel cells are shackled by the dehydration of PEM [66]. There are several different aspects of the effect of water on PEMFC performance. The proton conductivity of the PEM increases essentially linearly with water content of the membrane and the highest conductivity corresponds to a fully hydrated membrane [46]. In a fuel cell operated at a temperature above the boiling point of water, the membrane will lose conductivity due to dehydration. Drying also results in membrane shrinkage and leads to poor contact

and poor proton conduction between the membrane and the electrodes. Furthermore, it can result in increased gas crossover due to the increased accessibility of gas-phase diffuse/flow pathways within the membrane pores [67].

The maximum working temperature for Nafion membrane is around $100°C$. When fuel cell was operated at this temperature, the CO poisoning on the Pt (or Pt/Ru) catalyst can not be avoided. If the fuel is pure hydrogen, the fuel cell with Pt catalyst loading as low as 0.05-0.1 mg/cm^2 can still have satisfactory performance, with 0.7~1.2 A/cm^2 current density output at voltage of $0.5V$ [24, 25]. If there is trace amount of CO in hydrogen as impurity, the performance of fuel cell drops significantly even at high Pt (or Pt/Ru) catalyst loading. For example, when the concentration of CO is 10 ppm in hydrogen, the fuel cell with 4 mg/cm^2 Pt loading can only have 0.3 A/cm^2 current density output at $0.5V$ [23]. The hydrogen fuel is mainly from hydrocarbon reforming or cracking, so CO is one of the main by-product and it is not easy to be removed completely [68,69]. The CO poisoning is a result of the strong competitive chemisorption of CO to displace H_2 from the Pt surface [70]. Fortunately, since the chemisorption of CO is exothermic, it becomes weaker and weaker with the increase of temperature. Thus, the best way to solve the CO poisoning problem is to increase the PEMFCs working temperature [23]. However, Nafion membrane can not work properly at high temperature. New polymer electrolyte membranes for PEMFCs working at high temperature with low cost, high hydration and low fuel permeability are needed.

1.3. DEVELOPMENT OF PERFLUORINATED IONOMER MEMBRANE

1.3.1. INTRODUCTION

Polymer electrolyte membranes (PEMs) play a vital role in polymer electrolyte fuel cell systems. One of the limiting factors in PEMFCs is the membrane which serves as a structural framework to support the electrodes and transport protons from the anode

to the cathode. The limitations to large-scale commercial uses include poor ionic conductivities at low humidities and/or elevated temperatures, a susceptibility to chemical degradation at elevated temperatures and finally, membrane cost. These factors can adversely affect fuel cell performance and tend to limit the conditions under which a fuel cell may be operated. Consequently, the developments of new cheap solid polymer electrolytes, which can exhibit appropriate electrochemical properties, have become one of the most important fields for PEMFCs research.

Recently, other polymer electrolytes based on partially fluorinated ionomers [35, 36,71-76] and non-fluorinated ionomers are being developed by several groups around the world [35,72,77-81]. Ballard Advanced Materials has developed a group of materials, referred as a BAM3G, based on sulphonated copolymers incorporating α, β, β-trifluorostyrene (partially fluorinated ionomers) and a series of substituted-α, β, β-trifluorostyrene comonomers [35,72,73]. It has been shown that the water content of the sulphonated BAM3G is much higher than those of the Nafion® and Dow® membrane. It was claimed that in fuel cells, the BAM3G membrane exhibits performances superior to both the Nafion® and Dow® membranes at the currents above 600 A/ft^2 [35,72,73]. Unfortunately, some information related to the properties of BAM3G optimised parameters (thickness, ionic conductivity, conductance, exact chemical composition, mechanical strength, hydraulic permeation,etc.) is still not available.

Styrene-grafted and sulphonated membranes based on fluoropolymers have been developed by several groups [74,75,82-88]. They used γ-irradiation and electron-beam irradiation for grafting. 1t has been found that: (a) uncrosslinked membranes have lower resistance than crosslinked ones after they have been used for only a few hundred hours under fuel-cell operating conditions [82]; and (b) crosslinked membranes with divinylbenzene (DVB) have a rather high resistance, but better stability [82,84]. Styrene-grafted and sulphonated poly(vinylidene) membranes have also been developed. It has been shown that the total water uptake depends on the degree of

grafting (d.o.g.), and increases to around 40 H_2O/SO_3H (*mol/mol*) when the membrane is grafted at a d.o.g. of around 50% [85]. The effects of irradiation on sulphonation and on the thermal stability of poly(vinyl fluoride) have also been studied [75]. However, the major issue for these membranes is their stability in practical fuel-cell systems.

Several non-fluorinated ionomer membranes have also been studied [35,36,71]. As a result, the membrane based on poly(phenylquinoxaline) [35,36,72], poly(2,6 diphenyl-4-phenylene oxide) [35,36,72], acid-doped polybenzimidazole [77,89] polymer, polyimide [78] polymers, styrene/ethylene-butadiene/styrene triblock copolymer [79] and polyether ether ketone[80] polymers are still under active investigation by a lot of researchers. Up till now, there are still no membranes based on non-fluorinated polymers that have been used in practical fuel cell systems designed for long-term operation. .

Accordingly, Nafion membrane is still the most effective and available material that is used in practial systems. Although Nafion perfluorinated membrane material is advantaged by its stability and good performance, it still has some disadvantages for fuel cell applications. Nowadays, the modified Nafion is one important branch of new material developments. In order to improve the electrochemical performance of the Nafion membrane, some additives or impregnant were applied to modify the structure of the Nafion membrane.

1.3.2. DEVELOPMENT OF NEW INORGANIC ADDITIVES/NAFION COMPOSITE MEMBRANES

Inorganic materials were used for membrane structure modification in order to decrease the ionic resistance and improve the water retention characteristics of these perfluorinated membranes (i.e. Nafion). A number of hydrophilic materials have been

investigated based on physical and chemical properties such as hydrogen bonding, acidity, boiling point and proton conductivity. These materials include heteropolyacids, silicon oxide, metal oxide particles, zeolites, proton conducting glasses, sulfated zirconia and zirconium phosphate etc. The most promising composite membranes that have been investigated so far are Nafion/metal oxide, Nafion/zeolite, Nafion/silicon oxide and Nafion/zirconium phosphate membranes. These composite membranes show far superior performance as compared to unmodified Nafion at elevated temperatures up to and including $140°C$ and demonstrate excellent performance in the presence of CO in the hydrogen fuel stream as well.

Phosphoric Acid as Additive to Modify the Nafion Membrane Structure

Bhamidipati [92] found that a 1:1 mixture of phosphoric acid additives with Nafion resulted in a film that demonstrated 30% higher conductivity than a phosphoric acid equilibrated Nafion at $175°C$. In addition, thermal analysis data of the films suggested that the additive did not compromise the thermal stability of Nafion. The results suggested that the improved Nafion ionomer membranes could offer superior electrochemical performance, but they would retain the same degree of thermal stability as Nafion. However, the absorptions of phosphoric acid on the Pt electrocatalyst compromise the electrode performance [91].

Sulfonic Acid and Phosphoric Acid as Impregnant to Modify the Polymer Structure

Foulkes and Graydon [90] utilized (pre-Nafion) polystyrenesulfonic acid ion–exchange membranes in fuel cells with and without impregnation of the membrane with sulfuric acid. They found that the fuel cell with membranes pre-equilibrated with 8 N H_2SO_4 yielded substantially better current-voltage characteristics than those with only

water. Savinell *et al.* [91] incorporated 85% phosphoric acid (5 *mol* H_3PO_4 per mole sulfuric acid) in Nafion to increase its conductivity at higher temperatures for use in direct methanol fuel cell. They claimed good conductivity (~0.05 $\Omega^{-1}cm^{-1}$, compared with ~0.075 $\Omega^{-1}cm^{-1}$ for fully hydrated Nafion 117 at 80°*C*) could be obtained at 150°*C*. Although the phosphoric acid equilibrated membrane possesses substantial conductivity even in the absence of additional water (~0.02 $\Omega^{-1}cm^{-1}$), the presence of water dramatically increased its conductivity. Unfortunately, one disadvantage of the use of phosphoric acid is that it adsorbs on the *Pt* electrocatalyst, thus, compromising the electrode performance.

Heteropolyacid as Impregnant to Modify the Nafion Membrane Structure

Sanjiv Malhotra [93] *et al.* studied Nafion membrane modified with phosphotungstic acid (PTA) as impregnant. It is expected that the membrane modified by heteropolyacid can show a good electrochemical performance and can be used in high temperature fuel cell because heteropolyacid contains high concentration of protons.

It is well known that Nafion membrane is not suitable for high temperature fuel cell due to its dehydration at the high temperature. However, the Nafion 117 membrane impregnated with the solution of 12-phosphotungstic acid (PTA) (0.4*g* PTA in 30 *ml* of acetic acid) makes the fuel cell performance very different from that of non-impregnated Nafion membrane, as can be seen from Fig. 1-14 [93]. We can see that the current density obtained with PTA solution doped Nafion membrane at 110°*C* is much higher than that obtained with non-impregnated Nafion. Even though the Nafion membrane may loss its conductivity due to drying at high temperature, the PTA can provide a high concentration of protons in membrane pores, which makes the

impregnated Nafion membrane to maintain a high conductivity. Therefore, the high current density can still be obtained under high temperature operation of PEM fuel cell.

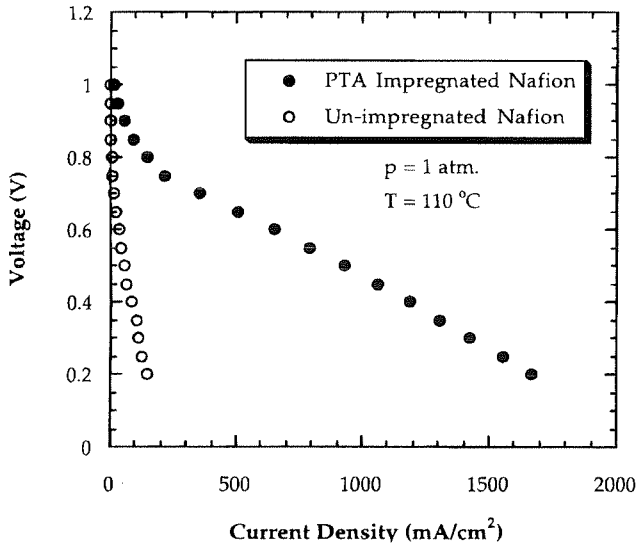

Figure 1- 14. Comparison of current-voltage curves at T=110°C and P=1 *atm,* for un-impregnated Nafion and Nafion impregnated with acetic acid solution of 12-phosphotungstic acid, along with 20% *Pt*-on-*C*, 0.35*mg Pt/cm*^{2}, gas-diffusion electrodes (E-TEK), $T_{\text{humidifiers}}$ =50°C for the impregnated Nafion case. [93]

The Inorganic Moisture Absorbing Reagents (Molecule Sieve, Silica gel, P_2O_5 etc.) as Additives to Modify Nafion Membrane Structure

In order to modify the structure of Nafion membrane, 10% Nafion solution was cast on a glass petri dish with a solvent dimethylformanide, together with some additives, which can be several kinds of inorganic moisture absorbing particles incorporated by 5 *wt%* relative to the polymer in the solution. The conductivity of the cast membrane was increased effectively compared with that of the blank membrane (Table 1-4).

P_2O_5 is a good water absorber, and shows twice as large conductivity as in comparison with the blank membrane. Molecular sieve shows also favourable effects, and this would be due to its rough surface structure. Porous silica gel, which has micropores of average size 21 *nm* and shows rough surface, has good accommodation of moisture and exhibits about 1.6 times increase of conductivity. However, non-porous type silica gel has few micropores and therefore gives almost no change in the conductivity performance in comparison with the blank membrane. This result verifies the correlation between membrane water content and ionic conductivity [46,95]. Increasing the amount of water by incorporating moisture absorbing particles would improve conductivity of the membrane [96], because these would expand the hydrophilic domains in the polymer structure.

Table 1- 4. The effect of the addition of moisture absorbents on the conductivity of Nafion cast membranes [94] (in dry state).

Additives	Content (*wt, %*)	Thickness (*mm*)	Conductivity ($10^{-2} S\ cm^{-1}$)
Blank	0	0.28	1.9
P_2O_5	0.5	0.29	2.3
	5.0	0.29	4.2
Molecular sieve	5.0	0.23	
Silica gel	5.0	0.27	3.1
Non-porous Silica gel	5.0[a]	0.32	2.0
	5.0[b]	0.36	1.8

[a]Treated to be hydrophilic. [b]Treated to be hydrophobic.

Calcium Phosphate/Nafion Composite Membrane

Calcium Phosphate was incorporated to form the composite membrane with Nafion [97]. The structure of calcium phosphate can be stable up to 1,000°C and has

high proton conductivity, which can be attributed to preventing methanol crossover. Solvent casting method was used to make membrane at 80°C onto the glass slides after sonicating and stirring of Nafion-calcium phosphate mixture. This has been confirmed by the following experimental trials.

Calcium Phosphate was incorporated to reduce methanol crossover in Nafion membrane. The characterization of composite membrane showed that there were channels along thickness direction similar to Nafion membrane, but the size of channel in composite membrane was smaller than that in Nafion. Saying, the smaller channel can reduce the flow of methanol through membrane. If it will be possible to control the size of channel, methanol crossover can be largely reduced. The decrease of crystallinity was confirmed in composite membrane using X-ray scattering. Nevertheless, the peak of hydronium ion was higher than Nafion, which leads to more water absorption capability and high proton conductivity. The proton conductivity of composite membrane was 5 x $10^{-2}/Scm^{-1}$ similar to that of Nafion, which gives the possibility for the composite membrane to be used in high temperature fuel cell.

Zirconium Phosphate/Nafion Composite Membranes

The physio-chemical properties of Nafion 115 and a composite Nafion 115/Zirconium Phosphate (25 *wt%*) membranes have been compared [98]. The composite membrane takes up more water than Nafion under the same water activity. However, the proton conductivity of the composite membrane is slightly less than that for Nafion 115. The result of Small angle X-ray scattering shows the hydrophilic phase domains in the composite membrane are spaced further apart than those in Nafion 115, and the composite membrane shows less restructuring with water uptake. Despite the lower proton conductivity of the composite membranes they display better fuel cell performance than Nafion 115 when the fuel cell is operated under-humidified. The data

suggest that the Zirconium Phosphate forms an internal rigid scaffold within the membrane that permits increased water uptake by the membrane in the confined environment of the fuel cell Membrane Electrode Assembly.

Composite membrane based on polyether ether ketone and heterpolyacids

In this study, a series of composite membranes have been prepared by the incorporation of tungstophosphoric acid, its disodium salt or molybdophosphoric acid into partially sulfonated PEEK polymer [99]. These membranes exhibited a rather high conductivity of 10^{-2} *S/cm* at ambient temperature and up to a maximum of about 10^{-1} *S/cm* above 100°C. The DSC studies of these membranes for the glass transition temperature showed an increase in the values due to the incorporation of both sulfuric acid groups and the solid HPA into the PEEK polymer. The increase in T_g of the composite membranes compared with that of pure SPEEK suggested an intermolecular interaction between SPEEK and HPAs. These membranes are thermally stable up to 250°C and above, as well as being mechanically strong and flexible. They maintain the high conductivity during storage in water for several months. These composite membranes are easy to be prepared and much less expensive than the commercial perfluorinated membranes. Their high proton conductivity combined with their long-term stability qualifies the HPA/SPEEK composite membrane which is considered for use in PEM fuel cells as alternatives to Nafion based membranes.

Perfluorosulfonic acid silicon oxide composite membrane

Silicon oxide/Nafion composite membranes were studied [100,101] for operation in hydrogen/oxygen proton-exchange membrane fuel cells (PEMFCs) from 80 to 140°C. The composite membranes were prepared either by an impregnation

of Nafion 115 via sol-gel processing of tetraethoxysilane or by preparing a cast film, using solubilized Nafion 115 and a silicon oxide polymer/gel. Tetraethoxysilane, when reacted with water in an acidic medium, undergoes polymerization to form a mixture of SiO_2 and siloxane polymer with product hydroxide and ethoxide groups. This material is referred to as *SiO_2/-OH/-OEt*. When Nafion is used as the acidic medium, the SiO_2/siloxane polymer will be found within the membrane. All composite membranes had a silicon oxide content of less than or equal to 10 *wt %*. The silicon oxide improved the water retention of the composite membranes, increasing proton conductivity at elevated temperatures. Attenuated total reflectance-Fourier transform infrared spectroscopy and scanning electron microscopy experiments indicated an evenly distributed siloxane polymer of *SiO_2/-OH/-OEt* in the composite membranes. At a potential of 0.4 *V*, silicon oxide/Nafion 115 composite membranes delivered four times the current density obtained with unmodified Nafion 115 in a H_2/O_2 PEMFC at 130 *°C* and a pressure of 3 *atm*. Furthermore, silicon oxide-modified membranes were more robust than the unmodified Nafion 115 and cast Nafion, which degrades after high operation temperature and thermal cycling.

Heteropolyacid ($H_3PW_{12}O_{40}$)/directly polymerized sulfonated poly(arylene ether sulfone) copolymer composite membrane

The feasibility of heteropolyacid (HPA)/sulfonated poly(arylene ether sulfone) composite membranes used in polymer electrolyte membrane (PEM) fuel cells was investigated [102]. Partially disulfonated poly(arylene-ether-sulfone)s (BPSH) copolymers were prepared by direct aromatic nucleophilic copolymerization and solution-blended with a commercial HPA, phosphotungstic acid. Fourier transform infrared (FTIR) spectroscopy band shifts showed that sulfuric acid groups on the polymer backbone interact with both bridging tungstic oxide and terminal tungstic oxide

in the phosphotungstic acid molecule, which indicated an intermolecular hydrogen bonding interaction between the copolymer and the HPA additive. The composite membranes generally exhibited a low HPA extraction after water vapor treatment, except for the 60 *mol%* disulfonated BPSH where significant HPA extraction from the composite membrane occurred because of excessive matrix swelling. The composite membrane not only had good thermal stability (decomposition temperature in nitrogen >300 *°C*), but also showed superior mechanical strength and lower water uptake than the unfilled membranes possibly due to the specific interaction. The composite membranes displayed good proton conductivity especially at elevated temperatures (e.g. 130 *°C*). For example, fully hydrated membranes consisting of 30 *wt.%* HPA and 70 *wt.%* BPSH with 40 *mol%* disulfonation had a conductivity of 0.08 S/cm at room temperature and it linearly increased up to 0.15 *S/cm* at 130 *°C*. In contrast, the pure copolymer had a proton conductivity of 0.07 *S/cm* at room temperature and only reached a maximum conductivity of 0.09 *S/cm*, most probably due to dehydration at elevated temperatures. The dehydration process was monitored by dynamic infrared spectra by observing the intensity reduction of the sulfonate group and distinctive changes of shape in the hydroxyl vibrations as the sample was heated. Combining infrared results with dynamic thermogravimetric data, it was shown that the composite membrane had much higher water retention from 100 to 280*°C* than the pure sulfonated copolymer. Those results suggested that the incorporation of HPA into these proton conducting copolymers should be good candidates for elevated temperature operation of polymer electrolyte membrane fuel cells.

New Cation Membranes Based on Nafion , Heteropolyacid and thiophene

Savadogo [103] and his coworkers studied Nafion membrane fabricated by blending Nafion solution with heteropolyacid and thiophene. It was shown that the synthesized membrane has higher conductivity.

Several new cation-exchange membranes of different thicknesses (15-500 μm) based on a Nafion® solution and silicotungstic acid with and without thiophene (named NASTATH and NASTA respectively) were synthesized by a simple chemical route for PEM fuel cell applications. The effect of membrane thickness, the concentrations of STA, and thiophene used during the preparation of NASTA and NASTATH on their water uptake and ionic conductivity were determined. Experimental results show that the water uptake of the NASTA membrane (60%) was significantly better than that of Nafion®117 (27%), while the water uptake of NASTATH (40%) was higher than that of Nafion®117 (27%). The ionic conductivities of both the NASTA (10.10 x 10^{-2} $\Omega^{-1}cm^{-1}$) and the NASTATH (9.5 x 10^{-2} $\Omega^{-1}cm^{-1}$) were found to be significantly higher than that of the Nafion®117 (1.23 x 10^{-2} $\Omega^{-1}cm^{-1}$). The membranes fabricated with Nafion® and silicotungstic acid with and without thiophene still exhibited good mechanical strength and stability after they had been dipped in an acid or a basic medium for at least 10 months. The voltage-current characteristics of PEMFCs were determined for Nafion®117, NASTA and NASTATH based membranes. The fuel cell parameters were correlated to the membrane water uptake and ionic conductivity. The current density at 0.600 V of the PEMFCs based on NASTATH (810 $mA\ cm^{-1}$) membranes was higher than that based on Nafion® 117 (640 $mA\ \ cm^{-1}$). It was shown that the better fuel cell parameters were obtained by the modified membranes with the higher water uptake.

This work was based on composite Nafion cast membrane from aqueous solution. However, they have not tried to cast membranes in high boiling point solvent like Dimethylformamide (DMF).

1.3.3. CONCLUSIONS

Inorganic materials as additives to modify the structure of polymer membranes become more and more active. Heteropolyacids (HPAs) are one of the most attractive

inorganic modifiers because these inorganic materials in crystalline form have been demonstrated to be highly conductive and thermally stable. Nowadays, the research concerning heteropolyacid and Nafion is of great interest. Heteropolyacids are the acid form of heteropolyanions, or metal oxide clusters with very good conductivity, which can be up to 0.2 $\Omega^{-1}cm^{-1}$ at $25°C$ [104]. In recent years, heteropolyacids based proton conducting electrolytes have aroused a considerable interest for their protonic activity. Among the various heteropolyacids, phosphotungstic (PTA), phosphomolibdic (PMoA) and silicotungstic (STA) acids, in their hydrate forms ($H_3PW_{12}O_{40} \cdot 29H_2O$, $H_3PMo_{12}O_{40} \cdot 29H_2O$ and $H_4SiW_{12}O_{40} \cdot 28H_2O$), are characterized by high protonic conductivity, which are 0.17, 0.18 and 0.027 $\Omega^{-1}cm^{-1}$, respectively [105,106]. Such high ionic conductivity together with the lower cost makes heteropolyacids very attractive for PEM fuel cell applications [116,117, 118]

1.4. THE FEASIBILITY OF THE PROJECT

This project is based on the modification of Nafion or Flemion membranes by using silicotungstic acids (STA) as additives. The new membrane is expected to be obtained by casting the polymer electrolyte solution containing STA and Nafion or Flemion. In order to improve the mechanical properties of new composite membrane, the high boiling point polar solvent DMF is used in the casting procedure.

1.4.1. THE PROPERTIES OF STA

The general formula of STA

Silicotungstic acid (STA) is a solid heterpolyacid. Usually, Heteropoly acid is highly hydrated [107], with up to 50 molecules of water per anion, and often forms

several solid hydrates. The formula of STA generally used is $H_4SiW_{12}O_{40} \cdot 26H_2O$ at room temperature.

Solubility and Molecular weight

STA is remarkably soluble in water (up to 85% by weight of solution), dilute acids, alcohols and ether. The density of a saturated aqueous solution at $18°C$ is $2.84\, g \cdot ml^{-1}$ [108]. X-Ray structural analysis of saturated aqueous solutions has shown that the structure of the 12-silicotungstic acid anion, $[SiW_{12}O_{40}]^{4-}$, is maintained when the lattice is dissolved in water [109]. This can be further confirmed by UV spectra of isostructural $H_4[SiW_{12}O_{40}]$ solutions [110]. Silicotungstic acids have high molecular weights. The anion $[SiW_{12}O_{40}]^{4-}$ has ionic weight of 2875.

The structure of STA

STA is known to have different hydrated structures depending on the environment [111,112]. In the dehydrated phase or in polar solvents the primary structure is called a Keggin unit (Fig.1-15a). The Keggin unit consists of a central atom in a tetrahedral arrangement of oxygen atoms surrounded by 12 oxygen octahedra connected with tungsten [113, 114]. There are four types of oxygen atoms found in the Keggin unit; the central oxygen atoms, two types of bridging oxygen atoms, and the terminal oxygen atoms. Each W is the center of an octahedron, and an oxygen atom is located at each vertex of the octahedron (Fig.1-15b). The ionic radius of W^{6+} (0.65 $\AA$) is smaller than that of O^{-2} (1.40 $\AA$) and an octahedron can share corners or edges or both with another WO_6 octahedron. The oxygen atoms may form part of each of the two octahedra sharing an edge. Silicon, which is the central atom, is similarly located in the center of a SiO_4 tetrahedron or SiO_6 octahedron. Each polyhedron is surrounded by WO_6 octahedron, which shares corners and/or edges with it

and with others. This makes that the total number of oxygen is utilized and each WO_6 is directly attached to a central atom through a shared oxygen atom. In the hydrated phase, STA has a secondary structure (Fig. 1-15c). The secondary structure takes the form of the Bravais lattices, with the Keggin units located at the lattice positions. STA possess waters of crystallization that bind the Keggin units together in the secondary structure by forming water bridges.

The diameter of the 12-silicotungstic acid anion ($[SiW_{12}O_{40}]^{4-}$) was found to be 11.2 $\AA$, and was of the same magnitude as that obtained from the sedimentation and diffusion studies (11 $\AA$) and from the X-Ray analysis of the solid (unit cell 12.1 $\AA$) [115].

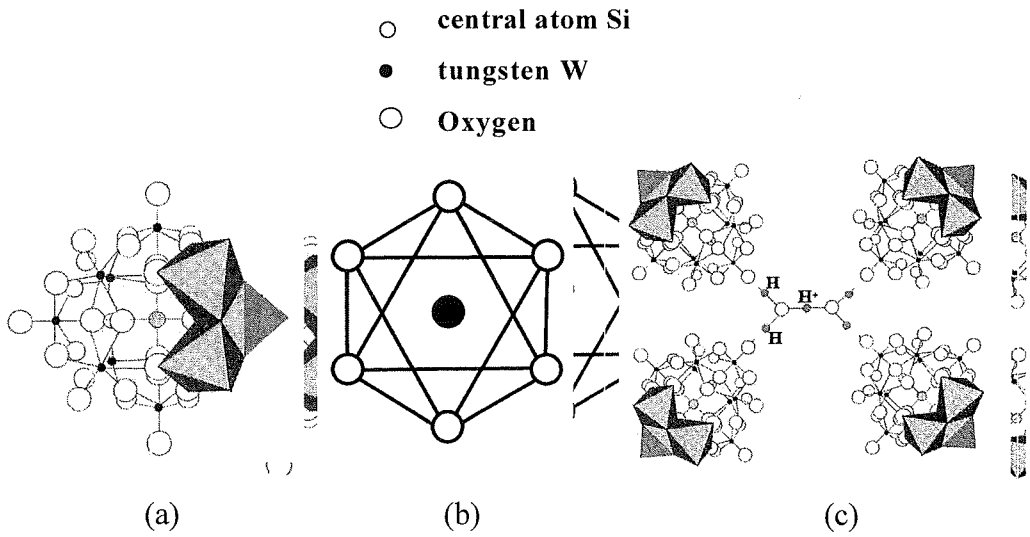

Figure 1- 15. The structure of STA. (a) Primary structure (Keggin); (b) Locations of W and O atoms in a WO_6 octahedron; (c) Secondary structure [111,112].

Ionic conductivity

Potentiometric titration of aqueous solutions shows the STA acid to be tetrabasic with all PK_A's (< 2) strong [108]. Silicotungstic acid (STA, $SiW_{12}O_{40}^{4-} \cdot 4H^+$) has good

conductivity and can provide high concentration of protons. Kreuer et al. [106] reported that the conductivity of a single crystal of STA ($28H_2O$) was $2.7\times10^{-2}\,S/cm$ at room temperature, which indicated that STA could be potentially used in solid electrolyte compositions with a sufficient conductivity to be used in a fuel cell at ambient temperature.

Thermal Stability

Thermoanalysis data, i.e. DTA, TG and DSC curves, of the pure STA sample in the temperature range of 20-1000°C are presented in Fig. 1-16 [118].

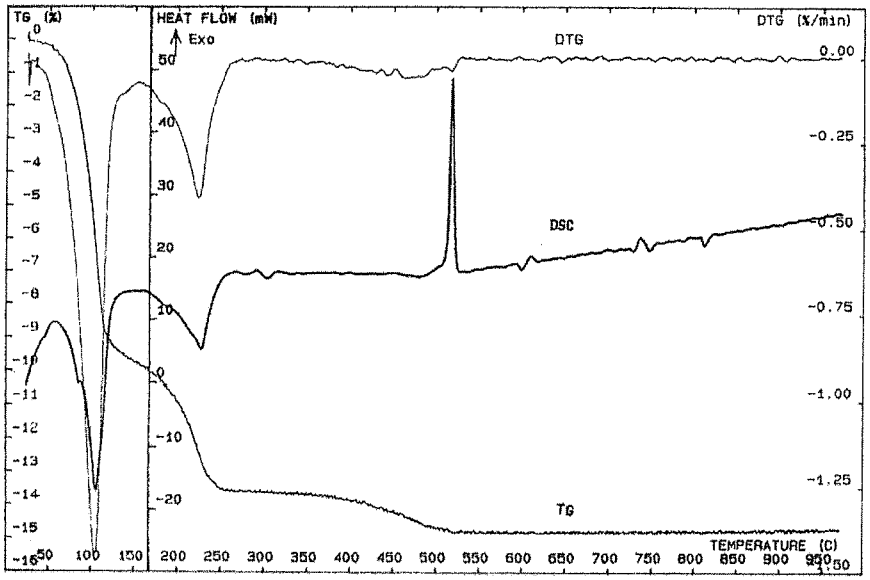

Figure 1- 16. Thermal curves of STA ($H_4SiW_{12}O_{40}\cdot 26H_2O$)(total weight loss: 15.05%).[118]

It can be calculated that the STA sample contains 26 water molecules for each silicotungstic acid unit, and the sample dehydrates 18 water molecules from 60 to

150°C, loses eight water molecules at around 240°C and removes a further two water molecules from $H_4SiW_{12}O_{40}$ at around 450°C. Therefore, it could be estimated that the dried STA used in this work (dried at 135°C in the oven overnight, will be discussed latter) would still contain at least eight crystal water molecules for each silicotungstic acid. Similar thermoanalysis results were reported in the literature for $H_4SiO_4 \cdot 12WO_3 \cdot 24.8H_2O$ [119] and $H_4SiO_4 \cdot 12WO_3 \cdot 29H_2O$ [120]. The exothermic peak at - 520°C in the DSC curve of Fig. 1-23 was previously assigned [119] to the spontaneous transformation of a highly disordered primary dehydroxylation product into a mixture of WO_3 and SiO_2.

1.4.2. MODIFICATION OF STA FOR NAFION STRUCTURE

The chemical structure of Nafion was discussed in section 1.2.1. Figure 1-17 is the cluster-network model for Nafion perfluorinated membranes [43].

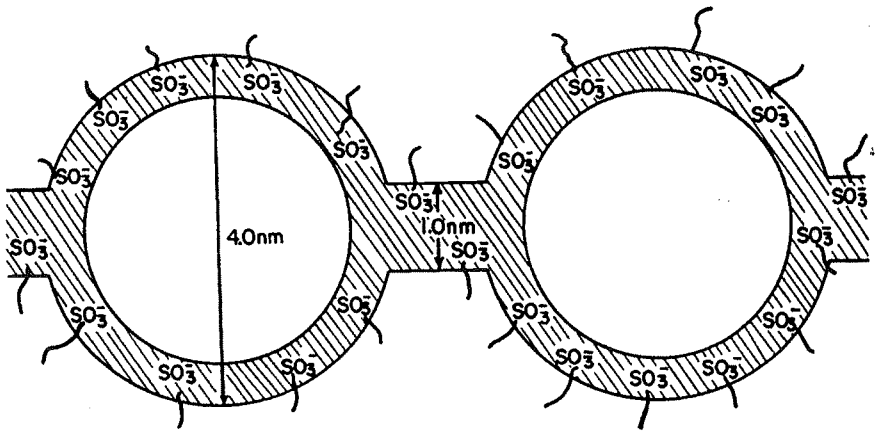

Figure 1- 17. Cluster-network model for Nafion perfluorinated membrane. [43]

The polymeric ions and absorbed electrolyte phase separate from the fluorocarbon backbone into approximately spherical clusters connected by short, narrow channels. The polymeric charges are most likely embedded in the solution near the

interface between the electrolyte and fluorocarbon backbone. This configuration minimizes both the hydrophobic interaction of water with the backbone and the electrostatic repulsion of proximate sulfonate groups. The dimensions shown were deduced from the experiments. The shaded areas around the interface and inside a channel are the double layer regions from which the hydroxyl ions are excluded electrostatically.

The diameter of these ion clusters is about 4 *nm* in fully hydrated Nafion. In the dry Nafion, the diameter of these ion clusters shrinks to 1.9 *nm* (Figure 1-18) [43]. So the STA (diameter is 11.2 *Å*) [115] can be embedded in the Nafion structure. Its high hydration and good conductivity can modify the properties of Nafion membrane. In this way, the electrochemical performance of Nafion membrane will be improved.

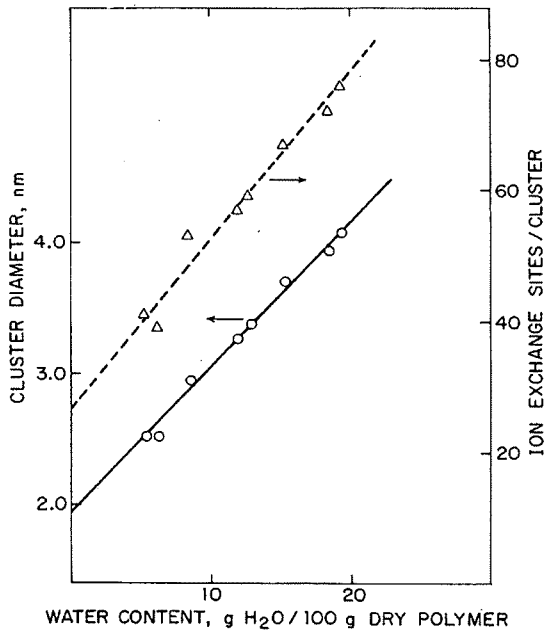

Figure 1- 18. The variation of cluster diameter (O) and ion exchange sites (Δ) per cluster with water content in 1200 *EW* polymer. [43]

Based on the above properties of STA and the polymer, it may be possible to cast Nafion or Flemion with and without STA from their solution. This project is the development of composite membrane based on Nafion or Flemion solution cast from Dimethylformamide (DMF) and Silicotungstic Acids (STA). The challenges of the work are to:

(i) determine the experimental conditions of the membrane casting;
(ii) evaluate the various properties of the composite membrane;
(iii) determine the performance of PEMFC single cell based on MEA using these composite membranes.

The electrochemical properties of the composite membrane are expected to be improved by using the Silicotungstic acid.

CHAPTER 2

EXPERIMENTAL PROCEDURE

In this chapter, the experimental techniques and methods involved in this project are described. Firstly, the synthesis procedure of the composite membrane based on the 5% Nafion solution (or 8.9 % Flemion solution) and heteropolyacid are introduced. And then, the measurement methods of composite membrane's properties (ionic conductivity, water uptake, performance of fuel cell etc.) are discussed. In addition, the analytical methods and experimental techniques (TG, AFM, SEM, FTIR, XRD and XPS) are also used for characterizing the composite membrane.

2.1. PREPARATION OF COMPOSITE MEMBRANE

The new composite membranes are based on the Nafion solution or Flemion solution and silicotungstic acid. In addition, *N, N'*-dimethylformamide (DMF) is also used in the preparing procedure.

2.1.1. NAFION SOLUTION AND FLEMION SOLUTION

NR - 005 Nafion® solution (Dupont) (*EW* = 1100):

Typical Analysis (*wt.%*):

50.0 % VOCs

45.0 % Water

5.0 % Perfluorosulfonic acid

Typical VOC Analysis (50 % Total):

1-propanol (15-30 %)

2-propanol (15-30 %)

1-butanol (<10 %)

Methanol (<5 %)

Mixed Ethers (<4 %)

Flemion Solution: 8.9 (*wt.%*) Flemion solution (*EW* = 910).

2.1.2. THE PROPERTIES OF DMF AND THE EFFECT OF DMF IN COMPOSITE MEMBRANE

N, N'-dimethylformamide (DMF) is a high-boiling polar solvent. Its general formula is $HCON(CH_3)_2$ and boiling point is 153°*C* [122]. The addition of the DMF during the preparation of composite membrane is only to improve the mechanical properties of the composite membrane. The improvement of mechanical properties can be attributed to the existence of crystallinity. If the polymer chains are immobile, crystallization cannot occur and low-quality cast membrane are obtained. In a high temperature procedure, the requisite mobility is provided by thermal excitation and by the plasticization effect of the high boiling point solvent. Therefore, the membrane has good mechanical properties.

The new composite membrane is fabricated by the evaporation of solvent (alcohol, water), where the solvent is evaporated from the mixed solution including the perfluorosulfonated polymer solution and STA. Usually, the temperature of solvent evaporation can affect the mechanical properties of the solution-cast membrane [121]. Low evaporation temperature (i.e. below ca. 70°*C*) leads to mud-cracked films that are very brittle. These films crumbled easily and could not be removed intact from the evaporation vial. However, very pliant and mechanically strong membranes can be obtained under high evaporation temperature (i.e. above ca. 125°*C*). In addition, these membranes could be easily removed intact from the evaporation vial [122]. Therefore, in order to get membranes with good mechanical proprieties, high-boiling solvent such

as *N*, *N*'-dimethylformamide (DMF) is added into mixed solution (STA and perfluorosulfonated polymer solution). Water and alcohol are firstly removed by evaporation at about $70°C$ – $80°C$, and then the high-boiling solvent is removed by vacuum heating around $20°C$ below its boiling point. Finally, the composite membrane, which is flexible and has good mechanical properties, can be obtained.

2.1.3. THE COMPOSITE MEMBRANE BASED ON NAFION SOLUTION (OR FLEMION SOLUTION) WITH STA

The new composite membrane is fabricated by a simple procedure of solvent evaporation. STA was firstly mixed with 5 *wt%* Nafion® solution (or 8.9 *wt%* Flemion solution), then *N, N*'-dimethylformamide (DMF) was added into the above solution, where the volume ratio of perfluorosulfonated polymer solution over DMF is 10:3 [122]. The mixed solution was cast on a petri dish, dried preliminarily at $70°C$ for 2 hours, then dried at $135°C$ in a vacuum till there is no more weight change (normally for 15 *h*). Finally, the composite Nafion/STA (or Flemion/STA) membranes were obtained, and the films were peeled off from the evaporation vial. By using the high temperature evaporation method, the composite Nafion/STA (Flemion/STA) membrane is flexible and has good mechanical properties.

Different composite membranes can be obtained by adding different amounts of STA and different volumes of Nafion solution (or Flemion solution). During the membrane preparation, the concentrations of STA used are ranged from 10^{-4} *M* to 10^{-3}*M* and the volumes of perfluorosulfonated polymer solution used are from 10 *ml* to 25 *ml*.

2.2. MEASUREMENT OF WATER UPTAKE

The water uptake and loss of STA of composite Nafion/STA (or Flemion/STA) membranes were measured by immersing a piece of composite membrane in boiling

deionized water for 4 hours. The procedure of measurement can be divided into 3 steps: firstly, the membrane was dried in vacuum oven at $70^{o}C$ overnight and the weight of the dried membrane is $W_1(g)$; secondly, the membrane was immersed in boiling deionized water for 4 hours and the wet weight is $W_2(g)$; thirdly, the membrane was dried in an oven vacuum at $70^{o}C$ overnight again and the final dry weight is $W_3(g)$. The water uptake and the loss of STA can be expressed as follows:

$$\text{Water uptake } \% = \frac{W_2(g) - W_3(g)}{W_3(g)} \times 100\%$$

$$\text{Loss of STA } \% = \left(\frac{W_1(g) - W_3(g)}{W_1(g)} / [STA]_0\right) \times 100\%$$

where $[STA]_0$ is the initial weight percentage of STA in dry membrane.

2.3. MEASUREMENT OF IONIC CONDUCTIVITY

The ionic conductivity of composite Nafion/STA (or Flemion/STA) membrane was measured by using a home made conductivity measurement cell, which is schematically illustrated in Figure 2-1. Membrane was inserted between a pair of Teflon blocks with openings (diameter is 1 *cm*), where 1 $M\ H_2SO_4$ solution was filled in order to avoid drying of the membrane during the measurements. Platinum foils were used as electrodes and connected to a power supply with an amperemeter. To measure the conductivity of the composite membrane, the potential drop between the two half cells was taken at different currents. Then a straight line of potential vs. current was plotted. The total resistance was determined from the slops. The potential drop across the composite membrane was obtained by taking off the solution's potential drop from total potential drop. The potential drop in the solution was measured after resetting the measurement cell without the composite membrane. The resistance of the composite

membrane was obtained by subtracting that of the solution from the total resistance. The ionic conductivity of the membrane can be calculated as follows:

$$\kappa = \frac{L}{S \cdot R}$$

where: L (cm): the thickness of the membrane,

S (cm^2): the measured surface of the membrane, which is 0.785cm^2 in our experiments,

R (ohm): the resistance of the membrane,

κ ($ohm^{-1} \cdot cm^{-1}$) : the ionic conductivity of the membrane.

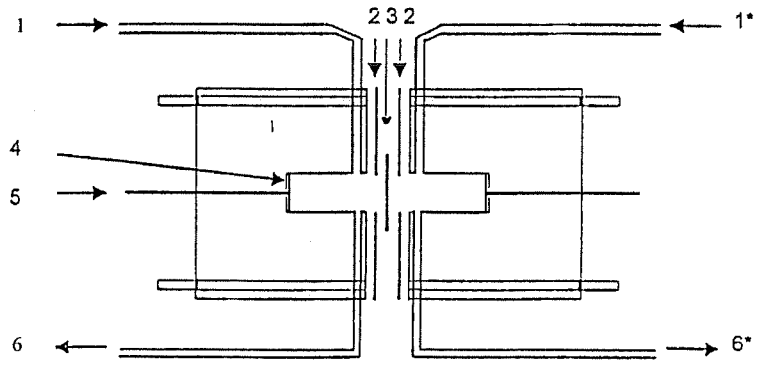

1,1*: capillaries
2: teflon supports
3: membrane
4: platinum electrodes
5: platinum wires
6,6*:solution coming from pumping system

Figure 2- 1. Cell diagram for ionic conductivity measurements.

The ionic conductivities of composite membranes are measured while the membranes are treated in the following pretreatment conditions respectively:

a) no immersion;

b) immersed in deionized water for 48 hours;

c) immersed in $1M\ H_2SO_4$ solution for 48 hours;

d) immersed in boiling deionized water for 4 hours;

e) immersed in boiling $1M\ H_2SO_4$ solution for 4 hours.

The following standard pretreatment step is applied only to the commercial Nafion 117 membrane [123]: the membrane was first immersed in boiling $3\%\ H_2O_2$ for 1 hour to remove any organic impurities and then it was cleaned in boiling deionized water for 1 hour. This was followed by treatment in boiling 1 $M\ H_2SO_4$ for 1 hour to remove any metallic impurities and then cleaning in boiling deionized water for 1 hour again. Finally, the membrane is kept in deionized water till it is used for experiments.

2.4. THERMAL AND MECHANICAL STABILITY OF THE MEMBRANE

The proton-exchange membrane fuel cell (PEMFC) is operated at lower temperatures than other fuel cells. The limitation on the operating temperature of the PEMFC is set by the thermal stability of the proton-exchange membrane that is used as electrolyte. For example, with Nafion, it is desirable not to exceed an operating temperature of $85°C$. Meanwhile, the PEMFC is generally operated under various pressures and thus the membranes should have good mechanical properties to make the system work properly. Therefore, it is of importance to study the thermal and mechanical stability of the membrane used in PEMFC system.

2.4.1. THERMAL ANALYSIS (TA)

Thermal analysis (TA) is an instrumental technique used to characterize thermal effects associated with either chemical or physical changes in a substance [124, 125]. These changes can be detected under different environments, either as a function of temperature from as low as $-120°C$ up to $1000°C$ or isothermally as a function of time. Complete TA results under usual operating conditions can be obtained from small-sized

samples in less than one hour depending on the heating/cooling rates and frequency used. These two factors make TA useful as both a research tool and a quality control technique.

The thermal stability of the composite membranes was investigated by thermogravimetric analysis (TGA). TGA can measure the weight loss or gain associated with sample oxidation, decomposition or volatilization as a function of time or temperature. TGA can be used to rank polymer systems in the order of their thermal stability. Kinetic data for decomposition processes are obtainable. The loss rate of moisture, diluent or unreacted monomer can be detected by TGA. TGA is also used to determine the weight percent of processing oils, carbon blacks, fillers and residual inorganic materials in a rubber compound analysis.

Dynamic TGA of composite membranes was performed on a **SETARAM Thermal Analyser** to assess the basic features of thermal stability and the dehydration processes for the HPA, polymer and the composite membranes. For the characterization of thermal stability, the samples were placed in the sample container and heated from $25°C$ to $800°C$ at $10°C/min$ while measuring the weight loss as a function of temperature in a nitrogen atmosphere.

2.4.2. TENSILE PROPERTIES OF THE MEMBRANES

Due to the following two reasons, the strain-stress behavior is normally used to characterize the mechanical property of the polymer membrane. Firstly, commercial users must know how the material will respond to the loads so that the component can be designed for satisfactory performance. Secondly, stress-strain measurements are useful to further understand the relationships between molecular structure and mechanical properties. The mechanical properties of polymers are dependent on temperature, humidity, strain rate, and specimen dimensions. For this reason, standard

test methods have been devised in which these parameters are kept constant and the values obtained are quoted as standard tensile, flexural, and compressive strengths or moduli. The American society for Testing and Materials (ASTM) has developed and approved many standard test methods for evaluating the mechanical properties of polymers.

Tensile properties of the composite membranes were measured on an **Instron (model 4400R)** using a grip separation rate of 10 mm/min. The films having a thickness of 180 um were prepared according to ASTM D882-02.

2.5. WIDE-ANGLE X-RAY DIFFRACTION

X-Ray diffraction is a versatile, non-destructive analytical technique for identification and quantitative determination of the various crystalline forms, known as 'phase', of compounds present in powdered and solid samples. Identification is achieved by comparing the X-ray diffraction pattern – or 'diffractogram' – obtained from an unknown sample with an internationally recognized database containing reference patterns for more than 70,000 phases. Modern computer-controlled diffractometer systems use automatic routines to measure, record and interpret the unique diffractograms produced by individual constituent even in highly complex mixtures.

2.5.1. THE PRINCIPLE OF WIDE-ANGLE X-RAY DIFFRACTION (WAXD)

X-ray diffraction can provide information about polymer morphology. Wide-angle X-ray diffraction (WAXD) is a very useful device for obtaining information about the size and shape of crystallites, as well as the degree of crystallinity in solid polymers. A schematic diagram of the working principle is given in Fig. 2-2, while Fig. 2-3 gives a plot of the scattering intensity as a function of the diffraction angle.

As shown in Fig. 2-2, an X-ray beam is allowed to impinge on the polymer sample and the intensity of the scattered X-rays is determined as a function of the diffraction angle (2θ) [126]. A crystal lattice is a regular three-dimensional distribution (cubic, rhombic, etc.) of atoms in space. These are arranged so that they form a series of parallel planes separated from one another by a distance *d*, which varies according to the nature of the material. For any crystal, planes exist in a number of different orientations – each with its own specific d-spacing. The *d*-spacing between two adjacent planes may be obtained from the Bragg relationship: $n\lambda = 2dsin\theta$. When a monochromatic X-ray beam with wavelength λ is incident on lattice planes in a crystal at an angle θ, diffraction occurs only when the distance traveled by the rays reflected from successive planes differs by a complete number *n* of wavelengths. By varying the angle θ, the Bragg's law conditions are satisfied by different *d*-spacings in polycrystalline materials.

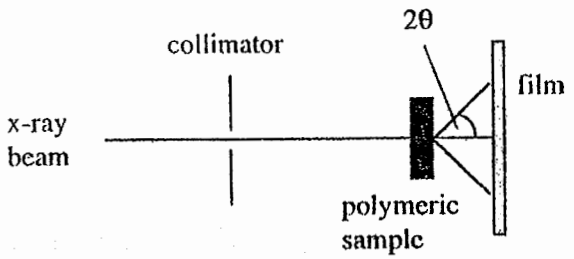

(a)

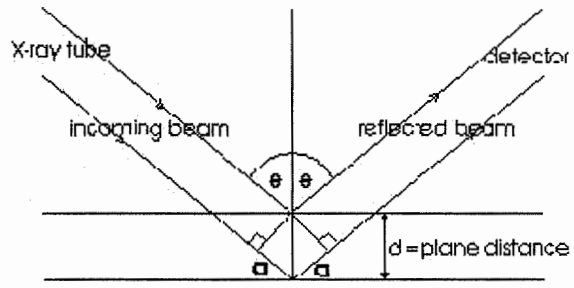

(b)

Figure 2- 2. Schematic diagram of the Wide-angle X-ray diffraction. (a) WAXD technique (b) the Bragg condition [126].

The diffractogram is multi-patterns, which are formed by addition of individual pattern. Each pattern, which is the result of plotting the angular positions and intensities of the resultant diffraction peaks, is the characteristic of each sample. A peak will only be detected when the Bragg condition $n\lambda = 2d\sin\theta$ is satisfied.

As seen in Fig. 2-3, crystalline regions show coherent scattering patterns and a sharp peak can be observed whereas an amorphous phase gives a broad peak. The degree of crystallinity can be obtained by measuring the area under each peak. However, it is normally difficult to differentiate crystalline and amorphous scattering. This indicates that the degree of crystallinity cannot be determined very accurately. Furthermore, the presence of small crystallites is difficult to characterize, because they exhibit similar scattering effects as the amorphous material. Nevertheless, small crystallites tend to broaden the peaks and sometimes information about crystal size can be obtained from such broadening. The result of an XRD measurement is a diffractogram, showing phase present (peak position), phase concentrations (peak height), amorphous content (background hump) and crystallite size/strain (peak widths).

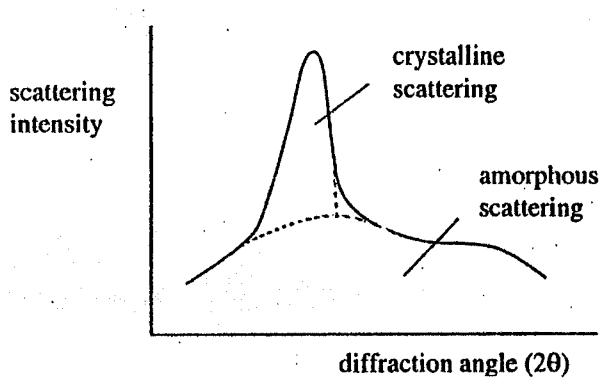

Figure 2- 3. A typical plot of scattering intensity versus diffraction angle obtained from wide-angle X-ray diffraction [126].

2.5.2. WAXD MEASUREMENT OF COMPOSITE MEMBRANE

The morphology of the composite membrane based on Nafion (or Flemion) and STA is studied with wide-angle x-ray diffraction where the reflection will be observed in the wide-angle x-ray scan from the different composite membrane samples. The effects of STA and water content on this reflection are studied.

To obtain the x-ray diffraction results from the different samples by **Philips X-Pert Diffractometer**, the composite Nafion/STA (or Flemion/STA) membrane samples were dried in vacuum oven at $70°C$ overnight or immersed in deionized water for 24 hours before they were used for x-ray analysis.

2.6. SCANNING ELECTRON MICROSCOPE (SEM)

2.6.1. THE PRINCIPLE OF SCANNING ELECTRON MICROSCOPY (SEM)

Scanning electron microscopy (SEM) provides a very convenient and simple method for characterizing and investigating the porous structure of microfiltration polymer membranes. The resolution limit of a simple electron microscope lies in the 0.01 μm (10 nm) range, whereas the pore diameters of microfiltration polymer membranes are in the 0.1 to 10 μm range. Resolutions of about 5 nm (0.005 μm) can be reached with more sophisticated microscopes.

The principle of the scanning electron microscope is illustrated in Fig. 2-4 [127]. A narrow beam of electrons with kinetic energies in the order of 1-25 kV hits the membrane sample. The incident electrons are called primary (high-energy) electrons, and those reflected are called secondary electrons. Secondary electrons (low-energy) are not reflected but liberated from atoms in the surface. The signals of secondary electrons are collected by detectors to form images of the sample displayed on the screen or on

the micrograph. When a membrane (or polymer) is placed in the electron beam, the sample can be burned or damaged, depending on the type of polymer and accelerating voltage employed. This can be avoided by coating the sample with a conducting layer, often a thin gold layer, to prevent charging up of the surface. The preparation technique is very essential to good images (but often overlooked) since bad preparation techniques give rise to artifacts.

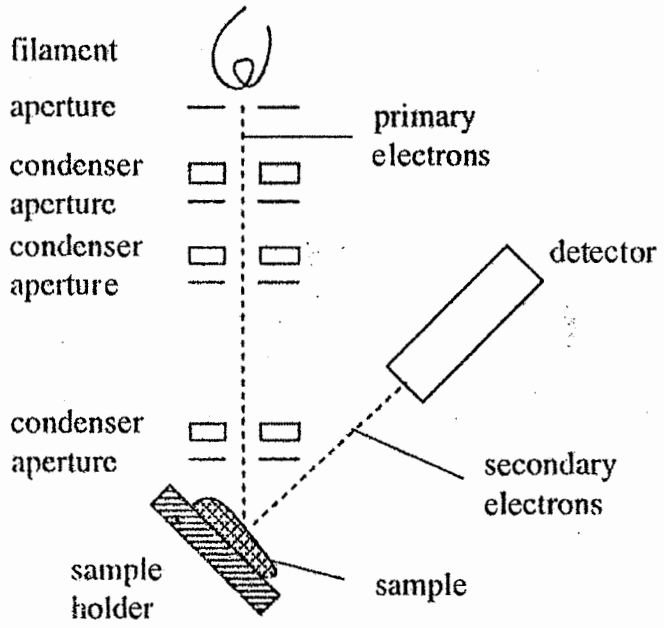

Figure 2- 4. The principle of scanning electron microscopy. [127]

Scanning electron microscopy allows a clear view of the overall structure of a microfiltration membrane; the top surface, the cross-section and the bottom surface can all be observed very nicely. In addition, the porosity and the pore size distribution can be estimated from the photographs. Care must be taken that the preparation technique does not influence the actual porous structure.

2.6.2. PREPARATION AND MEASUREMENT OF SAMPLES

Firstly, the composite Nafion/STA (or Flemion/STA) membranes are preteated in different condition: a) no immersion; b) immersed in deionized water or 1 M H_2SO_4 solution at different temperatures (25°C, 100°C) for 4 hours, and then, the samples are dried in vacuum oven at 70°C overnight. Secondly, the fresh cross-sectional cryogenic fractures of the membranes are vacuum sputtered with a thin layer of *Au/Pd* ready for SEM examination. Finally, the samples were measured in **JSM-840, JEOL SEM** equipment.

2.7. ATOMIC FORCE MICROSCOPY (AFM)

2.7.1. THE PRINCIPLE OF AFM

The Atomic Force Microcopy (AFM) uses a physical probe raster scanning across the sample using piezoelectric translator. The working principle of an AFM is based on the deflection of a very sensitive cantilever due to repulsive force between atoms on the sample surface and atoms at the cantilever tip. This deflection is measured using a laser beam while the sample is scanned. A feedback loop is used to maintain a constant interaction between the probe and the sample. The scanning in X, Y and Z positions is performed by a piezoelectric translator (Fig. 2-5 [128]). The position of the probe and the feedback signal are electronically recorded to produce a three dimensional map of the surface or other information depending on the specific probe used. Data Output is either a three dimensional image of the surface or a line profile with height measurements. The use of a micro fabricated cantilever allows us to operate at very low forces, less than 1 nN ($=10^{-9}$ N). This makes it possible to apply this technique for soft surfaces as in polymeric membrane.

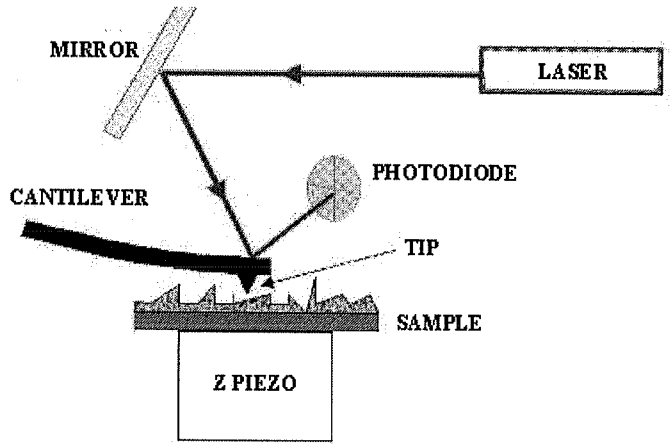

Figure 2- 5. Schematic the main components in an Atomic force Microscope. [128]

The surface of the membrane can be scanned in air without any pretreatment. The obtained line scans do not only reveal the possible position and size of a pore, but also give an indication of surface roughness or surface corrugations are obtained. Due to this surface roughness, it is often difficult to obtain a pore size distribution since the surface corrugations are in the same order or larger than the pore sizes. However, in combination with electron microscopy and other technique it might be a useful technique.

In summary, the atomic force microscopy (AFM) is a useful tool to determine surface structures [129]. The pore size and porosity can be obtained from the cross-sections of the AFM images. The advantage of this technique is that no pretreatment is required and the measurement can be carried out under atmospheric conditions. A disadvantage is that high surface roughness may result in images which are difficult to be interpreted. Moreover, high forces may damage the polymeric structure.

2.7.2. PREPARATION AND MEASUREMENT OF SAMPLES

The composite Nafion membrane with STA is preteated in different condition: a) no immersion; b) immersed in deionized water or 1 M H_2SO_4 solution at different temperatures (25°C and 100°C) for 4 hours, and then, the samples are dried in vacuum oven at 70°C overnight. And finally, the prepared samples were measured in **Digital Instruments NanoScope (R) III** AFM equipment.

2.8. FOURIER TRANSFORM INFRARED SPECTROSOPY (FTIR)

Fourier Transform Infrared Spectroscopy (FTIR) is a powerful tool for identifying types of chemical bonds in a molecule by producing an infrared absorption spectrum. FTIR spectroscopy is used primarily for qualitative and quantitative analysis of organic compounds, and also for the determination of the chemical structure of many inorganics.

2.8.1. THE PRINCIPLE OF FTIR

The diagrams of FTIR spectrophotometer system and optical system are shown in Figs. 2-6 and 2-7 [130]. Because chemical bonds can absorb infrared energy at specific frequencies (or wavelengths), the basic structures of compounds can be determined by the spectral locations of their IR absorption. The plot of a compound's IR transmission versus frequency is its "fingerprint", which identifies the material when compared to reference spectra.

When a molecule is irradiated with infrared radiation, it absorbs at frequencies that correspond to the vibrational/rotational energies of the molecule. Molecular motions that result in infrared absorption bands may be described in terms of bond stretches, bond angle deformations, torsions and rotations. The collection of absorption

bands over the IR frequency range (i.e., the infrared spectrum) is characteristic of the structure of the molecule. A typical IR spectrum will have absorbance bands which can be attributed to the presence of individual chemical group in the molecule under studying a "fingerprint" region distinctive of the individual compound. So the infrared spectrum can be used to identify the molecule.

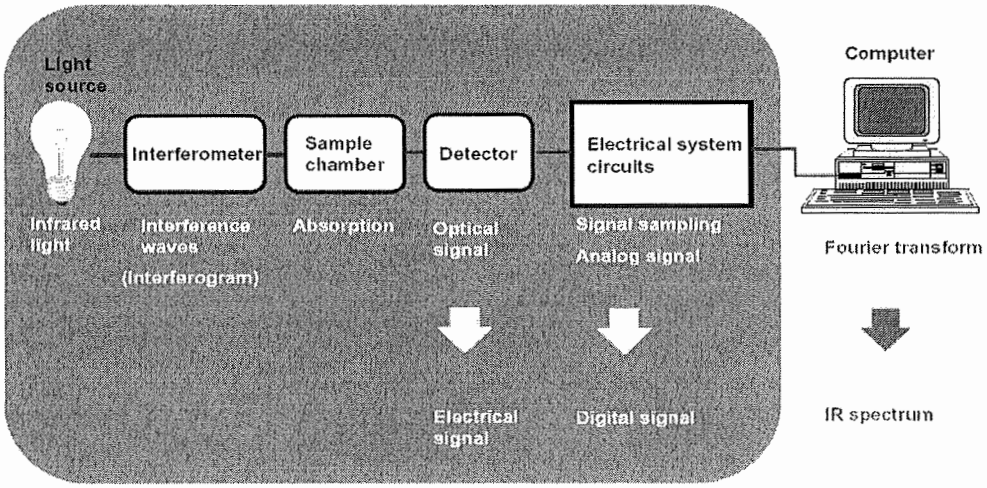

Figure 2- 6. The diagram of FTIR spectrophotometer system. [130]

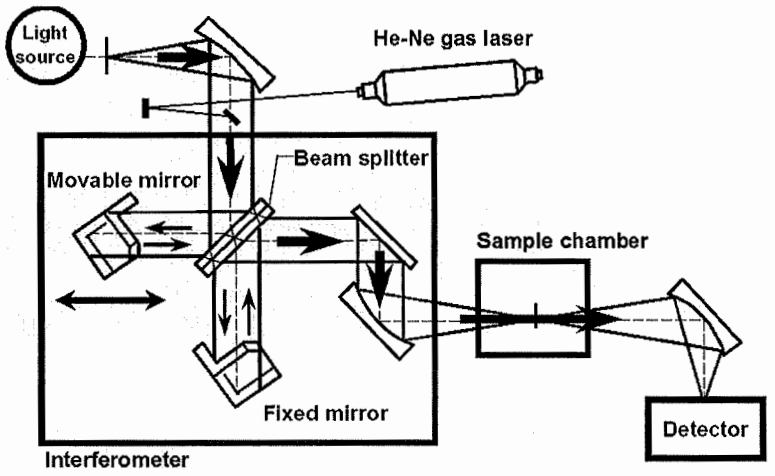

Figure 2- 7. FTIR optical system diagram. [130]

Fourier transform instruments offer many advantages over single scan instruments, including improved speeds of data collection and better signal-to-noise ratios. In an FTIR instrument, a specially "encoded" IR beam is passed through the sample and is automatically compared with a background spectrum. The resulting interferogram is Fourier transformed to produce the final FTIR spectrum.

2.8.2. MEASUREMENT OF COMPOSITE MEMBRANE

In this study, FTIR spectroscopy was used to confirm the pendant functional groups on the composite membrane. Measurements were recorded by using a **Perkin Elmer 2000 FTIR** spectrometer with the thin films.

2.9. X-RAY PHOTOELECTRON SPECTROSCOPY (XPS)

X-ray photoelectron spectroscopy (XPS), also known as Electron Spectroscopy for Chemical Analysis (ESCA), is a widely used technique for investigating the chemical composition of various material surfaces. Core-level electrons are emitted from a surface after it has been irradiated with soft X-rays. The low kinetic energy (0 – 1500 *eV*) of emitted photoelectrons limits the depth from which it can be emerged so that XPS is a very surface-sensitive technique and the sample depth is in the range of few nanometers. Photoelectrons are collected and analyzed by the instrument to produce a spectrum of emission intensity versus electron binding energy. In general, the binding energies of the photoelectrons are characteristic of the element from which they are emanated so that the spectra can be used for surface elemental analysis. Small shifts in the elemental binding energies provide information about the chemical state of the elements on the surface. Therefore, the high resolution XPS studies can provide the chemical state information of the surface.

2.9.1. THE PRINCIPLE OF XPS TECHNIQUE

Surface analysis by XPS is accomplished by irradiating a sample with monoenergetic soft x-rays and analyzing the energy of the detected electrons. Mg Kα (1253.6 *eV*) or Al Kα (1486,6 *eV*) x-rays are usually used. These photons have limited penetrating power in a solid on the order of 1-10 micrometers. They interact with atoms in the surface region, causing electrons to be emitted by the photoelectric effect [131]. The emitted electrons have measured kinetic energies given by:

$$KE = h\nu - BE - \phi_s$$

where $h\nu$ is the energy of the photon, BE is the binding energy of the atomic orbit from which the electron originates, and ϕ_s is the sample work function. Fig. 2-8 shows the principle of photoemission.

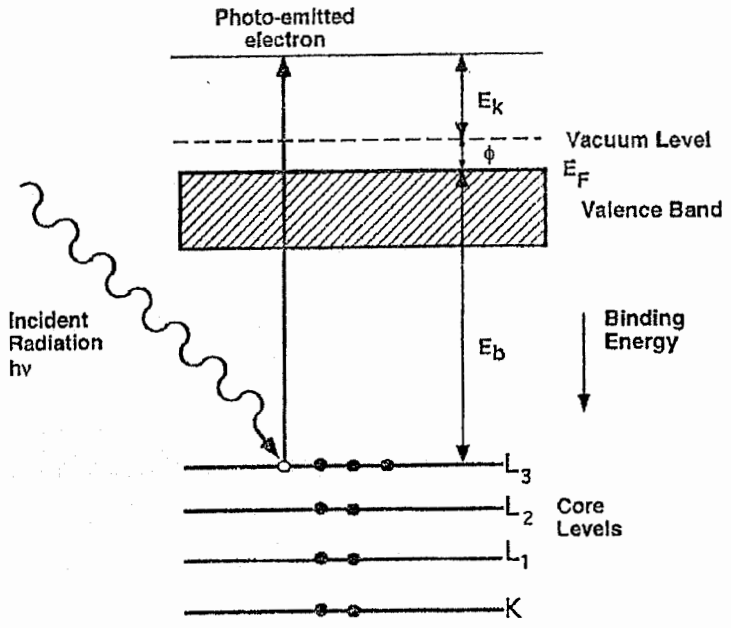

Figure 2- 8. Principle of photoemission. [131]

The binding energy may be regarded as the energy difference between the initial and final states after the photoelectron has left the atom. Because of a variety of possible final state of the ions from each type of atom, there is a corresponding variety of kinetic energies of the emitted electrons. Moreover, since each element has a unique set of binding energies, XPS can thus be used to identify and determine the concentration of the elements in the surface. Variations in the elemental binding energies (the chemical shifts) arise from differences in the chemical potential and polarizabilily of compounds. These chemical shifts can be used to identity the chemical state of the materials being analyzed.

In addition to photoelectrons emitted in the photoelectric process, Auger electrons may also be emitted because of relaxation of the excited ions remaining after photoemission. This Auger electron emission occurs roughly 10^{-14} seconds after the photoelectric event. The competing emission of a fluorescent x-ray photo is a minor process in this energy range. In the Auger process, an outer electron falls into the inner orbital vacancy, and a second electron is simultaneously emitted, carrying off the excess energy. The Auger electron possesses kinetic energy equal to the difference between the energy of the initial ion and the doubly charged final ion, and is independent of the mode of the initial ionization. Thus, photoionization normally leads to two emitted electrons: a photoelectron and an Auger electron. The sum of the kinetic energies of the electrons emitted cannot exceed the energy at the ionizing photons.

Probabilities of electron interaction with matter far exceed those of the photons, so while the path length of the photons is of the order of micrometers and that of the electrons is of the order of tens of angstroms. Thus, while ionization occurs to a depth of a few micrometers, only those electrons that originate within tens of angstroms below the solid surface can leave the surface without energy loss. These electrons which leave the surface without energy loss produce the peaks in the spectra and are the most useful.

The electrons that undergo inelastic loss processes before emerging form the background. The electrons leaving the sample are detected by an electron spectrometer according to their kinetic energy to produce the X-ray photoelectron spectroscopy (Fig.2-9).

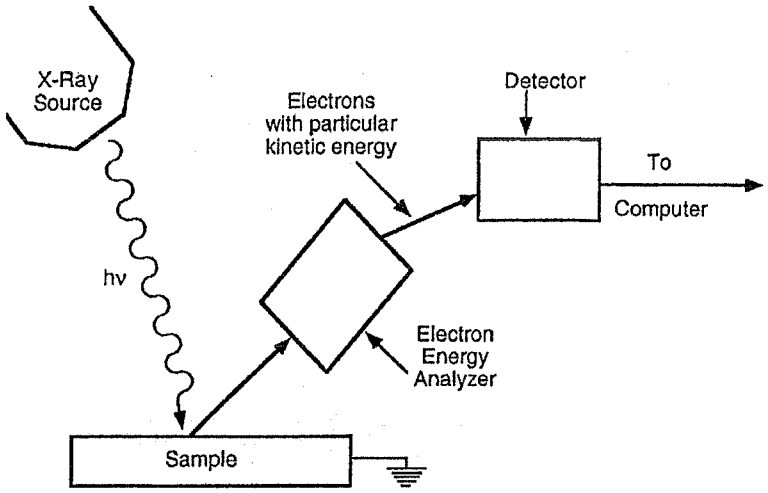

Figure 2- 9. Schematic arrangement of the basic elements of an X-ray photoelectron spectrometer. [131]

2.9.2. PREPARATION AND MEASUREMENT OF SAMPLES

The composite membranes based on Nafion (or Flemion) with or without STA are put in the high vacuum environment (10^{-8} *Torr*) for 24 hours and then are used to the measurement of XPS. The XPS spectra are recorded with an **ESCALAB MKII photoelectron spectrometer (VGScientific)** by using a *Mg* Kα Source and 240 *W* of power at 12 *KV*. The survey scan range is 1200 *eV* ~ 0 *eV* (*Mg* excitation) binding energy. The analytical surface of the sample is 2 *mm*×3 *mm* and the analytical depth of the sample is 50 *Å*. Detail scan of XPS spectrum of Carbon, Fluorine, Oxygen, Sulfur, Tungsten are used to analyze the element composition and chemical state of composite membranes.

2.10. APPLICATION IN THE H_2/O_2 FUEL CELL

2.10.1. PREPARATION OF MEMBRANE AND ELECTRODE ASSEMBLIES (MEA)

An MEA (Membrane and Electrode Assembly) is the heart of a polymer electrolyte membrane (PEM) fuel cell. It consists of a sheet of proton conducting polymer (the membrane) with two electrodes (an anode and a cathode) bonded to the opposite sides of the sheet. In the present experiments, MEA were prepared using the following steps:

a) brushing a 5% Nafion solution (Dupont) on to the commercial gas diffusion electrodes (E-TEK,1 *mg* Pt/cm^2, 20 % *Pt/C*);
b) evaporating solvent from the Nafion solution in the electrode under ambient conditions for 1 hour, followed by vacuum drying at 70°*C* for 30 *min*;
c) hot-pressing a pair of these electrodes on both sides of the membrane.

The optimized procedure for hot-pressing the MEA can be described as follows: two Nafion-impregnated electrodes are placed on both sides of a wet membrane. The assembly is then inserted into the two platens of the Carver Hot-Press equipment at a temperature of 110°*C*, and a pressure of 2 kg/cm^2 is applied for 4 minutes in order to obtain a good contact between the electrodes and the membrane.

During the hot-pressing procedure, the membrane dries out but is rehydrated adequately after insertion in the single cell test fixture and passage of the well-humidified gases through the anode and cathode gas chambers.

2.10.2. DESIGN AND ASSEMBLY OF SINGLE CELLS

The experiments were carried out in single cells made of carbon (Union Carbide nuclear grade graphite) and plates. The graphite and plates contain gas feed inlets and outlets, serpentine flow-field for gas flow behind the porous gas diffusion electrodes and holes for cartridge heaters and for a thermocouple (see Fig.2-10). After positioning the MEA between two gaskets and the graphite plates, the latter was tamped between stainless steel plates that were insulated from the cell body with PTFE sheets (see Fig.2-11). All cells were sealed using silicon rubber gaskets.

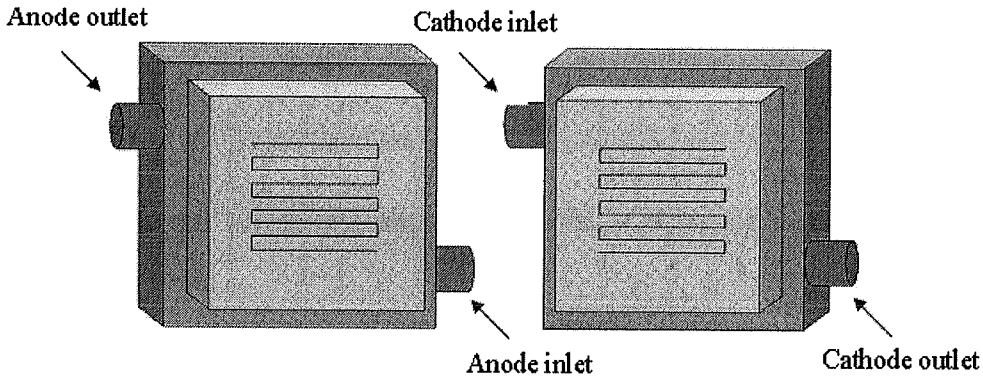

Figure 2- 10. Schematic diagram of graphite and plates.

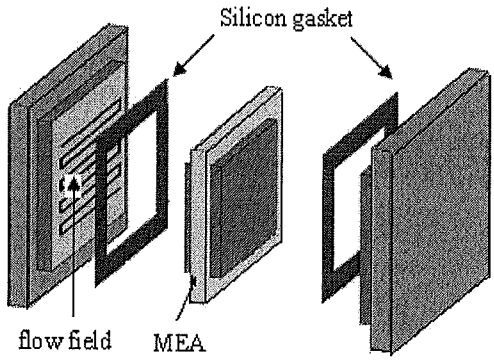

Figure 2- 11. Schematic of single cell.

2.10.3. MEASUREMENTS OF CELL POTENTIAL AS A FUNCTION OF CURRENT DENSITY

Fuel cells were tested by applying either a constant current or voltage from a potentiostat or power supply, voltage and current measurements were made using either a potentiostat or a digital multi-meter.

The fuel (H_2) and air stream (O_2, N_2) are heated and humidified before entering their respective channel where they are consumed in electrochemical reactions. Hydrogen gas diffuses through the porous electrode and is oxidized on platinum catalyst sites at the anode in a three-phase region containing polymer electrolyte, gaseous reactants, and carbon matrix. Oxygen passes through the gas-diffusion electrodes to the cathode. At the cathode, the hydrogen ions react with oxygen at similar catalyst sites to form water.

Humidification of reactant gases was carried out by passing the gases through stainless steel bottles containing water at about 5°-15°C above the cell temperature. The optimum condition for humidification was found to be a temperature of 5°C higher than that of the cell temperature for oxygen and a temperature of 10°-15°C higher than that of the cell temperature for hydrogen [132].

Measurements were made as a function of temperature and pressure. In present experiments, the temperature range is 50°C- 120°C and the pressure range is 1 – 4 atm. At the beginning, the single cell was fed with humidified H_2 and O_2 at atmospheric pressure (reactant gas and water vapor pressure equal to 1atm) and the temperatures of H_2 and O_2 humidifiers as well as the temperature of the single cell were slowly raised to 90, 85 and 80°C, respectively. During this period, the current of the single cell was maintained at a constant value of 200 mA, to reach an optimal hydration of the membrane using the water produced in the cell. After the single cell had reached steady-

state conditions (i.e. potential remained constant over time at a fixed current), cell potential versus current density measurements were then made under the desired conditions of temperature and pressure in the PEMFC.

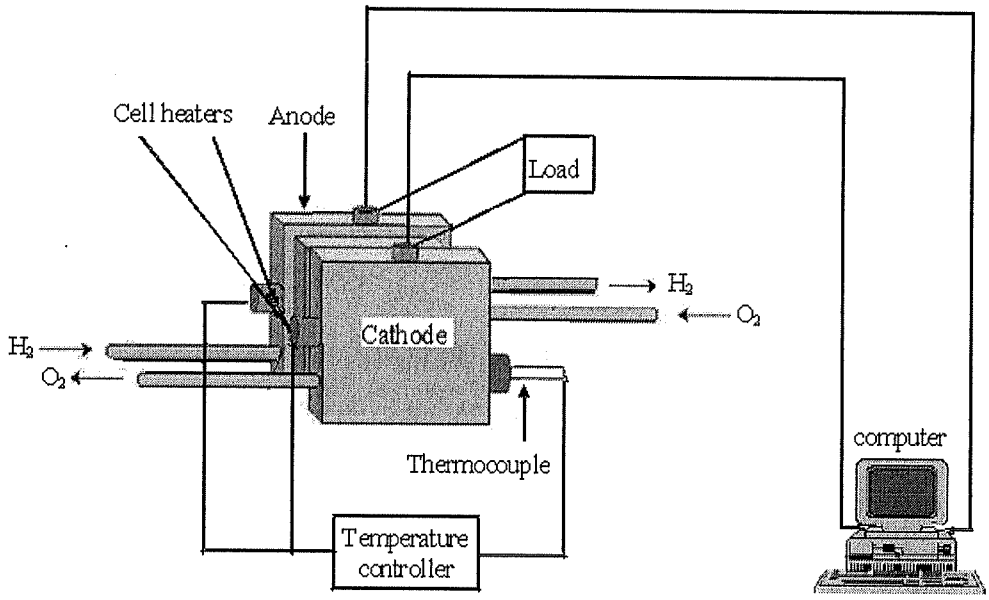

Figure 2- 12. Fuel cell system.

CHAPTER 3

RESULTS AND DISCUSSION

In this chapter, the experimental results will be presented and discussed. The experiments are classified as follows:

1. Preparation of the composite Nafion/STA or Flemion/STA membranes;
2. Study of the morphologies of the composite membranes using an atomic force microscopy (AFM) and scanning electron microscopy (SEM);
3. Investigation of the conductivities of the composite membranes under different immersion conditions;
4. Measurement of the water uptake of the composite membranes;
5. Study of the X-ray diffractions of the composite membranes;
6. Study of the thermal and mechanical stabilities of the composite membranes;
7. Study of the FTIR behaviors of the composite membranes;
8. Study of the XPS analysis of the composite membranes;
9. Study of the composite membrane in fuel cell appplication.

3.1. DESCRIPTION OF THE COMPOSITE MEMBRANES BASED ON CAST NAFION (OR FLEMION) WITH STA AND DMF

3.1.1. THE EFFECTS OF PREPARATION CONDITIONS ON THE PROPERTIES OF COMPOSITE MEMBRANE

Two different polymers, Nafion and Flemion, were used to prepare the composite membranes in this study. The membranes are elaborated according to the process described in chapter 2 (see section 2.1.3). Many membranes have been

fabricated with the presence of different amounts of polymer electrolyte solution, STA and DMF respectively. The effects of the evaporation temperature and the amount of STA on the membrane's mechanical behavior have also been studied. This part describes the visual observations based merely on the colors and the mechanical aspects. The other properties will be discussed in the later parts of this chapter.

During the preparation of the membranes, it can be observed that the mechanical properties of the solution-cast membranes are affected by the evaporation temperature. At the beginning of the experiments, the membranes were found to be easily cracked when they were cast at room temperature or 50°C. However, as the temperature reaches up to 70°*C*, the membranes obtained are clear and uncracked. Unfortunately, the membranes could not be removed intact from the evaporation beaker since they are brittle and could be gradually dissolved by water. Nevertheless, when the membranes are cast in the air at a temperature higher than 80°*C*, the solubility of membrane decreases with the increase of evaporation temperature but the color of the membrane becomes darker and darker due to the oxidation of membranes at high temperature. Furthermore, the obtained membrane is quite cirsp even though it could be completely peeled off from the evaporation beaker. It is well accepted that the mechanical properties of the membranes can be improved by the addition of polar solvent with high boiling point, as reported by other authors [122]. Therefore, DMF, which is high boiling point polar solvent, was added during the membrane preparation in this dissertation. The membranes had been cast at 70°*C* in the air and kept at this temperature for 2 hours firstly, and then they were placed in a vacuum oven at 135°*C* overnight. Finally, insoluble, flexible and clear light-brown membranes can be obtained.

The effects of the amount of STA on the mechanical properties of the membrane have been also investigated. When the concentration of STA in the casting electrolyte solution is between 10^{-2} *M* ~10^{-1} *M*, the membrane has poor flexibility and can be cracked easily. In addition, when the concentration of STA is more than 10^{-1}*M*, STA

powder is observed in the evaporation beaker after the solvent evaporation. This implies that the amount of STA exceeds the critical concentration value of its dispersion in Nafion. Our experimental results have shown that the optimum STA concentration range which can be used in the casting electrolyte solution is from $5\times10^{-4}\,M$ to $5\times10^{-3}\,M$ in this work. The membranes obtained within this STA concentration range exhibit good mechanical properties. Figure 3-1 gives some images of the composite membranes. From these images, we may see that the membranes are quite homogenous. This implies the STA is well dissolved in the polymer electrolyte solution, which will lead to a homogenous distribution of the STA in the composite membrane based on Nafion or Flemion solution with STA (see SEM micrograph Figs. 3-4 and 3-5).

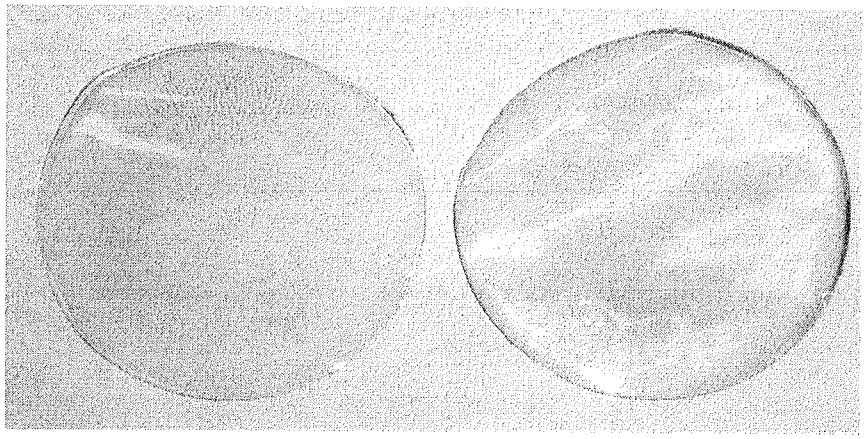

Figure 3- 1. The images of composite membranes cast from Nafion solution containing $5\times10^{-4}\,M$ STA (The diameter of the membrane is 6.5 *cm*).

Table 3-1 shows the different compositions of composite Nafion/STA membranes obtained from 5 *wt%* Nafion® solution, *N, N'*-dimethylformamide (DMF) and STA. The membranes with different thicknesses were respectively obtained using 10.00 *ml*, 15.00 *ml*, 20.00 *ml* and 25.00 *ml* Nafion solution. The corresponding volumes of DMF were 3.00*ml*, 4.50*ml*, 6.00*ml* and 7.50*ml*, respectively. During the membrane preparation, the concentrations of STA used in the casting electrolyte solution were respectively 0, $5\times10^{-4}M$, $1\times10^{-3}M$, $3\times10^{-3}M$, $5\times10^{-3}M$. The corresponding weight

percentages of STA in dry membrane were 0, 4.46%, 8.54%, 21.88%, 31.83%, respectively. The thicknesses of the obtained composite Nafion/STA membranes were varied from 50 to 320 μm.

Table 3- 1. Compositions of the casting electrolyte for the preparation of Nafion/STA composite membranes.

Number	Volume of Nafion Solution (mL)	Volume of DMF (mL)	[STA] (mol/L)
1	10.00	3.00	0
2	10.00	3.00	$5\times10^{-4}M$
3	10.00	3.00	$1\times10^{-3}M$
4	10.00	3.00	$3\times10^{-3}M$
5	10.00	3.00	$5\times10^{-3}M$
6	15.00	4.50	0
7	15.00	4.50	$5\times10^{-4}M$
8	15.00	4.50	$1\times10^{-3}M$
9	15.00	4.50	$3\times10^{-3}M$
10	15.00	4.50	$5\times10^{-3}M$
11	20.00	6.00	0
12	20.00	6.00	$5\times10^{-4}M$
13	20.00	6.00	$1\times10^{-3}M$
14	20.00	6.00	$3\times10^{-3}M$
15	20.00	6.00	$5\times10^{-3}M$
16	25.00	7.50	0
17	25.00	7.50	$5\times10^{-4}M$
18	25.00	7.50	$1\times10^{-3}M$
19	25.00	7.50	$3\times10^{-3}M$
20	25.00	7.50	$5\times10^{-3}M$

Table 3-2 shows the composite Flemion/STA membrane made from 8.9 *wt%* Flemion solution, *N, N'*-dimethylformamide (DMF) and STA. Five different concentrations of STA, 0, 5×10^{-4} *M*, 1×10^{-3} *M*, 3×10^{-3} *M* and 5×10^{-3} *M* were used in the casting electrolyte solution during the membrane casting process. The volumes of the Flemion solution and DMF were 10.00 *ml* and 3.00 *ml*. The thicknesses of the obtained composite Flemion/STA membranes were from 115 μ *m* to 240 μ *m*.

Table 3- 2. Compositions of the casting electrolyte for the preparation of Flemion/STA composite membranes.

Number	Volume of Flemion Solution (mL)	Volume of DMF (mL)	[STA] (mol/L)
1	10.00	3.00	0
2	10.00	3.00	$5\times10^{-4}M$
3	10.00	3.00	$1\times10^{-3}M$
4	10.00	3.00	$3\times10^{-3}M$
5	10.00	3.00	$5\times10^{-3}M$

3.1.2. SURFACE MORPHOLOGY AND THE CROSS SECTION VIEW OF THE COMPOSITE MEMBRANES

The surface morphologies of the Nafion/STA and Flemion/STA composite membrane ([STA]= $3\times10^{-3}M$) were investigated using an atomic force microscopy (AFM). The AFM images of the composite membranes are shown in Figs. 3-2 and 3-3. Figs. 3-2 (a, b) show the surface morphology of cast Nafion with and without STA whereas and Figs. 3-3 (a, b) show the surface morphology of cast Flemion with and without STA. From these figures, we may clearly see that the images exhibit a significant change of the surface morphology with the addition of STA. This may

indicate the relatively good retention of the STA particles in the composite membranes. Table 3-3 depicts the surface roughness analysis of the composite membrane. The surface roughness increases from 3.738 *nm* (Ra) for the cast Nafion without STA membrane to 21.663 *nm* (Ra) for the cast Nafion with STA membrane. The increase in the surface roughness of the cast Nafion with STA is due to the existence of the inorganic species, STA. The same trend was also found by comparing the roughness of cast Flemion with and without STA. The cast Flemion with STA exhibited the roughness of 23.674 *nm* (Ra) whereas that of the cast Flemion without STA was 2.084 *nm* (Ra).

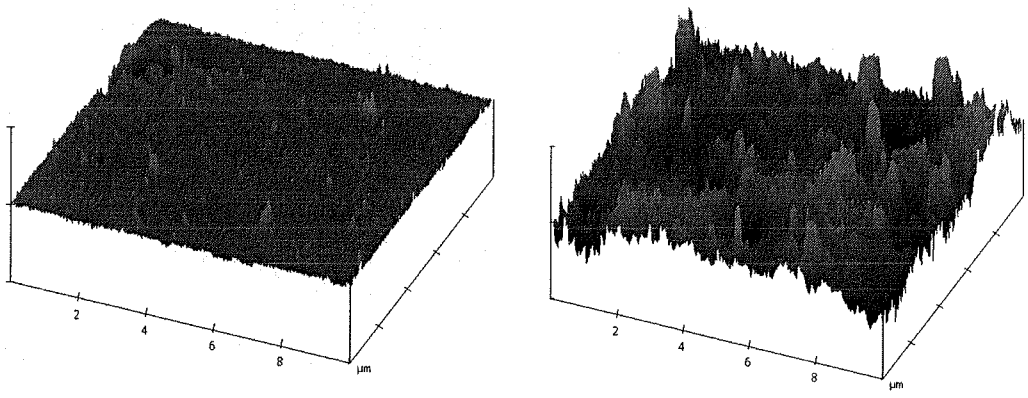

(a) (b)

Figure 3- 2. AFM surface images of the cast Nafion without (a) and with (b) STA.

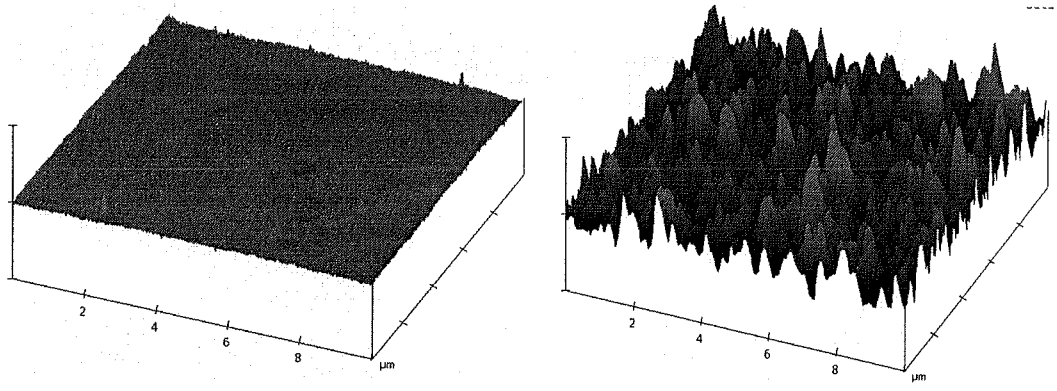

(a) (b)

Figure 3- 3. AFM surface images of the cast Flemion without (a) and with (b) STA.

Table 3- 3. The surface roughness analysis of composite membranes.

	Cast Nafion		*Cast Flemion*	
	Without STA	With STA ([STA]= $3\times10^{-3}M$)	Without STA	With STA ([STA]= $3\times10^{-3}M$)
Mean roughness (Ra)	3.738 *nm*	21.663 *nm*	2.084 *nm*	23.674 *nm*

The cross section views of the composite Nafion/STA and Flemion/STA membranes have been investigated using a scanning electron microscopy (SEM) respectively. The SEM micrographs of the composite membranes are shown in Fig. 3-4 and Fig. 3-5.

The SEM micrographs of cast Nafion without STA and with STA ([STA]= $3\times10^{-3}M$) membranes are presented in Fig. 3-4a and 3-4b, respectively. From Fig. 3-4a, it can be seen that the cast Nafion without STA has no agglomeration after membrane preparation. With the addition of STA, as can be seen in Fig. 3-4b, we may observe that STA particles, whose diameter is around 0.1-0.2 microns, are uniformly distributed within the cast Nafion with STA membrane. Figs. 3-5a and 3-5b show the influence of the STA as additives on the SEM micrographs of the cast Flemion without and with STA membranes. By comparing Fig. 3-5a and 3-5b, we can observe that the cast membrane containing the STA droplets shows nano-scale (0.05-0.1 μm in diameter) STA particle dispersed in the polymer matrix. We may also see a uniform distribution of STA across the cryogenic fracture of Flemion/STA composite membrane on a scale of 1 μm.

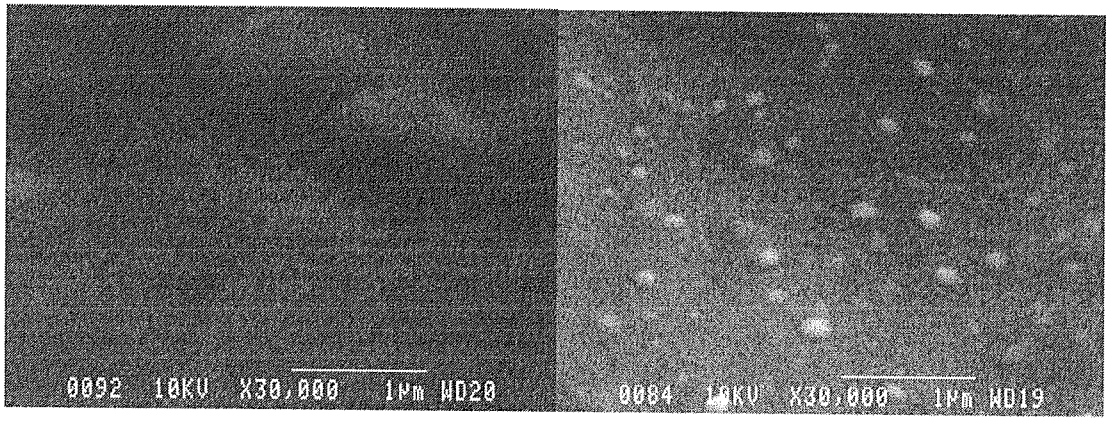

(a) (b)

Figure 3- 4. SEM micrograph (a cross section view) of the cryogenic fracture of the cast Nafion without (a) and with (b) STA.

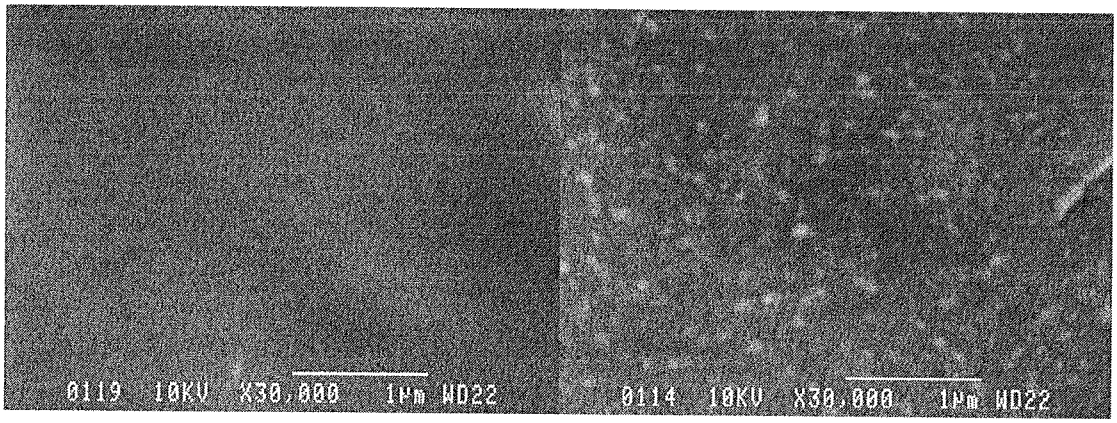

(a) (b)

Figure 3- 5. SEM micrograph (a cross section view) of the cryogenic fracture of the cast Flemion without (a) and with (b) STA.

3.1.3. THE EFFECTS OF THE TREATMENT CONDITIONS ON THE PROPERTIES OF COMPOSITE MEMBRANES

The morphologies of the composite membrane ([STA]= $3\times10^{-3}M$) immersed in deionized water or in 1 M H_2SO_4 were investigated using an atomic force microscopy (AFM) and a scanning electron microscope (SEM). Figs. 3-6, 3-7, 3-8 and 3-9 show the surface morphologies of the composite membranes under different immersion temperatures and different solutions. The analyses of the surface roughness of these membranes are summarized in Table 3-4.

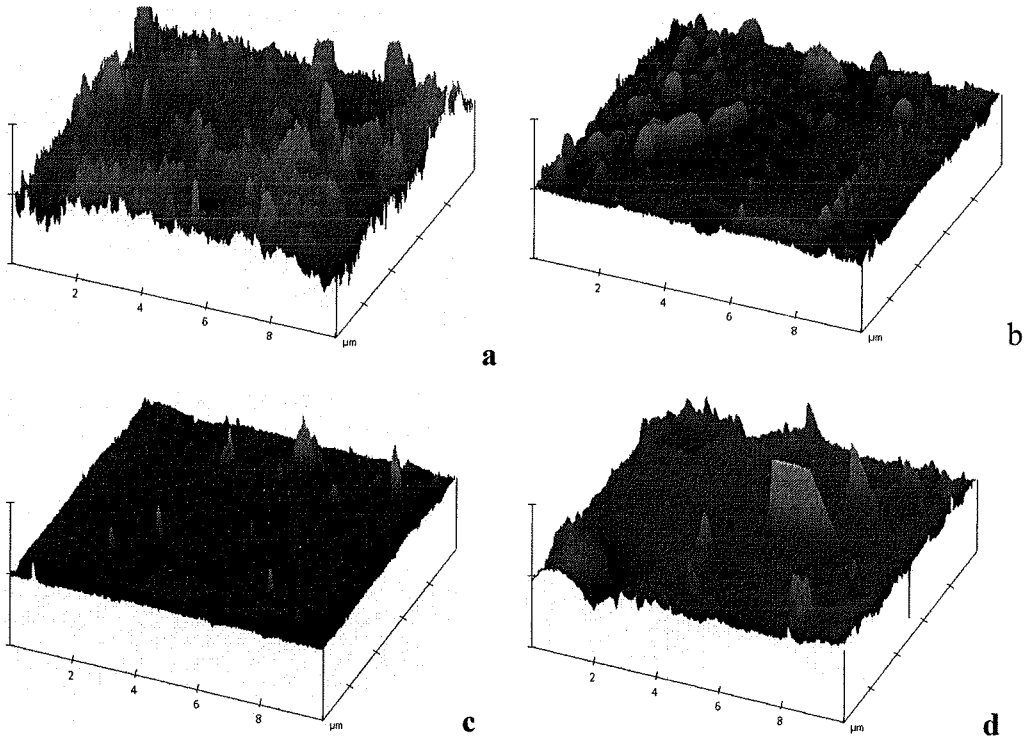

Figure 3- 6. AFM surface images of the Nafion/STA composite membranes under different immersion conditions. a) without any immersion; b) immersed in deionized water for 4 hours at room temperature; c) immersed in boiling deionized water for 4 hours; d) immersed in boiling 1 M H_2SO_4 for 4 hours.

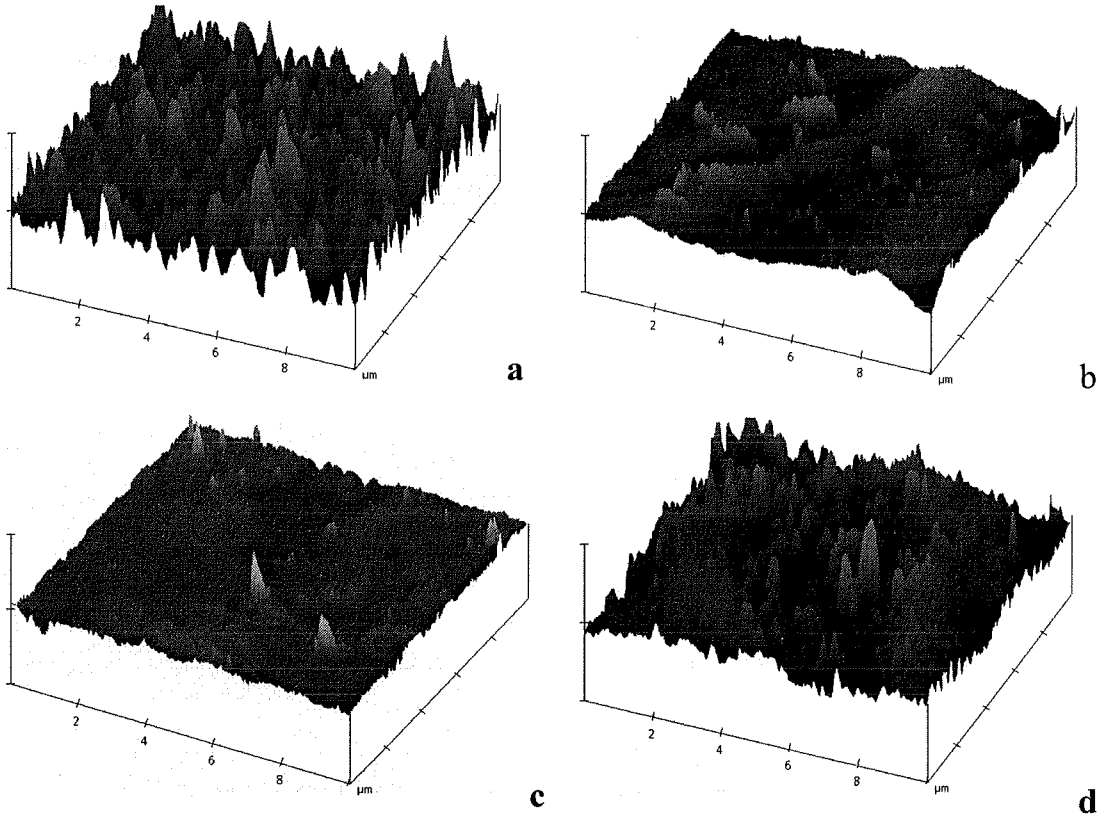

Figure 3- 7. AFM surface images of composite Flemion/STA membranes under different immersion conditions. a) without any immersion; b) immersed in deionized water for 4 hours at room temperature; c) immersed in boiling deionized water for 4 hours; d) immersed in boiling 1 *M* H_2SO_4 for 4 hours.

From these images, it can be seen that the immersion condition can affect the surface properties of composite membranes. Fig. 3-6c and 3-7c show the morphologies of composite Nafion/STA membrane and composite Flemion/STA membrane after immersion in boiling deionized water. Compared to the images in Fig. 3-6a and 3-7a which show the morphologies of composite Nafion/STA membrane and composite

Flemion/STA membrane without any immersion, Fig. 3-6c and 3-7c clearly indicate that there is significant change of the surfaces morphology of composite membrane after immersion in boiling deionized water. From the Table 3-4, it can be seen that the roughness of composite membrane decreases from 21.663 *nm* to 4.485 *nm* for Nafion/STA membrane and from 23.674 *nm* to 6.038 *nm* for Flemion/STA membrane after their immersion in boiling deionized water. These dramatic changes are suspected to be related to the loss of STA during the membranes immersed in deionized water. The STA loss increases with the increase of the immersion temperature. Fig. 3-6b and Fig. 3-7b show the morphologies of composite Nafion/STA and Flemion/STA membranes immersed in deionized water at room temperature. In this case, the surface roughness is 8.282 *nm* for Nafion/STA membrane and 9.577 *nm* for Flemion/STA membrane. Both values are larger than those in boiling deionized water.

Table 3- 4. The surface roughness analysis of composite membranes ([STA]= $3\times10^{-3}M$) in various treatment conditions.

	Nafion/STA composite membrane				*Flemion/STA composite membrane*			
	a	b	c	d	a	b	c	d
Mean roughness (Ra)	21.663 *nm*	8.282 *nm*	4.485 *nm*	10.169 *nm*	23.674 *nm*	9.577 *nm*	6.038 *nm*	22.110 *nm*

* a) without any immersion; b) immersed in deionized water for 4 hours at room temperature; c) immersed in boiling deionized water for 4 hours; d) immersed in boiling 1 $M\ H_2SO_4$ for 4 hours.

The losses of STA from the Nafion/STA and Flemion/STA composite membranes were also observed in SEM micrographes (Fig. 3-8 and 3-9). Fig. 3-8c and 3-9c show the SEM micrographs of the composite Nafion/STA and Flemion/STA

membranes after their immersion in boiling deionized water. In comparison with the Figure 3-8a and 3-9a which are the SEM micrographs of composite Nafion/STA and Flemion/STA membrane without any immersion, Fig. 3-8c and 3-9c show some holes on the SEM micrograph. These holes, which have similar size than the STA particles, are probably due to the loss of STA particles. However, the loss of STA is not clear when the composite membrane is immersed in deionized water at room temperature (no holes in Fig. 3-8b and 3-9b). Needless to say, the temperature has significant effect on the loss of STA in composite membrane. The agglomeration observed on the Fig. 3-8b may be caused by the secondary structure of STA in the presence of water (see section 1.5.1 and Fig. 1-22c). Nevertheless, by comparing Fig. 3-6b and 3-7b, we may find that the result obtained from SEM micrograph at room temperature is different from that obtained from the AFM images. This may be because the loss of STA in the surface of membrane is easier than that in the internal structure of the membrane, so the roughness of the composite membranes has significant changes whereas the SEM micrographs do not exhibit clear trace of STA loss at room temperature.

From the AFM surface images and SEM micrographs, it can be seen that the loss of STA in H_2SO_4 solution is less than that in deionized water. Fig. 3-6d and 3-7d show the surface morphologies of Nafion/STA and Flemion/STA membranes after immersion in boiling 1 M H_2SO_4. The roughnesses of composite membrane mentioned above are 10.169 nm for Nafion/STA membrane and 22.110 nm for Flemion/STA membrane. Needless to say, the roughnesses of both membranes after immersion in 1 M H_2SO_4 are larger than those in deionized water. Fig. 3-8d and 3-9d show the SEM micrographs of Nafion/STA and Flemion/STA membranes in boiling 1M H_2SO_4, respectively. It can be observed that there are many protuberances and a few holes on the SEM micrographs. The protuberance may be due to the interaction between the sulfuric acid and STA. The holes, which are obviously less than that in boiling deionized water, should be the place left by the STA loss from the membrane. We may conclude that the presence of sulfuric acid in the composite membrane can prevent the

dissolution of STA from the composite membrane. It is due to the synergetic effects, which can reduce the loss of STA in composite membrane, between the sulphonated group (-SO_3H) and the STA group. This synergetic effect will be discussed in the later part of this chapter.

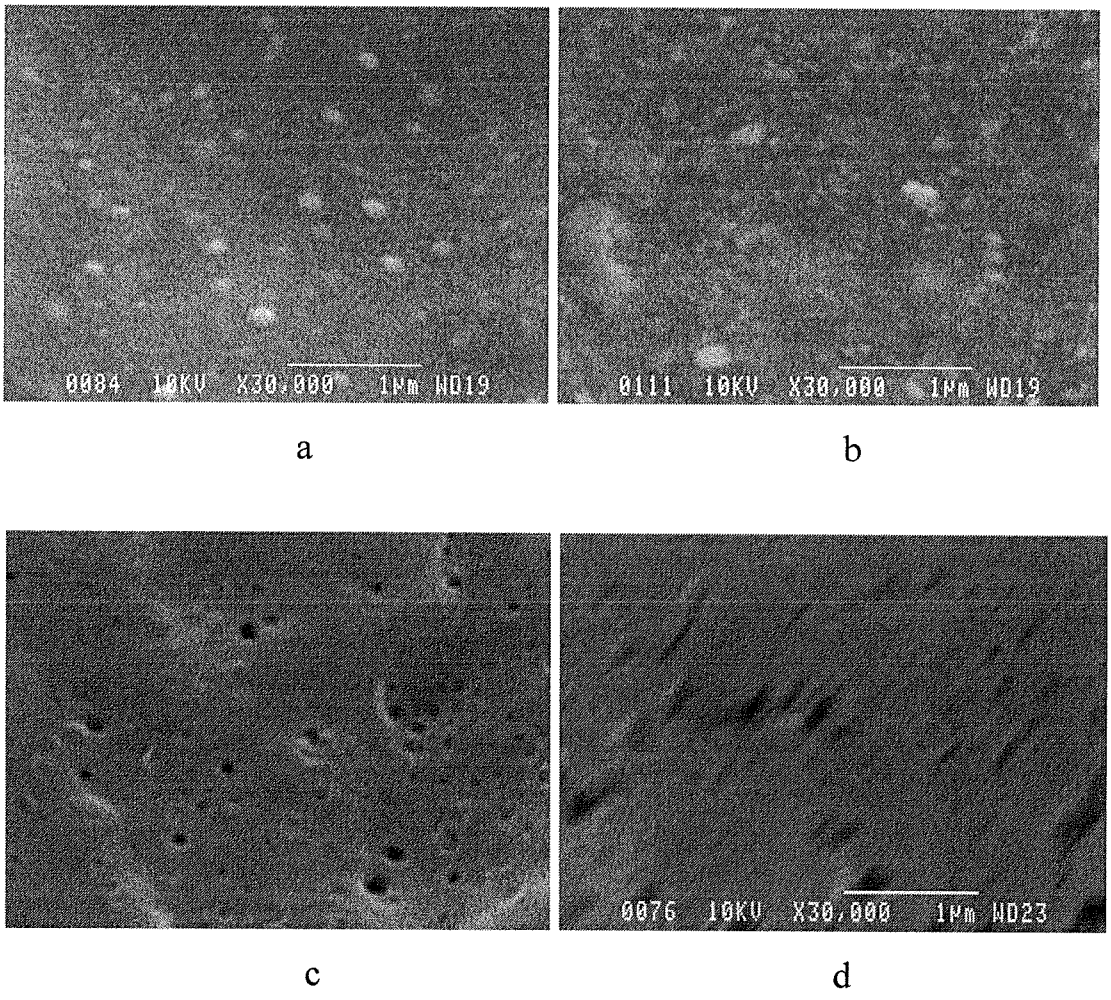

Figure 3- 8. SEM micrograph (a cross section view) of composite Nafion/STA membrane under different immersion conditions. a) without any immersion; b) immersed in deionized water for 4 hours at room temperature; c) immersed in boiling deionized water for 4 hours; d) immersed in boiling 1 M H_2SO_4 for 4 hours.

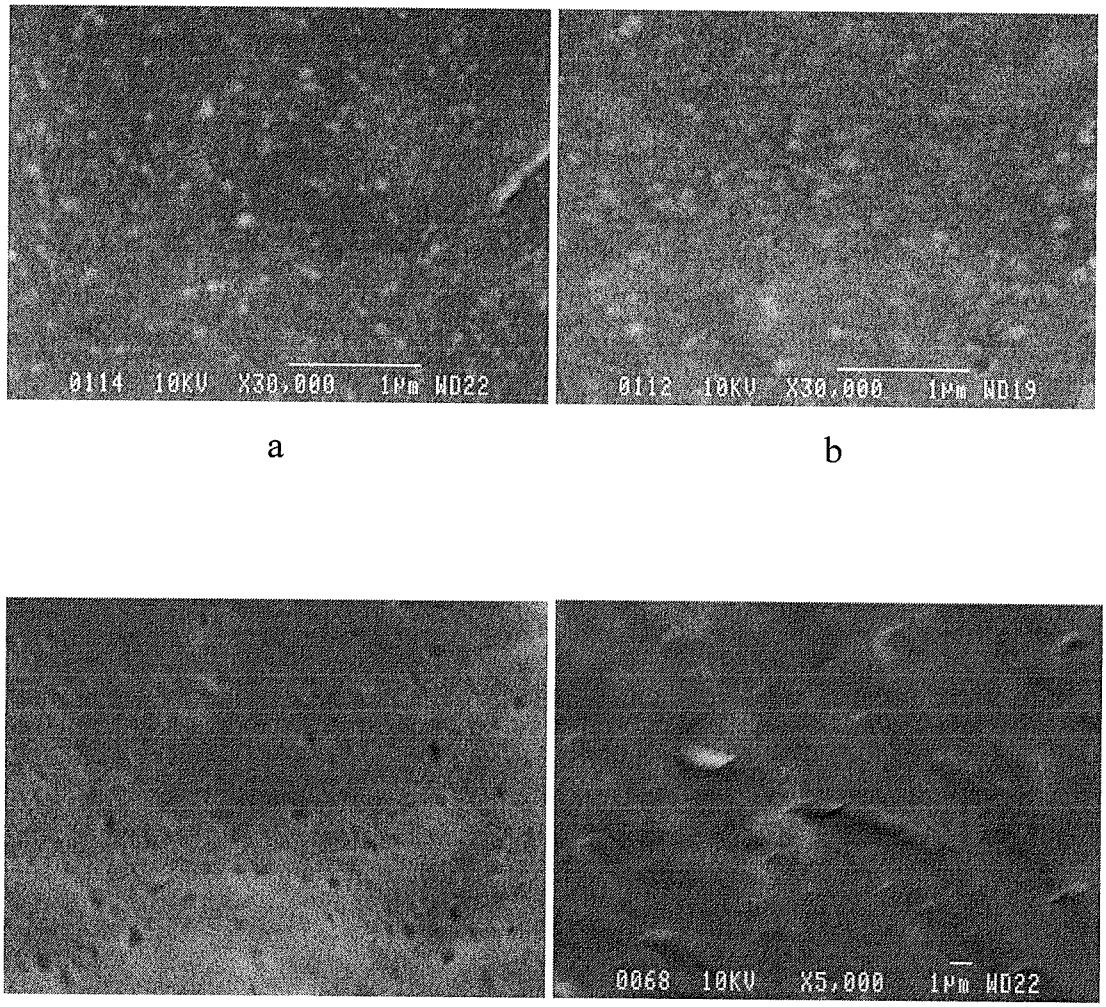

Figure 3- 9. SEM micrographs (a cross section view) of composite Flemion/STA membranes under different immersion conditions. a) without any immersion; b) immersed in deionized water for 4 hours at room temperature; c) immersed in boiling deionized water for 4 hours; d) immersed in boiling 1 M H_2SO_4 for 4 hours.

3.2. CONDUCTIVITIES OF COMPOSITE MEMBRANES

3.2.1. THE EFFECTS OF THE IMMERSION CONDITION (DEIONIZED WATER, SULPHURIC ACID ETC.) AND STA CONCENTRATIONS ON THE CONDUCTIVITY OF THE COMPOSITE MEMBRANES

3.2.1.1. Composite Nafion/STA membrane

The composite membranes based on Nafion were cast with 10 *ml* 5*wt%* Nafion solution, 3*ml* DMF and different amount of STA. The composite Nafion/STA membranes were respectively pretreated under the following different conditions before the conductivity measurements: a) no immersion; b) immersion in deionized water for 48 hours under room temperature; c) immersion in 1 *M* H_2SO_4 solution for 48 hours under room temperature; d) immersion in boiling deionized water for 4 hours; e) immersion in boiling 1 *M* H_2SO_4 solution for 4 hours. The variation of the membrane thickness was within ± 5% under different condition. The conductivities of these membranes were measured at room temperature and the results are shown in Fig. 3-10. The results were obtained when the membrane's conductivities had no more change, which would normally take 2 hours, since the conductivities were measured in 1M H_2SO_4 at room temperature and STA will be dissolved from the composite membrane. Furthermore, conductivities were determined for different regions of the same membrane. The results shown are the average values.

Fig. 3-10 shows the variation of conductivities of Nafion/STA composite membranes, which were pre-treated under various conditions. It can be seen that the composite Nafion/STA membrane exhibits higher conductivity than those without STA. Furthermore, the conductivity increases with the increase of STA concentrations. This may be due to the existence of STA ($SiW_{12}O_{40}^{4-} \cdot 4H^+$) which provides the high

concentration of the protons within the composite membrane and/or high mobility of the protons.

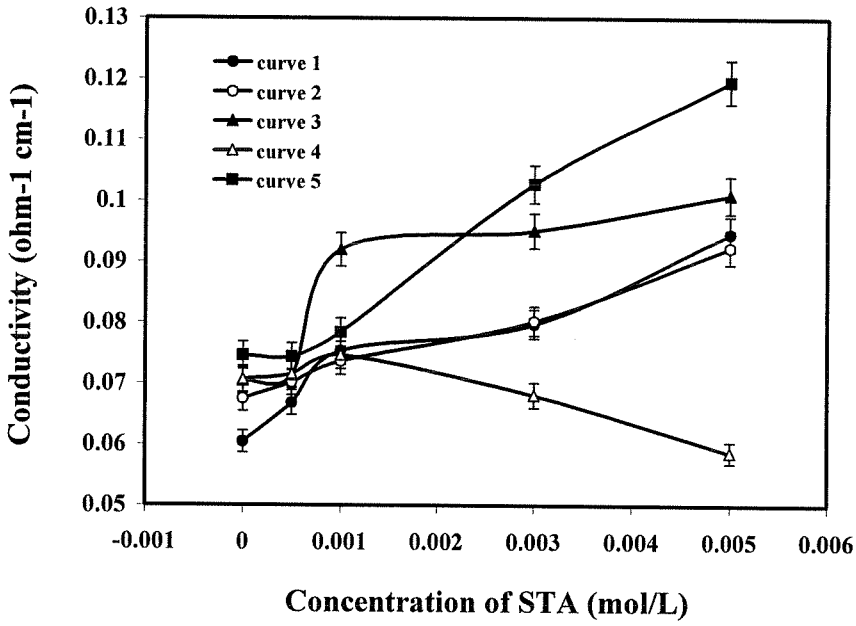

Figure 3- 10. Conductivities of composite Nafion membrane with and without STA under different conditions (curve 1: no immersion; curve 2: immersed in deionized water at room temperature; curve 3: immersed in 1 *M* H_2SO_4 solution at room temperature; curve 4: immersed in boiling deionized water; curve 5: immersed in boiling 1 *M* H_2SO_4 solution).

On the other hand, the variation of the conductivities depends on the membrane pre-treatment conditions. The lowest values of the conductivity were obtained where the membranes were previously immersed in boiling deionized water for 4 hours before conductivity measurements in 1 *M* H_2SO_4 solution (curve 4). In this case, the membrane conductivity is independent of STA concentration, which implies that the STA was washed out of the membrane. This is also supported by curves 1 and 2 which show the variation of the conductivity with STA concentration for the membranes immersed or not in deionized water at room temperature. These membranes exhibit higher

conductivity than those pre-treated in boiling water (curve 4). By comparing the curves 1 and 2, we may observe that the conductivity of composite Nafion/STA membrane pretreated in deionized water at room temperature is almost the same as that without immersion. This indicates that composite Nafion/STA membrane is stable in deionized water at room temperature and the immersion of the membrane in deionizd water at room temperature has almost no effect on the membrane conductivity. For the cast Nafion membrane without STA, the conductivity in deionized water or in 1 M H_2SO_4 solution is higher than that without any immersion. This due to the membrane absorbs a large amount of H_2O and H^+ during immersion, which is benefical for the transfer of the H^+ ion in the membrane and the improvement of the membrane conductivity.

A higher conductivity can be obtained for the composite membranes soaked in 1 M H_2SO_4 solution (curves 3 and 5). This may be due to the existence of synergetic effect between the sulfuric acid and the silicotungstic acid (STA). The high conductivity of the cast Nafion with STA membranes soaked in 1 M H_2SO_4 solution sustains the synergetic effect between H_2SO_4 and STA or/and the increase of the proton conductive sites coming from the contribution of sulfonated acid exchange sites, sulfuric acid and STA species. Experimental trials showed that the cast membrane with STA exhibited higher conductivity than that without STA when the membrane was soaked in sulphuric acid. In addition, a higher conductivity was obtained by soaking the membrane in sulfuric acid than soaking it in deionized water for the cast Nafion with STA membrane. These results confimed the synergetic effect discussed above. The existence of synergetic effect can be further verfied by the lower value of the conductivities of the cast Nafion with STA membrane soaked in boiling deionized water (curve 4) in comparison to those of the membranes soaked in boiling sulphuric acid (curve 5).

3.2.1.2. Composite Flemion/STA membrane

The composite Flemion/STA membranes were prepared with 10*ml*, 8.9*wt%* Flemion solution, 3*ml* DMF and different amount of STA. The conductivity of the composite Flemion/STA membranes was measured in 1 *M* H_2SO_4 solution after the membranes were pre-treated under the following respective conditions: a) no immersion before conductivity measurement; b) immersion in deionized water for 48 hours under room temperature; c) immersion in boiling deionized water for 4 hours; d) immersion in 1 *M* H_2SO_4 solution 48 hours under room temperature; e)immersion in boiling 1 *M* H_2SO_4 solution for 4 hours; and then the conductivities of these membranes were measured at room temperature. The conductivity variation of the composite membrane with the concentration of STA is shown in Fig. 3-11.

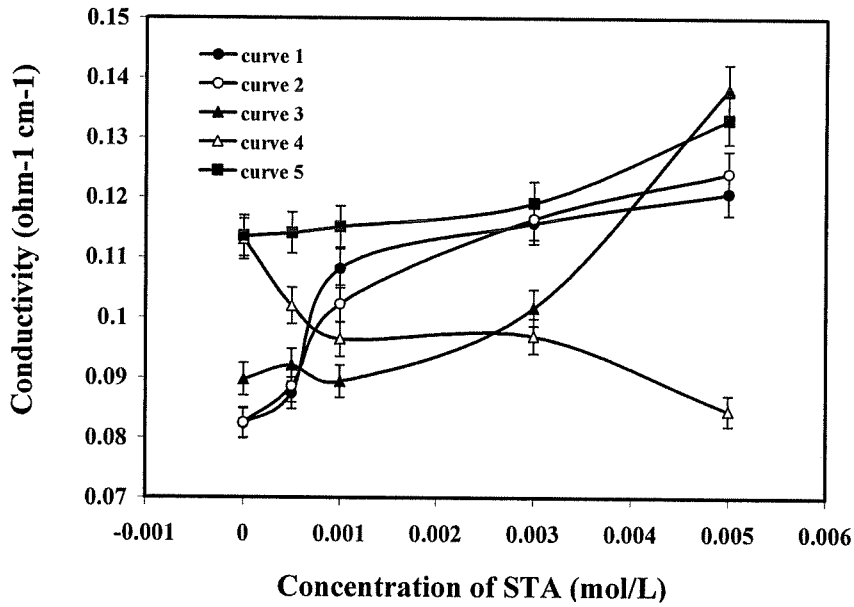

Figure 3- 11. Conductivities of composite Flemion with and without STA under different conditions (curve 1: no immersion; curve 2: immersed in deionized water under room temperature; curve 3: immersed in 1 *M* H_2SO solution under room temperature; curve 4: immersed in boiling deionized water; curve 5: immersed in boiling 1 *M* H_2SO_4 solution).

We can see that the cast Flemion with STA membrane exhibits higher conductivity than the cast Flemion without STA membrane as for the cast Nafion with and without STA. The conductivity of the membrane increases with the STA concentration. This is related to the increase of protonic sites provided by the STA species inserted in the membrane when the concentration of silicotungstic acid increases. These protonic sites are introduced to the membrane by STA ($SiW_{12}O_{40}^{4-} \cdot 4H^+$).

From the results of Fig. 3-11, we can also see that the pre-treatment conditions have significant effects on the conductivity of the composite membrane. The conductivities of composite membranes change with the immersion temperatures. At room temperature, the membrane is stable and the conductivity increases with the increase of STA concentration. It is supported by curves 1 and 2 which show that the conductivities of composite Flemion/STA membrane immersed or not in deionized water at room temperature are almost the same. This indicates that composite Flemion/STA membrane is stable in deionized water at room temperature. In other words, the immersion of the membrane in deionized water at room temperature has no effect on the membrane conductivity. However, the membrane conductivity is independent of STA concentration at high temperatures and we got the lowest conductivity value of membrane when the membranes were pretreated in boiling deionized water for 4 hours before conductivity measurement (curve 4). This may imply that STA was washed out of the membrane at this condition. For the cast Flemion membrane without STA, the variation of conductivity is about 0.03 $ohm^{-1} \cdot cm^{-1}$. This is due to the the same reason as discussed for cast Nafion without STA membranes. The absorption of H_2O and H^+ is benefical for the transfer of the H^+ ion in the membrane and the improvement of the membrane conductivity.

The dependence of the conductivity on the amount of STA is complex for the composite membrane pretreated in $1M$ H_2SO_4. It was found that the membranes pretreated in boiling $1M$ H_2SO_4 exhibited higher conductivity than membranes

pretreated in deionized water (curve 5). As discussed earlier for Nafion/STA composite membranes, the elevated conductivity was caused by the existence of synergetic effect between the sulfuric acid and STA or/and the increase of the concentration of the proton sites due to the sulfonated group and the STA species. It is also the case for Flemion/STA membrane. This synergetic effect can also be experimentally verified because the conductivity of the cast Flemion with STA membrane soaked in sulfuric acid is higher than that of the cast Flemion without STA membrane soaked in sulphonic acid and that of the cast Flemion with STA membrane soaked in deionized water. When the membrane was immersed in $1M$ H_2SO_4, the proton conductivity of the composite membrane should come from three contributions: sulfonated acid exchange sites, STA and H_2SO_4. Protons are produced by the dissociation of the H_2SO_4 which may compensate the decrease of proton due to the STA loss during the membrane operation. So there still keeps high concentration of mobile proton in composite membrane and the conductivity of the membrane still maintains high value.

3.2.1.3. The comparison of conductivities obtained from the two different types of composite membranes

Table 3-5 shows the conductivities obtained from composite Nafion/STA membrane and composite Flemion/STA membrane. Both membranes are based on 10 *ml* polymer solution (5% Nafion solution or 8.9 % Flemion solution), 3 *ml* DMF and different amount of STA. It can be seen that the Flemion/STA membrane exhibits better ionic conductivity than Nafion/STA membrane. The difference is mainly due to the difference of the equivalent weight between the two types of the membranes. Flemion membrane with 910 *EW* (I.E.C=1.1 *meq/g*) has better conductivity than Nafion with 1100 *EW* (I.E.C=0.91 *meq/g*). We may get the conductivity of commercial Nafion 117 membrane (0.06 $ohm^{-1} \cdot cm^{-1}$) using the same measuring condition. We see that the conductivies of the composite membranes are always better than that of commercial Nafion 117 membrane.

Table 3- 5. The comparison of conductivities obtained from different membranes.

Pretreatment condition	[STA] (mol/L)	Conductivity $(ohm^{-1} \cdot cm^{-1})$	
		Flemion/STA	*Nafion/STA*
No immersion	0	0.0823	0.0604
	$5\times10^{-4}M$	0.0874	0.0668
	$1\times10^{-3}M$	0.1082	0.0754
	$3\times10^{-3}M$	0.1158	0.0798
	$5\times10^{-3}M$	0.1208	0.0946
Immersed in deionized water for 48 hours	0	0.0825	0.0675
	$5\times10^{-4}M$	0.0885	0.0702
	$1\times10^{-3}M$	0.1022	0.0737
	$3\times10^{-3}M$	0.1165	0.0803
	$5\times10^{-3}M$	0.1241	0.0924
Immersed in 1 M H_2SO_4 Solution for 48 hours	0	0.0897	0.0705
	$5\times10^{-4}M$	0.0920	0.0714
	$1\times10^{-3}M$	0.0894	0.0920
	$3\times10^{-3}M$	0.1016	0.0951
	$5\times10^{-3}M$	0.1382	0.1010
Immersed in boiling deionized water for 4 hours	0	0.1130	0.0707
	$5\times10^{-4}M$	0.1019	0.0716
	$1\times10^{-3}M$	0.0964	0.0746
	$3\times10^{-3}M$	0.0969	0.0681
	$5\times10^{-3}M$	0.0846	0.0587
Immersed in boiling 1 M H_2SO_4 Solution for 4 hours	0	0.1135	0.0746
	$5\times10^{-4}M$	0.1140	0.0744
	$1\times10^{-3}M$	0.1151	0.0784
	$3\times10^{-3}M$	0.1191	0.1028
	$5\times10^{-3}M$	0.1330	0.1196

3.2.2. THE EFFECTS OF THE MEMBRANE THICKNESS ON THE CONDUCTIVITY OF COMPOSITE NAFION/STA MEMBRANE

The composite Nafion/STA membranes were prepared using 25 *ml* Nafion solution + 7.5 *ml* DMF + STA ($5\times10^{-3}M$), 20 *ml* Nafion solution + 6 *ml* DMF + STA ($5\times10^{-3}M$), 15 *ml* Nafion solution + 4.5 *ml* DMF + STA ($5\times10^{-3}M$), 10 *ml* Nafion solution + 3 *ml* DMF + STA, respectively. Various composite Nafion/STA membranes cast from various quantities of Nafion and DMF with different thicknesses were obtained. The thickness of the composite membrane increases with the increase of the volume of Nafion solution. In addition, the thickness variations for the membrane prepared from the same volume Nafion solution were within ± 10%, which implied the reproducibility of the membrane preparation method are quite good.

The above membranes were respectively pretreated under different conditions (same as sections 3.2.1.1 and 3.2.1.2) and then the conductivities of these membranes were measured. The comparisons of the measured conductivities of various composite Nafion/STA membranes are presented in Fig. 3-12.

The synergetic effects between the sulphonated group ($-SO_3H$) and the STA group or/and the increase of the protonic sites due to the presence of the STA make the ionic conductivities of the composite membranes with same STA concentration and different thicknesses exhibit different results. Fig. 3-12 shows the variation of the conductivities for the different thickness of the composite membranes with the same STA concentration ($5\times10^{-3}M$) under different pre-treated conditions. From Fig. 3-12, we may see that the conductivities of composite Nafion/STA membranes increase with the increase of the composite membrane thicknesses under different measuring conditions. When the composite Nafion/STA membranes were preteated by immersing the membrane in deionized water or without any immersion, the conductivities of membranes increase slightly with the increase of thickness of the membranes. For the

composite membrane with same concentration of STA, the above results may have relationship with the water uptake of membranes. It is well accepted that the ionic conductivity of the membrane is related to the water uptake of the membrane.

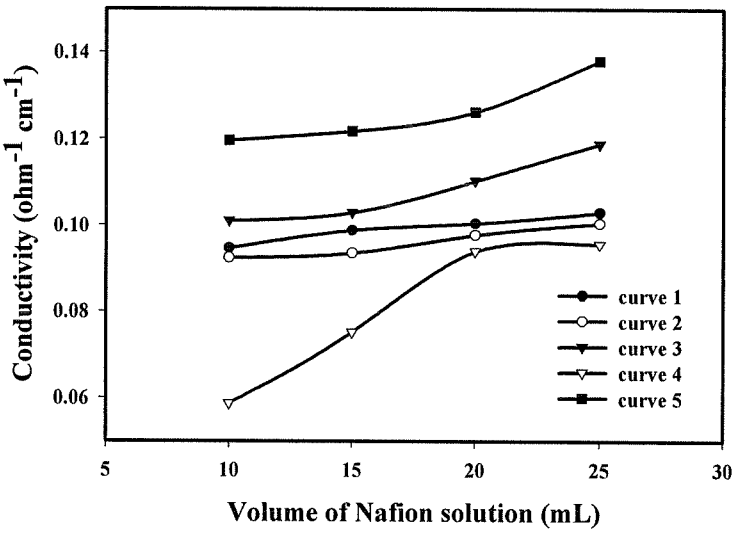

Figure 3- 12. Conductivities of different thickness composite Nafion/STA membranes under various pretreated conditions (Concentration of STA is $5\times10^{-3}M$) (curve 1: no immersion; curve 2: immersed in deionized water under room temperature; curve 3: immersed in 1 M H_2SO_4 solution under room temperature; curve 4: immersed in boiling deionized water; curve 5: immersed in boiling 1 M H_2SO_4 Solution.).

We may also observe that the conductivities of the membranes increase significantly with the increase of membrane thickness when the composite membranes were preteated in boiling deionized water or in 1 M H_2SO_4 solution. The difference of the STA loss with the membrane thickness and the synergetic effect between the sulphonated group ($-SO_3H$) and the STA group may be used to explain the above results. The thicker membrane exhibits better conductivities because they contain more

-SO_3H groups and STA. The effects of STA on the water uptake of membrane and STA loss in the membrane under different membrane thicknesses will be discussed later.

3.2.3. CONCLUSIONS

The addition of STA to the Nafion or Flemion solution during the membrane fabrication can effectively improve the ionic conductivity of composite membrane. The ionic conductivity of composite membrane increases with the increases of STA concentration in membranes and also increases with the increase of the composite membrane thickness. The experimental results show that the conductivity of the cast membrane with STA soaked in sulphonic acid is higher than that of the cast membrane without STA soaked in sulphonic acid and that of the cast membrane with STA soaked in deionized water, which is indicative of the synergetic effect between the STA and sulphonated group (-SO_3H) or /and the increase of the protonic sites concentration from the sulfonated group and the STA species. The variation of conductivity between the different conditions indicated the loss of STA in the membranes. The existence of H_2SO_4 can reduce the loss of STA.

3.3. WATER UPTAKE AND STA LOSS OF THE NAFION/STA COMPOSITE MEMBRANES

3.3.1. THE EFFECTS OF THE IMMERSION TIME OF THE MEMBRANES IN BOILING DEIONIZED WATER OR IN BOLILING 1M H_2SO_4 SOLUTION ON THEIR WATER UPTAKE

Tables 3-6 and 3-7 present the effects of the immersion time of the membranes in boiling deionized water or in boiling 1 M H_2SO_4 solution on their water uptake. The experimental results show that the water uptake does not change after 4 hours. Accordingly, the water uptake was measured after 4 hour immersion.

Table 3- 6. The effects of the immersion time in boiling deionized water on the water uptake of Nafion/STA membranes.

(Membrane preparation: 10 *ml* 5% Nafion +3 *ml* DMF+STA (5×10^{-3} *mol/L*))

Boiled time(hours)	4 hours	6 hours	8 hours
Water uptake (%)	20.13	20.93	20.36

Table 3- 7. The effects of the immersion time in boiling 1 *M* H_2SO_4 solution on the water uptake of Nafion/STA membranes.

(Membrane preparation: 10ml 5% Nafion +3ml DMF+STA (5×10^{-3} mol/L))

Boiled time(hours)	4 hours	6 hours	8 hours
Water uptake (%)	34.76	35.02	34.59

3.3.2. WATER UPTAKE AND STA LOSS OF COMPOSITE NAFION/STA MEMBRANES IN BOILING DEIONIZD WATER OR IN BOILNG 1M H_2SO_4 SOLUTION

The composite Nafion/STA membranes were prepared using different amount of STA and 10 *ml* 5 *wt%* Nafion solution + 3 *ml* DMF, 15 *ml* 5 *wt%* Nafion solution + 4.5 *ml* DMF, 20 *ml* 5 *wt%* Nafion solution + 6 *ml* DMF, 25 *ml* 5 *wt%* Nafion solution + 7.5 *ml* DMF, respectively. Then, the composite Nafion/STA membranes with different thicknesses and various STA concentrations were obtained. The variation of the water uptake and STA loss of these membranes was determined.

3.3.2.1. Water uptake and STA loss in boiling deionized water

Figs. 3-13 and 3-14 show the variation of the water uptakes of the composite Nafion/STA membranes with the different STA concentrations for various volumes of Nafion solution used for preparation of the composite membranes. The variation of Nafion solution volumes lead to different membrane thicknesses. As can be seen from Fig. 3-13 and 3-14, the water uptakes of the composite membranes change with the changes of the membrane thickness and the STA concentration. The water uptake increases with the increase of STA concentration for thicker membranes. However, it changes very slightly with the change of STA concentration for thinner membranes. For the composite membrane containing the same STA concentration, the water uptake increases with the increase of the membrane thickness.

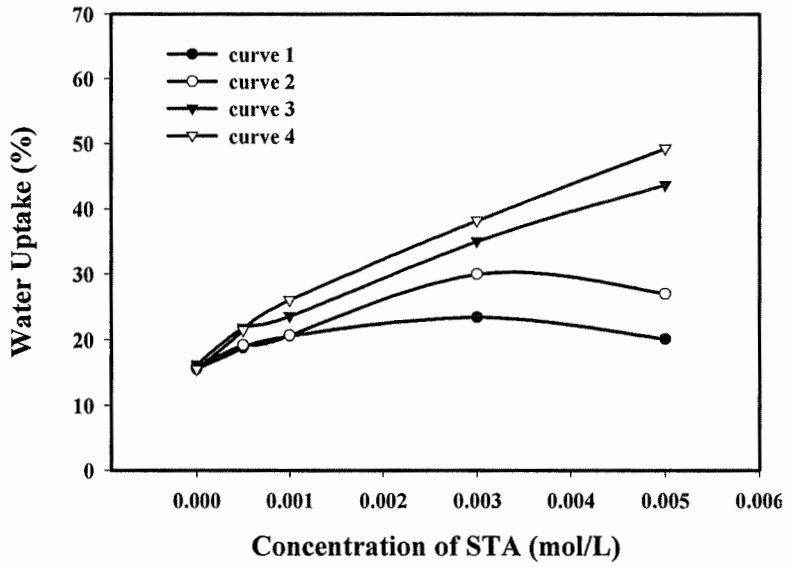

Figure 3- 13. Water uptakes of composite Nafion/STA membrane in boiling deionized water versus the concentrations of STA (curve 1: 10 *ml* 5 *wt.%* Nafion + 3 *ml* DMF + STA; curve 2: 15 *ml* 5 *wt.%* Nafion + 4.5 *ml* DMF + STA; curve 3: 20 *ml* 5 *wt.%* Nafion + 6 *ml* DMF + STA; curve 4: 25 *ml* 5 *wt.%* Nafion + 7.5 *ml* DMF + STA).

During the water uptake measurement, it can be observed that the STA loss is quite evident. That is to say, the composite membrane is unstable in the boiling deionized water and the STA in composite membrane is dissolved into the deionized water. Fig. 3-15 shows the variation of the STA loss of various membranes with the change of STA concentration. It can be seen that the STA loss increases with the increase of STA concentration in membranes, but it decreases with the increase of membrane's thickness. This can support the result of the conductivity decrease due to STA loss appeared in curve 4 of Fig. 3-10 (see section 3.2.1.1). Furthermore, it can also support the result of the increase of composite membrane conductivity because of the increase of membrane's thickness obtained in Fig. 3-12 (see section 3.2.1.2).

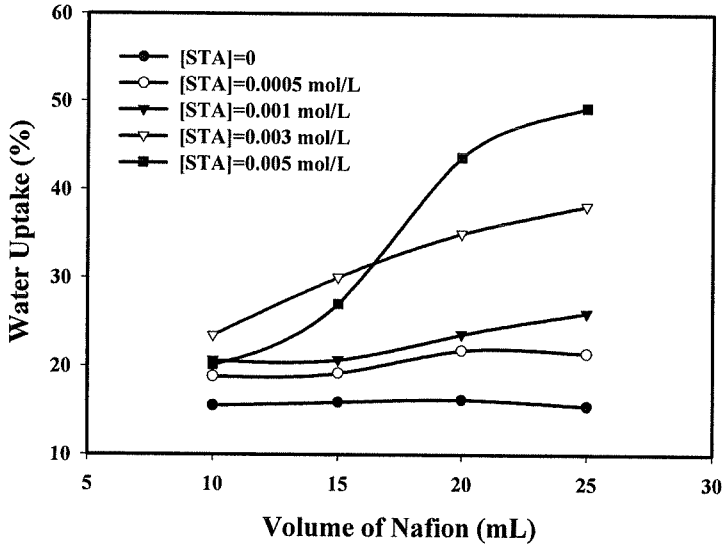

Figure 3- 14. Water uptakes of the composite Nafion/STA membrane in boiling deionized water versus the volumes of Nafion solution.

The effect of immersion temperature on the STA loss and the water uptake of composite membrane have also been investigated. As indicated in Fig. 3-16, the STA loss and water uptake of composite membrane vary with the change of immersion temperature. This variation can be attributed to the change of polymer structure when

the temperature increases (polymer is swollen). The STA loss of the composite Nafion/STA membrane immersed in deionized water at low temperature is, of course, less than that of the composite membrane immersed in boiling water. In other words, the cast Nafion with STA membrane at low temperature is more stable than that at high temperature. This makes a good agreement with the results described by curve 2 (composite membrane immersed in deionized water at room temperature) and curve 4 (composite membrane immersed in boiling deionized water) in Fig. 3-10. On the other hand, the swollen composite membrane has larger water absorption capacity at higher immersion temperatures.

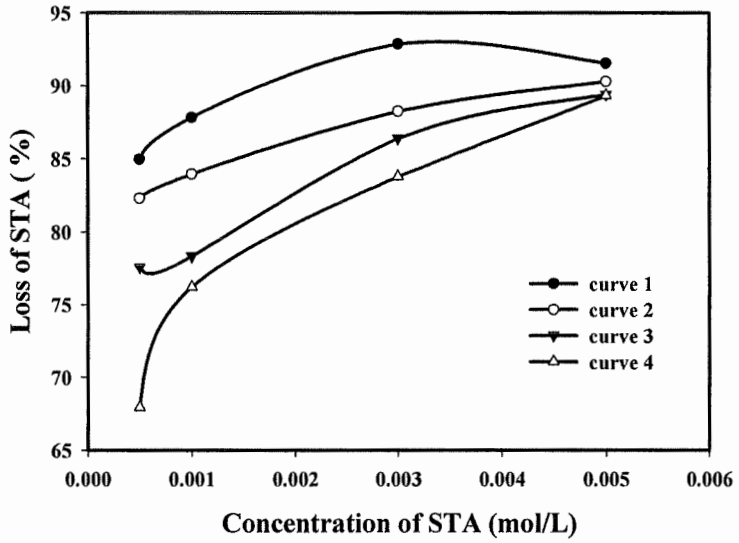

Figure 3- 15. STA loss for different thicknesses of composite Nafion/STA membranes in boiling deionized water versus STA concentrations (curve 1:10 *ml* 5 *wt.%* Nafion + 3 *ml* DMF + STA; curve 2: 15 *ml* 5 *wt.%* Nafion + 4.5 *ml* DMF + STA; curve 3: 20 *ml* 5 *wt.%* Nafion + 6 *ml* DMF + STA; curve 4:25 *ml* 5*wt.%* Nafion + 7.5 *ml* DMF + STA).

It can also be found that although the water uptake increases with the increase of immersion temperature, the STA weight percentage in dry membrane ([STA] *wt.*%) after the membrane had been immersed in boiling deionized water for 4 hours decreases

with the increase of immersion temperature. For example, the [STA](*wt.*%) decreased from 21.19 % (25°C) down to 1.46 % (100°C) for the given membrane shown in Fig. 3-16. Due to this reason, the conductivity of composite membrane immersed in low-temperature deionized water is, of course, higher than that of composite membrane immersed in boiling deionized water (Fig. 3-10, Fig. 3-12).

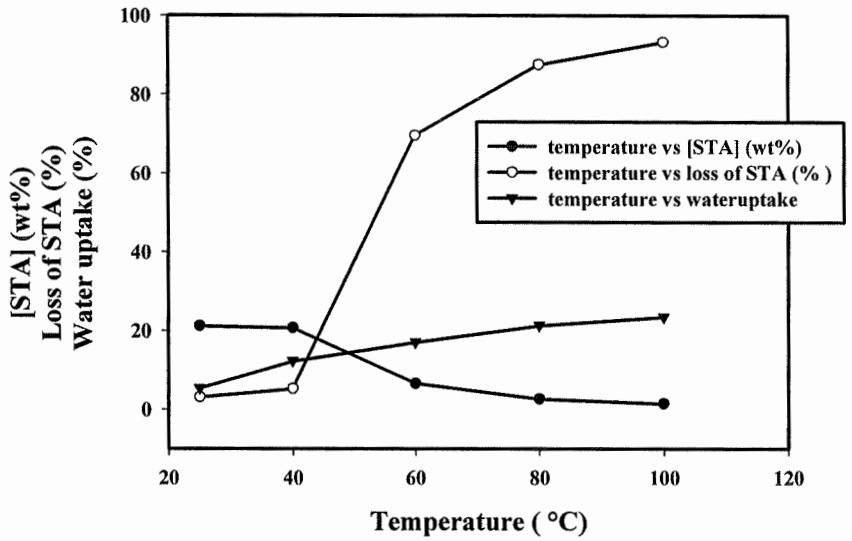

Figure 3- 16. STA loss, water uptake and [STA](*wt.%*) of the composite Nafion/STA membrane under different immersion temperatures (the STA concentration in membrane is 3×10^{-3} *M* (initial weight percentage is 21.88 %)).

3.3.2.2. Water uptake and STA loss in boiling 1 M H_2SO_4 solution

The water uptakes of composite Nafion/STA membranes in boiling 1 *M* H_2SO_4 solution are shown in Figs. 3-17 and 3-18. It can be seen that the water uptake of composite Nafion/STA membrane in boiling 1 *M* H_2SO_4 solution increases with the increase of the STA concentration and the membrane thickness. This can be used to explain the results that the conductivity of composite Nafion/STA membrane in boiling 1 *M* H_2SO_4 solution increases with the increase of both the STA concentration (Fig. 3-10, curve 5) and the membranes thickness (Fig. 3-12, curve 5).

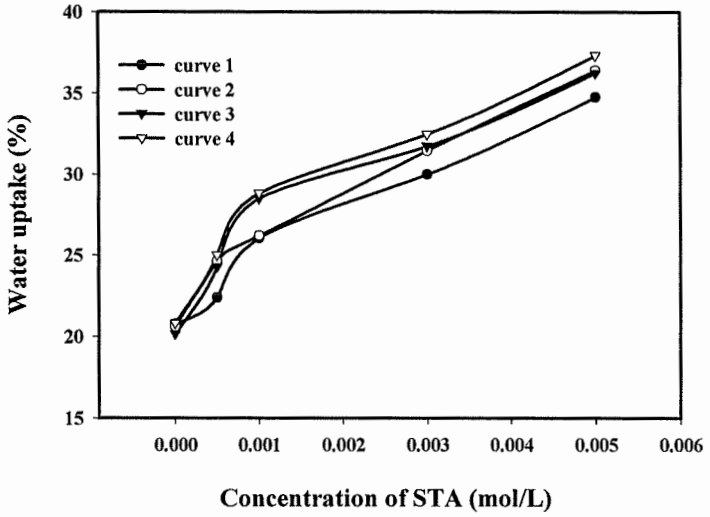

Figure 3- 17. Water uptakes of composite Nafion/STA membranes in boiling 1 *M* H_2SO_4 solution versus STA concentrations (curve 1:10 *ml* 5 *wt.%* Nafion + 3 *ml* DMF + STA; curve 2: 15 *ml* 5 *wt.%* Nafion + 4.5 *ml* DMF + STA; curve 3: 20 *ml* 5 *wt.%* Nafion + 6 *ml* DMF + STA; curve 4: 25 *ml* 5 *wt.%* Nafion + 7.5 *ml* DMF + STA).

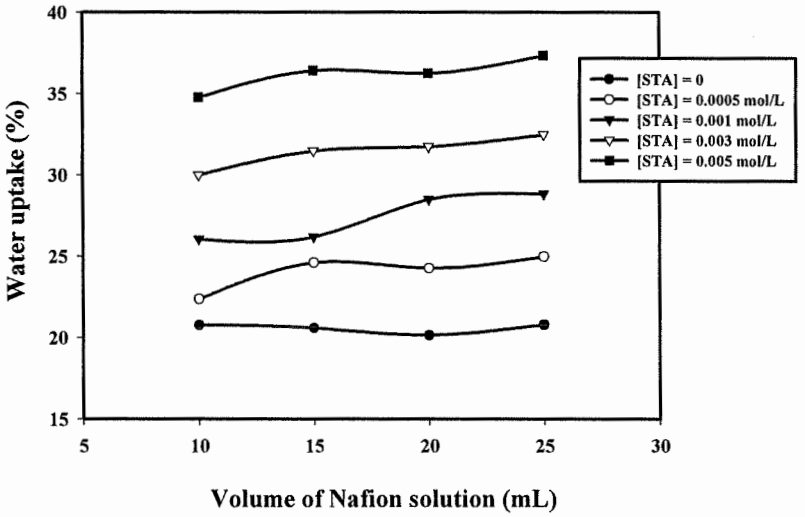

Figure 3- 18. Water uptakes of the composite Nafion/STA membranes in boiling 1 *M* H_2SO_4 solution versus the volumes of Nafion solution.

Fig. 3-19 shows the STA loss of composite membrane in boiling 1 *M* H_2SO_4 solution. The effect of the STA concentration on the STA loss in boiling 1 *M* H_2SO_4 solution is more complex than that in boiling deionized water. However, the relationship between the STA loss in boiling 1 *M* H_2SO_4 solution and the membrane thickness is evident. The STA loss decreases with the increase of the membrane thickness. This can also explain the result that the conductivity of composite Nafion/STA membrane in boiling 1 *M* H_2SO_4 solution increases with the increase of the membranes thickness (Fig. 3-12, curve 5).

Comparing the Fig. 3-19 to the Fig. 3-15, we can find that the STA loss in boiling 1 *M* H_2SO_4 solution is lower than that in boiling deionized water. This is the reason that the composite Nafion/STA membrane in boiling H_2SO_4 solution exhibits higher conductivity than that in boiling deionized water (Figs. 3-10 and 3-12).

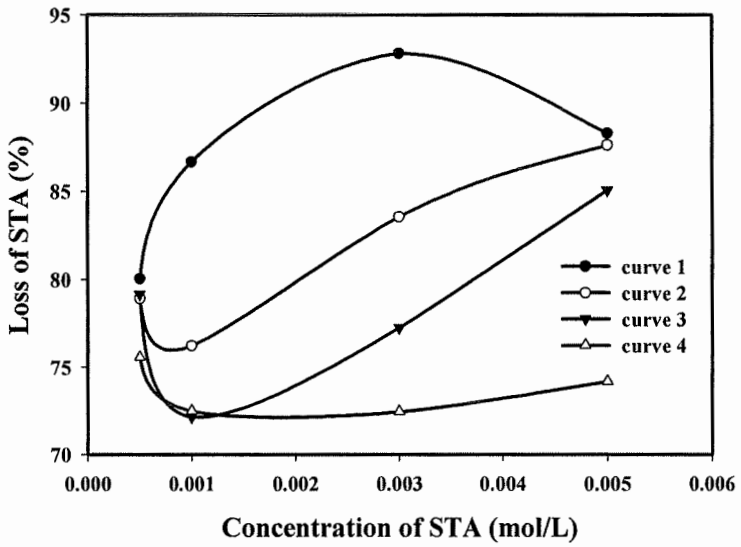

Figure 3- 19. STA loss of different thicknesses of composite Nafion/STA membranes in boiling 1 *M* H_2SO_4 solution versus STA concentrations (curve 1:10 *ml* 5 *wt.%* Nafion + 3 *ml* DMF + STA; curve 2: 15 *ml* 5 *wt.%* Nafion + 4.5 *ml* DMF + STA; curve 3: 20 *ml* 5 *wt.%* Nafion + 6 *ml* DMF + STA; curve 4:25 *ml* 5 *wt.%* Nafion + 7.5 *ml* DMF + STA).

3.3.3. EFFECTS OF STA ON WATER UPTAKE OF COMPOSITE MEMBRANE

The above results showed that the water uptake of composite membrane increased not only with the STA concentration in the membrane but also with the membrane thickness. The results can be explained by the highly hydrated ability of STA. During the preparation of composite Nafion membrane, the evaporation temperature was up to 135°C. From the results of the thermal stability analysis of STA (see Chapter 1, Fig. 1-23), it was shown that STA has at least 8 molecules of water under 135°C. Because the highly hydrated STA can contain 26 molecules of water at room temperature, the STA in the composite membranes can absorb more than 18 molecules of water when the composite membrane is immersed in deionized water.

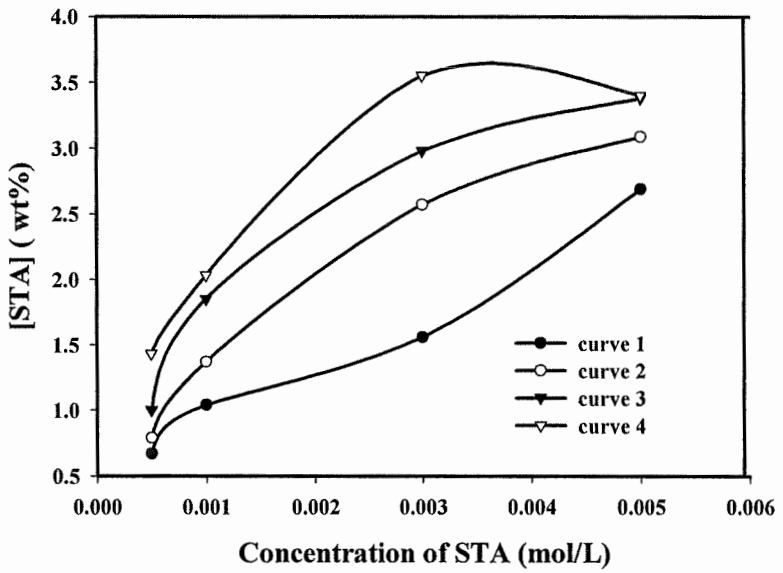

Figure 3- 20. The STA weight percentages in dry membrane after immersion in boiling deionized water 4 hours ([STA](*wt%*)) versus the initial STA concentrations (*mol/L*) (curve 1:10 *ml* 5 *wt.%* Nafion + 3 *ml* DMF + STA; curve 2: 15 *ml* 5 *wt.%* Nafion + 4.5 *ml* DMF + STA; curve 3: 20 *ml* 5 *wt.%* Nafion + 6 *ml* DMF + STA; curve 4:25 *ml* 5 *wt.%* Nafion + 7.5 *ml* DMF + STA).

When the composite membrane is immersed in boiling deionized water or boiling 1 *M* H_2SO_4 solution, there still has certain amount of STA left in membrane structure even though the loss of STA can be clearly observed. This implies that there may have the strong interaction, which will be discussed and verified in the later section, between the Nafion and STA. Figs. 3-20 and 3-21 show the weight percentage of STA in dry membrane after the membrane had been immersed in boiling deionized water or boiling 1 *M* H_2SO_4 solution 4 hours ([STA] *wt%*). The [STA] (*wt%*) increases with the increase of initial STA concentration and the membrane thickness. The STA left in membrane structure can absorb a large amount of H_2O which is beneficial for the transportation of the H^+ ion through membrane. The increase of the water uptake of the composite membrane may be due to the reason mentioned above. Moreover, the addition of STA leads to further improvement of composite membrane conductivity.

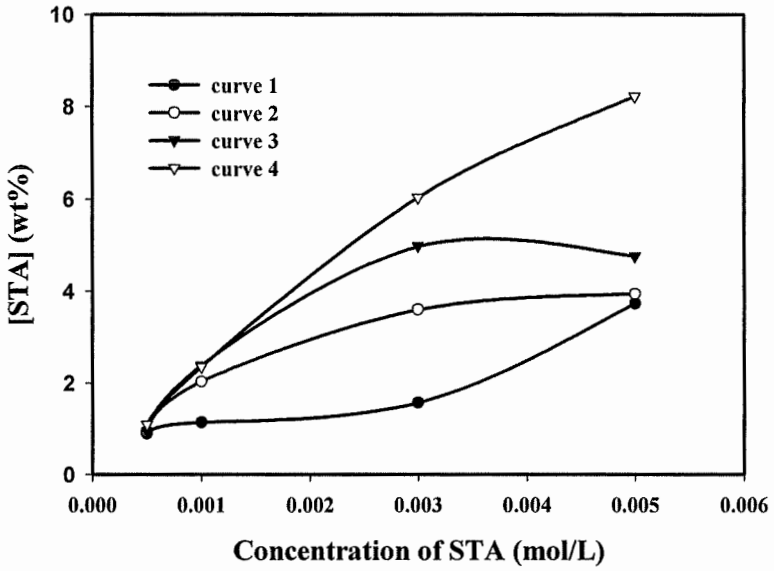

Figure 3- 21. The STA weight percentages in dry membrane after immersion in boiling 1 *M* H_2SO_4 solution 4 hours ([STA](*wt%*)) versus the initial concentration of STA (*mol/L*). (curve 1:10 *ml* 5 *wt.%* Nafion + 3 *ml* DMF + STA; curve 2: 15 *ml* 5 *wt.%* Nafion + 4.5 *ml* DMF + STA; curve 3: 20 *ml* 5 *wt.%* Nafion + 6 *ml* DMF + STA; curve 4:25 *ml* 5 *wt.%* Nafion + 7.5 *ml* DMF + STA).

By comparing the Figure 3-20 to Figure 3-21, we may see that the [STA] (*wt%*) in boiling 1 *M* H_2SO_4 solution (0.89% ~8.22%) is higher than that in boiling deionized water (0.67%~3.55%). This indicates that the existence of H_2SO_4 can reduce the loss of STA.

The phenomenon of STA loss can be explained by the structures of Nafion and STA. The ion cluster-network model of Nafion shows that the diameter of these ion-clusters is 1.9 *nm* in dry Nafion [43]. STA molecules (diameter of 1.12 *nm*) [115] can be embedded in the ion-cluster because the diameters both STA molecule and Nafion ion-cluster are in same magnitude. Further, the STA molecules can be dispersed into the surface layer as well. When temperature increases, the water uptake of composite membrane also increases and the ion-cluster becomes more and more swollen. In fully hydrated Nafion, the diameter of ion-cluster is about 4*nm* [43] where STA molecular can come out from the ion-cluster easily due to the fact that the diameter of STA keeps unchanged. High solubility of STA in water causes the loss of STA in the surface layer of polymer. The higher concentration of STA in membrane is, the more STA will be lost.

3.3.4. CONCLUSIONS

The water uptake of the composite Nafion/STA membrane changes with the change of membrane thickness and STA concentration in membrane. The water uptake increases slightly with the increase of STA concentration for thinner membrane. However, the increase of water uptake is quite significant with the increase of STA for thicker membranes. For the composite membrane containing the same STA concentration, the water uptake increases with the membrane thickness. It could not be denied that the addition of STA to the perfluoronated polymer solution makes the composite membrane with STA have an elevated capacity of water absorption than

those without STA. The experimental trials showed that the STA loss in boiling 1 M H_2SO_4 solution is lower than that in boiling deionized water, which indicates the existence of interaction between the STA and SO_3H group. Saying, the existence of H_2SO_4 reduces the loss of STA.

3.4. THERMAL STABILITY

The thermal stability of the composite membrane is very important for the application of composite membrane in PEMFC under higher operation temperature. Therefore, the thermogravimetry (TG) and Differential thermogravimetry (DTG) analysis of pure STA, composite Nafion/STA and Flemion/STA membrane (the concentration of STA is 3×10^{-3} M) are presented.

3.4.1. THERMAL CHARACTERIZATION OF STA SAMPLE UNDER DIFFERENT TEMPERATURES

Thermoanalysis data related to the percentage weight loss of the pure STA sample in the temperature range of 25-800°C are presented in Fig. 3-22 and 3-23 under different pretreatment conditions. Fig. 3-22 shows the thermoanalysis of STA without any treatment and Fig. 3-23 shows the thermoanalysis of STA dried at 135°C overnight. From Fig. 3-22, it can be calculated that the STA sample used in this work contains 20 water molecules for each silicotungstic acid unit. The STA sample will dehydrate 14 water molecules (product is $H_4SiW_{12}O_{40}\cdot 6H_2O$, weight loss is 7.60%) from 50 to 140°C and loses six water molecules around 250°C (product is $H_4SiW_{12}O_{40}$, weight loss is 11.01%). Furthermore, two water molecules will be removed from H_4SiO_4 around 500°C, which is due to the spontaneous transformation of dehydroxylation product into a mixture of WO_3 and SiO_2 [119]. The total weight loss is 12.22%.

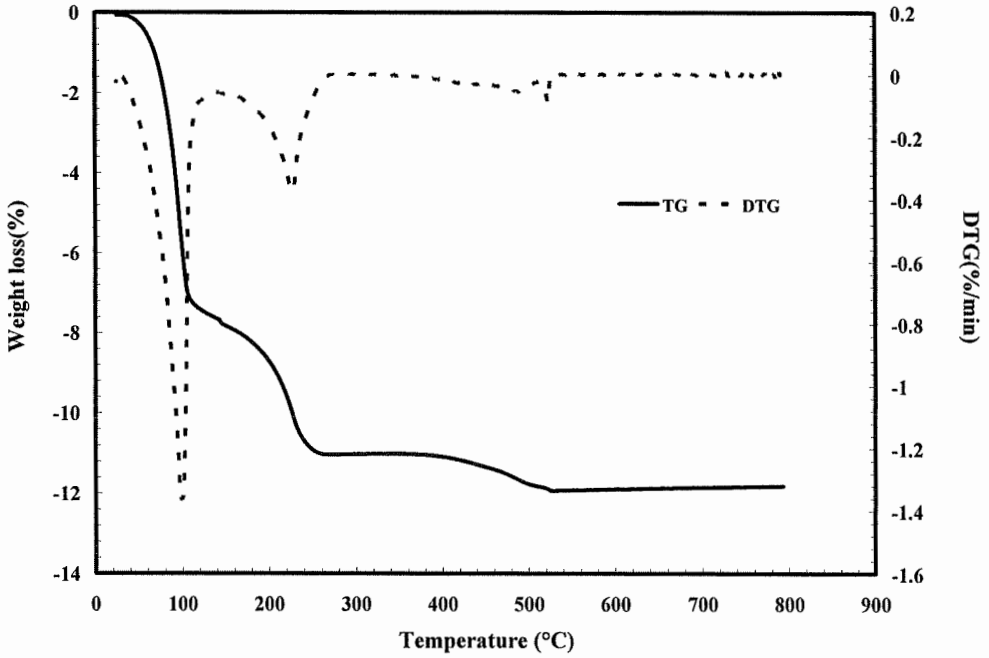

Figure 3- 22. TG and DTG curves of STA (obtained from room temperature).

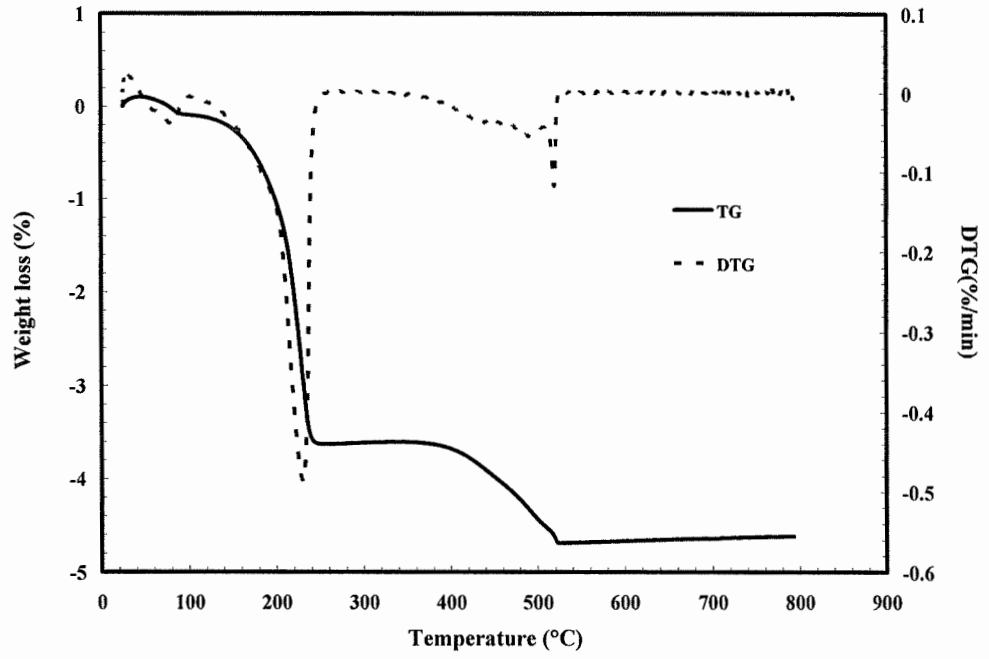

Figure 3- 23. TG and DTG curves of STA (the sample was dried in oven vacuum at 135°C overnight).

As mentioned in section 3.1.1.1, both the composite Nafion/STA and Flemion/STA membranes were obtained under 135°C. Therefore, it could be deducted that the STA existed in composite membrane would still contain at least six water molecules for each silicotungstic acid. This deduction can be also confirmed from Fig. 3-23 where the weight loss is 3.63% when the product is $H_4SiW_{12}O_{40}$. The calculated numbers of the water molecules in the dried (at 135°C) STA sample are six. We may conclude that STA has good thermal stability in fuel cell operating conditions. This supports the preparation of the electrolyte materials for fuel cells based on Silicontungstic acid and Nafion or Flemion solution.

3.4.2. THERMAL CHARACTERISTIZATION OF COMPOSITE NAFION/STA MEMBRANE AND COMPOSITE FLEMION/STA MEMBRANE

The following figures (Fig. 3-24, 3-25, 3-26, 3-27) show the thermogravimetry (TG) and Differential thermogravimetry (DTG) curves of the cast Nafion without STA membrane (cast Nafion), composite Nafion/STA membrane, cast Flemion without STA membrane (cast Flemion) and composite Flemion/STA membrane, respectively. The temperature range of thermoanalytical measurement is 25-800°C. The TG and DTG curves exhibit difference profiles for these membranes.

From Figs. 3-24 and 3-25, we can observe that the decomposition of cast Nafion and cast Flemion has at least two steps, as can be seen clearly in TG and DTG curves. The first step (290~400°C for cast Nafion, 280°C~390°C for cast Flemion) may be associated with a desulfonation process while the second step (400–550°C for cast Nafion and 390°C-560°C for cast Flemion) may be related to main-chain of polymer decomposition. This observation is in good agreement with the results observed in Nafion 117 (Fig. 1-12) [61] or other sulfonated copolymers reported by other authors [133,134].

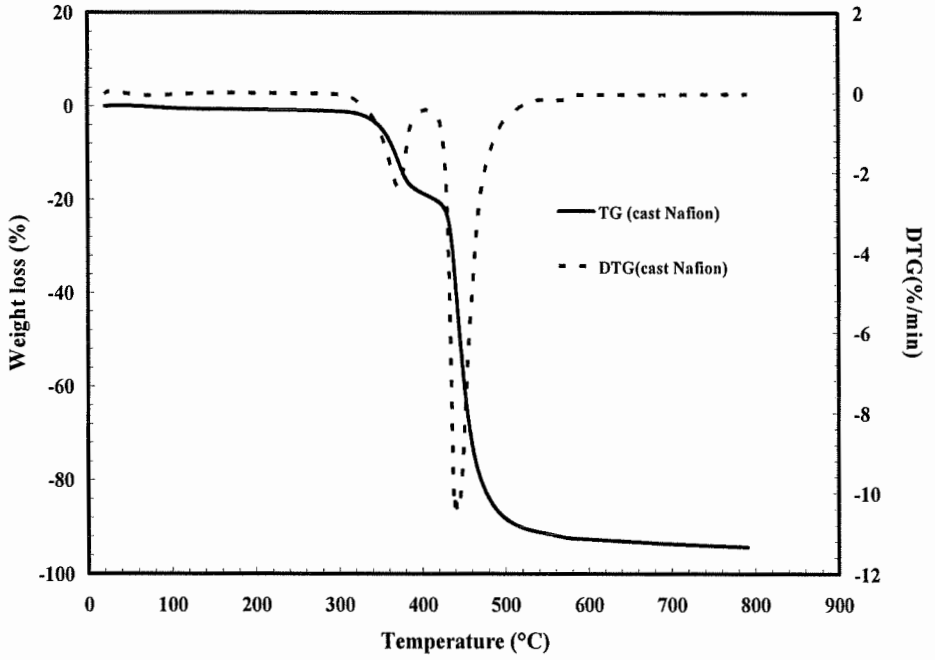

Figure 3- 24. TG and DTG curves of cast Nafion without STA (cast Nafion).

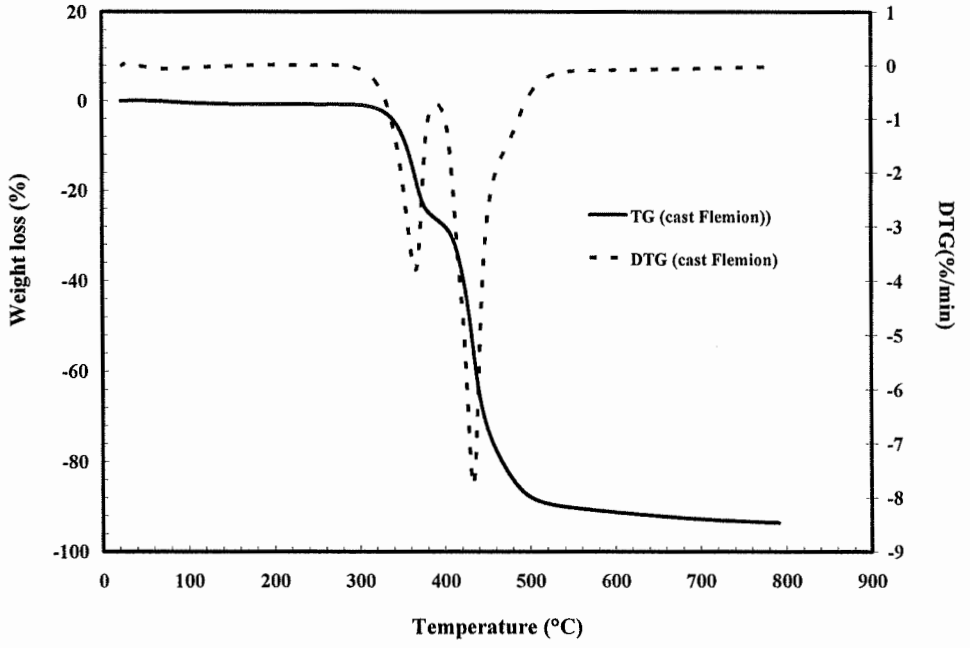

Figure 3- 25. TG and DTG curves of cast Flemion without STA (cast Flemion).

With the addition of STA, both composite Nafion/STA and Flemion/STA membranes also undergo two-step degradation process although the degradation temperatures were slightly higher than the composite membrane without STA, as can be seen from the TGA traces appeared in Figs.3-26 and 3-27. The first step is from 320°C to 425°C for Nafion/STA and 330°C to 422°C for Flemion/STA. The second step is from 425°C to 550°C for Nafion/STA and 422°C to 560°C for Flemion/STA. The comparison of the TGA of the composite Nafion/STA membrane and that of cast Nafion without STA membrane indicates that the two-step degradation of the composite membrane is mainly related to the degradation of the Nafion. In sum, the results of thermal analysis show the good thermal stabilities of both Nafion/STA and Flemion/STA composite membranes makes them feasible as electrolytes for polymer electrolyte fuel cell applications at high operation temperatures.

The thermal analysis results may also support the results that the water uptake of the membranes increased with the addition of STA. This might be related to the absorption of water by the STA in the composite membrane. According to the results discussed in section 3.4.1, the pure STA used in this work contains 20 water molecules for each silicotungstic acid unit. However, STA existing in the composite membrane would contain at least six crystal water molecule for each silicotungstic acid under the preparation temperature for composite membrane (135°C). The high hydrated ability of STA [107] makes it absorb at least 14 water molecules for each silicotungstic acid unit when the composite membrane is immersed in water. This is the reason why the water uptake increased when STA was added into the membrane.

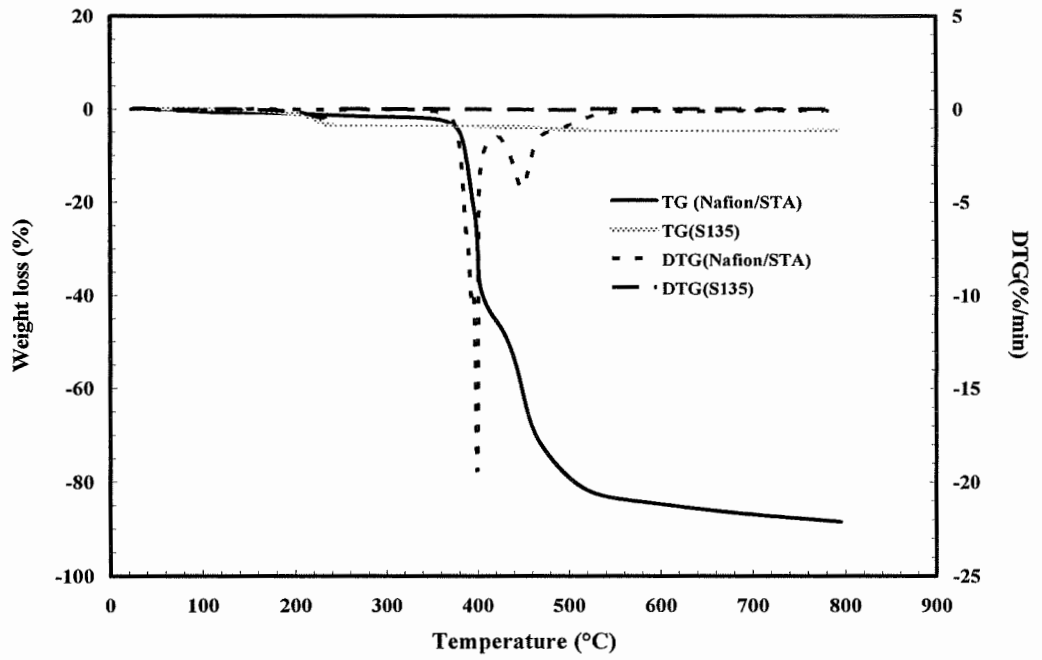

Figure 3- 26. TG and DTG curves of composite Nafion/STA membrane comparing with STA (STA sample dried in oven vacuum at 135°C overnight, S135).

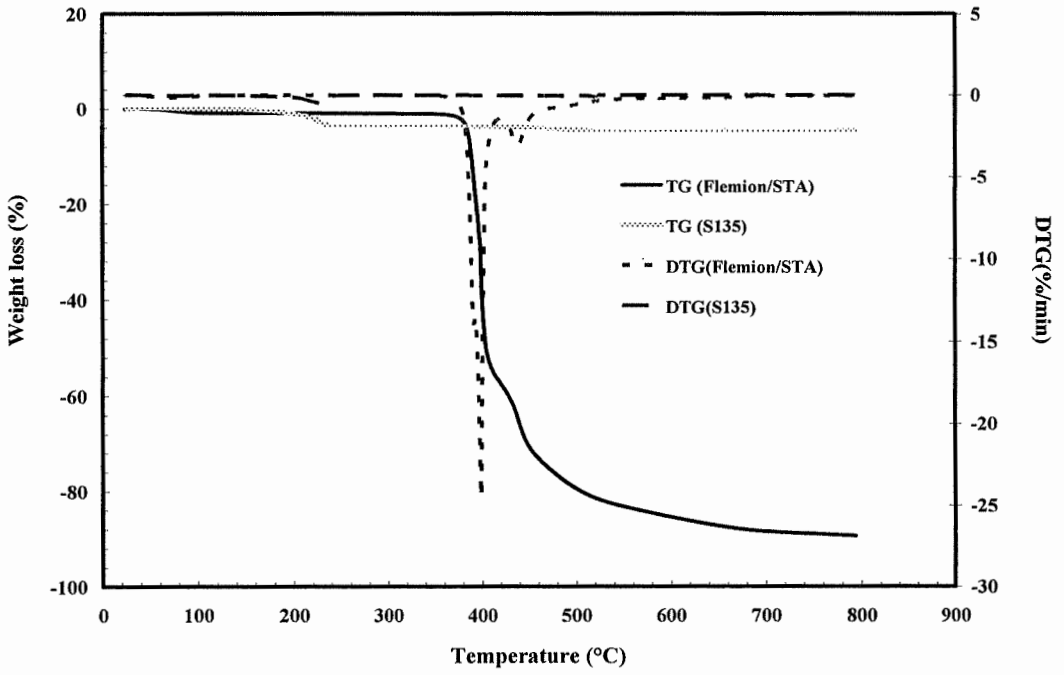

Figure 3- 27. TG and DTG curves of composite Flemion/STA membrane comparing with STA (STA sample dried in oven vacuum at 135°C overnight, S135).

3.4.3. THE EFFECT OF STA ON THE THERMAL CHARACTERISTICS OF COMPOSITE MEMBRAE

The composite Nafion/STA membranes cast with the same STA concentration ($3\times10^{-3}M$) were immersed in deionized water for 4 hours at $50°C$, $80°C$ and $100°C$, respectively. Then the membranes were dried in vacuum oven at $70°C$ overnight. Fig. 3-28 shows the TG curves of the above composite Nafion/STA membranes after immersion in the deionized water under different temperatures.

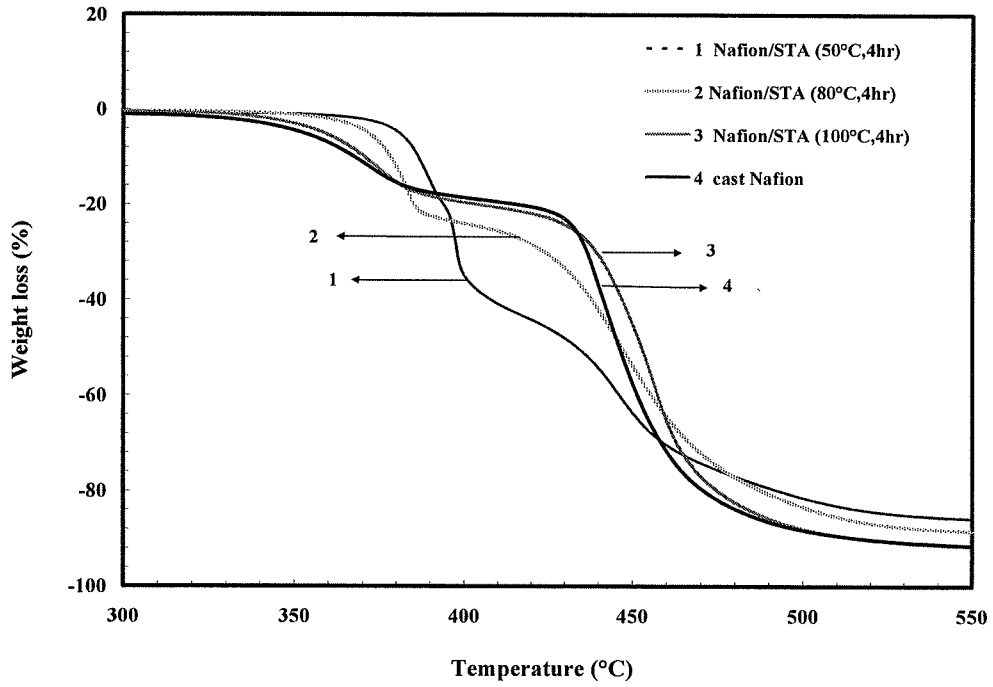

Figure 3- 28. TG curves of composite Nafion/STA membrane immersed in deionized water under different temperatures.

By comparing the TG curves of above composite membranes with that of the cast Nafion without STA (cast Nafion), we can find that the first step degradation temperature of the composite membrane decreases with the increase of the immersion

temperature. From the previous results, we know that the [STA] in the composite membrane decreases with the increase of the immersion temperature. Accordingly, the first step degradation temperature of the composite membrane decreases with the decrease of the [STA] in the membrane. Since the first step degradation corresponds to the reaction/or degradation of the sulfuric acid groups, the existence of STA in the composite membrane has an influence on the degradation of the sulfuric acid groups. This suggests that there is a specific interaction between the STA and the sulfuric acid which can contribute to an increase of the initial thermal stability of the cast Nafion with STA membrane. This is in good agreement with the results of the XPS which shows the existence of *W-S* link between the Nafion and STA (see section 3.7).

3.5. X-RAY STUDIES OF THE COMPOSITE MEMBRANE

The wide-angle X-ray diffraction (WAXD) technique was used to investigate crystallinity of composite membranes. Experiments were conducted on the films (0.1-0.2 *mm* thick) from the composite Nafion/STA membrane and cast Nafion without STA membrane. To obtain x-ray diffraction results of swollen and hydrolyzed sample or dry and dehydrated sample, the samples had to be dried in vacuum oven at $70\,^{\circ}C$ overnight or immersed in deionized water for 24 hours before they were used for x-ray analysis. Fig. 3-29 shows the WAXD spectra for the membranes mentioned above.

From Fig. 3-29, we can observe that all the membranes showed crystalline peaks for the perfluorocarbon backbone at $2\theta = 17.65$. This value is in good agreement with those measured using commercial Nafion 117 [135]. We also find that the intensity of this crystalline peak ($2\theta = 17.65$) of the dried cast Nafion (curve 1) is higher than that of the wet cast Nafion (curve 2). This indicates that the water content can affect the crystallinity of the cast Nafion membrane. In Nafion perfluorinated ion-exchange membrane, the ion exchange sites are generally observed to aggregate and form clusters. These ionic clusters have some effects on the membrane properties. The difference in

the crystalline peak intensity of the Nafion membrane may be due to less aggregation of the ion exchange site in the presence of water and leads to the decrease of the ionic clusters. The non-variation of the portion of the peak ($2\theta = 17.65$) for dried and wet membranes implies that the presence of water does not change the membrane crystalline structure. Although the crystallinity does slightly decrease upon hydrolysis, it is clear the hydrolyzed membrane is still partially crystallized. Thus, any ionic cluster existing in the polymer does not completely disturb the crystalline portion of the matrix. However, it can cause some changes on the amount of crystallines. This phenomenon can also be observed from Fig. 3-29 (curve 3 and curve 4). The ionic clusters can be studied using small-angle X-ray scattering (SAXS) technique. The size of the ionic cluster in the membrane can be calculated from the Bragg spacing and water content using Gierke's cluster-networking model [135]. This work is still under progress.

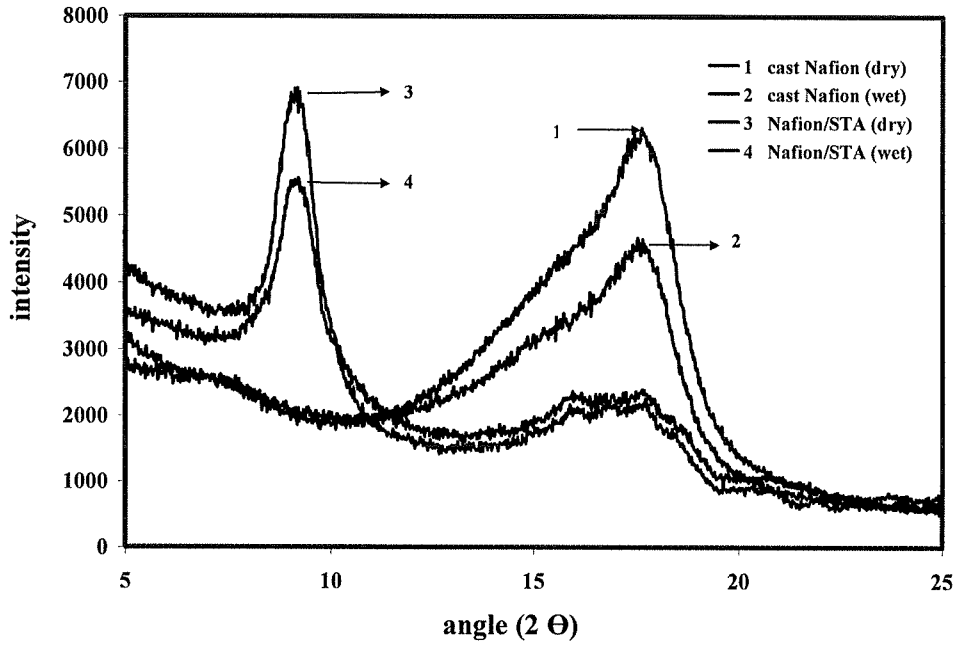

Figure 3- 29. Wide-angle X-ray diffraction spectra for the composite Nafion/STA, cast Nafion without STA in wet and dry conditions.

For the cast Nafion membrane with STA (curve 3 and curve 4), the intensity of the peaks at 2θ = 17.65 is very small. This means that the crystalline phase concentration of Nafion (2θ = 17.65) dramatically decreases in the composite membrane when STA is added into the membrane. Meanwhile, a new crystalline peak is observed at 2θ = 9.20. In order to study the effect of STA in the composite membrane, the X-ray Spectrum for STA is presented in Fig. 3-30. From the Fig. 3-30, we can see that the value of 2θ correspondents to the position of the peaks can be observed at 6.61, 7.97, 15.95, 18.13, 20.91, 22.87 and 23.71 for STA sample. Therefore, the crystalline peaks observed at 2θ = 15.96 for cast Nafion with STA membrane suggest that the STA remains present in the membrane matrix. The new crystalline peak at 2θ = 9.20 obtained from Fig. 3-29 should correspond to the interaction between the STA and Nafion. This agrees with the XPS results which showed the existence of *W-C* and *W-S* links between Nafion and STA (see section 3.7). The presence of the Silicontungstic Acid in the polymer matrix can explain the improvements of the conductivity and water uptake. Furthermore, it can also allow us to expect better fuel cell performances using the composite membranes.

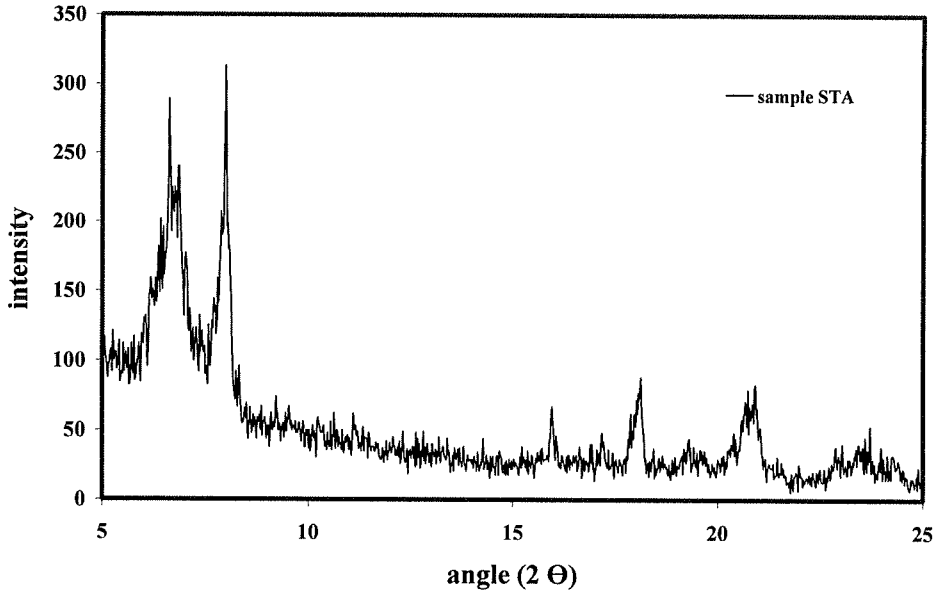

Figure 3- 30. Wide-angle X-ray diffraction spectra for STA

3.6. MECHANICAL PROPERTIES OF THE COMPOSITE MEMBRANES

An Instron (model 4400R) was used to investigate the tensile properties of the composite Nafion/STA membranes. The composite membranes were dried in vacuum oven at 70 °C for 12 hours and subsequently the specimens with a thickness of 180 μm were prepared according to ASTM D882-02. At least 5 specimens were tested for each sample and all the specimens were measured under the room temperature.

The Young's modulus, stresses (at break) and strains (at break) of the different composite membranes are summarized in Table 3-8. We may see that the maximum stress at break decreases slightly when the concentration of the STA increases. From the results of Table 3-8, it is worth noting that the stress of the commercial Nafion 117 (26.7 MPa) is higher than that of the cast Nafion (18.0 MPa) with the same thickness (~180 μm). The Young modulus of the cast membrane (362.67 MPa for Nafion without STA) is higher than that of commercial Nafion 117 (138.55 MPa). The strain at break of commercial Nafion 117 (450%) is larger than those of cast Nafion with or without STA (90.20% ~22.20%). The difference of mechanical properties observed between the cast Nafion and the commercial Nafion 117 can be attributed to the difference of the method of the membrane casting and the effect of STA. The addition of STA may increase the cristallinity of the cast membrane which may correspond to a high young modulus and a low strain at break. So when the concentration of the STA increases in the membrane, the strain at break and the maximum stress at break will decrease even though the effect is less important on the latter parameter. The Young modulus increases with the STA concentration. In other words, with the addition of certain amount of STA, the composite membrane becomes more rigid and crystalline (as shown by the XRD study) and the ductility deteriorated. These may indicate the existence of some specific interactions, which will be confirmed later by XPS, between the STA and the sulphonic acid group in the composite membrane. Therefore, in comparison to the cast Nafion with or without STA membranes, Nafion 117 exhibits higher maximum stress and strain

(at break). However, it has lower Young moudulus. The Nafion 117 membrane is less regid but has very good ductility.

Table 3- 8. The mechanical properties of composite Nafion/STA membranes.

Sample	Max. stress at break (MPa)	Young Modulus (MPa)	Strain at break (%)
NB	18.98	362.67	90.20
NS1	17.15	364.04	86.4
NS2	16.72	484.07	22.20
NF	26.78	138.55	450.00

NB: Cast Nafion without STA membrane;

NS1: Nafion/STA membrane (concentration of STA is $1\times10^{-3}M$);

NS2: Nafion/STA membrane (concentration of STA is $5\times10^{-3}M$);

NF: Commercial Nafion 117 membrane.

3.7. CHARACTERIZATION OF THE COMPOSITE MEMBRANES BY THE FOURIER TRANSFORM INFRARED SPECTROSCOPY (FTIR)

Specific interaction between STA and composite membranes, which represents one of the most important factors influencing the miscibility and electrochemical properties of the composite membrane, will be further elucidated by FTIR spectroscopy.

Before FTIR measurements, the composite Nafion/STA, composite Flemion/STA, cast Nafion without STA and cast Flemion without STA membranes had been dried in vacuum oven at 70°C overnight. Figs. 3-31 and 3-32 display the characteristic bands of above composite membranes. The frequencies are from 1400 cm^{-1} to 700 cm^{-1}. The absorption band located at 1056 cm^{-1} for Nafion-based membrane and 1057 cm^{-1} for the Flemion-based membrane were assigned to the symmetric stretch of

C-O-C in the composite membrane structure [136]. This band was insensitive to the addition of the STA. The symmetric stretch of SO_3 is observed at 1021 cm^{-1} [137] in cast Nafion without STA and cast Flemion without STA membranes and red shifted to 1017 cm^{-1} when the polymer membrane was blended with STA. This result indicates that STA can affect the characteristic band position of SO_3 group and there may have the interaction between STA particles and the sulfuric acid. Table 3-9 shows the infrared assignments of composite membrane [136,137,138,139].

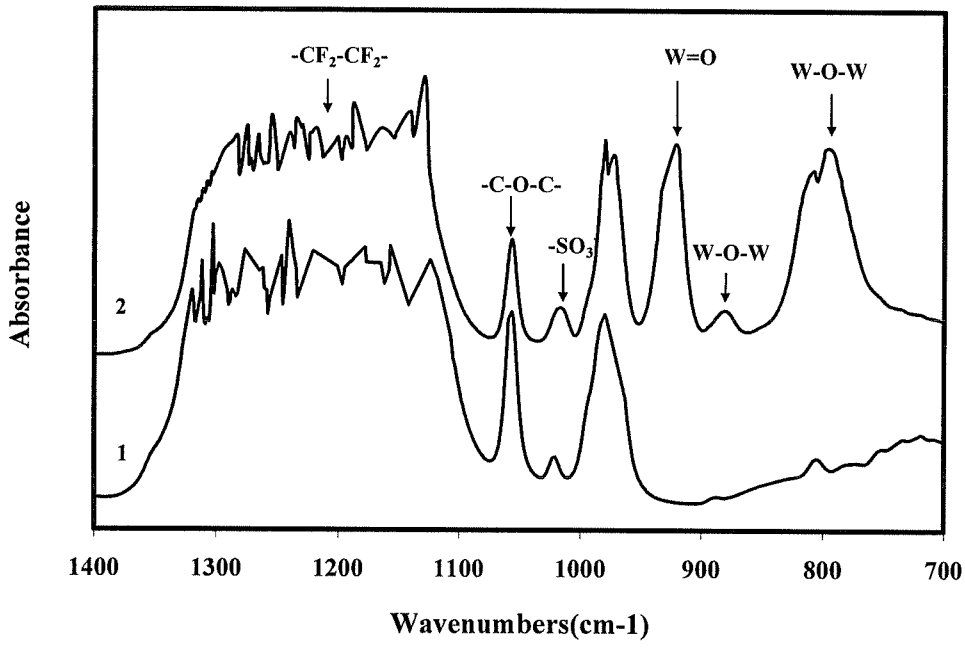

Figure 3- 31. FTIR spectra of cast Nafion without STA membrane (1) and composite Nafion/STA membrane (2).

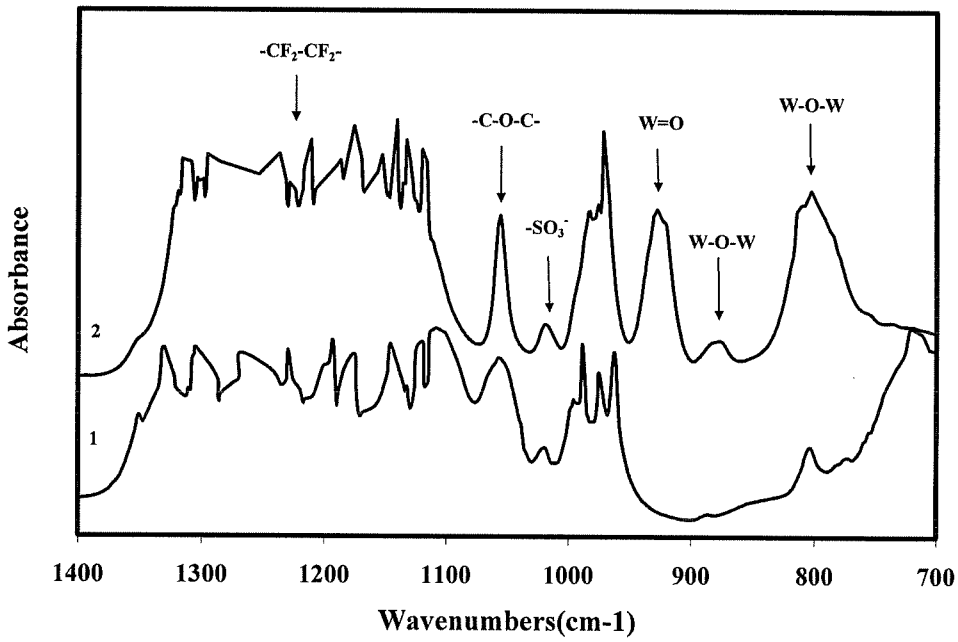

Figure 3-32. FTIR spectra of cast Flemion without STA membrane (1) and composite Flemion/STA membrane (2).

Table 3- 9. Infrared assignments of the composite membrane.

Sample	Wave number (cm^{-1})					
	$-(CF_2-CF_2)-$	$-SO_3^-$	C-O-C	$W=O_t$	$W-O_c-W$	$W-O_e-W$
Cast Nafion Without STA	1100-1375	1021	1056			
Nafion/STA	1100-1375	1017	1056	922	881	795
Cast Flemion Without STA	1100-1375	1020	1057			
Flemion/STA	1100-1375	1017	1056	928	877	803

* O_t is the terminal oxygen, O_c is the bridging oxygen of corner-shared octahedral, O_e is the bridging oxygen of edge-shared octahedral [112].

The frequency regions 1100 – 1375 cm^{-1} are assigned to the band -$(CF_2$-$CF_2)$- [137]. However, it is difficult to investigate the effect of STA on -$(CF_2$-$CF_2)$- band because the region correspond to the -$(CF_2$-$CF_2)$- is very wide. The interaction between STA and main-chain of polymer will be elucidated by XPS experiment.

The IR spectra of the composite Nafion/STA and Flemion/STA membranes have clearly shown the existence of STA in composite membranes. For the Keggin unit of STA, several distinct components should have the characteristic band at 1010-930 cm^{-1} (W=O), 900-870 cm^{-1} (W-O_c-W) and 850-700 cm^{-1} (W-O_e-W) [138]. In curve 2 of Figs. 3-31 and 3-32, we can find that the bands at 922 cm^{-1}(W=O) for Nafion/STA membrane and 928 cm^{-1}(W=O) for Flemion/STA membrane, 881 cm^{-1} (W-O_c-W) for Nafion/STA membrane and 877 cm^{-1} (W-O_c-W) for Flemion/STA membrane, 795 cm^{-1} (W-O_e-W) for Nafion/STA membrane and 803 cm^{-1} (W-O_e-W) for Flemion/STA membrane. This corresponds to the structure of STA. According the results of the FTIR spectra, it is confirmed that the STA is inserted in the polymer matrix.

3.8. CHARACTERIZATION OF COMPOSITE MEMBRANE BY X-RAY PHOTOELECTRON SPECTROSCOPY (XPS)

The x-ray photoelectron spectroscopy (XPS) is a powerful technique for chemical analysis. For a typical XPS investigation where the surface composition is unknown, a broad scan survey spectrum should be firstly done. This survey spectrum is used to identify the surface element composition. Once the surface element composition is determined, detailed scans of selected peaks can be used for a more comprehensive picture of the chemical composition. In this study, the composite membranes were evaluated by both survey and detail scans to analyze the chemical composition and the chemical state of different elements in the composite membranes.

3.8.1. SURVEY SCANS AND CHEMICAL COMPOSITION OF COMPOSITE MEMBRANE

The samples of Nafion/STA and Flemion/STA membranes had been exposed under high vacuum (10^{-8} *Torr)* for 24 hours before XPS measurements. The XPS spectra were recorded with a scan range of 1200 *eV* ~ 0 *eV* (*Mg* excitation) binding energy. The survey spectra of composite Nafion/STA membrane, cast Nafion without STA membrane, composite Flemion/STA membrane and cast Flemion without STA membrane are presented in Figs. 3-33, 3-34, 3-35 and 3-36. The lines observed in these spectra are identified by comparing them to the standard XPS spectra of elements [131,140]. The peak positions are respectively located at the binding energies of 690.0 *eV*, 533.0 *eV*, 402.0 *eV*, 285.0 *eV*, 170.0 *eV* and 36.0 *eV*. These positions respectively correspond to the elements of Fluorine (*F*), Oxygen (*O*), Nitrogen (*N*), Carbon (*C*), Sulfur (*S*) and tungsten (*W*). In addition, the peaks located at the binding energies of 599 *eV* and 625 *eV* are Auger lines. Auger lines have kinetic energies which are independent of the ionizing radiation. They appear on a binding energy plot to be in different positions when ionizing photons of different energies (i.e. different x-ray source) are used.

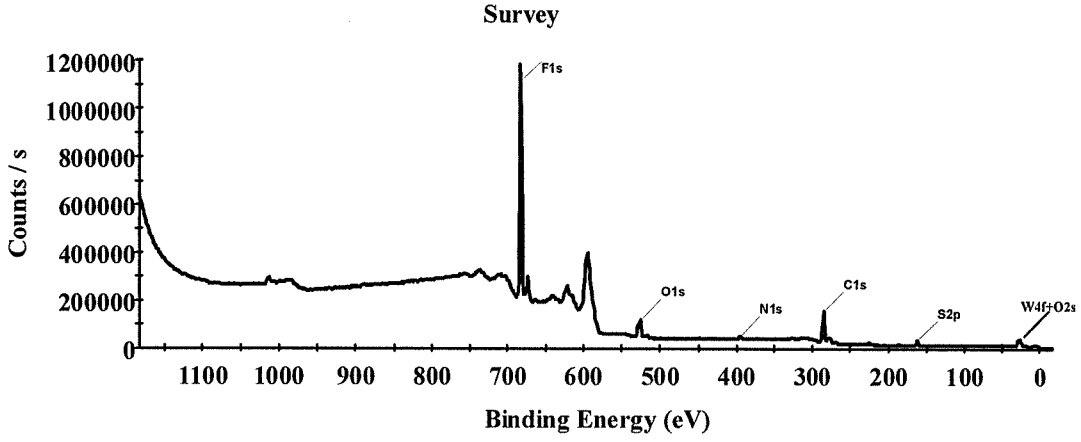

Figure 3- 33. XPS survey spectra of composite Nafion/STA membrane.

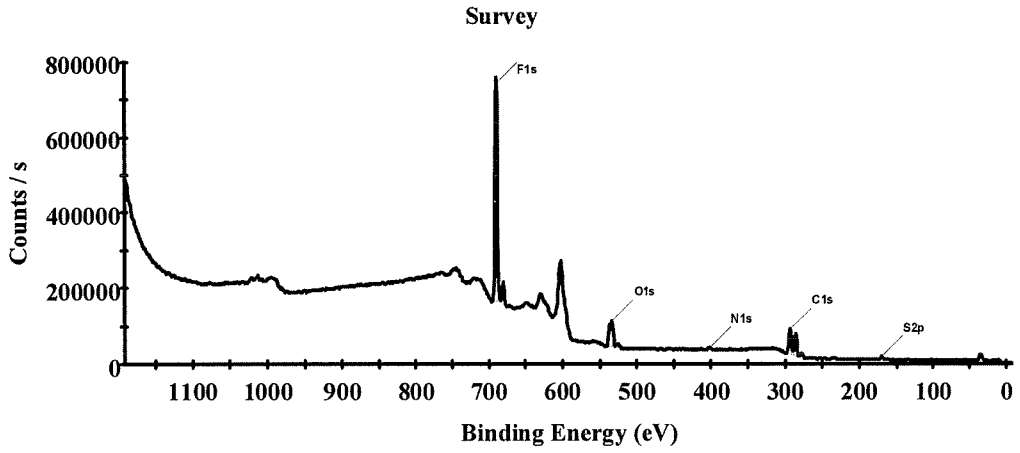

Figure 3- 34. XPS survey spectra of cast Nafion without STA membrane.

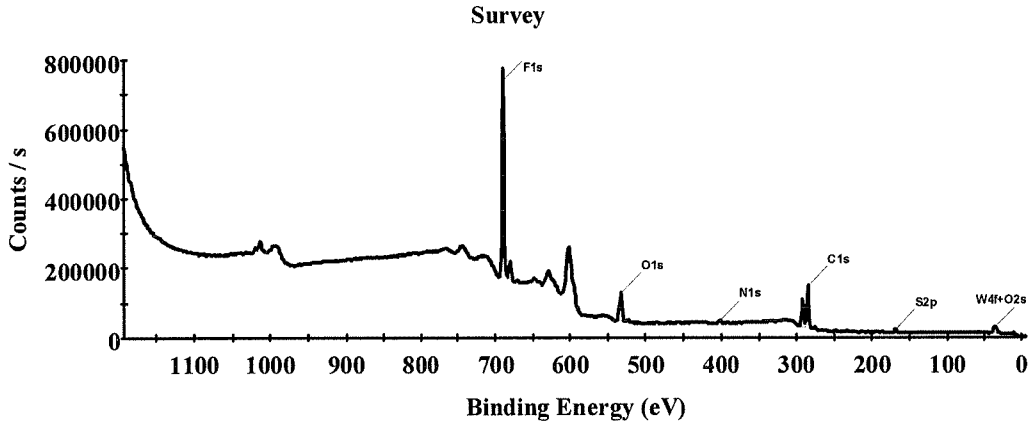

Figure 3- 35. XPS survey spectra of composite Flemion/STA membrane.

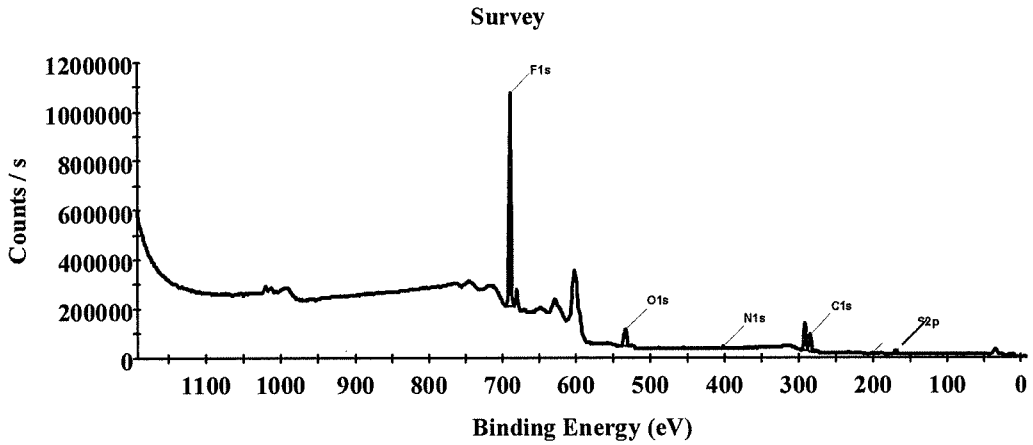

Figure 3- 36. XPS survey spectra of cast Flemion without STA membrane.

Table 3-10 summarizes the results of the line identification which show the chemical composition of the membranes and the relative concentration of the various elements. It can be found that Fluorine (*F*), Oxygen (*O*), Nitrogen (*N*), Carbon (*C*) and Sulfur (*S*) exist in each membrane. However, Tungsten (*W*) only appears in the spectra of Nafion/STA membrane and Flemion/STA membrane. The observation of *W* in the survey spectra of the composite Nafion/STA and Flemion/STA is an indication of the presence of STA species in the composite membrane. Unfortunately, the XPS spectra do not show the binding energy associated to the presence of silicon (*Si*) in the sample. This may be due to the lower concentration and the weak sensitivity of Silicon. The XPS sensitivity factor of *Si* is 0.27 whereas that of *W* is 2.75.

Table 3- 10. The surface chemical composition of the composite membranes.

Name	Centre BE (eV)	Relative atomic %					Sensitivity factor (SF)
		Nafion without STA	Nafion /STA	Flemion without STA	Flemion /STA	Nafion 117*	
F1s	690.0	52.5	49.3	51.8	49.8	60.0	1.00
O1s	533.0	9.6	12.6	9.0	11.6	7.6	0.66
N1s	402.0	1.0	1.6	0.9	1.7		0.42
C1s	285.0	35.8	34.6	36.9	34.9	30.8	0.25
S2p	170.0	1.1	1.0	1.4	1.3	1.5	0.54
W4f	36.0	-	0.8	-	0.6		2.75

* by M. Schulze, M. Lorenz, N. Wagner, E. Gulzow [141].

The atomic percentage concentrations of the elements detected in the cast membranes with and without STA are also presented in table 3-10. The atomic concentrations of the various elements in the cast Nafion without STA membrane are

52.5%, 9.6%, 1.3%, 35.8% and 1.1% for Fluorine (*F*), Oxygen (*O*), Nitrogen (*N*), Carbon (*C*) and Sulfur (*S*), respectively. Similar results were obtained with cast Flemion without STA membrane. These values are slightly different from those obtained elsewhere [141] where the following atomic concentrations were obtained for Nafion: Fluorine 60%, Oxygen 7.6%, Carbon 30.8% and Sulfur 1.5%. The difference in the elements atomic concentration between the cast Nafion without STA and the commercial Nafion could be attributed to the effect of the solvent and DMF used to prepare the cast membrane.

3.8.2. DETAIL SCAN AND THE CHEMICAL STATE IDENTIFICATION OF ELEMENTS IN THE COMPOSITE NAFION/STA MEMBRANE AND FLEMION/STA MEMBRANE

The detail scanning XPS spectra of F_{1s}, O_{1s}, C_{1s}, S_{2p} and W_{4f} of the composite membranes are shown in Figs. 3-37, 3-38, 3-39 and 3-40. Moreover, tables 3-11 and 3-12 give the analytical results of the chemical state of the elements for the composite Nafion/STA and Flemion/STA membranes, respectively. In comparison, the analytical results of the chemical state of the elements for cast Nafion without STA membrane and cast Flemion without STA membrane are respectively presented in tables 3-13 and 3-14. **Avantage** from **VGScientific** is used for the data calculation. The full width of the half maximum (FWHM) average of each peak` from literature and from standard is used for the determination of the number of components under the various peaks. These binding energies are in agreement with those obtained by other authors in the literature [131,140,141,142] for the same species. It can be seen from tables 3-11 and 3-12 that various tungsten compounds, e.g. *W-C*, *W-S*, *W-F*, WO_2 and WO_3, are detected in both composite Nafion/STA and Flemion/STA membranes. The presence of the tungsten in the cast membranes with STA is an indication that the STA species is in the membranes.

From the results of *C* in tables 3-11 ~ 3-14, it can be seen that the *C-C* (285.0 *eV*), *C-O* (286.0 *eV*), *O-C=O* (288.5 *eV*), *C-F* (289.2-290.0 *eV*), *O-C-F* (289.2-290.0 *eV*), $-CF_2$ (291.9-292.9 *eV*) and $C-F_3$ (293-294 *eV*) bands were detected in all the membranes whereas *C-W* (284.3 *eV*) band can be detected in composite Nafion/STA and Flemion/STA membranes and *N-C=O* (287.2 *eV*) in cast Nafion without STA and cast Flemion without STA membranes. The bands of *C-C*, *C-O*, *C-F*, *O-C-F*, $-CF_2$ and $C-F_3$ are in agreement with the composition of Nafion and Flemion. The band of *C-W* is due to the interaction between the STA and Nafion or Flemion. The presence of the organic solvents like VCO and DMF during the preparation of the membranes may explain the presence of the binding energies of *O-C=O* and *N-C=O* in the spectra.

The analytical results of *F* indicate that the CF_x (289.0-289.8 e*V*), which corresponds to the backbone of Nafion and Flemion, can be observed in all the membranes.

The binding energy of the S_{2p} electrons is 170.3 *eV* whereas the polymer decomposition creates a new sulfur state at a binding energy of 165.5 *eV*. These can be attributed to $CF-SO_3$ and $C-SO_3$, respectively. The values of the binding energies of S_{2p} electrons obtained at 170.3 *eV* and 165.5 *eV* are in agreement with those of the literature [131,141].

The binding energies of the O_{1s} states are 533 *eV* and 535 *eV*. According to the data obtained by other research groups [131,140], these binding energies can be attributed to the oxygen in the sulfuric acid groups and the oxygen in the ether configuration. The SO_3 and *C-O-C* groups are detected in the membranes. The binding energy detected at 532 *eV* is related to the *C=O* group and may come from the organic solvent because we have verified that the cast membrane in aqueous electrolyte does not exhibit the *C=O* binding energy [103].

The *W* can only be detected in the composite Nafion/STA and Flemion/STA membranes. The peaks located in 32.2 *eV* and 33.5 *eV* respectively correspond to the binding energies of *W-C* and *W-S*. This may indicate that there have chemical interactions between the STA and the sulfuric acid, and also between the STA and the main-chain of the polymer. The binding energies of *W* which found at 32.2, 34.6 and 36.5 *eV* can be respectively attributed to WO_2, WO_3 and WO_4. The total atom percentages of *W* are 0.8% and 0.6% for composite Nafion/STA membrane and Flemion/STA membrane, respectively. Therefore, the certain amount of STA species can be introduced in the Nafion or Flemion structure.

3.8.3. CONCLUSIONS

The results of Thermal analysis, X-ray diffraction and FTIR analysis have shown the possible interactions between the STA and the polymer in the composite membrane. These interactions have been supported by the XPS analysis which has shown the presence of W-C and W-S bonds in the composite Nafion/STA or Flemion/STA membrane. These various results can be correlated to the performance of the H_2/O_2 PEMFC based on the composite Nafion/STA or Flemion/STA membrane.

The improvements of the conductivities for the Nafion/STA or Flemion/STA membranes can be proved to be due to the increase of proton sites concentrations coming from the introduction of the STA species in the composite membranes. The high protonic sites should correspond to the high conductivity. From the results of XPS study (see Table 3-10), we can obtain the total relative concentration of the active protonic sites which were considered from the the sulfuric acid group and the addition of STA species in the membranes for various membranes: 1.1% for cast Nafion (from SO_3^-), 1.27 % for composite Nafion/STA (from SO_3^- and STA), 1.4% for cast Felmion (from SO_3^-) and 1.5% for composite Flemion/STA (from SO_3^- and STA). This result is in agreement with the earlier results obtained in Table 3-5.

Table 3- 11. The analysis of chemical state of the elements for composite Nafion/STA membrane.

Name	Identification	Centre BE (eV)
*	Satellite Kα 3	281.9
*	Satellite Kα 4	283.6
C1	*C-W*	284.3
C2	*C-C*	285.0
C3	*C-O*	286.9
C4	*O-C=O*	288.5
C5	*C-F + O-C-F*	289.2
C6	$C\text{-}F_2$	292.0
C7	$C\text{-}F_3$	293.7
F	$C\text{-}F_x$	689.0
O1	*?*	531.8
O2	*C=O*	532.7
O3	SO_3	533.7
O4	*C-O-C*	535.1
O5	*?*	536.0
W1	*W*	30.9
W2	$W\text{-}C + WO_2$	32.2
W3	*W-S*	33.4
W4	WO_3	34.6
W5	WO_4	36.1
W6	*W-F*	37.6
S1	$C\text{-}SO_3$	165.6
S2	$CF_x\text{-}SO_3$	170.8

Table 3- 12. The analysis of chemical state of the elements for composite Flemion/STA membrane.

Name	Identification	Centre BE (eV)
*	Satellite Kα 3	281.8
*	Satellite Kα 4	283.5
C1	*C-C*	285.0
C2	*C-O*	286.7
C3	*O-C=O*	288.5
C4	*C-F + O-C-F*	289.8
C5	$C\text{-}F_2$	291.9
C6	$C\text{-}F_3$	293.5
F	$C\text{-}F_x$	689.2
O1	*C=O*	532.2
O2	SO_3	533.0
O3	H_2O adsorbed	534.1
O4	*C-O-C*	535.2
O5	*?*	536.0
W1	$W\text{-}C + WO_2$	32.2
W2	*W-S*	33.5
W3	WO_3	34.8
W4	WO_4	36.5
S1	$C\text{-}SO_3$	165.7
S2	$CF_x\text{-}SO_3$	169.6

Table 3- 13. The analysis of chemical state of the elements for cast Nafion without STA.

Name	Identification	Centre BE (eV)
C1	*C-C*	285.0
C2	*C-O*	286.0
C3	*N-C=O*	287.2
C4	*O-C=O*	288.5
C5	*C-F + O-C-F*	290.0
C6	$C\text{-}F_2$	292.9
C7	$C\text{-}F_3$	294.3
F	$C\text{-}F_x$	689.8
O1	*C=O*	532.7
O2	SO_3	533.7
O3	H_2O adsorbed	534.6
O4	*C-O-C*	535.8
O5	*?*	537.0
S1	$C\text{-}SO_3$	165.5
S2	$CF_x\text{-}SO_3$	170.3

Table 3- 14. The analysis of chemical state of the elements for cast Flemion without STA.

Name	Identification	Centre BE (eV)
*	Satellite Kα 3	282.0
*	Satellite Kα 4	283.8
C1	*C-C*	285.0
C2	*C-O*	286.1
C3	*N-C=O*	287.3
C4	*O-C=O*	289.0
C5	*C-F + O-C-F*	290.0
C6	$C\text{-}F_2$	292.2
C7	$C\text{-}F_3$	294.1
F	$C\text{-}F_x$	689.3
O1	*C=O*	532.0
O2	SO_3	533.0
O3	H_2O adsorbed	534.0
O4	*C-O-C*	535.2
O5	*?*	536.2
S1	$C\text{-}SO_3$	165.4
S2	$CF_x\text{-}SO_3$	169.5

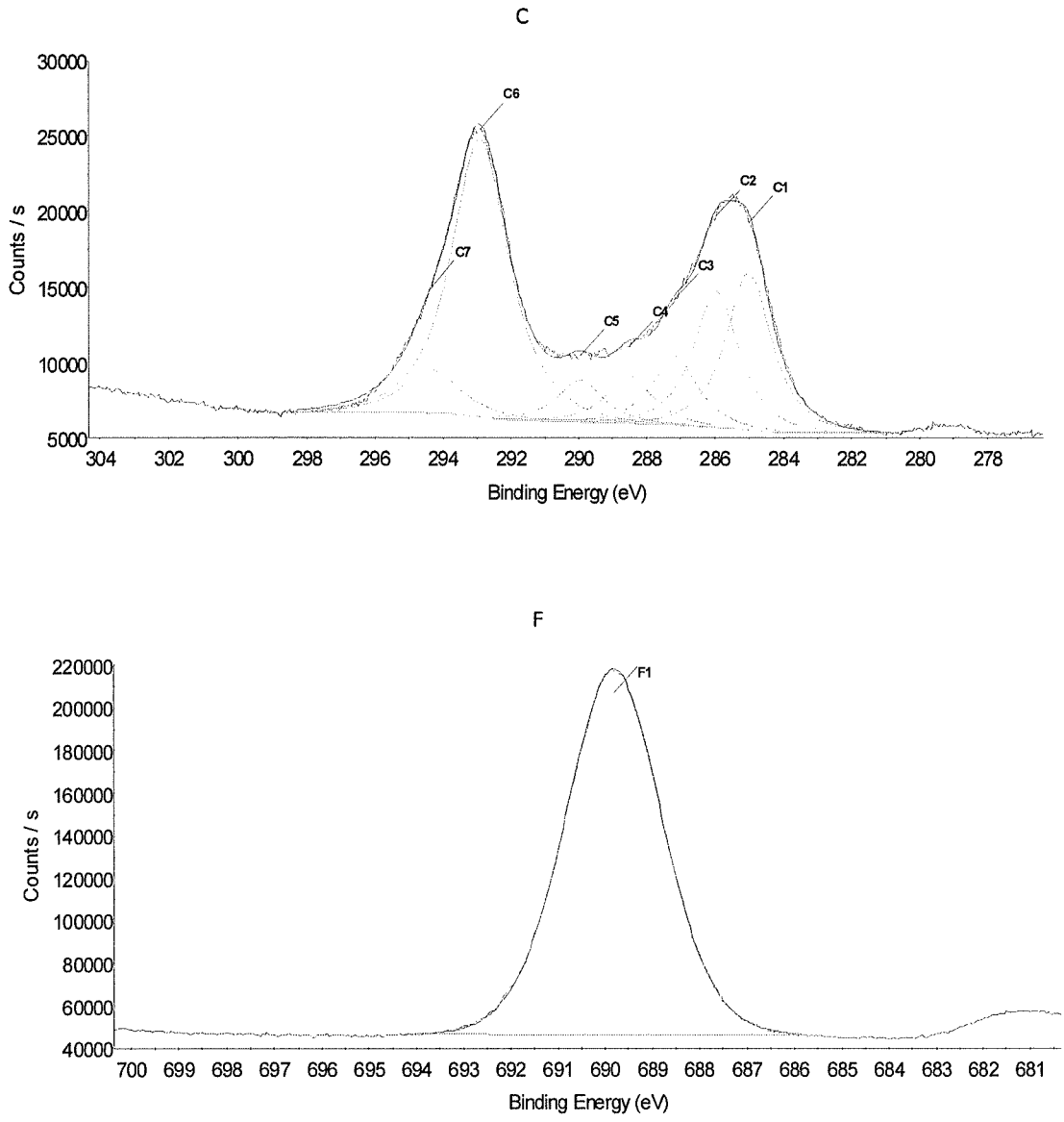

Figure 3-37. Spectral distribution of C_{1s}, F_{1s}, O_{1s}, S_{2p} of cast Nafion without STA membrane (suite).

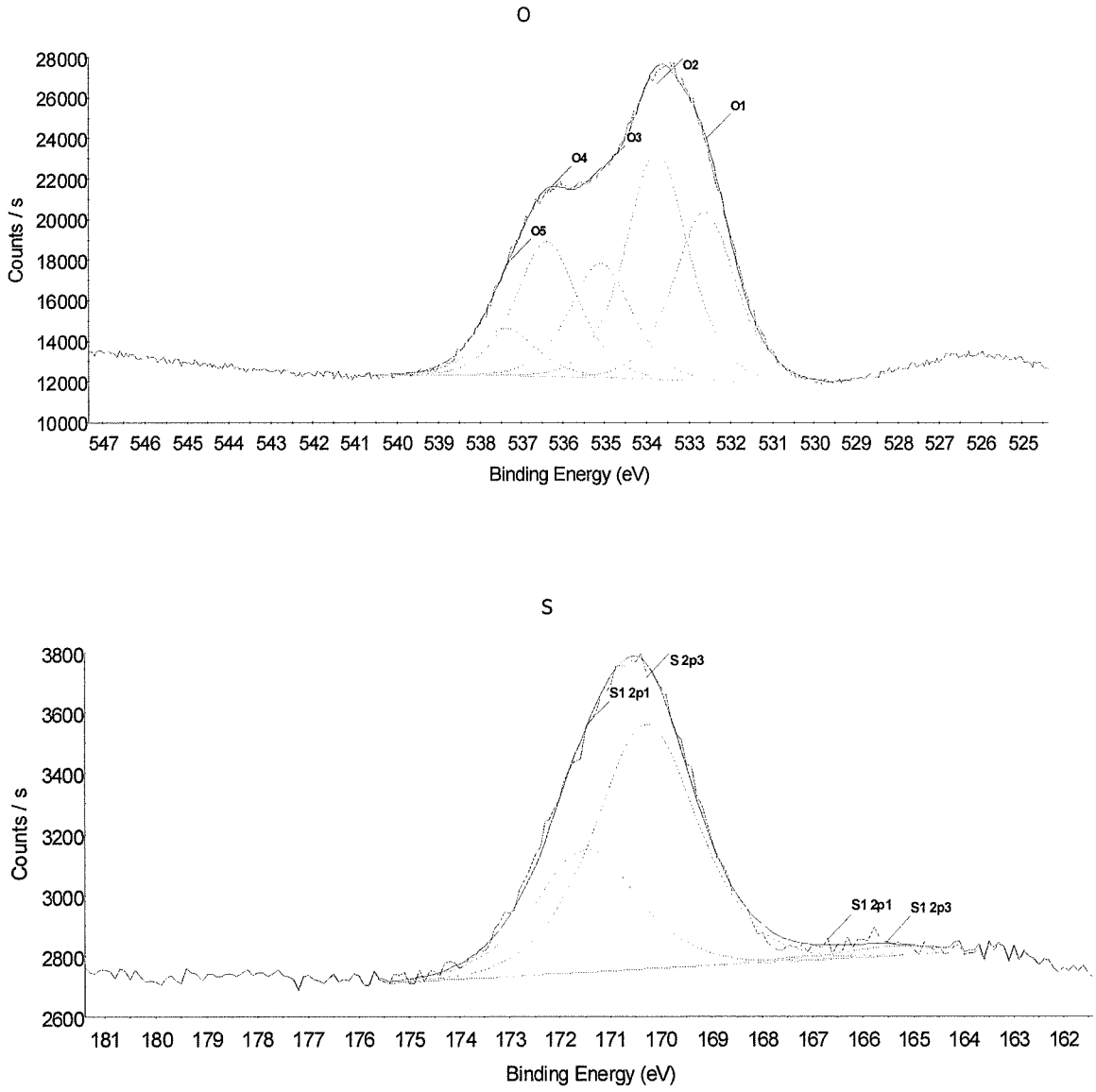

Figure 3- 37. (suite)Spectral distribution of C_{1s}, F_{1s}, O_{1s}, S_{2p} of cast Nafion without STA membrane.

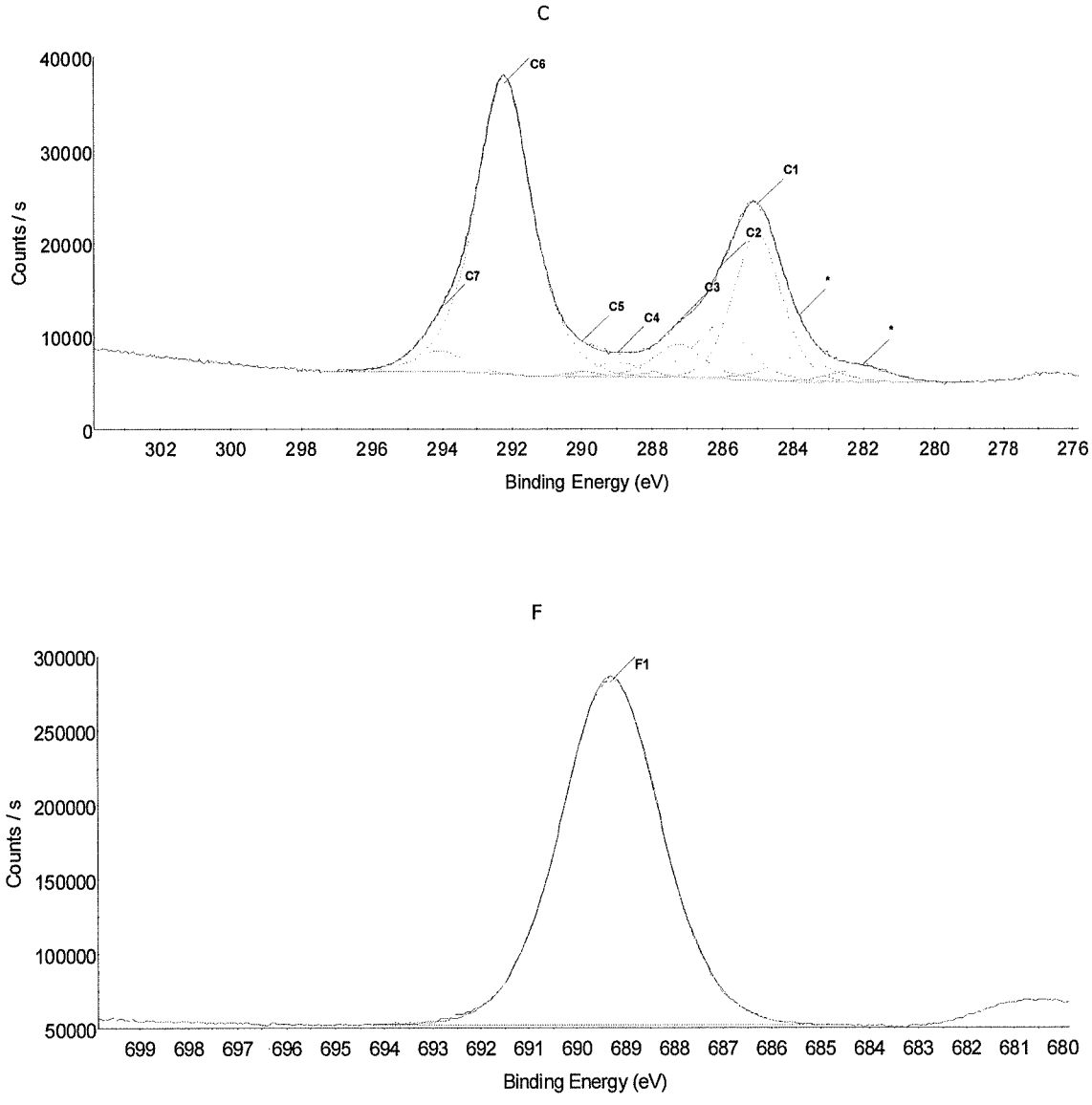

Figure 3-38. Spectral distribution of C_{1s}, F_{1s}, O_{1s}, S_{2p} of cast Flemion without STA membrane (suite).

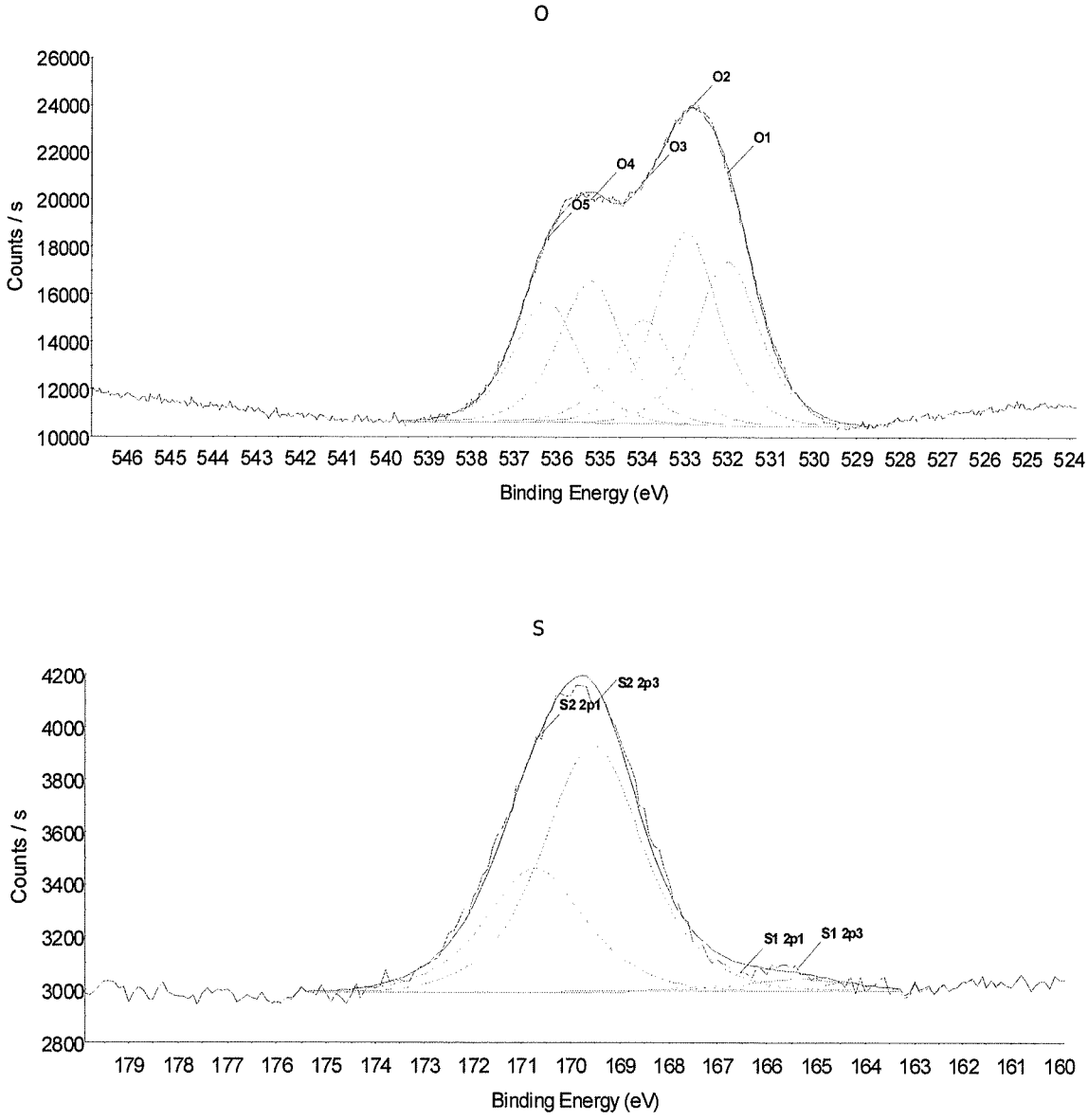

Figure 3- 38. (Suite)Spectral distribution of C_{1s}, F_{1s}, O_{1s}, S_{2p} of cast Flemion without STA membrane.

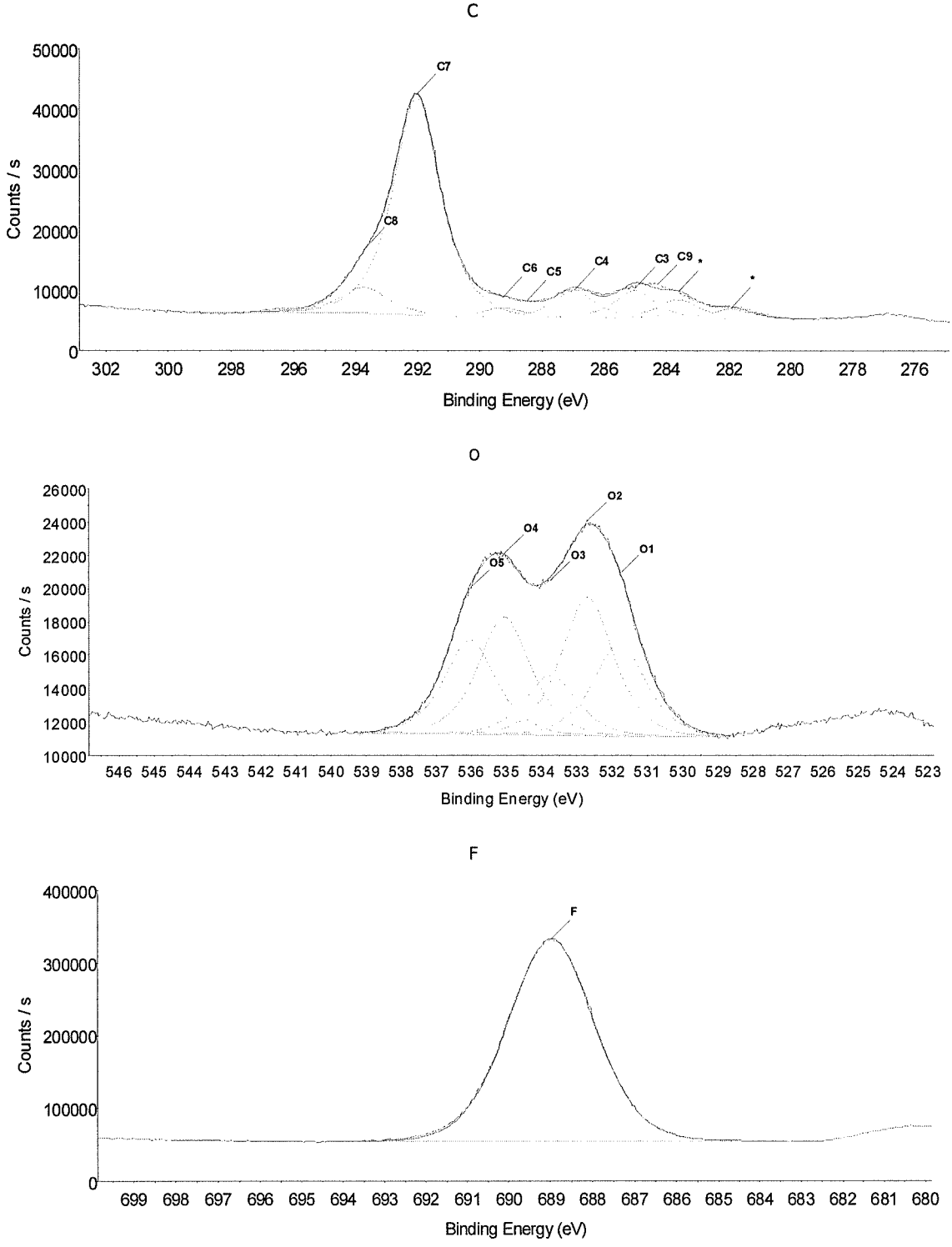

Figure 3-39. Spectral distribution of C_{1s}, O_{1s}, F_{1s}, S_{2p}, W_{4f} of composite Nafion/STA membrane (suite).

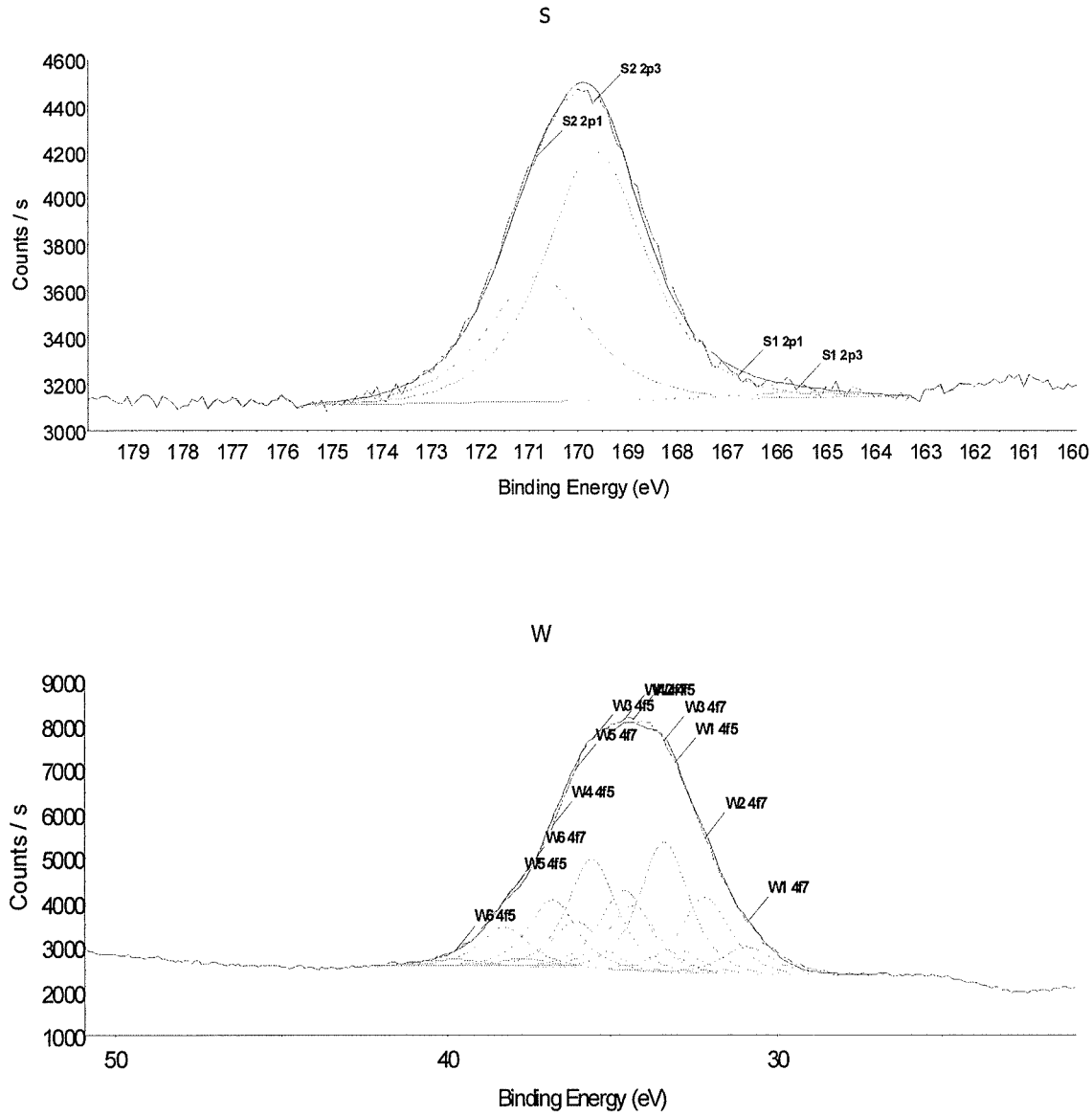

Figure 3- 39. (Suite) Spectral distribution of C_{1s}, O_{1s}, F_{1s}, S_{2p}, W_{4f} of composite Nafion/STA membrane.

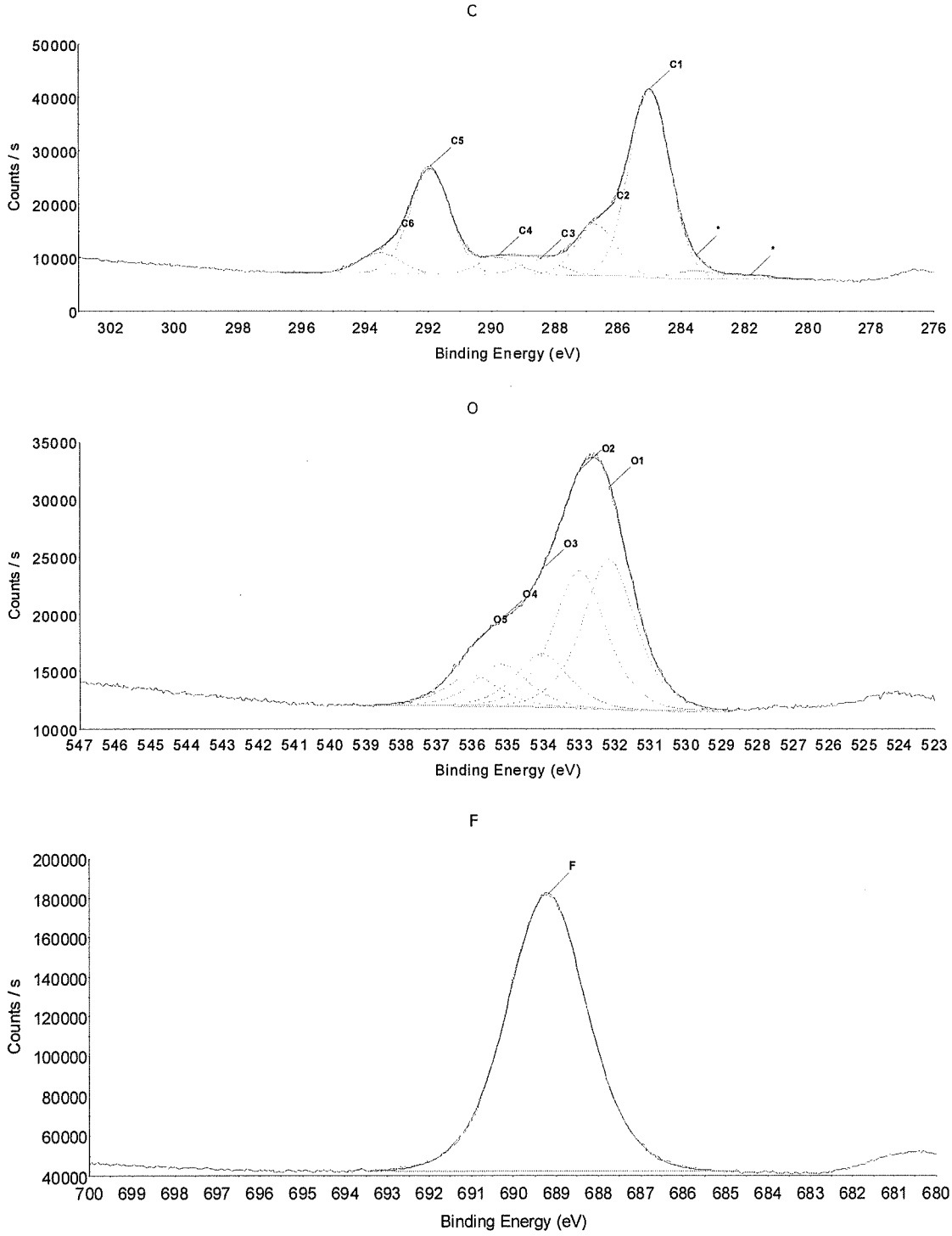

Figure 3-40. Spectral distribution of C_{1s}, O_{1s}, F_{1s}, S_{2p}, W_{4f} of composite Flemion/STA membrane (suite).

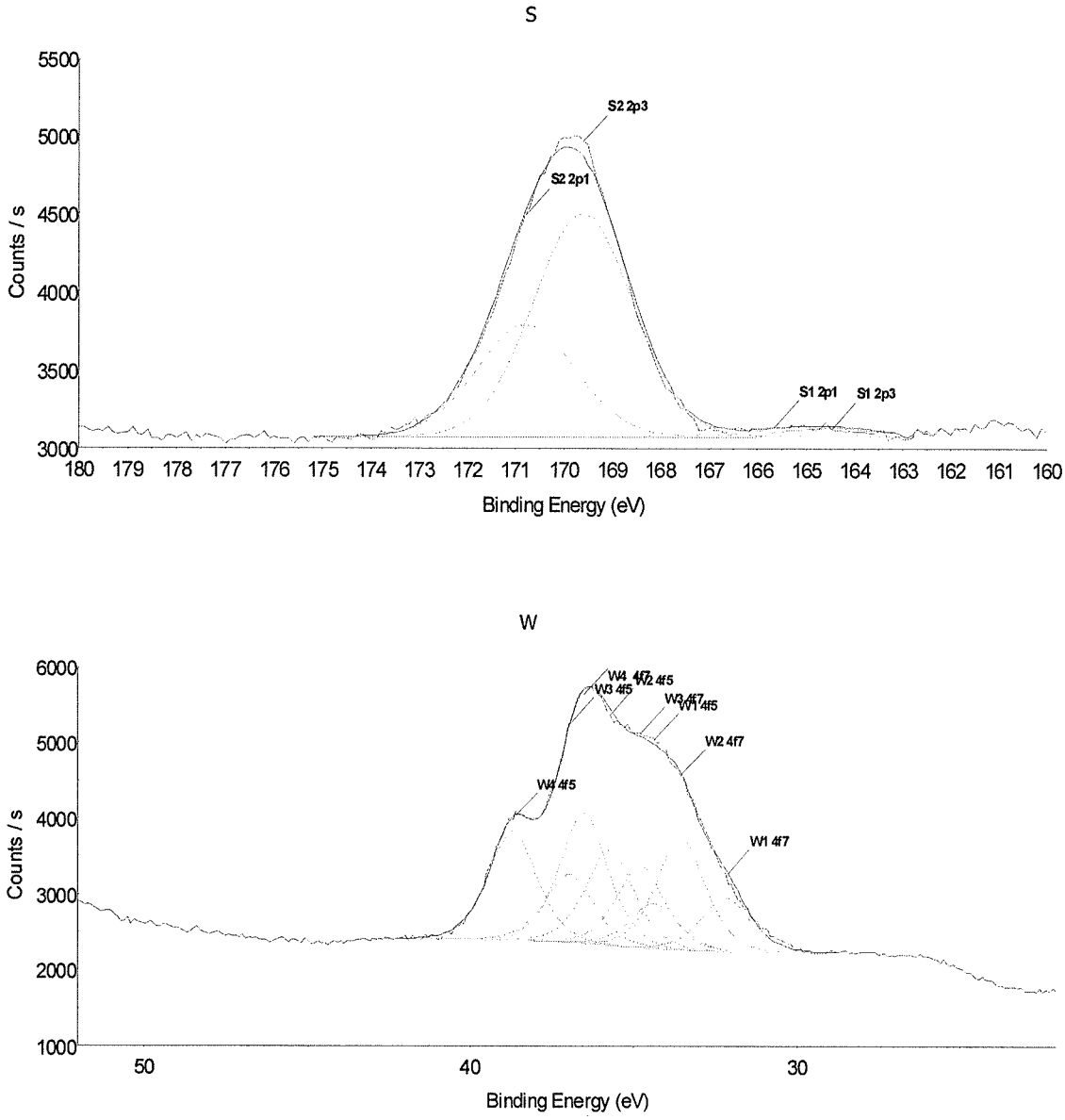

Figure 3- 40. (Suite) Spectral distribution of C_{1s}, O_{1s}, F_{1s}, S_{2p}, W_{4f} of composite Flemion/STA membrane.

3.9. PERFORMANCE OF THE H_2/O_2 PEM FUEL CELL BASED ON PERFLURINATED POLYMER/STA COMPOSITE MEMBRANES

The main objective of this study is to demonstrate the effects of STA on the composite Nafion/STA and Flemion/STA membranes for PEMFC applications. The fuel cell performances were compared for various composite membranes. The cell current–potential polarization curves were obtained using 2.25 cm^2 MEA which is made of the commercial carbon cloth gas diffusion electrode (E-TEK, 1 $mg\ Pt/cm^2$, 20 $\%\ Pt/C$) and the cast membranes with or without STA. These membranes were not pretreated. The electrode kinetics, mass transport and ohmic parameters can be obtained by fitting experimental data (current density versus cell potential) into equations (3) and (4) (see section 1.1.1).

3.9.1. CURRENT-POTENTIAL CHARACTERISTICS OF NAFION/STA MEMBRANE

The current-potential polarization curves based on cast Nafion with and without STA at different pressures are shown in Figs. 3-41~3-43 and the corresponding cell temperatures are 50°C, 80°C and 110°C, respectively. The pressures used for both H_2 and O_2 are 1, 2 and 4 *atm,* respectively. The concentration of STA in the casting electrolyte solution is $3 \times 10^{-3}\ M$ for the membrane cast with STA. Althrough the conductivity of this membrane is lower than that of the membrane containing $5 \times 10^{-3}\ M$ concentration STA, it is more flexible and more suitable than the latter one for the electrode membrane assembly (MEA). The thicknesses of the cast Nafion with and without STA membranes are 140 μm and 124 μm respectively.

From Figs. 3-41~3-43, we can observe that the current density based on composite Nafion/STA membrane always exhibit a higher value than that based on the cast membrane without STA (cast Nafion). It is worth noting that the current density at

0.6*V* of MEAs based on composite Nafion/STA membrane is higher than that of the cast Nafion without STA. Table 3-15 shows the current densities of composite Nafion/STA membrane and the cast Nafion membrane without STA at cell potential of 0.6*V* under different conditions.

Table 3- 15. The current density of composite Nafion/STA and cast Nafion without STA membrane at 0.6 *V* cell potential under different conditions.

		$I_{(E=0.6V)}$ (mA/cm^2)		
Cell temperature (°C)	Pressure / Cast Nafion Membrane	1 *atm*	2 *atm*	4 *atm*
50°C	without STA	172	195	239
	With STA	314	336	426
	$\Delta I = I_{with\ STA} - I_{without\ STA}$	142	141	187
80°C	without STA	328	425	477
	With STA	455	574	708
	$\Delta I = I_{with\ STA} - I_{without\ STA}$	127	149	231
110°C	without STA	60	97	120
	with STA	164	194	261
	$\Delta I = I_{with\ STA} - I_{without\ STA}$	104	97	141

When the cell operating temperature is at 80°C, the current densities of MEAs made from composite Nafion/STA membrane and the cast Nafion without STA are 455 and 328 (1 *atm*) , 574 and 425 (2 *atm*), 708 and 477 mA/cm^2 (4 *atm*), respectively. In comparison to the cast Nafion without STA, the improvements in the cell current density at 0.6*V* are 127 (1 *atm*), 149 (2 *atm*) and 231 mA/cm^2 (4 *atm*) at 80°C for the composite Nafion/STA membrane. Furthermore, as the temperature is increased to

110°C, the current density differences between the composite Nafion/STA membrane and the cast Nafion without STA membrane are 104 (1 *atm*), 97 (2 *atm*) and 141mA/cm^2 (4 *atm*). That is to say, the current density improvement from composite Nafion/STA membrane to the cast Nafion without STA membrane is also quite significant at higher temperature even though the difference is not as large as that at 80°C. Accordingly, the effect of STA on the cell performance is quite significant.

In order to make the picture clearer, we plot the difference of the current density between the composite Nafion/STA membrane and the cast Nafion without STA membrane at the cell potential of 0.6 *V* under different conditions in Fig. 3-44. We may easily give the order of the current density improvements from high to low as follows: ΔI (at *80°C*) > ΔI (at *50°C*) > ΔI (at *110°C*) under 2 atm or 4 atm pressure and ΔI (at *50°C*) > ΔI (at *80°C*) > ΔI (at *110°C*) under 1 atm.

The electrode kinetic parameters for oxygen reduction and the values of *R* were evaluated by fitting the experimental data to Equation (3) and (4). The calculated results are presented in Table 3-16. This table shows the effect of cast Nafion with or without STA membrane on the parameters under different temperatures and pressures, when oxygen is used as the cathodic reactant.

From Table 3-16, we can observe that the resistance (*R*) of MEA based on the Nafion/STA membrane is less than that of MEA based on cast Nafion without STA, which is due to the high conductivity and high hydrated ability of STA. This is in agreement with the results that the ionic conductivities of the composite Nafion/STA are always higher than those of the cast Nafion without STA (see section 3.2). The overpotential (η) of the composite Nafion/STA is lower than that of cast NAfion at 400mA/cm^2 which can explain the results that the composite Nafion/STA exhibits better potential-current characteristics than the cast Nafion without STA in PEMFCs

Table 3-16. Electrode-kinetic parameters for PEMFC with Nafion-based membranes

	Cell temperature (°C)	*50°C*		*80°C*		*110°C*	
	Membrane / Pressure	Cast Nafion	Nafion /STA	Cast Nafion	Nafion /STA	Cast Nafion	Nafion /STA
E_0 *(V)*	1 *atm*	0.908	0.908	0.942	0.925	0.942	0.875
	2 *atm*	0.958	0.925	0.975	0.958	0.908	0.908
	4 *atm*	0.942	0.925	0.975	0.975	0.925	0.942
b (mV/dec)	1 *atm*	66.9	53.0	62.0	47.0	94.7	48.2
	2 *atm*	59.0	44.6	61.9	48.1	76.9	45.7
	4 *atm*	45.8	34.4	56.9	43.3	70.7	46.7
R *(ohm.cm^2)*	1 *atm*	0.904	0.549	0.543	0.429	2.75	0.975
	2 *atm*	0.913	0.610	0.487	0.386	1.49	0.991
	4 *atm*	0.990	0.555	0.435	0.360	1.42	0.872
$I_{(E=0.9V)}$ *(mA/cm^2)*	1 *atm*	1	1	1	10	1	-
	2 *atm*	8	11	15	22	1	1
	4 *atm*	8	18	16	30	1	12
$\eta_{(400mA/cm^2)}$ *(V)*	1 *atm*	0.597	0.358	0.382	0.295	-	0.546
	2 *atm*	0.597	0.365	0.355	0.273	-	0.498
	4 *atm*	0.532	0.305	0.325	0.266	0.780	0.472

application. It is well accepted that the variation of R is due to the charge-transfer resistance, ohmic resistance and mass-transfer resistance. The charge transfer resistance due to the hydrogen oxidation reaction has been found to be relatively small when platinum is used as an electrocatalyst with carbon supported. Even at about 2 A/cm^2, the charge transfer resistance is of the order of 0.25 $ohm\ cm^2$ for the hydrogen-oxygen fuel cell operated under 5 atm [132]. Therefore, the ionic resistance of the membrane and mass transport in the reaction interface must be the main contribution in the variation of R. The mass-transport resistance at low pressure which is evidenced by the R values, the low hydration of Nafion at low temperature and the high hydrated ability of STA may result in a big difference of the current density between the composite Nafion/STA membrane and cast Nafion without STA membrane at 0.6 V cell potential at 50°C and 1 atm. It is well known that the hydration of Nafion at 50°C is lower than that at 80°C and Nafion will dehydrate above 100°C, which leads to the lowest ionic resistance at 80°C and the highest ionic resistance at 110°C for the Nafion/STA membrane. In addition, the mass-transport resistance decreases with the increase of the pressure which is the routine way to overcome mass transport problems in fuel cell technology. So the combined effects of mass-transfer resistance at higher pressure and ionic resistance can explain the results that the order of current improvement at the cell potential of 0.6 V for Nafion/STA membrane is: ΔI (at $80°C$) > ΔI (at $50°C$) > ΔI (at $110°C$) under 2 atm or 4 atm pressure. The best fuel cell performance can be obtained at 80°C and 4 atm pressure when the MEA is based on the composite Nafion/STA membrane.

The Tafel slope b changes from 34.4mV/dec to 53.0 mV/dec for composite Nafion/STA membrane and from 45.8 mV/dec to 94.7 mV/dec for cast Nafion without STA membrane. The existence of STA can clearly affect the value of Tafel slope b. The Tafel slope of composite Nafion/STA membrane is lower than that of cast Nafion without STA (Table 3-16). The change of Tafel slope for the composite Nafion/STA indicates an influence of the active surface area or active sites or both, and an influence of charge transfer. These influences, coming from the existence of STA in composite

membrane, gives rise to a mixed activation/mass-transport control which is limited by the diffusion of oxygen through electrode, oxygen reduction reaction at the catalyst/electrolyte interface and transport of the proton in electrolyte and catalyst/electrolyte interface. A poor membrane/electrode interface due to membrane dehydration could be one of the reasons for the large value of Tafel slope obtained with MEA based on cast Nafion without STA. The decrease of b for MEA based on cast Nafion with STA is due to the significantly decreased dehydration of the membrane. From the results of Tafel slope b at 110°C, we may suspect that the membrane/electrode interface properties are improved when STA is introduced to the membrane structure.

The E_0 values for composite Nafion/STA membrane are lower than those of the cast Nafion without STA, which may be because the existence of STA affects the effective utilization of electrocatalysts and results in the decrease of the electrode reaction rate.

The current-power density curves of the composite Nafion/STA membrane and cast Nafion without STA membrane are also compared and presented in Figs. 3-41~3-43, 3-45 and Table 3-17. The power density based on composite Nafion/STA membrane is always higher than that based on composite membrane without STA (cast Nafion). The improvements in the cell power output at $0.6V$ are 77 (1 *atm*), 91 (2 *atm*) and 141 mW/cm^2 (4 *atm*), respectively, at $80°C$. And at $110°C$, the improvements in the cell power output at $0.6V$ are 64 (1 *atm*), 59 (2 *atm*) and 86 mW/cm^2 (4 *atm*), respectively. The results of fuel cell test can keep good reproducibility during 36 hours.

The improvement in the fuel cell characteristics for the composite Nafion/STA membrane is due to a combined effects of Nafion and STA. The existence of STA improves the fuel cell performance and makes this operation feasible under high temperature. The long-term tests are still under progress.

Table 3- 17. The power density at 0.6V cell potential for composite Nafion/STA and cast Nafion membrane under different conditions.

		$P_{(E=0.6V)}$ (mW/cm^2)		
Cell temperature (°C)	Pressure / Cast Nafion Membrane	1 *atm*	2 *atm*	4 *atm*
50°C	without STA	105	119	146
	With STA	191	205	260
	$\Delta P = P_{with\ STA} - P_{without\ STA}$	86	86	114
80°C	without STA	200	259	291
	With STA	277	350	432
	$\Delta P = P_{with\ STA} - P_{without\ STA}$	77	91	141
110°C	without STA	36	59	73
	with STA	100	118	159
	$\Delta P = P_{with\ STA} - P_{without\ STA}$	64	59	86

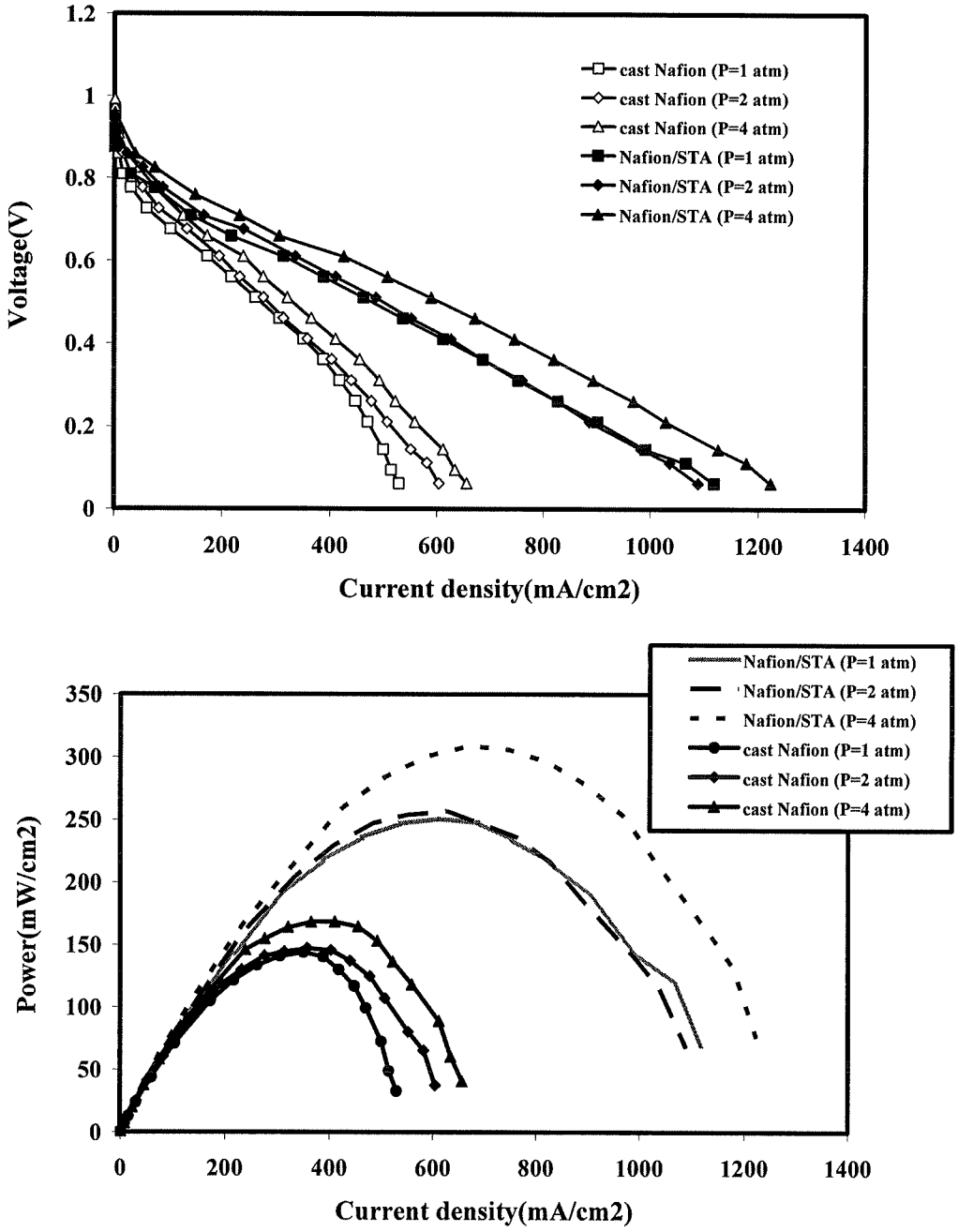

Figure 3- 41. Current-potential and current-power characteristics under different pressures for cast Nafion with or without STA membrane (Nafion/STA or cast Nafion) H_2/O_2 fuel cell, along with 20 % *Pt*-on-*C*, 1 *mg* Pt/cm^2, gas-diffusion electrodes. T *(humidifiers)* = 65 °C for *T(cell)* = 50 °C.

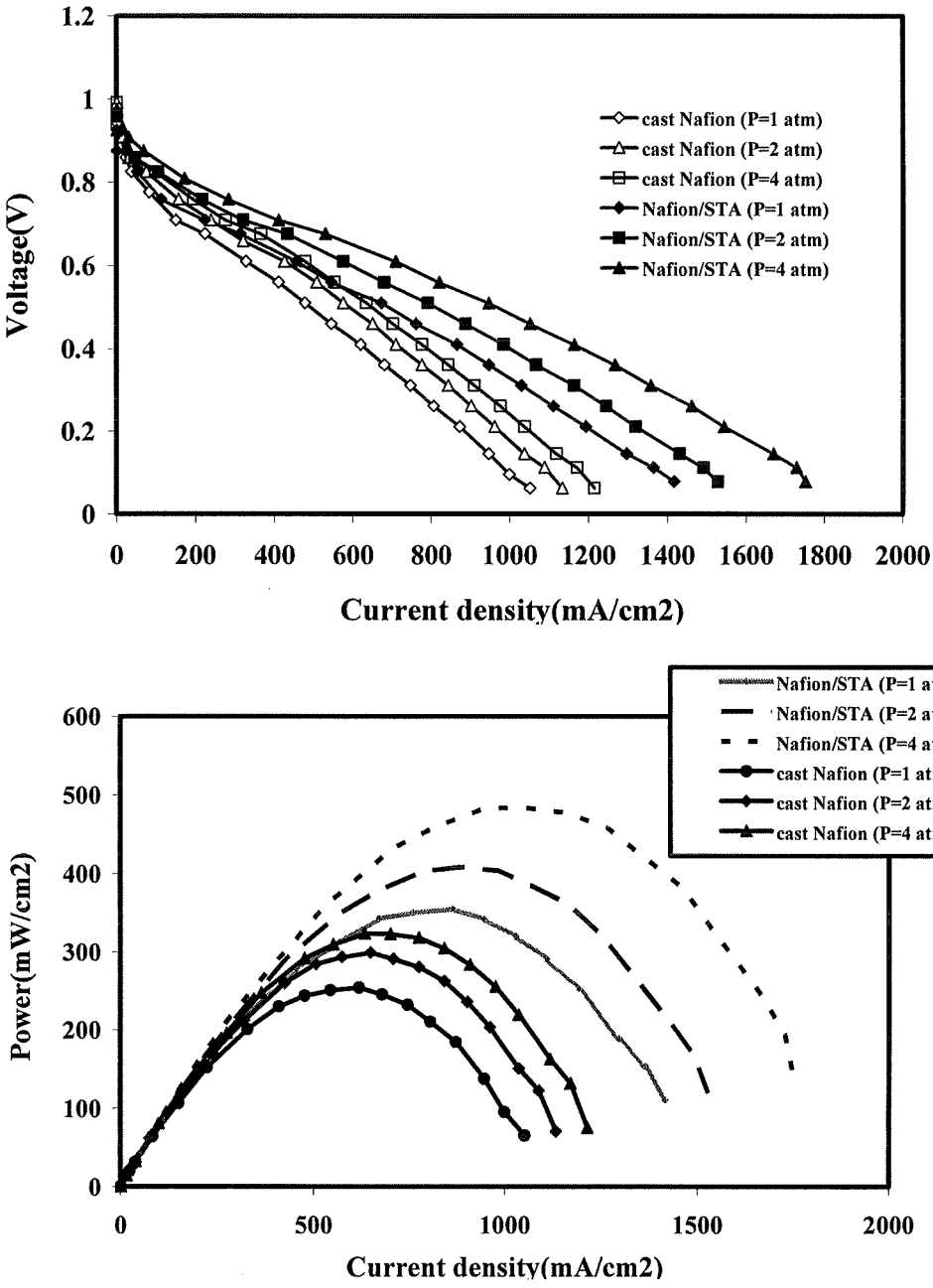

Figure 3- 42. Current-potential and current-power characteristics under different pressures for cast Nafion with or without STA membrane (Nafion/STA or cast Nafion) H_2/O_2 fuel cell, along with 20 *% Pt*-on-*C*, 1 *mg* Pt/cm^2, gas-diffusion electrodes. *T (humidifiers)* = 95 °*C* for *T(cell)* = 80 °*C*.

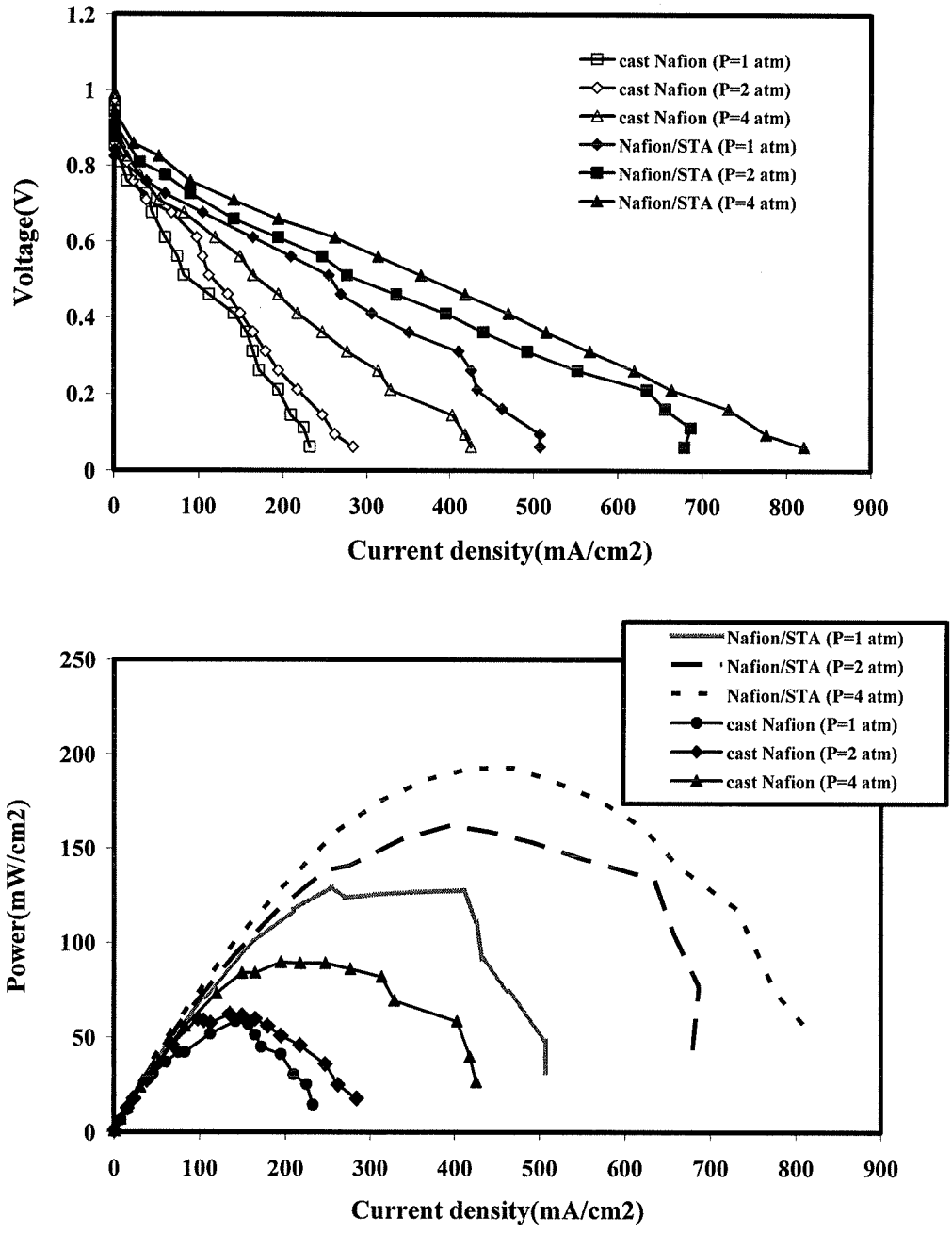

Figure 3- 43. Current-potential and current-power characteristics under different pressures for cast Nafion with or without STA membrane (Nafion/STA or cast Nafion) H_2/O_2 fuel cell, along with 20 *% Pt*-on-*C*, 1 *mg* Pt/cm^2, gas-diffusion electrodes. *T (humidifiers)* = 95 °*C* for T(cell) = 110 °*C*.

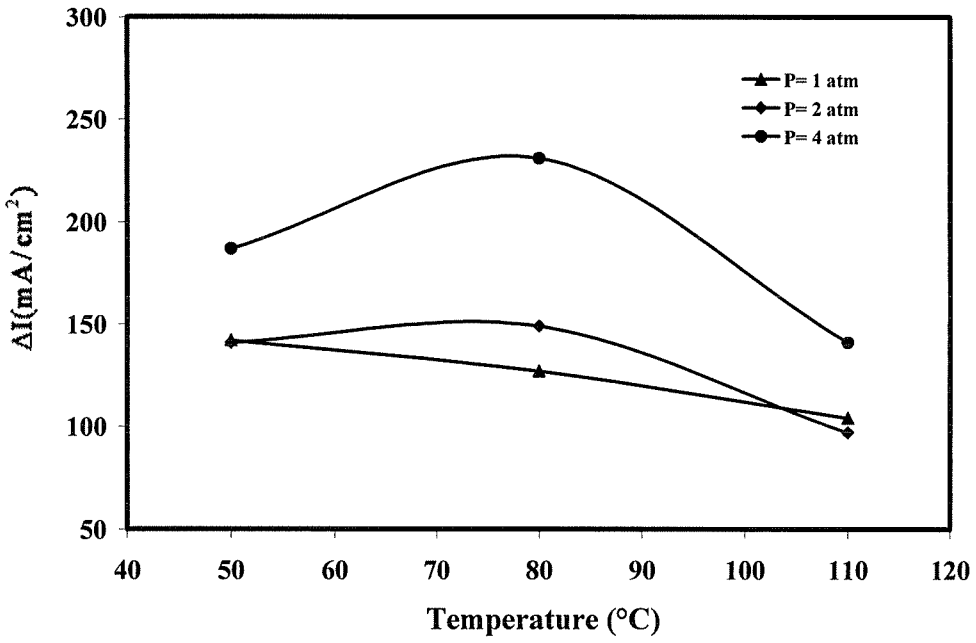

Figure 3- 44. The differences of the current density between the composite Nafion/STA membrane and cast Nafion without STA membrane at 0.6 V cell potential under different conditions ($\Delta I = I_{\text{Nafion with STA}} - I_{\text{Nafion without STA}}$).

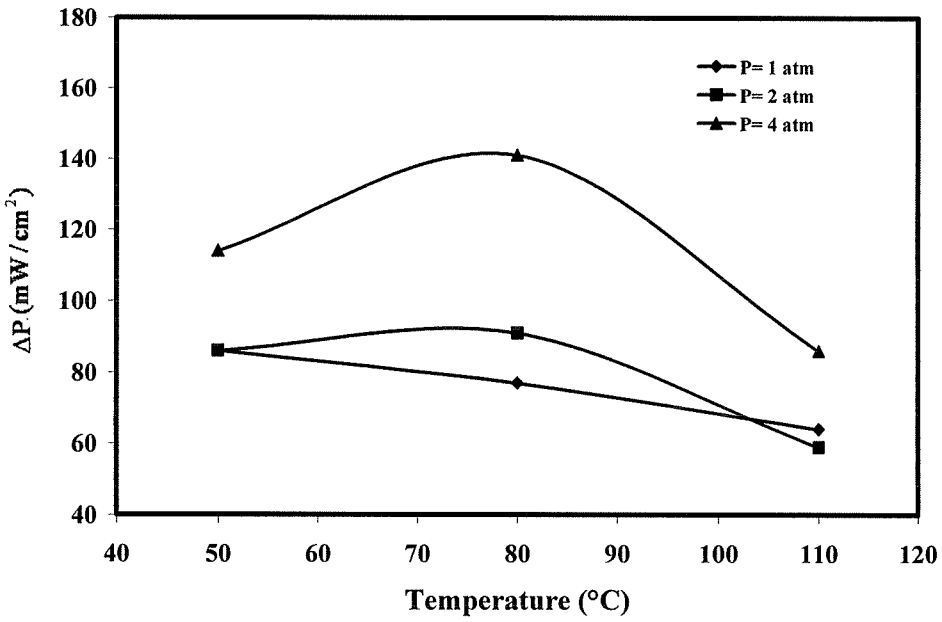

Figure 3- 45. The differences of the power density between the composite Nafion/STA membrane and cast Nafion without STA membrane at 0.6 V cell potential under different conditions ($\Delta P = P_{\text{Nafion with STA}} - P_{\text{Nafion without STA}}$).

3.9.2. THE CURRENT-POTENTIAL CHARACTERISTICS OF FLEMION/STA MEMBRANE

The current-potential polarization curves based on cast Flemion with or without STA membrane under different conditions are presented in Figs. 3-46~3-49. Four cell temperatures (50, 80, 110 and 120°*C*) were used during the fuel cell test. The pressures of H_2 and O_2 used are the same as that used for Nafion-based membrane, which are 1 atm, 2 and 4 atms, respectively. The concentration of STA in casting electrolyte solution is also $3\times10^{-3}M$ for composite Flemion/STA membrane. The thicknesses of the cast Flemion with and without STA membranes are 114 μm and 102 μm respectively.

From the current-potential curves, we may see that the composite Flemion/STA membrane exhibits better polarization characteristics than cast Flemion without STA membrane. It is worth being noted at 0.6*V* the current density of MEAs based on composite Flemion/STA membrane is higher than that of MEAs based on cast Flemion without STA membrane. We may also observe that at 0.6*V* the current density of MEAs made from composite Flemion/STA membrane and cast Flemion with STA membrane are 604 and 515 (1 *atm*), 813 and 597 (2 *atm)*, 1014 and 776 mA/cm^2 (4 *atm*) respectively, at 80°*C*. So the improvements in the cell current density at 0.6*V* are 89 (1 *atm*), 216 (2 *atm*) and 238 mA/cm^2 (4 *atm*), respectively, at 80°*C* for the composite Flemion/STA membrane. When the temperature was increased to 110°C, the current density obtained with the composite Flemion/STA membrane is still higher than that obtained with the cast Flemion without STA membrane (Fig. 3-48). The improvements in the cell current density at 0.6*V* are 134 (1 *atm*), 202 (2 *atm*) and 283 mA/cm^2 (4 *atm*). The current densities of composite Flemion/STA and cast Flemion without STA membrane at 0.6 *V* cell potential under different conditions are summarized in Table 3-18. Note that the current density obtained with the composite Flemion/STA membrane at 0.6*V* can reach up to 209 mA/cm^2 (4 *atm*) at 120°*C*. This indicates that STA can significantly affect the PEMFC performance of cast Flemion membrane and Flemion-

based membrane can keep better current-potential characteristics under high temperature (120°C) when STA is used as additive to modify the properties of cast Flemion.

Table 3- 18. The current densities of composite Flemion/STA and cast Flemion without STA membrane at the cell potential of 0.6 *V* under different conditions.

		$I_{(E=0.6V)}$ (mA/cm^2)		
Cell temperature (°C)	Pressure / Cast Flemion Membrane	1 *atm*	2 *atm*	4 *atm*
50°C	Without STA	239	388	478
	With STA	247	396	530
	$\Delta I = I_{with\ STA} - I_{without\ STA}$	8	8	52
80°C	Without STA	515	597	776
	With STA	604	813	1014
	$\Delta I = I_{with\ STA} - I_{without\ STA}$	89	216	238
110°C	Without STA	105	157	202
	With STA	239	359	485
	$\Delta I = I_{with\ STA} - I_{without\ STA}$	134	202	283
120°C	Without STA	69	90	172
	With STA	70	135	209
	$\Delta I = I_{with\ STA} - I_{without\ STA}$	2	45	37

The current density improvement of composite Flemion/STA membrane at the cell potential of 0.6*V* under different temperatures and pressures are also presented in Fig.3-50. Althrough the best fuel cell performance is based on the Flemion/STA

membrane at 80°C, we may also find that the current density improvement based on the Flemion/STA membrane can be of satification at 110°*C*, which is even higher than that at 80°*C* and 4 *atm*. The current density based on the Flemion/STA membrane at 120°C can keep almost same improvement with that at 50°C. This indicates that the application of Flemion/STA membrane in PEMFC should be more and more attentive.

Tables 3-19 and 3-20 show the electrode-kinetic parameters for PEMFC with Flemion-based membrane. The E_0 values for Flemion/STA membrane are always larger than that of cast Flemion without STA membrane, which is different with the Nafion-based membrane. The increase of the E_0 value may due to the mixed effects of the electrode reaction rate and the gas transport in electrode. The high E_0 might imply the enhancement of gas transport in electrode with the addition of STA in membrane. We can also find that the resistance (R) of cast Flemion with STA membrane is less than those of cast Flemion without STA membrane. These are in agreement with the results that the ionic conductivity values of the composite Flemion/STA membrane are always larger than those of cast Flemion without STA membrane. The results of overpotentials (η) at 400mA/cm^2 can give the best explanation for the result that the composite Flemion/STA membranes exhibit better potential-current characteristics than cast Flemion without STA membrane in PEMFCs application because the η for composite Flemion/STA membrane is always lower than that of the cast Flemion without STA.

From table 3-20, we may also note that the Tafel slope b changes from 20.8 *mV/dec* to 44.3 *mV/dec* for composite Flemion-based membrane and from 21.8 *mV/dec* to 48 *mV/dec* for cast Flemion when the cell temperature range is from 50°C to 110°C. We may see that the addition of STA can affect the value of Tafel slope b and make the composite Flemion/STA membranes exhibite the low Tafel value which due to the same reason as we discussed for Nafion-based membrane (section 3.9.1). Moreover, the STA significantly affects the value of b at 120°C. The large value of composite Flemion/STA

Table 3-19. Electrode-kinetic parameters for PEMFC with Flemion-based membranes (1)

Cell temperature *(°C)*		E_0 *(V)*			$\eta_{(400mA/cm2)}$ **(V)**		
	Membrane	1 *atm*	2 *atm*	4 *atm*	1 *atm*	2 *atm*	4 *atm*
50°C	Cast Flemion	0.842	0.859	0.892	0.322	0.259	0.252
	Flemion/STA	0.842	0.875	0.892	0.302	0.265	0.232
80°C	Cast Flemion	0.859	0.892	0.925	0.209	0.232	0.210
	Flemion/STA	0.875	0.942	0.942	0.195	0.232	0.182
110°C	Cast Flemion	0.809	0.842	0.875	0.664	0.572	0.535
	Flemion/STA	0.825	0.925	0.908	0.415	0.335	0.248
120°C	Cast Flemion	0.776	0.825	0.859	-	-	-
	Flemion/STA	0.859	0.925	0.942	0.797	0.780	0.681

Table 3-20. Electrode-kinetic parameters for PEMFC with Flemion-based membranes (2)

Cell temperature (°C)		*b (mV/dec)*			*R (ohm.cm²)*			$I_{(E=0.9V)}$ (mA/cm²)		
	Membrane	1 *atm*	2 *atm*	4 *atm*	1 *atm*	2 *atm*	4 *atm*	1 *atm*	2 *atm*	4 *atm*
50°C	Cast Flemion	48.0	41.2	42.6	0.495	0.381	0.354	-	-	-
	Flemion/STA	44.3	41.3	34.8	0.477	0.389	0.345	-	-	-
80°C	Cast Flemion	34.0	44.7	41.2	0.296	0.262	0.258	-	1	1
	Flemion/STA	26.5	43.7	32.7	0.306	0.250	0.233	-	20	45
110°C	Cast Flemion	31.6	29.8	21.8	1.25	1.09	1.10	-	-	-
	Flemion/STA	20.8	28.7	22.7	0.684	0.683	0.484	-	15	30
120°C	Cast Flemion	36.6	23.8	20.0	1.52	1.84	1.11	-	-	-
	Flemion/STA	52.3	58.7	40.9	2.32	1.40	1.15	-	1	12

membrane at 120°C may be due to the poor electrode/membrane interface which is caused by membrane dehydration at high temperature and result in the unstable of the fuel cell performance.

The current-power densities of the composite Flemion/STA membrane and cast Flemion without STA membrane were also compared and the results are presented in Figs. 3-46~3-49, 3-51. From these figures, we may see that the power density based on composite Flemion/STA membrane is always higher than that based on composite membrane without STA (cast Flemion). The improvements in the cell power output at $0.6V$ are 54 (1 *atm*), 132 (2 *atm*) and 146 mW/cm^2 (4 *atm*), respectively, at 80°C. And at 110°C, the improvements in the cell power output at $0.6V$ are 82 (1 *atm*), 123 (2 *atm*) and 173 mW/cm^2 (4 *atm*). The cell power densities for Flemion with and without STA membranes under different temperatures and pressures are summarized in table 3-21. From table 3-21, we may also see that the power density based on composite Flemion/STA membrane at $0.6V$ can still reach up to 128 mW/cm^2 (4 *atm*), at 120°C. The improvement in the fuel cell characteristics for the composite Flemion/STA membrane is due to a combined effect of Flemion and STA. The MEA based on cast Flemion with STA membrane can give good performance at 110°C, which give us an indication that composite Flemion/STA membrane can be used in high temperature fuel cell system. The results of fuel cell test can keep good reproducibility during 36 hours. However, The long-term tests still need to be investigated.

Table 3- 21. The power densities at 0.6 V cell potential for composite Flemion/STA and cast Flemion membrane in PEMFC under different conditions.

		$P_{(E=0.6V)}$ (mW/cm^2)		
Cell temperature (°C)	Pressure / Cast Flemion Membrane	1 *atm*	2 *atm*	4 *atm*
50°C	Without STA	146	237	291
	With STA	150	241	323
	$\Delta P = P_{with\ STA} - P_{without\ STA}$	4	4	32
80°C	Without STA	314	364	473
	With STA	368	496	619
	$\Delta P = P_{with\ STA} - P_{without\ STA}$	54	132	146
110°C	Without STA	64	96	123
	With STA	146	219	296
	$\Delta P = P_{with\ STA} - P_{without\ STA}$	82	123	173
120°C	Without STA	41	55	105
	With STA	41	82	128
	$\Delta P = P_{with\ STA} - P_{without\ STA}$	0	27	23

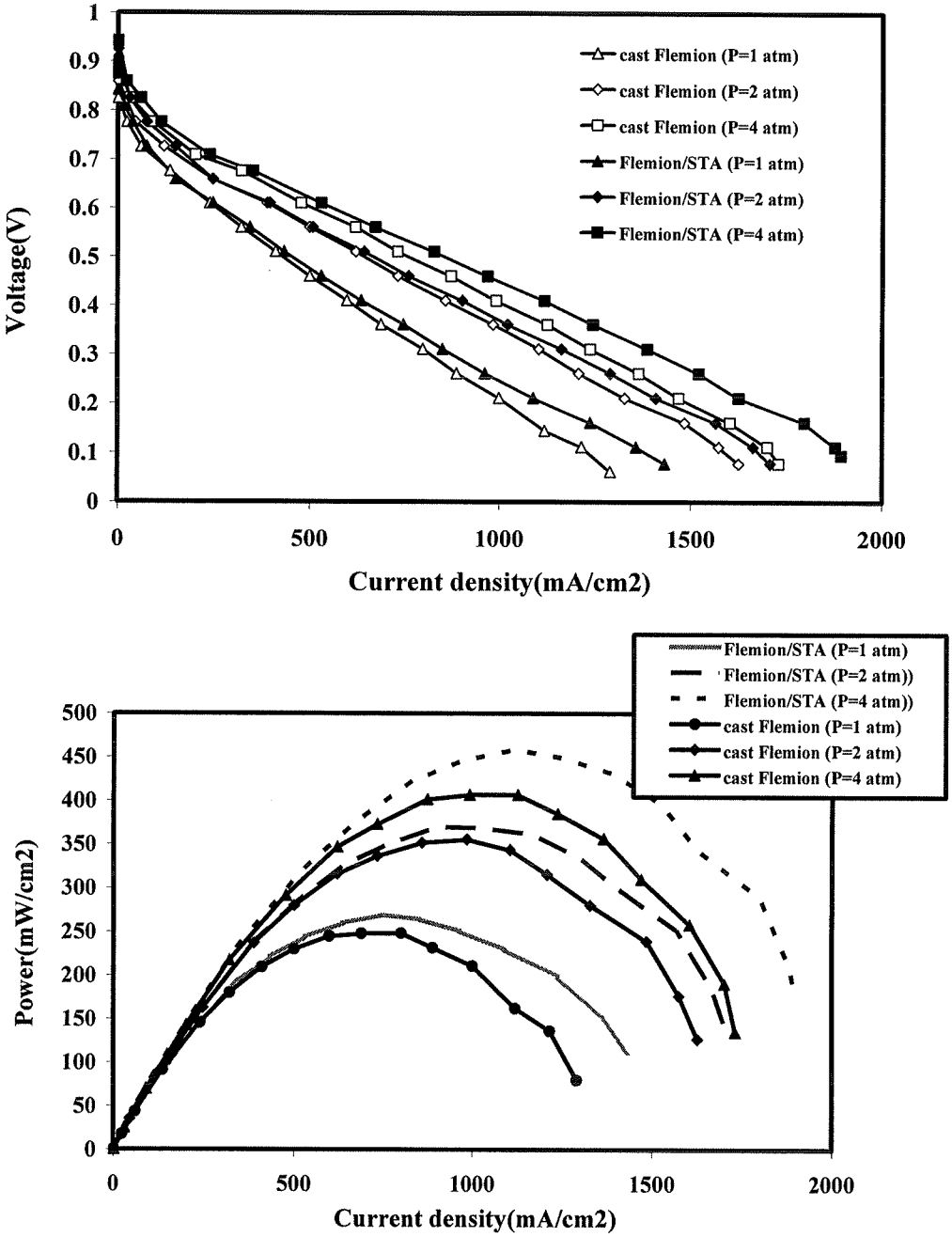

Figure 3- 46. Current-potential and current-power characteristics under different pressures for cast Flemion with or without STA membrane (Flemion/STA or cast Flemion) H_2/O_2 fuel cell, along with 20 *% Pt*-on-*C*, 1 *mg* Pt/cm^2, gas-diffusion electrodes. *T (humidifiers)* = 65 °C for *T(cell)* = 50 °C.

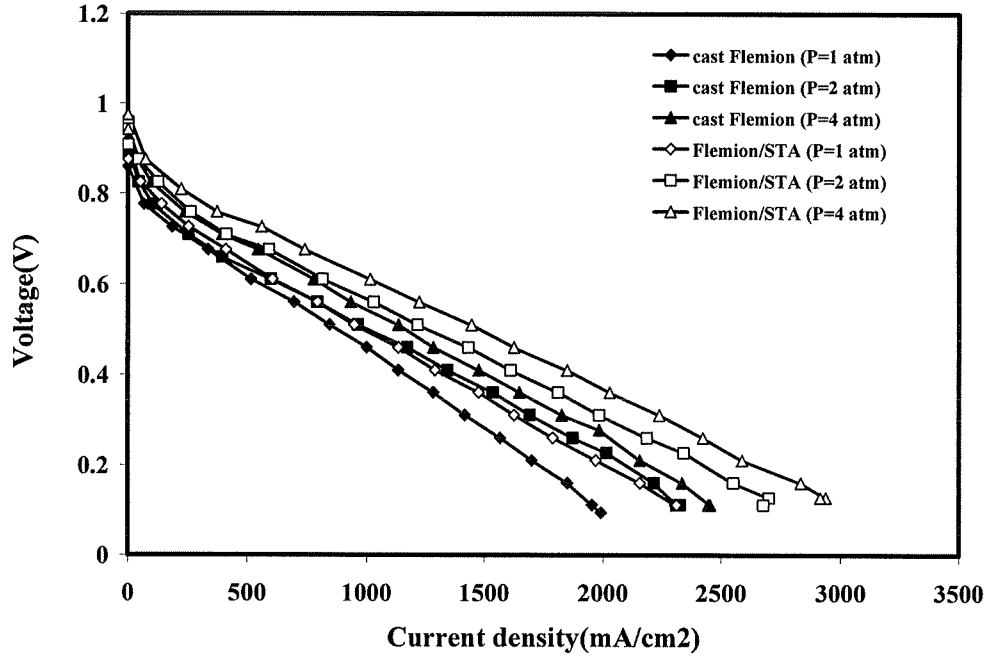

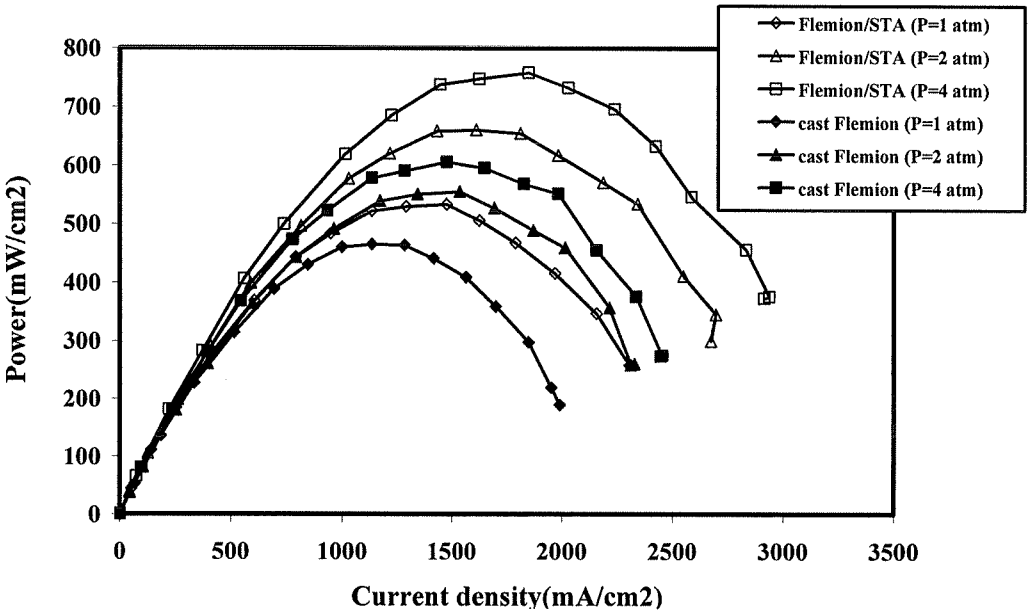

Figure 3- 47. Current-potential and current-power characteristics under different pressures for cast Flemion with or without STA membrane (Flemion/STA or cast Flemion) H_2/O_2 fuel cell, along with 20 % *Pt*-on-*C*, 1 *mg* Pt/cm^2, gas-diffusion electrodes. *T (humidifiers)* = 95°*C* for *T(cell)* = 80°*C*.

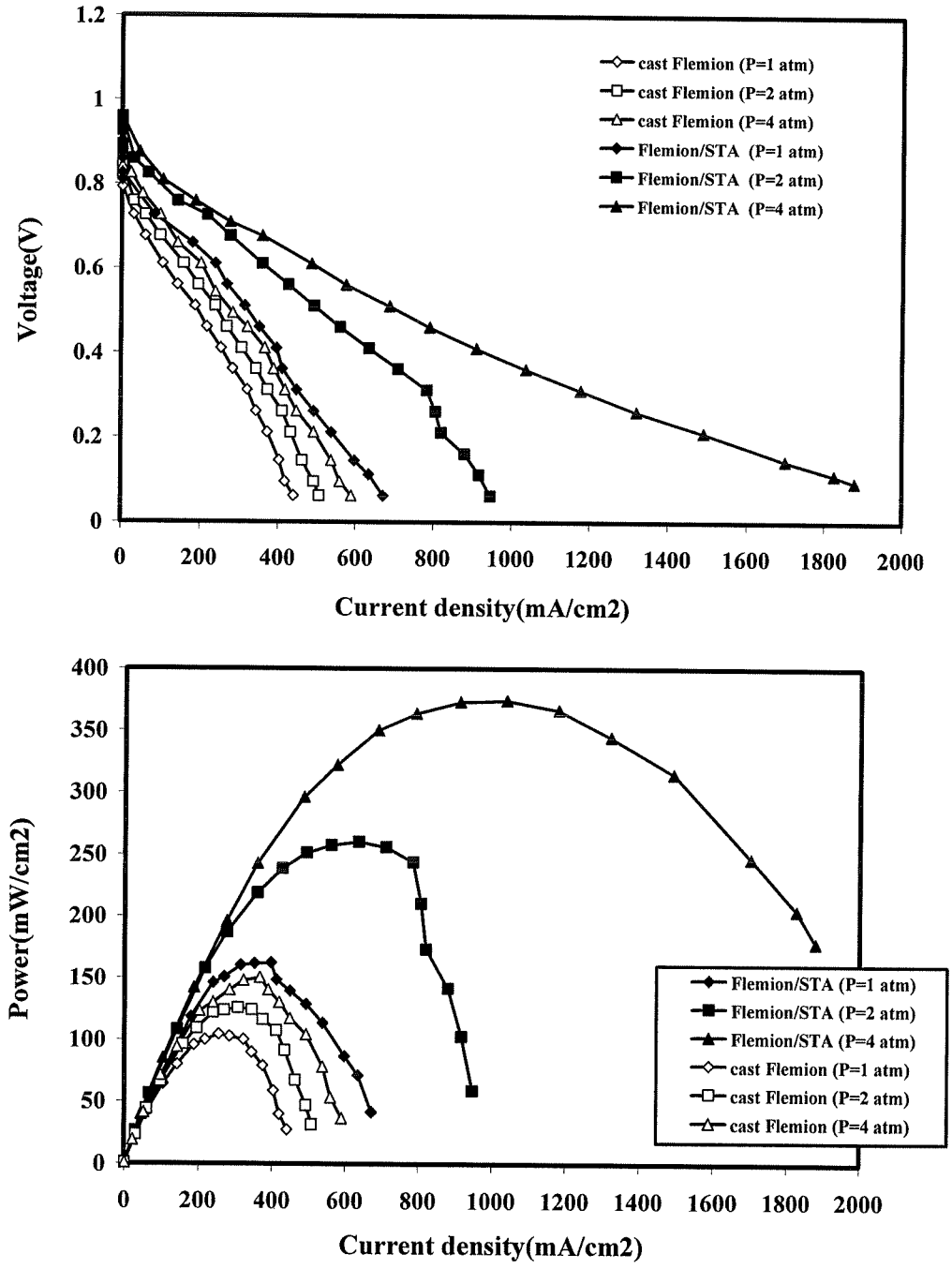

Figure 3- 48. Current-potential and current-power ancharacteristics under different pressures for cast Flemion with or without STA membrane (Flemion/STA or cast Flemion) H_2/O_2 fuel cell, along with 20 % *Pt*-on-*C*, 1 *mg* Pt/cm^2, gas-diffusion electrodes. *T (humidifiers)* = 95°C for *T (cell)* = 110°C.

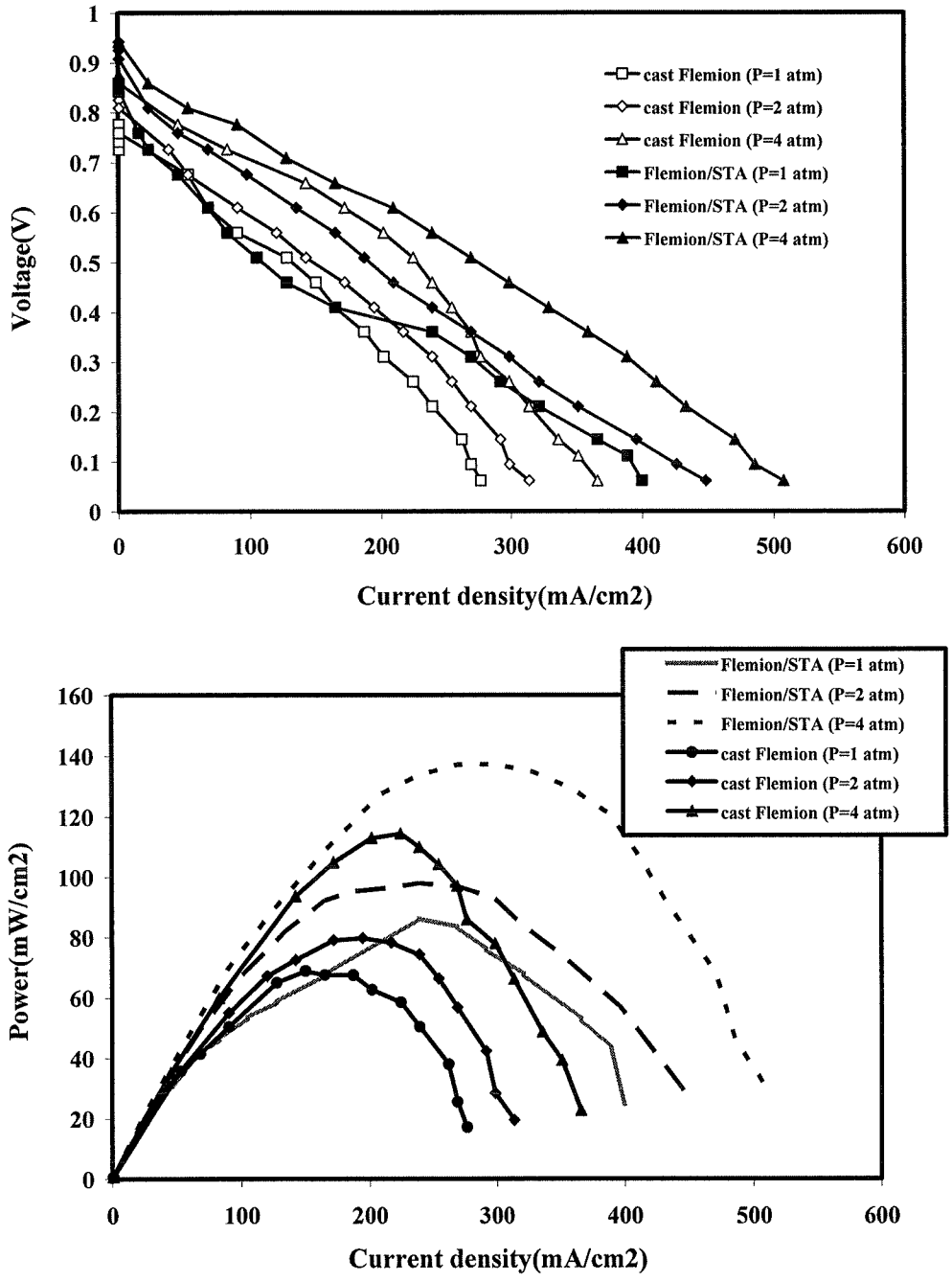

Figure 3- 49. Current-potential and current-power characteristics under different pressures for cast Flemion with or without STA membrane (Flemion/STA or cast Flemion) H_2/O_2 fuel cell, along with *20 % Pt*-on-*C*, 1 *mg* Pt/cm^2, gas-diffusion electrodes. *T (humidifiers)* = 95 °*C* for *T (cell)* = 120 °*C*.

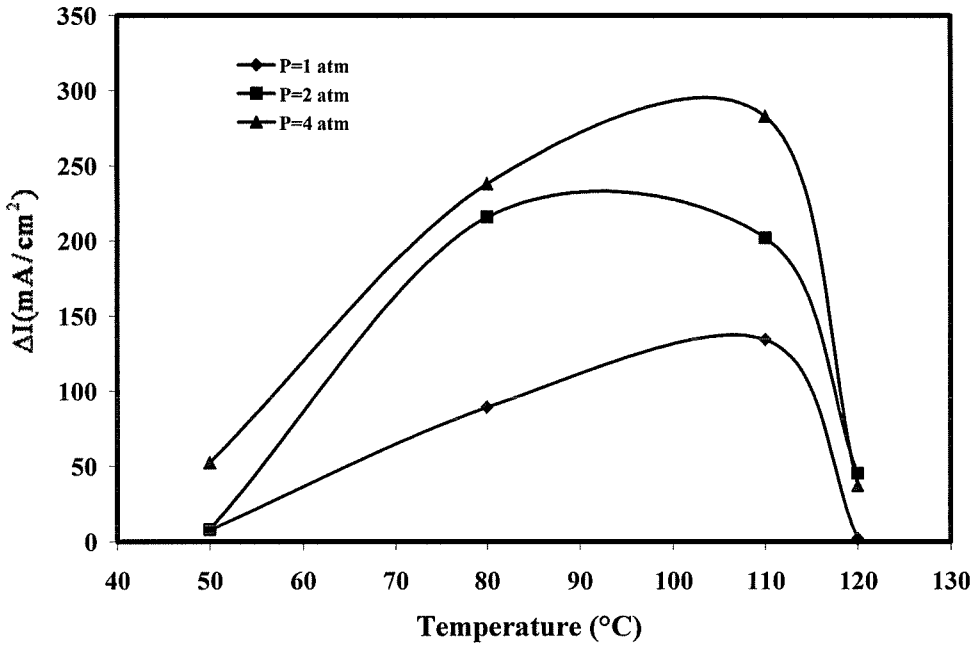

Figure 3- 50. The differences of the current densities between the composite Flemion/STA membrane and cast Flemion without STA membrane at 0.6 V cell potential under different conditions ($\Delta I = I_{\text{Flemion with STA}} - I_{\text{Flemion without STA}}$).

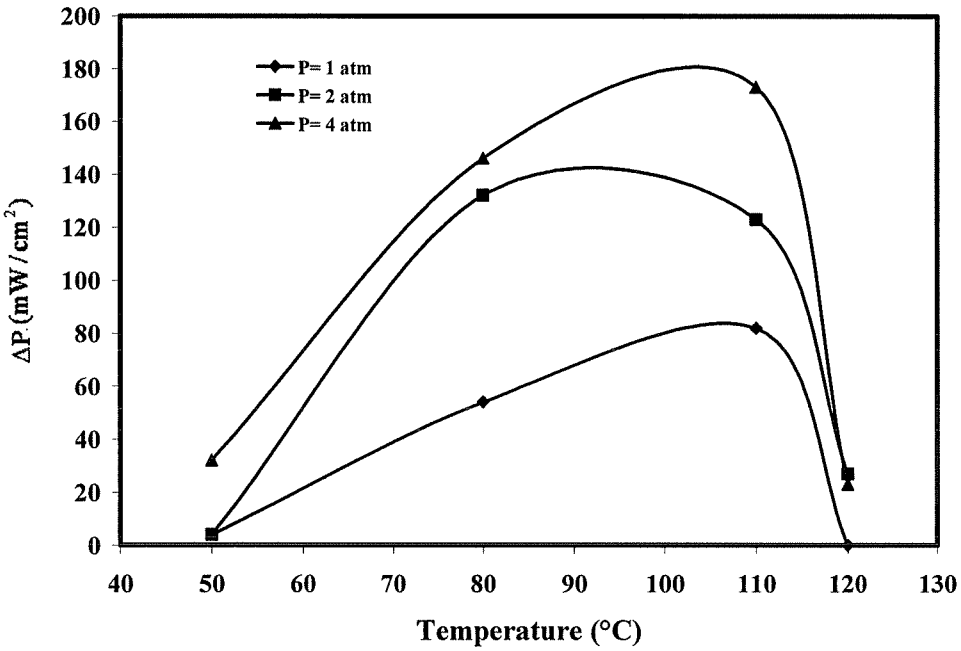

Figure 3- 51. The differences of the power densities between the composite Flemion/STA membrane and cast Flemion without STA membrane at 0.6 V cell potential under different conditions ($\Delta P = P_{\text{Flemion with STA}} - P_{\text{Flemion without STA}}$).

3.9.3. COMPARISON OF CURRENT POTENTIAL CHARACTERISTICS FOR NAFION/STA, FLEMION/STA AND NAFION 117 MEMBRANES

The comparison of the current–potential polarization curves of 2.25 cm^2 MEA based on cast Nafion with STA ([STA] = 3×10^{-3} M) and without STA ([STA] = 0) membranes, cast Flemion with STA ([STA] = $3\times10^{-3}M$) and without STA ([STA] = 0) membranes as well as commerical Nafion 117 membrane, with the cell temperature varying from 50°C to 120°C and the pressure of 4 atm for both H_2 and O_2, are demonstrated in Figs. 3-52~3-54 .

Compared to Nafion-based membrane, Flemion-based membrane exhibits better current-potential polarization characteristics which is due to the low EW of the Flemion. In addition, both composite Nafion/STA and composite Flemion/STA membranes exhibit the better fuel cell performance than Nafion 117 membrane. For example, at 80°C and 4 atm, the cell current densities at 0.6V are 1014 mA/cm^2 for composite Flemion/STA membrane, 708 mA/cm^2 for composite Nafion/STA membrane and 604 mA/cm^2 for Nafion 117 membrane. Fig. 3-55 shows the difference of the current density between the composite Flemion/STA membrane, composite Nafion/STA membrane and commercial Nafion 117 membrane at 0.6V cell potential under different conditions. These results indicate that composite Flemion/STA membrane and composite Nafion/STA membrane have much more advantages than commercial Nafion 117 membrane in PEMFC application. Therefore, it is safe to say that the application of composite membranes in PEMFC is becoming more and more feasible with the addition of STA.

Table 3-22 shows the electrode-kinetic parameters analysis results of commercial Nafion 117 membrane for PEMFC at 4 atm. By comparing the table 3-22 with tables 3-16, 3-19 and 3-20, we can see that the commercial Nafion 117 membrane has larger E_0 value than composite Nafion/STA and composite Flemion/STA

membranes. We may also observe Nafion 117 membrane has the low ionic resistance at 50°C and 80°C. In addition, the high R value of Nafion 117 at 110°C implies the dehydration of Nafion 117 which can lead to poor membrane/electrode interface and result in the bad PEMFC performance. By comparing the R and the $\eta_{(400mA/cm2)}$ of the Nafion/STA membrane (NS), cast Nafion without STA (NB), Flemion/STA membranes (FS), cast Flemion without STA (FB) and Nafion 117 memebrane (NF) at 4 atm pressure, we can get the following results:

$R_{(FS)} < R_{(FB)} < R_{(NF)} < R_{(NS)} < R_{(NB)}$ and $\eta_{(FS)} < \eta_{(FB)} < \eta_{(NS)} < \eta_{(NF)} < \eta_{(NB)}$ at 50°C;
$R_{(FS)} < R_{(FB)} < R_{(NS)} < R_{(NF)} < R_{(NB)}$ and $\eta_{(FS)} < \eta_{(FB)} < \eta_{(NS)} < \eta_{(NB)} = \eta_{(NF))}$ at 80°C;
$R_{(FS)} < R_{(NS)} < R_{(FB)} < R_{(NB)} < R_{(NF)}$ and $\eta_{(FS)} < \eta_{(NS)} < \eta_{(FB))} < \eta_{(NB)}$ at 110°C.

These are in agreement with the fuel cell performance shown in Figs. 3-52~3-54. The addition of STA makes the Nafion/STA and Flemion/STA membranes exhibit lower R and $\eta_{(400mA/cm2)}$ than Nafion 117 at high temperature, so Flemion/STA membrane and Nafion/STA membrane can exhibit the better PEMFC performance than commercial Nafion 117 under high temperature.

Table 3- 22. Electrode-kinetic parameters for PEMFCs with Nafion 117 membrane at 4 atm pressure.

Cell temperature (°C)	E_0 *(V)*	b *(mV/dec)*	R *(ohm.cm^2)*	$I_{(E=0.9V)}$ *(mA/cm^2)*	$I_{(E=0.6V)}$ *(mA/cm^2)*	$\eta_{(400mA/cm2)}$ *(V)*
/50°C	1.025	103	0.398	16	411	0.415
80°C	1.025	71.4	0.370	23	604	0.325
110°C	1.008	152	1051	1	82	-

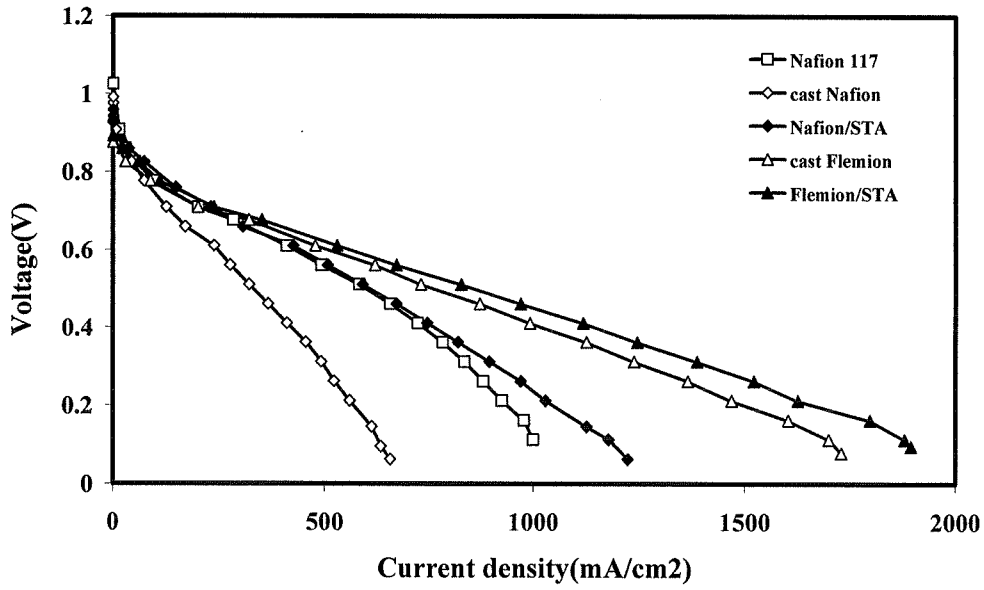

Figure 3- 52. A comparison of current-potential curves at 4 atm pressure, for the different PEM H_2/O_2 fuel cell, Along with 20 % *Pt*-on-*C*, 1 *mg* Pt/cm^2 gas-diffusion electrodes. *T (cell)* =50°*C*, *T(humidifiers)* =65°*C*.

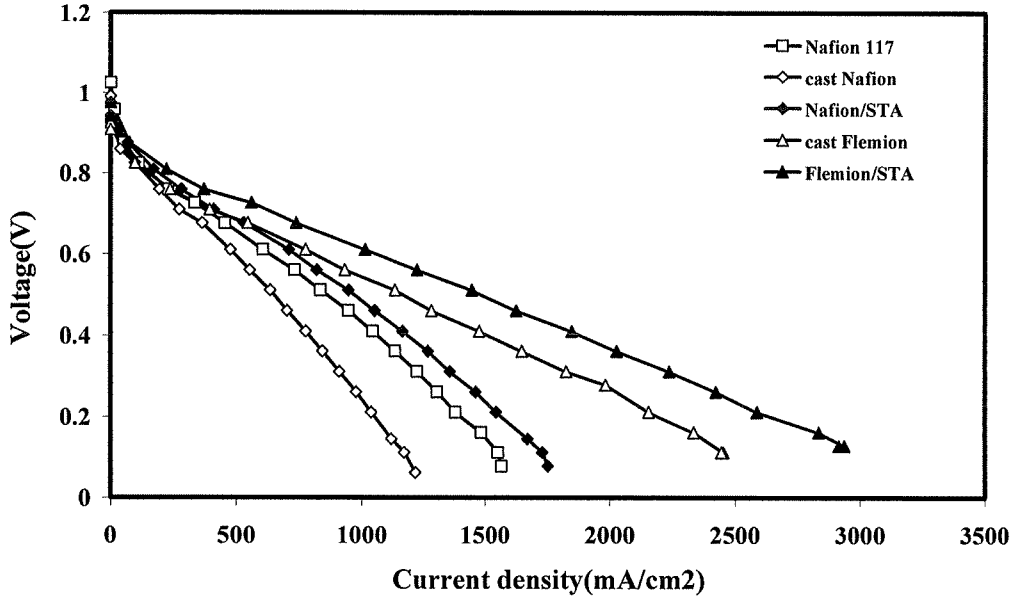

Figure 3- 53. A comparison of current-potential curves at 4 atm pressure, for the different PEM H_2/O_2 fuel cell, Along with 20 % *Pt*-on-*C*, 1 *mg* Pt/cm^2 gas-diffusion electrodes. *T (cell)* =80°*C*, *T(humidifiers)* =95°*C*.

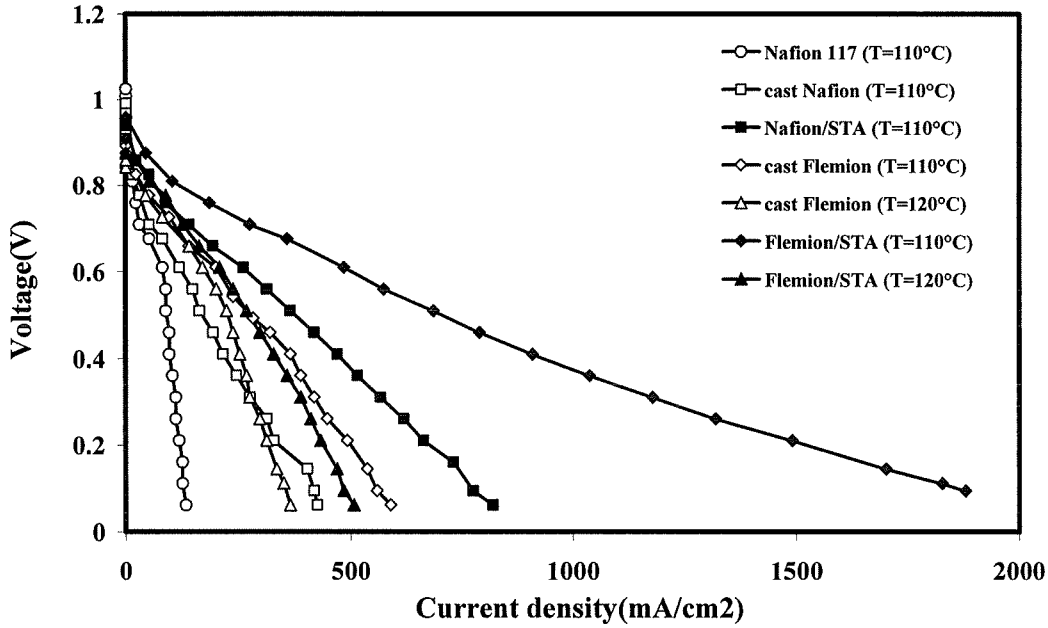

Figure 3- 54. A comparison of current-potential curves at 4 atm pressure, for the different PEM H_2/O_2 fuel cell, Along with 20 *% Pt*-on-*C*, 1 *mg Pt/cm*^{2} gas-diffusion electrodes. *T (cell)* =110°*C* and 120°*C*, *T (humidifiers)* =95°*C*.

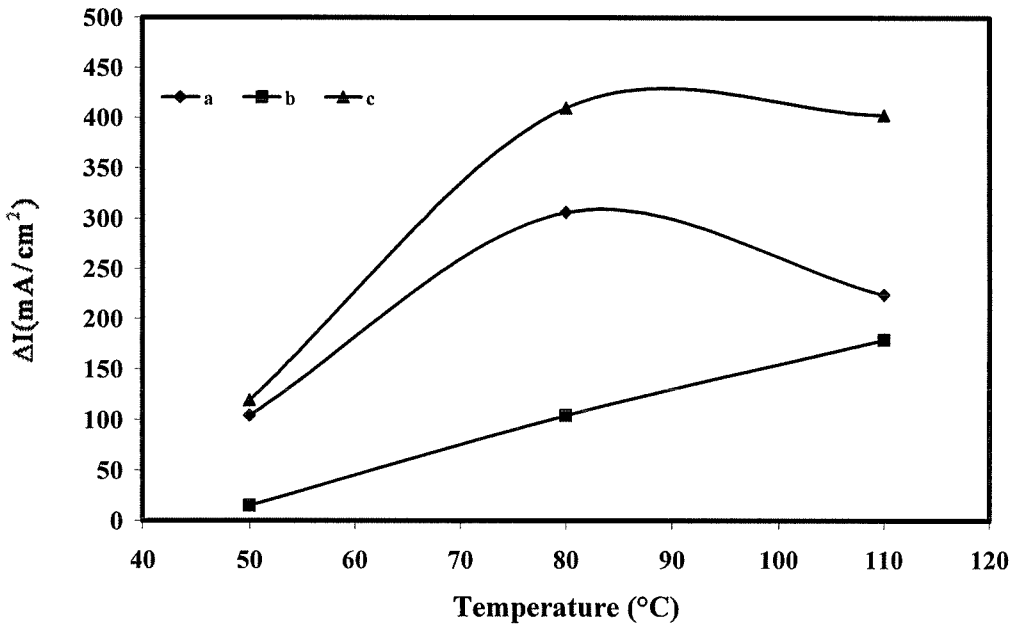

Figure 3- 55. The differences of the current density between the composite Flemion/STA membrane, composite Nafion/STA membrane and commercial Nafion 117 membrane at 0.6V cell potential under 4 atm pressure and different temperatures. a) $\Delta I = I_{Flemion/\ STA} - I_{Nafion/\ STA}$; b) $\Delta I = I_{Nafion/\ STA} - I_{Nafion117}$; c) $\Delta I = I_{Flemion/\ STA} - I_{Nafion117}$.

3.9.4. CONCLUSIONS

From the results obtained in PEM fuel cell test, we may conclude that the composite Nafion/STA and Flemion/STA membranes have the superior performances than the membranes without STA. The improvement in the fuel cell characteristics for the composite Nafion/STA and Flemion/STA membrane is due to a combined effect between Nafion or Flemion and STA. The presence of STA improves the fuel cell performance and make this operation feasible under high temperature.

CONCLUDING REMARKS

New composite membranes cast from Nafion or Flemion solution with and without STA in *N, N'*-dimethylformamide (DMF) were obtained. The preparation procedure of the composite membrane has been determined. The preparation method was based on solvent evaporation. During the casting of composite membranes, DMF was added in the mixed solution which included perfluorosulfonated polymer solution and STA. The high boiling point of DMF makes the composite membrane be able to be cast under high temperature (135°C). Compared to the composite membrane cast at low temperature (<70°C) from the initial Nafion solution without DMF, which is brittle, the composite membrane cast from DMF at 135°C is very flexible.

The surface and cross-section morphologies of the composite Nafion/STA and Flemion/STA membranes have been studied using atomic force microscopy (AFM) and scanning electron microscopy (SEM). It was seen that the solid STA is uniformly distributed in Nafion and Flemion membrane and shows no agglomeration after membrane preparation. From the SEM micrograph, the STA particles are observed and their size was estimated to be 0.1-0.2 μm (in diameter) within Nafion/STA membrane and 0.05-0.1 μm (in diameter) within Flemion/STA membranes.

The ionic conductivities of the Nafion/STA or Flemion/STA composite membranes were investigated under different conditions including the effect of STA concentration on the ionic conductivity and different pretreatment for the composite membrane. The ionic conductivity of composite membrane increases with the STA concentration in composite membrane. This is attributed to the high concentration of protons provided by STA when STA was introduced in the membrane. The composite membranes were stable at room temperature in deionized water and their ionic conductivity increases with STA concentration in the membrane when the composite membrane was immersed in deionized water or $1M\ H_2SO_4$ solution at room temperature.

However, the ionic conductivity is independent of the STA concentration when the composite membranes were pretreated in boiling deionized water. This result was attributed to the loss of STA in composite membrane. The ionic conductivity of composite membrane for the membrane pretreated in 1 $M\ H_2SO_4$ is always higher than that pretreated in deionized water. This indicates that there has the synergetic effect between the sulphuric acid and STA. The existence of this synergetic effect was further investigated using the TGA, FTIR and XPS characterization of the samples. The ionic conductivity of cast membrane with STA is larger than that without STA and it can reach up to 0.120 $ohm^{-1} \cdot cm^{-1}$ for Nafion/STA membrane and 0.133 $ohm^{-1} \cdot cm^{-1}$ for Flemion/STA membrane.

It was also shown that the water uptake of the composite membranes with STA is higher than that without STA in boiling deionized water. This is due to the high hydration capacity of STA. The thermal analysis results of STA showed that the STA in the composite membranes could absorb more than 18 molecules of water. Accordingly, the water uptakes of composite membranes increase with STA concentration.

The wide-angle X-ray diffraction (XRD) technique was used to determine the composite membrane structure. A new peak was observed at $2\Theta = 9.20$ for the composite membrane with STA. In comparison to the x-ray diffraction spectrum of the membrane without STA, this new peak was attributed to the interaction between the STA and the Nafion. Accordingly, it was concluded that some STA species are detected in the membrane matrix and is combined to the perfluoronated polymer.

The thermoanalysis data of the composite membranes showed that these membranes have two-step degradations in the temperature range scanned (25°C~800°C). The first step degradation temperature of the composite membrane decreases with the decrease of [STA] in the membrane. Since the first step degradation corresponds to the reaction/or degradation of the sulfuric acid groups, the existence of STA in the

composite membrane has an influence on the degradation of the sulfuric acid groups. This result suggests a possible specific interaction between the STA and sulfuric acid. This is in good agreement with the XRD results. The TG analysis evidenced that the composite membrane has quite sufficient thermal stability within conceivable temperature range of PEMFC application.

The IR spectrum has clearly shown the existence of STA in composite membrane. The symmetric stretch of SO_3 is observed at 1021cm^{-1} in cast Nafion or cast Flemion and red shifted to 1017 cm^{-1} when the polymer membrane was blended with STA. This result indicates that STA particles interact with the sulfuric acid moiety of composite membrane.

The samples of Nafion/STA and Flemion/STA membranes were evaluated by using XPS to analyze the chemical composition of composite membranes. The observation of *W* in the survey spectra of the composite Nafion/STA and Flemion/STA proved the presence of STA in composite membrane. The detection of W-S and W-C bond in the Nafion/STA and Flemion/STA samples confirms the interactions between STA and the sulfuric acid, STA and main-chain of polymer. The results of XRD, FTIR, TG, XPS provide support for the existence of synergetic effect between the sulphonic acid and STA. This interaction can be used to explain the increase of the composite's ionic conductivity and water uptake with the increase of STA concentration in the membrane. The improvements of the conductivities for the Nafion/STA or Flemion/STA membranes can be proved to be due to the increase of proton sites concentrations coming from the introduction of the STA species in the composite membranes. From the results of XPS, we can obtain the total relative concentration of the active protonic sites which were considered from the the sulfuric acid group and the addition of STA species in the membranes for various membranes: 1.1% for cast Nafion (from SO_3^-), 1.27 % for composite Nafion/STA (from SO_3^- and STA), 1.4% for cast Felmion (from SO_3^-) and 1.5% for composite Flemion/STA (from SO_3^- and STA).

Obviously, the active protonic sites of composite membranes with STA are higher than that without STA. The high protonic sites should correspond to the high conductivity.

The evaluation of composite membrane performance in fuel cell test was carried out under different temperatures and different pressures of H_2 and O_2. Composite membrane with STA exhibits higher potential than those without STA at each current density, temperature and pressure. When the cell temperature is $80°C$ and the pressures of both H_2 and O_2 are 4 atm, the current densities of MEAs made from composite Nafion/STA membrane and cast Nafion without STA membrane at $0.6V$ are 708 and 477 mA/cm^2. In comparison to cast Nafion without STA, the improvement in the cell current density at $0.6V$ for composite Nafion/STA membrane is 231 mA/cm^2. Furthermore, as the temperature is increased to 110°C, the current density differences between the composite Nafion/STA membrane and the cast Nafion without STA membrane is 141 mA/cm^2 (4 atm). And by comparing the composite Flemion/STA membrane with the cast Flemion without STA membrane, we may find the improvements in the cell current density at $0.6V$ are 238 mA/cm^2 (at 80°C), 283 mA/cm^2 (at 110°C) and 37 mA/cm^2 (at $120°C$) under same operation pressure. It is clear that the composite membrane with STA can still keep good performance in fuel cell test even at higher temperature. The above experimental results show that the addition of STA can improve the electrochemical properties of composite membrane and enhance the feasibility of polymer electrolyte membrane applying in high temperature fuel cell system.

In sum, new Nafion/STA and Flemion/STA composite membranes have been successfully prepared and their properties have been extensively investigated. The results of thermal analysis, X-ray diffraction and FTIR analysis have shown the existence of STA in composite membrane and the possible interactions between the STA and the polymer. These interactions have been supported by the XPS analysis which has shown the presence of W-C and W-S bonds in the composite Nafion/STA or

Flemion/STA membrane. The presence of STA is responsible for the improvement of the ionic conductivities, the capacity of water absorption by the membranes as well as the performances of the composite membranes in H_2/O_2 fuel cell.

RECOMMENDATIONS

To pursue this work, the following recommendations deserve to be considered:

1. The ion-exchange capacity of composite membrane with STA should be determined.
2. The study of the water uptake of the composite membrane with STA in water vapor is very important to search the electrochemical properties of the composite membrane in high temperature fuel cell operation.
3. How to reduce the loss of STA in composite membrane must be further investigated.
4. The form of STA in composite membrane should be further ascertained.
5. Flemion is a perfluorinated polymer developed by Asahi Glass Company. It has a structure which is quite similar to Nafion. The study of composite Flemion with STA membrane should be further explored.

REFERENCES

1. KALHAMMER, F.R. 2000. << Polymer electrolytes and the electric vehicle>>. *Solid State Ionics*. 135. 315-323.
2. PRATER, K. B. 1990. <<The renaissance of the solid polymer fuel cell>>. *J. Power Sources*. 29. p. 239-250.
3. CONNELLY, D.J. AND GRESHAM, W.J. 1966. *US Patent*. 4,3,282,875.
4. EZZEL, B.R., CARL, W.P. AND MOD, W.A. 1982. *US Patent*. 4,358,412.
5. YOSHIDA, N., ISHISAKI, T., WATANABE, A. AND YOSHITAKE, M. 1998. <<Characterization of Flemion membranes for PEFC>>. *Electrochim. Acta*. 43:24. 3749.
6. WAKIZOE, M., KIM, J.; SRINIVASAN, S.; MCBREEN, J. 1993. << A novel method for determination of transport parameters of H_2 and O_2 in PEMFCs >>. Presented at *the 183rd Electrochemical Society Meeting*, Honolulu, HI, 16-21 May 1993. 13W.
7. SAVADOGO, O. 2004. <<Emerging membranes for electrochemical systems Part II. High temperature composite membranes for polymer electrolyte fuel cell (PEFC) applications>>. *J. Power Sources*. 127. 135-161.
8. YOUNG LEE K., ARAL, T., NAKATA, S.I., ASAOKA, S., OKUHURA, T. AND MISONO, M. 1992. <<Catalysis by heteropoly compounds. 20. An NMR study of ethanol dehydration in the pseudoliquid phase of 12-tungstophosphoric acid>>. *J. Am. Chem. Soc.* 114. 2836.
9. MISUMO, N., WATANABE, T., MISONO, M. 1985. <<Catalysis by heteropoly compounds. VIII. Reduction-oxidation and catalytic properties of 12-molybdophosphoric acid and its alkali salts. The role of redox carriers in the bulk>>. *J. Phys. Chem.* 89. 80.
10. FOGG, A.G., BSEBSU, N.K., 1981. <<Differential-pulse anodic voltammetric determination of phosphate, silicate, arsenate and germanate as β -

heteropolymolybdates at a stationary glassy-carbon electrode>>. *TALANTA. Short communication.* 28. 473.

11. SAVADOGO, O. AND MANDAL, K.C. 1994. <<Low Cost Schottky Barrier Solar Cells Fabricated on CdSe and Sb_2S_3 Films Chemically Deposited with Silicotungstic Acid>>. *J. Electrochem. Soc.* 141:10. 2871.
12. TELL, B. 1979. <<Electrochromic effects in solid phosphotungstic acid and phosphomolybdic acid>>. *J. Appl. Phys.* 50. 5944.
13. TELL, B. AND WAGNER, S. 1978. <<Electrochemichromic cells based on phosphotungstic acid>>. *Appl. Phys. Lett.* 33. 837.
14. SHIMIDSU, T., OHTANI, A. AIBA, M. HONDA, K. 1988. <<Electrochromism of a conducting polypyrrole–phosphotungstate composite electrode>>. *J. Chem. Soc. Faraday Trans.* 184. 3941.
15. MAHESWARI, S.P. AND HABIB, M.A. 1988. <<Electrochromic Aspects of Phosphotungstic Acid>>. *Solar Energy Mater.* 18. 75.
16. FRICOTEAUX, P., SAVADOGO, O. 1999. <<Electrocatalytic parameters of the electrodeposition of copper with silicotungstic acid (STA)>>. *Electrochim. Acta.* 44. 2927
17. SRINIVASAN, S. 1992. <<Electrode Kinetic and Electrocatalytic Aspects of Electrochemical Energy Conversion>>. *Electrochemistry in Transition.* Edited by Murphy O. J. *et al.*, Plenum Press, New York, p.577-602.
18. PRATER, K.B. 1994. <<Polymer electrolyte fuel cells: a review of recent developments>>. *J. Power Sources.* 51. 129.
19. SHOESMITH, J. P., COLLINS, R. D., OAKLEY, M. J. AND STEVENSON, D. K. 1994. <<Status of solid polymer fuel cell system development>>. *J. Power Sources.* 49. 129.
20. PRATER, K.B. 1992. << Solid polymer fuel cell developments at Ballard>>. *J. Power Sources.* 37. 181-188.
21. BERGER, C. 1968. *Hand Book of Fuel Cell Technology.* Prentice-Hall, Inc., Englewood Cliffs, New Jersey. p.221.

22. ALENONS, R. 1990. <<Fuel cells for transportation>> *J. Power sources.* 29. 251.

23. WILKINSON, D.P. AND THOMPSETT, D. 1997. <<Materials and approaches for CO and CO_2 tolerance for polymer electrolyte membrane fuel cells>>. *Proceeding of the second International Symposium on New Materials for Fuel Cell and Modern Battery system.* Eds. Savadogo, O. and Roberge, P.R., Montreal, Canada, July 6-7, p.266.

24. ESCRIBANO, S., MIACHON, S. AND ALDEBERT, P. 1995 << low platinum loading wide electrodes for internal humidification hydrogen/oxygen polymer electrolyte membrane fuel cells>>. *Proceeding of the first International Symposium on New Materials for Fuel Cell and Modern Battery system.* Eds. Savadogo, O., Roberge P.R. and Veziroglu, T.N. Montreal, Canada, July 9-13, p.135.

25. BESSE, S., BRONOEL, G., TASSIN, N., NAIMI, Y. AND TOUNSI, A. 1995. << Development and manufacture of electrodes for proton exchange membrane fuel cell>>. *Proceeding of the first International Symposium on New Materials for Fuel Cell and Modern Battery system.* Eds. Savadogo, O., Roberge P.R. and Veziroglu, T.N. Montreal, Canada, July 9-13, p.144.

26. BLOMEN L. J. M. J. AND MUGERWA M. N. 1993. *Fuel Cell Systems.* New York and London: Plenum Press, p.81.

27. BARD, A. J. AND FAULKNER, L. R. 1980. *Electrochemical methods: Fundamentals and Applications.* John Wiley & Sons, New York, p.86.

28. WOO RHO, Y., SRINIVASAN, S. 1994 <<Mass transport phenomena in proton exchange membrane fuel cells using O_2/He, O_2/Ar, and O_2/N_2 mixtures. I. experimental analysis>>. *J. Electrochem. Soc.*, 141:8. 2089.

29. WOO RHO, Y., VELEV, O.A. AND SRINIVASAN, S. 1994. <<Mass transport phenomena in proton exchange membrane fuel cells using O_2/He, O_2/Ar, and O_2/N_2 mixtures. II. Theoretical analysis>>. *J. Electrochem. Soc.* 141:8. 2084.

30. KIM, J., LEE, S.-M. AND SRINIVASAN, S. 1995. <<Modeling of proton exchange membrane fuel cell performance with an empircal equation>>. *J. Electrochem. Soc.* 142:8. 2670.

31. TICIANELLI, E.A., DEROUIN, C.R., REOLONDO, A. AND SRINIVASAN, S. 1988. << Methods to advance technology of proton exchange membrane of proton exchange membrane fuel cells>>. *J. Electrochem. Soc.,* 135:9. 2209.

32. SRINIVASAN, S., VELEV, O. A., PARTHASARATHY, A., MANKO, D.J. AND APPLEBY, A.J. 1991. <<High energy efficiency and high power density proton exchange membrane fuel cells — electrode kinetics and mass transport>>. *J. Power Sources*, 36. 299.

33. SRINIVASAN, S., TICIANELLI, E.A., DEROUIN, C.R. AND REDONDO, A. 1988. <<Advances in solid polymer electrolyte fuel cell technology with low platinum loading electrodes>>. *J. Power Sources*, 22. 359.

34. RIKUKAWA, M. AND SANUI, K. 2000. <<Proton-conducting polymer electrolyte membranes based on hydrocarbon polymers>>. *Prog. Polym. Sci.* 25. 1464.

35. SAVADOGO, O. 1998. <<Emerging membranes for electrochemical systems: (I) solid polymer electrolyte membranes for fuel cell systems>>. *J. New. Mat. Electrochem.Systems.* I. 47.

36. STECK, A. 1995. << Membrane materials in fuel cells>>. *Proceedings of the First International symposium on New Materials for Fuel cell Systems.* Eds. Savadogo O., Roberge P. R. AND Veziroglu T.N., Montreal, Canada, July 9-13, p.74.

37. RIKUKAWA, M. AND SANUI, K. 2000. <<Proton-conducting polymer electrolyte membranes based on hydrocarbon polymers>>. *Prog. Polym. Sci.* 25. 1466.

38. EISMAN, G.A. 1987. *Fuel cell Technology and Applications. International Seminar*. The Netherlands, Oct. 26. p.287.

39. APPLEBY, A. J. AND YEAGER, E. B. 1986. <<Polymer electrolyte fuel cells (SPEFCs)>>. *Energy.* 11. 137.

40. RIEDINGER, H. AND FAUL, W. 1988. <<The focussing of membrane R&D on areas of commercial potential>>. *J. Membrane Sci.* 36. 5.

41. NUTTAL, L. J. AND BROWN, W.A. 1971. <<Solid polymer electrolyte water electrolysis system>>. *SAE/ASME/A Conference*, Los Angeles.

42. YEAGER, H. L. 1982. << Transport properties of perfluorosulfonate polymer membranes>>. *Perfluorinated Ionomer Members*. Eisenberg A. and Yeager H. L. Editors. ASC. Symp. Ser. 180, ACS, Washington, DC. p. 41.

43. GIERKE, T. D. AND HSU, W.Y. 1982. << The cluster-network model of ion clustering in perfluorosulfonated membranes>>. *Perfluorinated Ionomer Members*. Eisenberg A. and Yeager H. L. Editors. ASC. Symp. Ser. 180, ACS, Washington, DC. p.283.

44. BOCKRIS J.O'M. AND REDDY, A. K. N. 1970. *Modern Electrochemistry.* New York: Plenum Press. Vol. 1, p.474.

45. FALK, M. 1982. <<Infrared Spectra of perfluorosulfonated polymer and of water in perfluorosulfonated polymer>>. *Perfluorinated Ionomer Members.* Eisenberg A. and Yeager H. L. Editors. ASC. Symp. Ser. 180, ACS, Washington, DC. p. 139.

46. ZAWODZINSKI, T. A., SPRINGER, T. E., DAVEY, J., JESTEL, R., LOPEZ, C., VALERIO, J. AND GOTTESFELD, S. 1981. <<A comparative study of water uptake by and transport through ionomeric fuel cell membranes>>. *J. Electrochem. Soc.* 140. 1981.

47. SPRINGER, T. E., ZAWODZINSKI, T. A. AND GOTTESFELD, S. 1991. <<Polymer electrolyte fuel cell model>>. *J. Electrochem. Soc.* 138. 2334.

48. FULLER, T. F. AND NEWMAN, J. 1993. <<Water and thermal management in solid-polymer-electrolyte fuel cells>>. *J. Electrochem. Soc.* 140. 1218.

49. NGUYEN, T. V. AND WHITE, R. E. 1993. <<A water and heat management model for proton-exchange-membrane fuel cells>>. *J. Electrochem. Soc.*, 140. 2178.

50. ZAWODZINSKI, T.A., JR., DEROUIN, C., RADZINSKI, S., SHERMAN, R. J., SMITH, V. T., SPRINGER, T. E. AND GOTTESFELD, S. 1993. <<Water uptake by and transport through Nafion 117 membranes>>. *J. Electrochem. Soc.* 140. 1041.

51. YEO, R. S. AND YEAGER, H. L. 1985. *Modern aspects of electrochemistry.* No. 16, Conway B.E., White R.E., and Bockris J. O'M., Editors, New York: Plenum Press. p.437-504.

52. LOPEZ, M., KIPLING, B. AND YEAGER, H. L. 1976. <<Exchange rates and water content of a cation exchange membrane in aprotic solvents>>. *Anal. Chem.* 48. 1121.

53. ZAWODZINSKI, T.A., NEEMAN, M., SILLERUD, L. AND GOTTESFELD, S. 1991. <<Determination of water diffusion coefficients in perfluorosulfonate ionomeric membranes>>. *J. Phys. Chem.* 95. 6040.

54. HINATSU, J. T., MIZUHATA, M. AND TAKENAKA, H. 1994. <<Water uptake of perfluorosulfonic acid membranes from liquid water and water vapor>>. *J. Electrochem. Soc.* 141. 1493.

55. EISENBERG, A. 1970. <<Clustering of ions in organic polymers. A theoretical approach>>. *Macromolecules.* 3. 147.

56. YEO, S. AND EISENBERG, 1977. <<A. Physical properties and supermolecular structure of perfluorinated ion-containing (nafion) polymers>>. *J. Appl. Polym. Sci.* 21. 875.

57. ZAWADZINSKI, T.A. JR., GOTTESFELD, S. SHOICHET, S. AND MCCARTHY, T. J. 1993. <<The contact angle between water and the surface of perfluorosulfonic acid membranes>>. *J. Appl. Electrochem.* 23. 86.

58. SIMPSON, J. H. AND CARR, H. Y. 1958. <<Diffusion and Nuclear Spin Relaxation in Water>>. *Phys. Rev.* 111. 1201.

59. BRESLAU, B. R. AND MILLER, I. F. 1971. <<A hydrodynamic model for electroosmosis>>. *Ind. Eng. Chem. Fundam.* 10. 554.

60. RIEKE, P.C. AND VANDERBORGH, N. E. 1987. <<Temperature dependence of water content and proton conductivity in polyperfluorosulfonic acid membranes>>. *J. Memb. Sci.* 32. 313.

61. ALMEIDA S.H.DE. AND KAWANO, Y. 1999. <<Thermal behavior of Nafion membranes>>. *J. Therm. Anal. Cal.*, 58. 569.

62. WILKIE, C.A., THOMSEN, J.R. AND MITTLEMAN, M.L. 1991. <<Interaction of poly(methyl methacrylate) and Nafions>>. *J. appl. Polym. Sci.,* 42. 901.

63. BUNCE, N.J., SONDHEIMER S.S., AND FYFE, C.A. 1986. <<Proton NMR method for the quantitative determination of the water content of the polymeric fluorosulfonic acid Nafion-H>>. *Macromolecules.* 19. 333.

64. KYU, T., HASHIYAMA, M. AND EISENBERG, A. 1983. <<Dynamic mechanical studies of partially ionized and neutralized Nafion polymers>>. *Can. J. Chem.,* 61. 680.

65. FUJIMURA, M., HASHIMOTO, T. AND KAWAI, H. 1981. <<Small-angle X-ray scattering study of perfluorinated ionomer membranes. 1. Origin of two scattering maxima>>. *Macromolecules,* 14. 1309.

66. BERNARDI, D.M. 1990. <<Water-balance calculations for solid-polymer-electrolyte fuel cells>>. *J. Electrochem. Soc.,* 137. 3344.

67. DATA, R. AND RINKER, R.G. 1985. <<Supported liquid-phase catalysis : I. A theoretical model for transport and reaction>> . *J. Catal.*, 95. 181.

68. KUMER, R. AND AHMED, S. 1995. << Fuel cells processing for transportation fuel cell systems>>. *Proceeding of the first International Symposium on New Materials for Fuel Cell and Modern Battery system.* Eds. Savadogo O., Roberge P.R. and Veziroglu T.N., Montreal, Canada, July 9-13. P.224.

69. KAHLICH, M., SCHUBERT, M.M., HUTTNER, M., NOESKE, M., GASTEIGER, H.A. AND BEHM, R.J. 1997. << Kinetics of the selective CO oxidation in H_2-rich gas on supported noble metal catalysis>>. *Proceeding of the Second International Symposium on New Materials for Fuel Cell and Modern Battery system.* Eds. Savadogo O. and Roberge P.R., Montreal, Canada, July 6-10. p.642.

70. DHER, H.P., CHRISTNER, L.G. AND K.KUSH, A. 1987. <<Nature of CO adsorption during H_2 oxidation in relation to modeling for CO poisoning of a fuel cell anode>>. *J. Electrochem. Soc.,* 134. 3021.

71. LIEBHABSKY, H.A., CAIRNS ET. 1968. *Fuel cells and fuel batteries.* New York: Wiley. p. 425.

72. STECK, A.E. 1997. << Development of the BAM membrane for fuel cell application>>. *Proceedings of the Second International Symposium on New Materials for Fuel-Cell and Modern Battery Systems.* Eds. Savadogo O. and Roberge P.R., Montreal, Canada. p. 792.

73. WEI, J., STONE, C. AND STECK, A. E. 1995. *US Patent.* No. 5,422,411.

74. HASS, O., BRACK, H. P., BUCHI, F. N., GUPTA, B. AND SCHERER, G. G. 1997. <<Properties of radiation grafted membranes for fuel cell applications>>. *Proceedings of the Second International Symposium on New Materials for Fuel-Cell and Modern Battery Systems.* Eds. Savadogo O. and Roberge P.R., Montreal, Canada. p.836.

75. HIETALA, S., KOEL, M., SKOU, E., ELOMAA, M. AND SUNDHOLM, F. 1998. <<Thermal stability of styrene grafted and sulfonated proton conducting membranes based on poly(vinylidene fluoride)>>. *J. Mater. Chem.* 8. 1127.

76. KERRES, J., CUI, W., EIGENBERGER, G., BEVERS, D., SCHNURNBERGER, W., FISHER, A. AND WENDT, H. 1996. <<New ionomers and their application In PEM fuel cells>>.*Proceedings of the 11th Hydrogen Conference.* Veziroglu T.N.. Winter C.J., Baselt J.P., Kreysa G. (Eds.), Stuttgart, Germany. p.1951.

77. J.S. WAINRIGHT, R.F. SAVINELL, M.H. LITT, 1997. <<Acid doped polybenzimidazole as a polymer electrolyte for methanol fuel cells>>. *Proceedings of the Second International Symposium on New Materials for Fuel-Cell and Modern Battery Systems*. Eds. Savadogo O. and Roberge P.R., Montreal, Canada. p.808.

78. FAURE, S., CORNET, N., GEBEL, G., MERCIER, R., PINERI, M. AND SILLON B. 1997. <<Sulfonated polyimides as novel proton exchange membranes for H_2/O_2 fuel cells>>. *Proceedings of the Second International Symposium on New Materials for Fuel Cell and Modern Battery Systems.* Eds. Savadogo O. and Roberge P.R., Montreal, Canada. p.818.

79. EHRENGERG, SCOTT G., SERPICO, JOSEPH M., SHEIKH-ALI, BASHIR M., TANGREDI, TIMOTHY N., ZADOR, E. AND WNEK, G. E. 1997. << Hydrocarbon PEM/electrode assemblies for low-cost fuel cells: Development, Performance and Market opportunities>>. *Proceedings of the Second International Symposium on New Materials for Fuel-Cell and Modern Battery Systems.* Eds. Savadogo O. and Roberge P.R., Montreal, Canada. p.828.

80. SCHMELLER, A., RITTER, H., LZDJEFF, K., NOLTE, R. AND R. THORWIRTH, 1993. *EP. 0574791 A2.*

81. WIECZOREK, W., FLORJANCZYK, Z. AND STEVENS, J. R. 1995. <<Proton conducting polymer gels based on a polyacrylamide matrix>>. *Eletrochim. Acta* 40. 2327.

82. BURNETT. 1985. *US Patent.* No 4,506,035.

83. SCHERER, G. 1990. <<XPS studies of radiation grafted PTFE-g-polystyrene sulfonic acid membranes>>. *Ber. Bunsenges. Phys. Chem.* 94. 1008.

84. BUCHI, F.N., GUPTA, B., HAAS, O. and SCHERER, G. 1995. <<Performance of Differently Cross-Linked, Partially Fluorinated Proton Exchange Membranes in Polymer Electrolyte Fuel Cells>>*J. Electrochem. Soc.* 142:9. 3044.

85. GUPTA, B., BUCHI, F.N. AND SCHERER, G.G. 1993. <<Research aspects of organic solid proton conductors>>. *Solid State Ionics.* 61. 213.

86. LEHTINEN, T., SUNDHOLM, G., HOLMBERG, S., SUNDHOLM, F., BJORNBOM, P. AND BURSELL, M. 1998. <<Electrochemical characterization of PVDF-based proton conducting membranes for fuel cells>>. *Electrochim. Acta.* 43. 1991.

87. PARANEN, M., SUNDHOLM, F., RANHALA, E., LEHTINEN, T. AND HEITALA, S. 1997. <<Effects of irradiation on sulfonation of poly(vinyl fluoride)>>. *J. Mat. Chem.* 7. 2401.

88. OSTROVSKII, D.I., TORELL, L.M., PARONEN, M., HEITALA, S. AND SUNDHOLM, F. 1997. <<Water sorption properties of and the state of water in PVDF-based proton conducting membranes>>. *Solid State Ionics,* 97. 315.

89. XING, B. AND SAVADAGO, O. 1999. <<The effect of acid doping on the conductivity of polybenzimidazole (PBI)>>. *J. New Mat. Electrochem. Systems.* 2. 95.

90. FOULKES, F. R. AND GRAYDON, W. F. 1971. << Transport in membrane fuel cells>>. *Electrochim. Acta.* 16. 1577.

91. SAVINELL, R., YEAGER, E., TRYK, D., LANDAU, U., WAINRIGHT, J., WENG, D., LUX, K., LITT, M. AND ROGERS, C. 1994. <<A Polymer Electrolyte for Operation at Temperatures up to 200°C>>. *J. Electrochem. Soc.* 141. L46.

92. BHAMIDIPATI, M., LAZARO, E., LYONS, F. AND MORRIS, R. S. 1998. <<Novel Proton Exchange Membrane for High Temperature Fuel Cell>>. *Materials Research Society Symposium Proceedings Materials for Electrochemical Energy Storage and Conversion II – Batteries, Capacitors and Fuel Cell Proceedings of the 1998 MRS Fall Symposium.* Dec. 1-5 1997 v496 1998 Boston, MA, USA. p.201.

93. MALHOTRA, S. AND DATTA, R. 1997. <<Membrane-supported nonvolatile acidic electrolytes allow higher temperature operation of proton-exchange membrane fuel cells>>. *J Electrochem. Soc.* 144. 2.

94. ARIMURA, T., OSTROVSHII, D., OKADA, T. AND XIE, G. 1999. <<The effect of additives on the ionic conductivity performances of perfluoroalkyl sulfonated ionomer membranes>>. *Solid State Ionics.* p.118.

95. OKADA, T., XIE, G., GORSETH, O., KJELSTRUP, S. AND NAKAMURA, N. T. 1998. <<Arimura Ion and water transport characteristics of Nafion membranes as electrolytes>>. *Electrochim Acta.* 43. 3741.

96. WATANABE, M., UCHIDA, H., SEKI, Y. AND EMORI, M. 1996. <<Self-humidifying polymer electrolyte membranes for fuel cells>>. *J. Electrochem. Soc.* 143. 3847.

97. YOUNG-SUN Park, MOON-YUP Jang AND YOHTARO Yamazaki. 2003. << Development of High Crystalline Nafion/Calcium Hydroxy Apatite Composite membrnae For Direct methanol Fuel Cells >>. Presented at *the 44th Japan Battery Symposium*, Sakai, Japan, November 4-6 (2003). 1A03.

98. YANG, C., SRINIVASAN, S., BOCARSLY, A.B., TULYANI, S. AND BENZIGER, J.B. 2004. <<A comparison of physical properties and fuel cell performance of Nafion and zirconium phosphate/Nafion composite Membranes>>. *J. Membrane Science.* 237. 145-161.

99. ZAIDI, S.M.J., MIKHAILENKO, S.D., ROBERTSON, G.P., GUIVER, M.D. AND KALIAGUINE, S. 2000. <<Proton conducting composite membranes from polyether ether ketone and heteropolyacids for fuel cell applications>>. *Journal of Membrane Science,* 173. 17-34.

100. ADJEMIAN, K.T., LEE, S.J., SRINIVASAN, J., BENZIGER, S. AND BOCARSLY, A.B. 2002. <<Silicon oxide Nafion composite membranes for proton-exchange membrane fuel cell operation at 80-140°C>>. *J. Electrochem. Soc.,* 149. A256-A261.

101. ADJEMIAN, K.T., SRINIVASAN, S., BENZIGER, J. AND BOCARSLY, A.B. 2002. <<Investigation of PEMFC operation above 100 °C employing perfluorosulfonic acid silicon oxide composite membranes>>. *Journal of Power Sources.* 109. 356-364.

102. KIM Y. S., WANG, F., HICKNER, M., ZAWODZINSKI, T. A. AND MCGRATH J. E. 2003. <<Fabrication and characterization of heteropolyacid ($H_3PW_{12}O_{40}$)/directly polymerized sulfonated poly(arylene ether sulfone) copolymer composite membranes for higher temperature fuel cell applications>>. *Journal of Membrane Science*. 212. 263-282.

103. TAZI, B. AND SAVADOGO, O. 2000. <<Parameters of PEM fuel-cells based on new membranes fabricated from Nafion®, silicotungstic acid and thiophene>>. *Electrochimica Acta.* 45. 4329.

104. CLEARFIELD, A. 1998. <<Role of ion exchange in solid-state chemistry>>. *Chem. Rev.* 88. 125.

105. NAKAMURA, O., KODAMA, T., OGINO, I. AND MIYAKE, Y. 1979. <<High-conductivity solid proton conductors: Dodecamolybdophosphoric acid and Dodecatungstophosphoric acid crystals>>. *Chem. Letters.* 17.

106. KREUER, K. D., HAMPELE, M., DOLDE, K. AND RABENAU, A. 1988. <<Proton Transport in Some Heteropolyacidhydrates A single Crystal PFG-NMR and Conductivity Study>>. *Solid State Ionics* .28-32. 589-593.

107. POPE, M. T. 1983. *Heteropoly and isopoly oxometalates.* Edited by Springer-Verlag, Germany. p.30.

108. POPE, M. T. 1983. *Heteropoly and isopoly oxometalates.* Edited by Springer-Verlag, Germany. p.60.

109. LEVY, H. A., AGRON, F. A., DANFORD, M. O. 1959. <<Structure of silico-Tungstic acid in aqueous solution>>. *J. Chem. Phys.* 30. 1486.

110. GLEMSER, O., HOLZNAGEL, W., HOLTJE, W., SCHWARZMANN, E. 1965. <<New Methods and Results in the Study of Polyacids>>. *Z. Naturforsch.* 206. 725.

111. LEE, K.Y., MIZUNO, N., OKUHARA, T. AND MISONO, M. 1989. <<Catalysis by heteropoly compounds. XIII. An infrared study of ethanol and diethyl ether in the pseudoliquid phase of 12-tungstophosphoric acid>>. *Bull. Chem. Soc. Jpn.* 62. 1731.

112. BARDIN, B.B., BORDAWEKAR, S.V., NEUROCK, M. AND DAVIS, R.J. 1998. <<Acidity of Keggin-type heteropolycompounds evaluated by catalytic probe reactions, sorption microcalorimetry, and density functional quantum chemical calculations>>. *J. Phys. Chem.* B 102. 10817.

113. TSIGDINOS, G. A. 1978. <<Heteropoly: compound of molybdenum and tungsten>>. *Aspect of molybolenum and related chemistry, Topics in current chemistry*. Edited by Springer-Verlag, Germany. p.18.

114. FRICOTEAUX, P. AND SAVADOGO, O. 1999. <<Electrocatalytic parameters of the electrodeposition of copper with silicotungstic acid (STA)>>. *Electrochim. Acta.* 44. 2927.

115. KURUSCEV, T., SARGESON, A. M. AND WEST, B. O. 1957. <<Size and hydration of inorganic macroions from viscosity and density measurements>>. *J. Phys. Chem.* 61. 1567

116. KUCERNAK, A. R. J., BARNETT, C. J., BURSTEIN, G. T. AND WILLIAMS K. R. 1995. <<Tungsten containing electrodes and electrolytes for low temperature methanol electrooxidation>>. *New Materials for Fuel Cell System 1, Proceedings of the First International Symposium on New Materials for Fuel Cell Systems.* Eds. Savadogo O., Roberge P.R. and Veziroglu T.N., Montreal, Quebec, Canada. p. 337.

117. STAITI, P., FRENI, S. AND HOCEVAR, S. 1999. <<Synthesis and characterization of proton-conducting materials containing dodecatungstophosphoric and dodecatungstosilic acid supported on silica>>. *J. Power Sources.* 79. 250.

118. SUN, J., MACFARLANE, D. R. AND FORSYTH, M. 2001. <<Characterization of a proton conductor based on silicotungstic acid>>. *Electrochimica Acta.* 46. 1673.

119. BIELANSKI, A., POZNICZEK, J. AND HASIK, M. 1995. <<THERMAL-BEHAVIOR OF HYDRATED DODECATUNGSTOSILICIC>>. *J. Thermal Analysis.* 44. 717.

120. MIOC, U., DAVIDOVIC, M., TJAPKIN, N., COLOMBAN, P. AND NOVAK, A. 1991. <<Equilibrium of the protonic species in hydrates of some heteropolyacids at elevated temperatures>> .*Solid State Ionics.* 46. 103.

121. MOORE, R. B. AND MARTIN, C. R. 1986. <<Procedure for preparing solution-cast perfluorosulfonate ionomer films and membranes>>. *Anal Chem.* 58. 2570.

122. MOORE, R.B. AND MARTIN, C.R. 1988. <<Chemical and morphological properties of solution-cast perfluorosulfonate ionomers>>. *Macromolecules.* 21. 1334.

123. YOSHIDA, N., ISHISAKJ, T., WATAKABE, A. AND YOSHITAKE, M. 1998. <<Characterization of Flemion® membranes for PEFC>>. *Electrochimica Acta.* 43. 3749.

124. FAVA, A. 1980. <<Polymers, PART B: crystal structure and morphology>>. *Methods of Experimental Physics.* Marton, L. AND Marton, C. Editors- in-Chief, Volume 16, Academic Press, Inc. p.287.

125. MULDER, M. 1996. *Basic principles of membrane technology.* The Netherlands: Kluwer Academic Publishers. p.195.

126. MULDER, M. 1996. *Basic principles of membrane technology.* The Netherlands: Kluwer Academic Publishers. p.199.

127. MULDER, M. 1996. *Basic principles of membrane technology.* The Netherlands: Kluwer Academic Publishers. p.162.

128. THE UK's NATIONAL MEASUREMENT LAB. << Theory of Atomic Force Microscopy>>. http://www.npl.co.uk/smd/npl_research/afm_theory.html

129. MULDER, M. 1996. *Basic principles of membrane technology.* The Netherlands: Kluwer Academic Publishers. p.164.

130. JAS.CO, <<FTIR Seminar>>. http://www.jascofrance.fr/pdf/ftir.pdf

131. MOULDER, F. J., STICKLE, W. F., SOBOL, P. E. AND BOMBEN, K. D. 1992. *Handbook of X-ray photoelectron spectroscopy.* Edited by Jill Chastain, Perkin-Elmer Corp.

132. MOSDALE, R. AND SRINIVASAN, S. 1995. <<Analysis of performance and of water and thermal management in proton exchange membrane fuel cells>>. *Electrochimica Acta.* 40. 413.

133. ALMEIDA, S.H.D. AND KAWANO, Y.J. 1999. <<Thermal behavior of Nafion membranes>>. *J. Therm. Anal. Cal.* 58. 569.

134. LUO, Y., HUO, R., JIN, X. AND KARASZ, F.E. 1995. <<Thermal degradation of sulfonated poly(aryl ether ether ketone)>> . *J. Anal. Appl. Pyrolysis.* 34. 229.

135. GIERKE, T.D., MUNN, G.E. AND WILSON, F.C. 1981. <<The morphology in Nafion perfluorinated membrane products, as determined by wide-and small-angle x-ray studies>>. *J. Polym.Sci: Polym.Phys.Ed.* 19. 1687.

136. ALPERT, N. L., KEISER, W. E. AND SZYMANSKI, H. A. 1970. *IR theory and practice of infrared spectroscopy.* New York:Plenum Press. p. 276-277.

137. ALPERT, N. L., KEISER, W. E. AND SZYMANSKI, H. A. 1970. *IR theory and practice of infrared spectroscopy.* New York:Plenum Press. p. 288-289.

138. PAZÉ, C., BORDIGA, S. AND ZECCHINA, A. 2000. <<H_2O interaction with solid $H_3PW_{12}O_{40}$: An iR study>>. *Langmuir.* 16. 8139.

139. TSIGDINOS, G. A. 1978. <<Heteropoly compound of molybdenum and tungsten>>. *Aspect of molybolenum and related chemistry, Topics in current chemistry.* Edited by Springer-Verlag, Germany. p.55.

140. BEAMSON, G. AND BRIGGS, D. 1992. <<High resolution XPS of organic polymers>>. *The scienta ESCA300 database.* John Wiley & sons. p. 79.

141. SCHULZE, M., LORENZ, M., WAGNER, N. AND GULZOW, E. 1999. <<XPS analysis of the degradation of Nafion>>. *Frenesius J. Anal. Chem.* 365. 106.

142. HUSLAGE, J., RAGER, T., SCHNYDER, B. AND TSUKADA, A. 2002. <<Radiation-grafted membrane/electrode assemblies with improved interface>>. *Electrochimica acta.* 48. 247.